Universitat Autònoma de Barcelona

New therapeutic strategies targeting dendritic cell-mediated dissemination of enveloped viruses

Daniel Pérez Zsolt

Universitat Autònoma de Barcelona

Department of Biochemistry and Molecular Biology

New therapeutic strategies targeting dendritic cell-mediated dissemination of enveloped viruses

Daniel Pérez Zsolt

Institut de Recererca de la SIDA – IrsiCaixa

Hospital Universitari Germans Trias i Pujol

2019

Doctoral thesis to obtain the PhD degree in Biochemistry, Molecular Biology and Biomedicine of the Universitat Autònoma de Barcelona

Directors: **Dr. Javier Martínez-Picado**

Dr. Nuria Izquierdo-Useros

Tutor: **Dr. Maria Victòria Nogués Bara**

Cover illustrations: Òscar Blanch Lombarte, 2019.

The Spanish Secretariat of State of Research, Development and Innovation (SEIDI) supported the research performed in this thesis through grants SAF2013-49042-R and SAF2016-80033-R. Grifols provided additional support. Daniel Pérez Zsolt was supported by the Spanish Ministry of Science, Innovation and Universities and the European Regional Development Fund under agreement BES-2014-069931. The Spanish AIDS Network 'Red Española de Investigación en SIDA' (RIS) provided additional support for congress assistance.

IrsiCaixa
Institut de Recerca de la Sida

El Dr. Javier Martínez-Picado, investigador principal i professor de recerca ICREA a l'Institut de Recerca de la SIDA, IrsiCaixa (Hospital Universitari Germans Trias i Pujol).

Certifica:

Que el treball experimental i la redacció de la memòria de la Tesi Doctoral titulada "New therapeutic strategies targeting dendritic cell-mediated dissemination of enveloped viruses" han estat realitzats per en Daniel Pérez Zsolt sota la seva direcció, i considera que l'esmentada Tesi és apta per a ser presentada per optar al grau de Doctor en Bioquímica, Biologia Molecular i Biomedicina per la Universitat Autònoma de Barcelona.

I per tal que en quedi constància, signa aquest document.

Badalona, 9 de desembre de 2019.

Dr. Javier Martínez-Picado

IrsiCaixa
Institut de Recerca de la Sida

La Dra. Nuria Izquierdo-Useros, investigadora a l'Institut de Recerca de la SIDA, IrsiCaixa (Hospital Universitari Germans Trias i Pujol).

Certifica:

Que el treball experimental i la redacció de la memòria de la Tesi Doctoral titulada "New therapeutic strategies targeting dendritic cell-mediated dissemination of enveloped viruses" han estat realitzats per en Daniel Pérez Zsolt sota la seva direcció, i considera que l'esmentada Tesi és apta per a ser presentada per optar al grau de Doctor en Bioquímica, Biologia Molecular i Biomedicina per la Universitat Autònoma de Barcelona.

I per tal que en quedi constància, signa aquest document.

Badalona, 9 de desembre de 2019.

Dra. Nuria Izquierdo-Useros

Universitat Autònoma de Barcelona

La Dra. Maria Victòria Nogués Bara, catedràtica de Bioquímica i Biologia Molecular de la Universitat Autònoma de Barcelona.

Certifica:

Que el treball experimental i la redacció de la memòria de la Tesi Doctoral titulada "New therapeutic strategies targeting dendritic cell-mediated dissemination of enveloped viruses" han estat realitzats per en Daniel Pérez Zsolt sota la seva tutela, i considera que l'esmentada Tesi és apta per a ser presentada per optar al grau de Doctor en Bioquímica, Biologia Molecular i Biomedicina per la Universitat Autònoma de Barcelona.

I per tal que en quedi constància, signa aquest document.

Badalona, 9 de desembre de 2019.

Dra. Maria Victòria Nogués Bara

A mis padres. Y a los suyos.

'I understood for the first time that I didn't understand what I thought I understood'

Seiji Ozawa

SUMMARY

Dendritic cells are key inducers of specific adaptive immune responses due to their capacity to capture, process and present pathogen-derived antigens to T lymphocytes. However, they might also contribute to early HIV-1 dissemination by capturing HIV-1 particles and transmitting them to target $CD4^+$ T cells, a process known as *trans*-infection. This mechanism relies on the expression of Siglec-1 receptor (CD169), which recognizes sialylated gangliosides on the viral membrane. Siglec-1 is potently up-regulated upon dendritic cell stimulation with interferon-alpha and lipopolysaccharide, which are both immune-activating factors present during the course of HIV-1 infection. Here, we demonstrated that interferon-alpha secreted by HIV-1-infected plasmacytoid dendritic cells and autocrine interferon-alpha secreted by myeloid cells in response to lipopolysaccharide up-regulate Siglec-1 on dendritic cells. Importantly, plasmacytoid dendritic cells derived from women secreted higher amounts of interferon-alpha than those derived from men, highlighting the relevance of studying HIV-1 *trans*-infection in key female tissues for HIV-1 acquisition.

Thus, we next studied the role of Siglec-1 in HIV-1 transmission mediated by primary dendritic cells directly isolated from cervical tissues, identifying a subset of cervical myeloid cells that expressed Siglec-1 and captured HIV-1 particles in a Siglec-1-dependent manner. This capacity was enhanced upon activation with interferon-alpha. Moreover, HIV-1 cell-to-cell transmission mediated by these cells could be efficiently blocked using an anti-Siglec-1 monoclonal antibody, indicating the potential use of antibodies directed against Siglec-1 in prevention of sexually transmitted HIV-1 acquisition in women. Thus, we generated a set of new anti-Siglec-1 monoclonal antibodies with the capacity to block dendritic cell-mediated HIV-1 *trans*-infection. Five new clones were produced, demonstrating high affinity for different epitopes located in the N-terminal region of Siglec-1 receptor. Moreover, they efficiently blocked HIV-1 capture and *trans*-infection mediated by dendritic cells, indicating their potential use in microbicidal strategies targeting this type of viral cell-to-cell transmission.

Aside from HIV-1, dendritic cells can play important roles in the pathogenesis of other viruses, including Ebola and Marburg filoviruses. In contrast to HIV-1, dendritic cells are permissive to filoviral infection and act as early targets in viral pathogenesis. The host factors governing filoviral entry into these cells are not fully characterized, but both Ebola and Marburg are enveloped viruses that incorporate sialylated gangliosides during the

budding process. Moreover, Siglec-1-activating factors such as interferon-alpha and lipopolysaccharide have been found during Ebola virus disease. Thus, we investigated the role of Siglec-1 in filoviral entry into dendritic cells. We found that Siglec-1-mediated capture of non-infectious Ebola virus-like particles into these cells, especially upon interferon-alpha and lipopolysaccharide activation. Interestingly, captured Ebola virus-like particles accumulated in the same cellular compartment where HIV-1 was previously detected. Siglec-1 also facilitated Ebola cytoplasmic entry into dendritic cells, so we tested the capacity of novel anti-Siglec-1 monoclonal antibodies to interfere with this process. We found that capture and cytoplasmic entry of Ebola virus-like particles into activated myeloid cells was blocked by these novel antibodies. Overall, the activity of anti-Siglec-1 monoclonal antibodies inhibits the access of both retroviruses and filoviruses into myeloid cells and suggests their potential use as broad-spectrum antiviral agents.

RESUM

Les cèl·lules dendrítiques són clau en la inducció de respostes immunitàries adaptatives gràcies a la seva capacitat de capturar, processar i presentar antígens derivats de patògens als limfòcits T. Tanmateix, aquestes cèl·lules també podrien contribuir a la disseminació inicial del VIH-1 a través de la captura de partícules virals i de la seva transmissió a les cèl·lules T $CD4^+$ diana, un procés conegut com a *trans*-infecció. Aquest mecanisme es basa en l'expressió del receptor Siglec-1 (CD169), que reconeix gangliòsids sialilats a la membrana viral. Els nivells de Siglec-1 augmenten en cèl·lules dendrítiques estimulades amb interferó-alfa i lipopolisacàrid, factors immuno-activadors presents durant el decurs de la infecció per VIH-1. En aquesta tesi, hem demostrat que l'interferó-alfa secretat per cèl·lules dendrítiques plasmacitoides infectades per VIH-1, així com l'inteferó-alfa autocrí secretat per cèl·lules mieloides en resposta a lipopolisacàrid, augmenten l'expressió de Siglec-1 en cèl·lules dendrítiques. A més, les cèl·lules dendrítiques plasmacitoides provinents de dones secreten quantitats superiors d'interferó-alfa que les derivades d'homes, posant de manifest la rellevància d'estudiar la *trans*-infecció del VIH-1 en teixits clau per a l'adquisició del virus en dones.

Així, també hem estudiat el paper de Siglec-1 en la transmissió del VIH-1 per part de cèl·lules dendrítiques primàries aïllades directament de teixit cervical, identificant una població de cèl·lules mieloides cervicals que expressen Siglec-1 i capturen partícules de VIH-1 a través d'aquest receptor. Aquesta capacitat augmenta amb l'activació per interferó-alfa. A més, la transmissió cèl·lula-cèl·lula del VIH-1 per cèl·lules mieloides del cèrvix es bloqueja de forma eficient amb un anticòs monoclonal dirigit contra Siglec-1, indicant el potencial ús d'aquests anticossos en la prevenció de la transmissió sexual del VIH-1 en dones. Per tant, hem generat una sèrie de nous anticossos monoclonals contra Siglec-1 amb la capacitat de bloquejar la *tans*-infecció del VIH-1 per cèl·lules dendrítiques. S'han produït cinc nous clons, que han demostrat tenir una alta afinitat per diferents epítops localitzats a la regió N-terminal de Siglec-1. A més, aquests anticossos bloquegen de forma eficaç la captura i *trans*-infecció del VIH-1 per cèl·lules dendrítiques, de forma que podrien ser un component en estratègies microbicides dirigides contra aquest tipus de transmissió viral cèl·lula-cèl·lula.

A banda del VIH-1, les cèl·lules dendrítiques juguen un paper important en la patogènesi d'altres virus, com ara els filovirus d'Ebola i Marburg. A diferència del VIH-1, les cèl·lules dendrítiques són permissives a la infecció per filovirus i són dianes primerenques en la

patogènesi viral. Els factors cel·lulars implicats en l'entrada de filovirus en aquestes cèl·lules no han estat totalment caracteritzats, però tant Ebola com Marburg són virus embolcallats que incorporen gangliòsids sialilats durant el procés de gemmació viral. A més, els factors que activen l'expressió de Siglec-1 com ara interferó-alfa i lipopolisacàrid s'han trobat durant la infecció pel virus d'Ebola. Per tant, en aquesta tesi hem estudiat el paper de Siglec-1 en l'entrada de filovirus en cèl·lules dendrítiques. Hem trobat que Siglec-1 està implicat en la captura de partícules no infeccioses d'Ebola per part d'aquestes cèl·lules, especialment després de l'activació per interferó-alfa i lipopolisacàrid. A més, les partícules capturades són acumulades en el mateix compartiment cel·lular en què prèviament s'havia detectat el VIH-1. Siglec-1 també facilita l'entrada citoplasmàtica del virus a les cèl·lules dendrítiques, així que hem determinat la capacitat dels nous anticossos monoclonals contra Siglec-1 d'interferir amb aquest procés, i hem vist que aquests bloquegen tant la captura com l'entrada citoplasmàtica de partícules no infeccioses d'Ebola en cèl·lules mieloides activades. En general, l'activitat dels anticossos monoclonals contra Siglec-1 inhibeix l'accés de retrovirus i de filovirus a les cèl·lules mieloides, cosa que indica el seu potencial ús com a agents antivirals d'ampli espectre.

COMMON ABBREVIATIONS

AIDS: acquired immunodeficiency syndrome
AMPK: AMP-activated protein kinase
APC: antigen-presenting cell
APOBEC3G: apolipoprotein B mRNA editing enzyme catalytic subunit 3G
ART: antiretroviral treatment

BlaM: β-lactamase
BDCA1: blood dendritic cell antigen 1
BSA: bovine serum albumin

CCR5: C-C chemokine receptor type 5
CLR: C-type lectin receptor
CTSB: cathepsin B
CXCR4: C-X-C chemokine receptor type 4

DAPI: 4,6-diamidino-2-phenylindole
DC: dendritic cell
DC-SIGN: dendritic cell-specific intercellular adhesion molecule-3-grabbing non-integrin
DMEM: Dulbecco's Modified Eagle Medium
DNA; deoxyribonucleic acid
dsDNA: double-stranded deoxyribonucleic acid

EBOV: Ebola virus
eGFP: enhanced green fluorescent protein
ELISA: enzyme-linked immunosorbent assay
EMEM: Eagle's minimum essential medium
ESCRT: endosomal sorting complexes required for transport

FACS: fluorescence-activated cell sorting
FBS: fetal bovine serum
Fc: fragment crystallizable (constant fraction; antibodies)
FITC: fluorescein isothiocyanate
FSC: forward scatter channel (flow cytometry)

FVD: filovirus disease

GALT: gut-associated lymphoid tissue
GFP: green fluorescent protein
GM-CSF: granulocyte/macrophage-colony stimulating factor
GP: glycoprotein

HEK: human embryonic kidney
HIV: human immunodeficiency virus
HIV-1: human immunodeficiency virus type 1
HIV-2: human immunodeficiency virus type 2
HLA-DR: human leukocyte antigen DR
HRP: horseradish peroxidase
HUGTiP: Hospital Universitari Germans Trias i Pujol
HUVH: Hospital Universitari Vall d'Hebron

iDC: immature DC
Ig: immunoglobulin
IFN: interferon
IFNα: interferon-alpha
IL-4: interleukin-4
IU: International Units

LPS: lipopolysaccharide
LPS-DC: dendritic cell treated with lipopolysaccharide
LSECtin: liver/lymph node sinusoidal endothelial cell C-type lectin
L-SIGN: liver/lymph node-specific intracellular adhesion molecule-3-grabbing non-integrin

mAb: monoclonal antibody
MARV: Marburg virus
MDDC: monocyte-derived dendritic cell
MFI: mean fluorescence intensity
MHC: major histocompatibility complex
MHC-I: major histocompatibility complex class I
MHC-II: major histocompatibility complex class II
mRNA: messenger ribonucleic acid

NIH: National Institutes of Health
NK: natural killer cell
NP: nucleoprotein
NPC1: Niemann-Pick C1 receptor

PAMP: pathogen-associated molecular pattern
PBS: phosphate-buffered saline
pDC: plasmacytoid dendritic cell
PE: phycoerythrin
PE-Cy7: phycoerythrin-cyanine 7 conjugate
PerCP: peridinin chlorophyll protein
PerCP-Cy5.5: peridinin chlorophyll protein-cyanine 5.5 conjugate
PFA: paraformaldehyde
PRR: pattern-recognition receptor

RLU: relative light unit
RNA: ribonucleic acid
RPMI: Roswell Park Memorial Institute medium
RT: room temperature

SAMHD1: sterile alpha-motif (SAM) and histidine-aspartate (HD) domain-containing protein 1
SD: standard deviation
SEM: standard error of the mean
shRNA: short hairpin ribonucleic acid
Siglec-1: sialic acid-binding immunoglobulin-like lectin 1
SIV: simian immunodeficiency virus
SPR: surface plasmon resonance
SSC: side scatter channel
ssRNA: single-stranded ribonucleic acid

TAM: Tyro-Axl-Mer receptor
TBS: Tris-buffered saline
$TCID_{50}$: median tissue culture infectious dose
TCR: T cell receptor
Th: T helper cells

TIM: T-cell immunoglobulin and mucin domain receptor
TLR: toll-like receptor
TPC: two-pore channel

VCC: virus-containing compartment
VLP: virus-like particle
VP24: viral protein 24
VP30: viral protein 30
VP35: viral protein 35
VP40: viral protein 40
VSV: vesicular stomatitis virus

TABLE OF CONTENTS

Chapter 1

INTRODUCTION

In our daily life we are constantly exposed to agents such as viruses and bacteria with the capacity to cause infection and disease. Most of the times, however, our immune system efficiently detects and eliminates these pathogens, thus maintaining the organism in a healthy state. As part of the immune system, dendritic cells (DCs) act as sentinels of the mucosal surfaces and are among the first cells to recognize incoming microbes, contributing to initiate immune responses against them[1,2]. However, in this thesis we will focus on how two distant viruses such as the human immunodeficiency virus type 1 (HIV-1) and Ebola virus (EBOV) can subvert the function of DCs as a pathogenic strategy.

In this chapter, we provide an overview of the role of DCs in immunity, and a general description about the biology and pathogenesis of HIV-1 and EBOV, highlighting the role that DCs have in the course of the infection-associated diseases caused by such different viruses.

1. DCs in antiviral host defense

All the elements of the immune system act in an orchestrated manner to detect and eliminate pathogens, and immune responses are generally classified in two main categories: the early mechanisms of innate immunity, and the more potent and specific adaptive immune responses. As pivotal players in the initiation of immunity against invading viruses, DCs participate in these two types of responses[3–5].

1.1 DCs in innate immunity

Elements of the innate immunity are present even before pathogen invasion, and induce a rapid reaction to either eliminate the threat or control it until the adaptive responses are mounted[6,7]. DCs form an integral part of innate immunity, along with other leukocytes and tissue cells. Present at the portals of pathogen invasion such as mucosal surfaces and the skin, DCs are among the first cells encountering these pathogens, and the early interaction with these cells will impact the outcome of the infection. As innate immune cells, DCs detect molecular patterns shared by broad groups of pathogens, which are termed pathogen-associated molecular patterns (PAMPs). Viral RNA or DNA genomes, bacterial lipopolysaccharide (LPS) and yeast mannans are just a few examples of PAMPs[6,8]. DCs recognize these conserved motifs through germ-line encoded receptors called pattern-recognition receptors (PRRs)[9].

Toll-like receptors (TLRs) conform a well-studied family of PRRs recognizing a variety of ligands[10–13]. There are 10 human TLRs (TLR1-10), each with particular sub-cellular localization and ligand specificity[14–16]. For example, endosomal TLR7 and TLR8 recognize ssRNA, while TLR9 binds DNA moieties. TLR4 is involved in response against bacteria as it recognizes LPS, an integral component of the outer membrane of gram-negative bacteria. Another group of PRRs found on DCs are C-type lectin receptors (CLRs), such as the closely related DC-SIGN (CD209), L-SIGN (CD299, Clec4M) and LSECtin (Clec4G), that recognize high mannose-containing glycans[17–19]. I-type lectins constitute a group of glycan-binding receptors within the immunoglobulin (Ig) superfamily[20,21]. The sialic-acid-binding Ig-like lectins (Siglecs) are the best characterized members in this group. They are expressed by DCs, macrophages and monocytes and recognize sialic acids found on pathogens and also in host cells[20–27]. While TLRs and lectins are transmembrane proteins, other PRRs are found in the cytosol. For example, the cyclic GMP-AMP synthase (cGAS) in DCs triggers innate immune responses upon recognition of HIV-1 complementary DNA[28–30].

In most cases, pathogen recognition via cellular PRRs initiates a signalling cascade that can trigger DC activation, altering gene expression and shaping the cell function[31,32]. In general, viral recognition by DCs induces an antiviral and inflammatory state that relies on the secretion of different cytokines and chemokines. Type I interferons (IFNs) such as interferon-alpha (IFNα) and IFNβ are the main antiviral cytokines, and plasmacytoid DCs (pDCs) are the major producers of these cytokines in blood[33]. For example, upon HIV infection viral genome is recognized via TLR7 and TLR9 on pDCs, which induces the expression of type I IFNs by these cells[34–37]. Once secreted, type I IFNs activate the expression of interferon-stimulated genes that mediate different antiviral activities such as inhibition of viral transcription and translation[38].

Taken together, the innate immune response in general and DCs in particular rely on pathogen sensing via PRRs. Signalling through these receptors can result in cell activation and in the secretion of antiviral and inflammatory cytokines, which creates an environment that either eliminates the pathogen or limits its replication until the mechanisms of adaptive immunity are mounted.

1.2 DCs in adaptive immunity

Immature DCs (iDCs) efficiently capture pathogens at the entry sites, degrade them in endosomal lytic compartments and load pathogen-derived peptides onto molecules of the major histocompatibility complex (MHC). Upon activation, they migrate to the secondary lymphoid tissues[39], where fully mature DCs present these antigens to naïve T lymphocytes, a crucial step for the initiation of adaptive immunity. As DCs specialize in this process of antigen presentation, they are often referred to as professional antigen-presenting cells (APCs)[1,2]. Upon contact with microbial products, DCs maturation regulates antigen processing and presentation by lowering the pH of endocytic compartments, activating proteolysis, and transporting peptide-MHC complexes to the cell surface[40]. Moreover, maturation enhances the expression of co-stimulatory molecules such as CD80 and CD86 that, along with antigen presentation, are required for priming T cell responses[41–43]. Each individual T cell expresses a surface T cell receptor (TCR) with a given antigen specificity, and becomes activated upon the formation of cognate DC:T cell conjugates, thus establishing 'immunological synapses'[44,45]. Once activated, T cells proliferate and differentiate into effector cells which mediate adaptive immune responses aimed to eliminate pathogens[46]. The effector functions of $CD4^+$ and $CD8^+$ T cells are different, and so are the pathways by which DC present antigens to each T cell subset.

The pathways of antigen presentation are partially defined by the origin of such antigens, that can be endogenous or exogenous. Endogenous antigens are those expressed by the APC itself, for example viral proteins synthesized in the cytoplasm upon viral infection. These antigens undergo proteasomal cleavage and the derived peptides are loaded onto MHC class I (MHC-I) molecules that are directed towards the cell surface[3] (**Figure 1, left panel**). MHC-I:peptide complexes are presented to $CD8^+$ T cells, which once activated exert a cytotoxic function aimed to eliminate infected cells[46]. In contrast, exogenous antigens are internalized by DCs through different mechanisms such as pinocytosis, phagocytosis and receptor-mediated endocytosis[47]. These antigens undergo processing by endosomal proteases such as cathepsins, and the derived peptides are incorporated onto MHC class II (MHC-II) molecules that also reach the cell surface[48] (**Figure 1, centre panel**). MHC-II:peptide complexes are recognized by $CD4^+$ T cells, which differentiate into several effector cell subtypes that help in the development of specific antimicrobial responses[49].

Of note, the endogenous and exogenous pathways are not completely independent. Indeed, DCs have the unique capacity of presenting exogenous antigens to $CD8^+$ T cells via MHC-I, a process known as 'cross-presentation'[50,51] (**Figure 1, right panel**). This mechanism allows antigen presentation to $CD8^+$ T cells without productive DC infection, and is an efficient presentation pathway for viruses such as influenza A virus (IAV)[52,53] and HIV-1[54–56]. Moreover, and although it is widely assumed that exogenous antigens constitute the only source for presentation via MHC-II, numerous exceptions have been found to this rule as well. Indeed, endogenous antigens from measles virus[57,58], IAV[59–61] and HIV-1[62] are loaded onto MHC-II molecules and presented to $CD4^+$ T cells following this non-classical presentation pathway (**Figure 1, dotted line**). Taken together, DCs are specialized in presenting pathogen-derived antigens to T lymphocytes, which occurs through several pathways and initiates different types of adaptive immune responses.

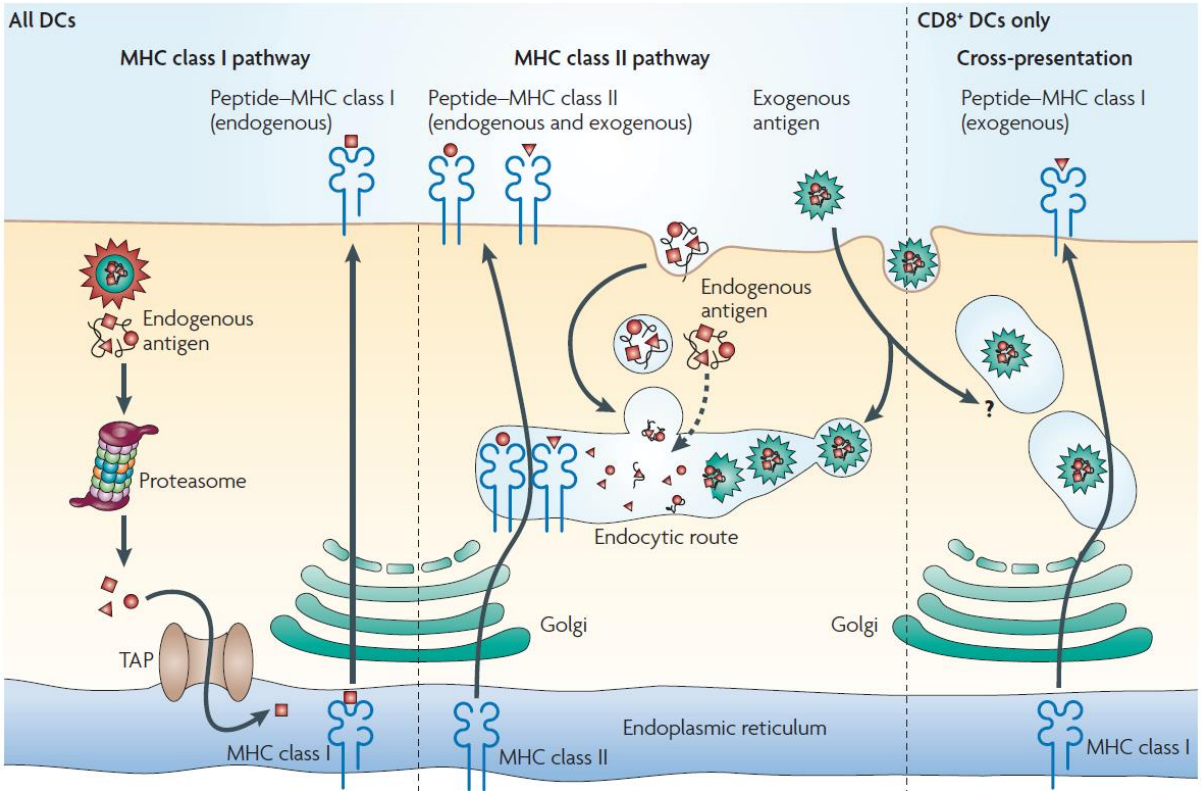

Figure 1. Antigen presentation pathways in DCs. Endogenous antigens are processed by the proteasome and loaded onto MHC-I molecules, or alternatively access the endocytic route and are presented in the context of MHC-II molecules. In turn, exogenous antigens are internalized, digested in endocytic compartments and presented via MHC-II. Moreover, DCs are able to present internalized antigens onto MHC-I molecules via cross-presentation. From ref.[63].

The functional paradigm of DC biology states that the particular DC that interacts with incoming viruses in the mucosa would be the one processing these viruses and then traveling to the lymphoid tissue. However, this classical notion should also be reviewed, as these cells might not always be the only ones presenting the captured antigens. Rather, pathogen-interacting DCs might transfer captured antigens to other APCs by several mechanisms, including secretion of extracellular vesicles bearing antigen-loaded fragments, which can even be already processed and presented in MHC molecules[64,65] (**Figure 2**). By these means, the number of DCs bearing viral-specific antigens can be increased very quickly upon infection, thus amplifying the initiation of primary adaptive immune responses[66–68]. Importantly, to induce naïve T cell stimulation *in vitro*, these extracellular vesicles require a competent activated DC to deliver the co-stimulatory signals to T cells[67]. Thus, antigen-containing extracellular vesicles do not overcome the need for a competent DC to activate naïve T cells.

Among the distinct cellular receptors expressed by DCs, the sialic acid-binding Ig-like lectin 1 (Siglec-1/CD169) is key to capture secreted extracellular vesicles (**Figure 2**). Siglec-1 interacts with extracellular vesicles via recognition of sialylated gangliosides packaged on the nanovesicle membrane[69], which has been confirmed not only *in vitro*[70,71] with extracellular vesicles derived from cell lines or primary cells, but also in murine models where Siglec-1 expressed on lymphoid tissues was required to trap extracellular vesicles *in vivo*[72]. Upon capture of extracellular vesicles on activated DCs via Siglec-1, they are trafficked along with the receptor towards a sac-like compartment invagination that is continuous with the plasma membrane and allows for extracellular vesicle retention[70,73]. This Siglec-1-positive compartment formed within activated DCs might serve as an antigen depot, controlling and sustaining adaptive immunity even if the source of antigen is not directly in contact with the DC, that still can trigger antigen-specific immune responses. These antigens could maintain immunity for prolonged periods, as it happens when DCs control endosomal acidification to preserve antigen cross-presentation over time[74]. Although mature or activated DCs markedly down-regulate their macropinocytic capacity, these cells are still able to capture, process, and present antigens internalized via endocytic receptors[75], and that may also be the case for Siglec-1 via extracellular vesicle trapping. Moreover, as DCs continue to capture and present antigens after maturation *in vivo*[76], they could also initiate responses to newly encountered antigens during the course of viral infections, a process that would be boosted by Siglec-1 expression.

The fate of trapped extracellular vesicles on DCs is diverse (**Figure 2**), as they provide a source not only for antigen cross-presentation to $CD8^+$ T cells, but also to stimulate antigen-specific naïve $CD4^+$ T cell responses *in vivo*[66,67]. This $CD4^+$ T cell stimulation can take place either by reprocessing the antigens contained in the captured extracellular vesicles or by the direct presentation of previously processed functional MHC:peptide complexes exposed in the vesicle surface[66,67]. Direct extracellular vesicle antigen presentation in the absence of lytic degradation within DCs was initially described using DC populations devoid of particular MHC-II molecules, that were still able to activate $CD4^+$ T cells because the necessary MHC-II molecules were already presenting the antigen on the extracellular vesicles trapped by those DCs[67]. Thus, extracellular vesicles displaying previously processed functional MHC-peptide complexes on their surface can be recognized, retained and directly transferred from DCs to antigen-specific $CD4^+$ T cells[67]. In turn, Siglec-1 up-regulation on activated DCs, which are competent APCs, could boost extracellular vesicle uptake and magnify antiviral immune responses.

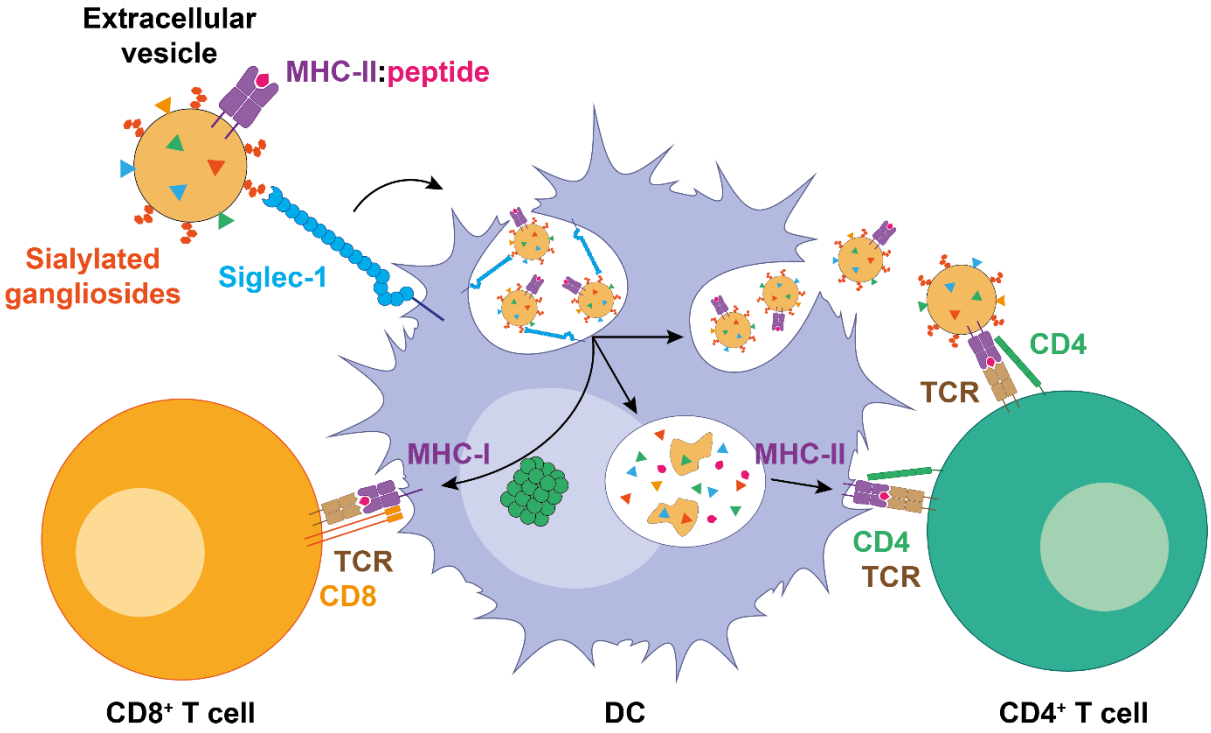

Figure 2. Presentation of extracellular vesicle-derived antigens by DCs. DCs capture extracellular vesicles bearing antigens loaded onto MHC molecules, a process mediated by Siglec-1 that directs them to a non-classical compartment that is connected to the plasma membrane. Antigens can be presented to target cells upon release of extracellular vesicles. Alternatively, they can be further processed and presented on the surface of DCs via MHC-I and MHC-II molecules. This mechanism of antigen dissemination allows presentation by DCs in the absence of a direct contact with the original antigenic source.

Taken together, DCs are key cells in defense against viruses due to their capacity to initiate both innate and adaptive immune responses. Of note, different functions are exerted by different DC subsets, as the term 'DC' englobes a heterogeneous group of cell subpopulations that share some common features but also have specific functions.

1.3 DC classification and subset functionality

DCs were first identified in human skin by Paul Langerhans, who noticed their striking 'tree-like' or 'dendritic' (from the Greek *dendron*, 'tree') morphology[77]. In 1973, Ralph Steinmann and Zanvil Cohn identified a population of phagocytic cells in murine spleen that were officially termed 'dendritic cells'[78]. Traditionally, DCs have been described as MHC-II$^+$ (HLA-DR$^+$) cells lacking other lineage-defining antigens such as CD3 (T cells), CD19 (B cells) or CD56 (natural killer cells, NK)[79]. Moreover, they were further subdivided based on their phenotypical and functional features into 'conventional' or 'classical' DCs (cDCs), and 'plasmacytoid' DCs[31,32]. In the last years, however, techniques such as single-cell transcriptomics and multiparameter cytometry have expanded our understanding in DC function and subtypes. Currently, at least seven distinct DC subpopulations have been identified: cDCs, pDCs, Axl$^+$ Siglec-6$^+$ DCs, Langerhans cells, CD14$^+$ dermal DCs, CD16$^+$ non-classical monocytes and monocyte-derived DCs (MDDCs)[31,32,80]. The main features of the different DC subsets are described in **Table 1**. However, in this thesis we will focus on cDCs, pDCs and MDDCs.

cDCs, also known as 'myeloid DCs' due to their hematopoietic origin, typically express CD11c but not CD123 and participate in antigen uptake, thus representing the classical APC described in the previous section[32]. This subset has been divided in CD141$^+$ conventional DCs 1 (cDC1) and CD1c$^+$ conventional DCs 2 (cDC2)[79,81,82]. pDCs express CD123 while lack CD11c, and are best known for their capacity to secrete type I IFNs during viral infection[83]. MDDCs differentiate *in vivo* during inflammation and are also known as 'inflammatory DCs'[31]. Noteworthy, it is possible to differentiate MDDCs *in vitro* upon monocyte treatment with granulocyte/macrophage-colony stimulating factor (GM-CSF) and interleukin-4 (IL-4)[84]. Throughout this thesis, we will refer to MDDCs and myeloid DCs as 'DCs'. Moreover, we will employ the term 'myeloid cells' as a general term to designate APCs of myeloid origin: DCs, macrophages and monocytes.

Table 1. Characteristics of the main human DC subsets. Adapted from refs.[31,32,80].

DC subpopulation		Phenotype	Location	Main function
Conventional DCs (cDCs)	**cDC1**	**Blood:** CD11c^{lo}, CD141^{+}, Clec9A^{+}, CADM1^{+}, XCR1^{+}, BTLA+, CD123^{-}. **Tissues:** CD11c^{lo}, CD141^{++}, Clec9A^{+}, CD123^{-}, CD1c$^{-/low}$, CD14^{-}.	Blood, lymph nodes, tonsils, spleen, bone marrow, skin, lung, intestine, liver.	Cross-presentation to CD8^{+} T cells.
	cDC2	**Blood:** CD11c^{+}, CD1c^{+}, CD11b^{+}, CD33^{+}, CD123^{-}. Tissues: CD11c^{+}, CD1a^{+}, CD1c^{+}, CD11b^{+}, CD141^{-}.	Blood, lymph nodes, skin, lung, intestine, liver.	Cytokine release, antigen presentation.
Plasmacytoid DCs (pDCs)		**Blood:** CD123^{hi}, BDCA-2^{hi} (Clec4C^{hi}), BDCA-4^{+} (CD304^{+}), CD11c^{-}, Axl^{-}, Siglec-6^{-}.	Blood, inflamed tissues, lymph nodes.	Type I IFN response.
Axl^{+} Siglec-6^{+} DCs ('AS' DCs)		**Blood:** CD123^{+}, Axl^{++}, Siglec-6^{+}, (CD327^{+}), Siglec-1^{+} (CD169^{+}), Siglec-2^{+} (CD22^{+}), Siglec-3^{+} (CD33^{+}), CD11c^{+}.	Blood	Cytokine secretion, antigen presentation.
Langerhans cells (LCs)		**Tissues:** Langerin^{+} (CD207^{+}), CD1a^{++}, CD1c^{lo}, CD11c^{lo}, CD39, Birbeck granules^{+}.	Skin (epidermis), lymph nodes.	Antigen presentation, epithelial integrity.
CD14^{+} dermal DCs		**Tissues:** CD14^{+}, CD1c$^{+/-}$, CD11c$^{+/-}$.	Skin	T follicular helper (Tfh) differentiation
CD16^{+} non-classical monocytes		**Blood:** CD16^{+}, CD11c^{+}, CD141^{-}, CD1c^{-}, Slan$^{+/-}$.	Blood	Endothelium 'patrolling', cytokine secretion
Monocyte-derived DCs (MDDCs)		CD11c^{+}, CD1c^{+}, CD1a^{+}, FcεR1^{+}, MR^{+} (CD206^{+}), DC-SIGN^{+} (CD209)	Inflamed tissues	Th17 polarization.

Despite the immune activity exerted by different DC subsets upon viral infection[3–5], it has been known for decades that viruses evolved different strategies to escape DC antiviral activity[85–87]. Furthermore, certain viruses exploit the migratory function of DCs as a way to colonize distant tissues, using them as 'Trojan Horses' to effectively disseminate systemically[88–97]. A key example to illustrate this viral escape mechanism is provided by Siglec-1 receptor. In spite of its proposed function as a PRR[26] and in antigen trapping via extracellular vesicle recognition[70–72], Siglec-1 has also been identified as a key player in viral subversion of DC function[98,99]. Indeed, in this thesis we focus on how two distant viruses such as HIV-1 and EBOV can hijack Siglec-1 function to gain access into DCs, which might facilitate systemic viral spread from the entry sites. In the following sections, we will introduce the general features of HIV-1 and EBOV, highlighting the proposed role for DCs and Siglec-1 in the pathogenesis of both infectious agents.

2. Human immunodeficiency virus (HIV)

The human immunodeficiency virus (HIV) is the causative agent of the acquired immunodeficiency syndrome (AIDS). HIV infects immune cells and escapes from immune responses, causing a chronic disease for which neither prophylactic vaccines or cure strategies are currently available.

2.1 History and epidemiology

In the early 1980s, a number of cases of what would be known as AIDS were detected in the United States[100]. In 1983, Françoise Barré-Sinoussi and Luc Montagnier isolated a new human retrovirus from the lymph node from an infected patient with a generalized lymphadenopathy, which was denominated 'lymphadenopathy-associated virus' (LAV)[101]. Molecular cloning of the virus[102–104] led to its full nucleotide sequencing in 1985[105–107]. The following year, the International Committee on Taxonomy of Viruses recommended the use of 'human immunodeficiency virus' or 'HIV' to refer to the novel retrovirus. Since the beginning of the pandemic, more than 70 million people have been infected by HIV, which has caused 32 million AIDS-related deaths[108]. In 2018, 37.9 million people were living with HIV worldwide, and 1.7 million new infections were reported, 61% of those in sub-Saharan Africa[108]. Currently, the African region is the most severely affected, with nearly 1 in 25 adults (3.9%) living with HIV, which accounts for more than two-thirds of people living with HIV worldwide[109].

2.2 Classification and viral structure

HIV belongs to the *Retroviridae* family, *Orthoretrovirinae* subfamily and *Lentivirus* genus, which includes the related simian immunodeficiency virus (SIV)[110]. HIV isolates are grouped in two types, HIV-1 and HIV-2. HIV-1 is the main cause of AIDS worldwide, while HIV-2 is endemic of some regions of Western and Central Africa and causes a less virulent disease as compared to HIV-1[111]. Further HIV-1 classification subdivides the virus in the groups M, N, O and P[112], and M viruses are distributed in clades A-L, where subtypes E and I are missing because they are Circulating Recombinant Forms (CRFs)[113,114].

HIV-1 genome is composed by two copies of ssRNA of approximately 9,2 kb with positive polarity[105–107]. The viral genome is flanked by two long terminal repeats (LTRs) and encodes for the structural genes *gag*, *pol* and *env*, plus a number of regulatory/accessory proteins; Vif, Vpr, Tat, Rev, Vpu and Nef[115] (**Figure 3A**). The *gag* gene encodes the p55 polyprotein, precursor of the structural capsid (p24), nucleocapsid (p7) and matrix proteins (p17). The *pol* gene encodes the reverse transcriptase, the integrase and the protease enzymes. These proteins convert viral RNA into DNA, incorporate viral DNA into the host DNA genome, and cleave both Gag and Pol precursors into their components, respectively, which are crucial steps for viral replication. The *env* gene encodes gp160, precursor of gp120 and gp41, which assemble to constitute the viral envelope glycoprotein[116].

At a structural level, mature HIV-1 virions are spherical particles with a diameter of approximately 150 nm[116,117] (**Figure 3B**). They are enveloped by a lipid membrane that derives from the host cell from which the virus buds, and also bears host-derived proteins such as MHC-I, MHC-II, the intercellular adhesion molecule-1 (ICAM-1) and co-stimulatory molecules[118]. HIV-1 surface displays glycoprotein spikes, composed by gp120-gp41 heterotrimers, which are linked through non-covalent interactions. While gp41 is a type I transmembrane protein, heavily glycosylated gp120 is the only viral protein exposed on the virion surface. Beneath the membrane, the p17 icosahedral matrix surrounds the p24 conical capsid core. The capsid contains the two copies of ssRNA genome stabilized by the p7 nucleoprotein, as well as reverse transcriptase, integrase and protease enzymes[116] (**Figure 3B**).

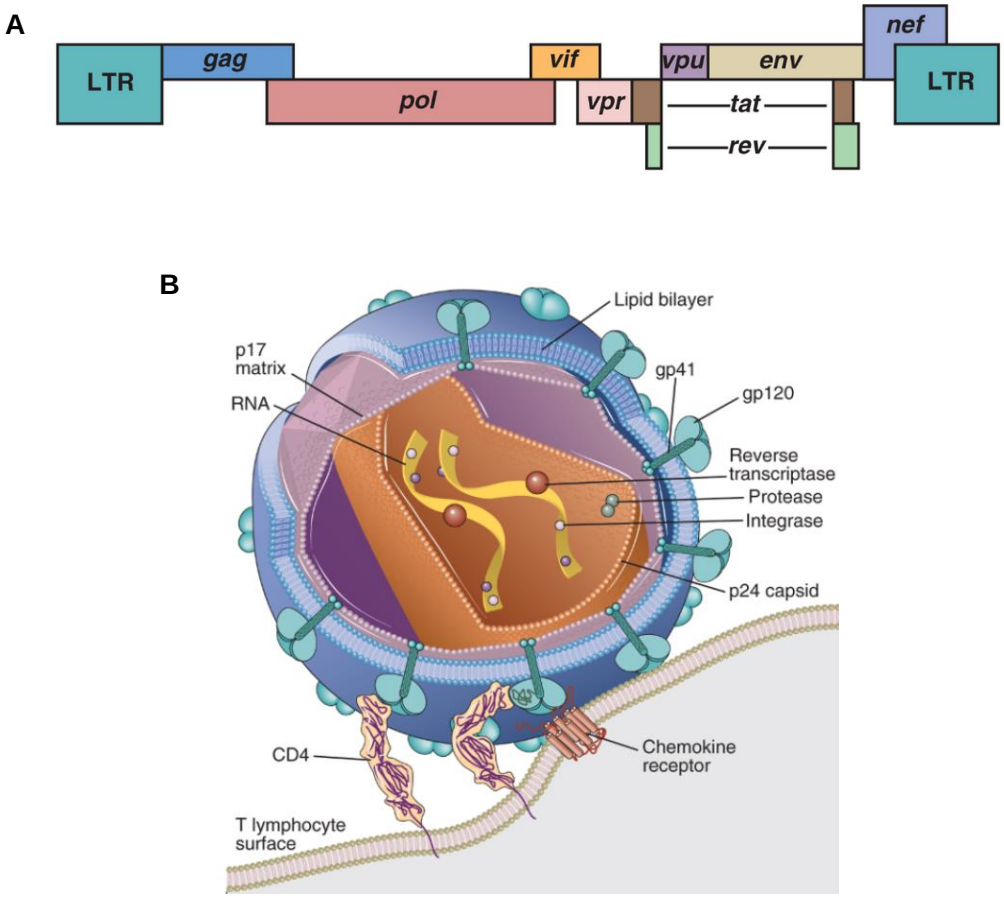

Figure 3. HIV-1 genome and viral structure. A. HIV-1 9,2 kb RNA genome encodes *gag*, *pol*, *env* and accessory viral proteins. **B.** HIV-1 virions are 150-nm spherical particles in which the viral ssRNA genome is contained within the viral capsid (p24) and the matrix (p17). A lipoprotein membrane containing host-derived and viral proteins envelops the virion, with gp120-gp41 spikes projecting from the membrane. LTR: long terminal repeat. Reverse transcriptase, integrase and protease are also contained in the virion. From ref.[119].

2.3 Tropism and replication cycle

The different proteins encoded by the HIV-1 genome have specific functions during the viral life cycle, which also relies on the target cell machinery. HIV-1 replication cycle consists of the following steps: i) viral entry, ii) reverse transcription and integration, iii) transcription and translation of viral proteins, and iv) viral assembly, budding and maturation (**Figure 4**).

Viral entry into target cells is allowed by the presence of the CD4 receptor and co-receptors CCR5 or CXCR4, which defines the R5-tropic and X4-tropic HIV-1 strains, respectively[120]. All these receptors are found in $CD4^+$ T cells, the main HIV-1 targets, but also in other immune cells such as DCs and macrophages[121]. HIV binding to CD4 and CCR5/CXCR4 is

mediated by gp120, which upon CD4 binding undergoes a conformational change that exposes the specific co-receptor-binding domain. Following CCR5/CXCR4 binding, the N-terminal fusion peptide of gp41 interacts with the cell membrane, allowing fusion between the viral and the cell membranes and subsequent cytoplasmic release of the viral capsid. Once in the cytoplasm, capsid uncoating occurs and viral genome is also released[120] (**Figure 4**).

Viral reverse transcriptase converts HIV-1 RNA genome into linear dsDNA[122], and newly synthesized DNA complexes with other proteins in the pre-integration complex (PIC)[123]. This complex is translocated into the cell nucleus and integrated within the host genome, a process that relies on the viral integrase activity[116,123] (**Figure 4**). In the absence of cell activation, proviral DNA is poorly transcribed, and the virus can remain in a latent form. Conversely, activation of the latently infected cell can induce transcription of the provirus, resuming the viral replication cycle[116]. The cell transcription and translation machinery facilitates the synthesis of viral mRNAs in a two-phase process. First, Tat and Rev are expressed, which facilitates the transcription of longer RNA transcripts. Then, mRNAs encoding Env and several accessory proteins are synthesized. Eventually, Rev mediates translocation of mRNAs encoding structural proteins from the nucleus to the cytoplasm, where the translation machinery allows the synthesis of structural viral proteins[116,123,124] (**Figure 4**).

Proteins encoded by *gag* and *pol* assembly at the plasma membrane to form the nucleus of the nascent HIV-1 particle, while *env* products form the glycoprotein spikes of the envelope[116] (**Figure 4**). These precursor molecules are cleaved by the viral protease in a maturation step that is necessary step for the infectivity of new virions[125]. The assembled viral proteins, together with two viral ssRNA strands associated to replication enzymes, bud from the infected cell from specialized cholesterol-enriched domains of the plasma membrane, incorporating glycosphingolipids such as gangliosides and host proteins[126]. Release of the newly synthesized viral particle is dependent on the host endosomal sorting complexes required for transport (ESCRT)[123,125]. Once released, the maturation process continues and gives rise to fully infectious new virions[125] (**Figure 4**). Of note, expression of the Gag polyprotein alone results in membrane binding, assembly and release of spherical particles that bud from the producing cell[127]. This allows for the generation of virus-like particles (VLPs), which can contain a reporter protein such as green fluorescent protein (GFP) fused to Gag and be used as tools for the study of different virological processes.

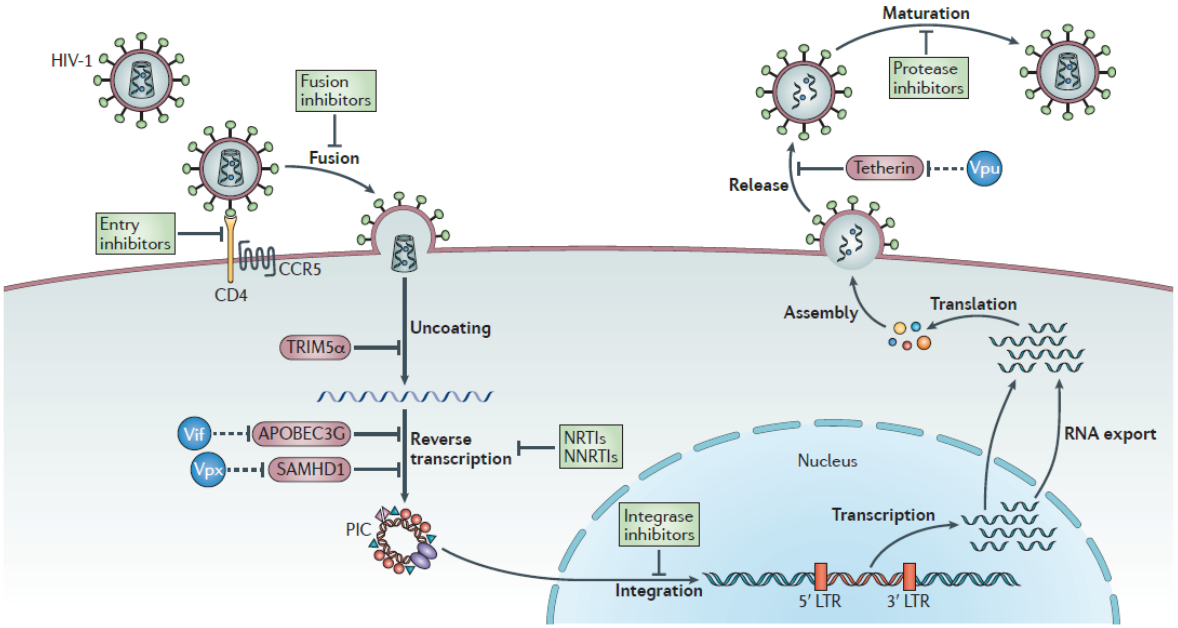

Figure 4. HIV-1 replication cycle. Binding of HIV-1 gp120 to CD4 and CCR5 (or CXCR4) induces viral fusion with the plasma membrane of the target cells. In the cytoplasm, viral RNA is converted into dsDNA by the viral reverse transcriptase. Complexed with host proteins, viral DNA enters the nucleus and is inserted within the host genome, a process driven by viral integrase. Viral mRNAs are transcribed upon cell activation, and viral proteins are synthesized in the cytoplasm. Viral proteins assemble under the plasma membrane, and newly synthesized virions bud incorporating a host-derived lipid membrane. Maturation driven by viral protease is essential for the infectivity of newly synthesized virions. From ref.[128].

2.4 Natural course of HIV-1 infection and treatment

As highlighted in the previous section, HIV-1 requires the host cell metabolism to replicate, but it depends also on a biological environment to persist, as virions are labile and cannot survive long outside biological fluids. HIV-1 can be acquired following tissue disruption with contaminated objects such as needles or sharp tools. However, the main route of HIV-1 transmission is via direct exposition of mucosae or disrupted skin to infected body fluids such as blood, breast milk, semen and vaginal secretions[129]. Currently, sexual transmission is the most common HIV-1 acquisition route worldwide[108]. Following viral exposure, the natural course of HIV-1 infection includes the following stages: primary infection, acute phase, clinical latency and AIDS (**Figure 5**).

The primary infection (1-2 weeks post-exposure) that follows HIV-1 sexual transmission is characterized by infection of permissive cells in the mucosa, such as $CD4^+$ T cells, myeloid DCs, Langerhans cells and macrophages[130]. In order to establish a systemic

infection, the small founder population of viruses infecting a limited amount of cells at the entry sites must expand via lymphatic drainage to establish a self-propagating infection in the genital draining lymph nodes[131,132]. Given their migratory capacity, DCs are thought to play an important role in this initial dissemination of the virus[89,132–134]. The primary infection is characterized by the lack of detectable plasma viremia and clinical symptomatology[135].

During the acute phase of HIV-1 infection (3-12 weeks post-exposure) viral RNA is detectable in blood[136]. Plasma viremia reaches a peak that approximately coincides with the phase of antibody seroconversion[136–138], and viremia subsequently decreases due to the generation of adaptive immune responses that partially control viral replication[139–144]. In addition, this phase is characterized by a reduction in the number of $CD4^+$ T cells in blood, that are partially recovered upon the decrease of plasma viral load[116,145]. Gastrointestinal $CD4^+$ T cells are also importantly reduced, but no recovery is observed following the decrease in plasma viremia[146] (**Figure 5**). As a consequence of destruction of the gut-associated lymphoid tissue (GALT), the intestinal barrier is compromised and bacteria are translocated to the blood[147,148]. At a clinical level, during this phase a flu-like or mononucleosis-like condition can occur in some individuals[139].

Acute phase is followed by a period of clinical latency (1-10 years post-exposure) characterized by the absence of symptomatology[116,135]. During this stage, that reflects the antiviral action exerted by innate and adaptive immune responses, $CD4^+$ T cell counts gradually decrease, while viral load progressively augments[149] (**Figure 5**). As a consequence of viral replication and the chronic activation of immune cells, this stage of the disease is characterized by the progressive destruction of the lymphoid tissue architecture[116].

When $CD4^+$ T cell counts fall below 200 cells/µl, the risk of opportunistic infections and tumours increases due to immune impairment[150,151]. During this AIDS phase, the number of $CD4^+$ T cells further decreases, while HIV-1 viremia increases as a consequence of the loss of immune control over the virus[116,135]. Eventually, immune deficiency leads to the death of the patient, with a mean survival of 11 years after infection[116] (**Figure 5**).

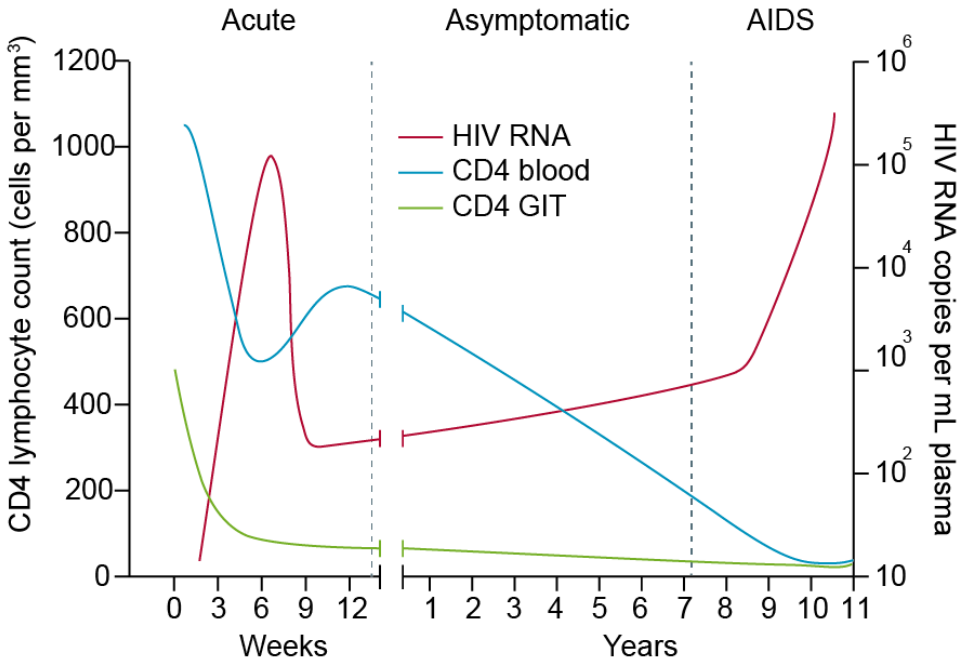

Figure 5. Natural course of HIV-1 infection. Following primary infection, the acute HIV-1-associated disease is characterized by a peak viremia and a decrease in $CD4^+$ T cell counts in blood and in the gastrointestinal tract (GIT). Adaptive immune responses reduce HIV-1 plasma levels while partially recover blood $CD4^+$ T cells, which progressively decrease along the chronic phase of the disease. When blood $CD4^+$ T cell counts fall below the threshold of 200 cells/μl the AIDS phase begins, in which recurrent opportunistic diseases appear and eventually causes the death of the patient. From ref.[146].

The implementation of antiretroviral treatment (ART) has greatly reduced morbidity and mortality associated to HIV-1 infection[128,152–154], turning a previously fatal condition to a manageable chronic disease with little impact on life expectancy[128]. In the late 1980s and early 1990s, the antiretroviral azidothymidine (AZT, Zidovudine) demonstrated to reduce HIV-1-associated morbi-mortality[155], and since then the efficacy of ART has been importantly improved, with a progressive reduction of ART-associated adverse effects. Today, the combination of nucleoside and non-nucleoside reverse transcriptase inhibitors with other drugs such as protease and integrase inhibitors effectively suppresses plasma viremia of treated patients below detectable levels (< 50 RNA copies/ml) and recuperates $CD4^+$ T cell counts. However, ART interruption invariably leads to a rebound of plasma viremia, and thus ART must be maintained for life.

Aside from its beneficial role in HIV-1 treatment, ART has been proposed as a pre-exposure prophylactic strategy to prevent new infections, especially those transmitted via

sexual intercourse through topic ART administration in microbicides[156]. These strategies effectively block HIV-1 productive replication at the entry sites. However, HIV-1 takes advantage of the migration capacity of DCs to reach the lymph nodes, where ART might be less efficient. Thus, understanding the interactions of these cells with HIV-1, especially at critical locations for HIV-1 acquisition such as the reproductive tract, is essential to understand the how HIV-1 subverts DC function and also to design new strategies to combat HIV-1 transmission.

2.5 The role of DCs in HIV-1 pathogenesis

In the early 1990s, it was observed that DCs can transmit a vigorous HIV-1 infection to target $CD4^+$ T cells in co-culture, a mechanism of viral transmission that was much more effective than infection by cell-free virions[88]. In agreement with these data, mathematical models predict that in lymphoid tissues, approximately 10% of new infections are caused by cell-free virions, while the remaining 90% is mediated through cell-to-cell transmission[157]. However, following the initial observations, the mechanism behind DC-mediated cell-to-cell transmission remained elusive for some time, with two complementary models being assessed in parallel. On the one hand, work initiated by Knight and Patterson studied the capacity of productively infected DCs to transfer newly synthesized viral particles to bystander $CD4^+$ T cells[158]. And on the other hand, pioneering work by Cameron and Steinman identified a mechanism by which DCs can transmit HIV-1 to target $CD4^+$ T cells in the absence of productive infection[88] (**Figure 6**).

DCs express CD4 and HIV-1 co-receptors, especially CCR5[159–161], which makes these cells susceptible to productive HIV-1 infection or infection in *cis*[158,162,163]. Infected DCs and also Langerhans cells can transmit *de novo* synthesized viral particles to bystander $CD4^+$ T cells upon the establishment of cell-to-cell contacts[164,165] (**Figure 6A**). However, this mode of HIV-1 transmission is limited due to their lower infectivity rates of DCs as compared to $CD4^+$ T cells[164,166–169]. This is partially explained by the lower expression of HIV-1 receptor and co-receptors on DCs[170] and by the capacity of these cells to readily degrade incoming viral particles[171,172]. Moreover, DCs express restriction factors that interfere with viral productive replication, including the SAM and HD domain-containing protein 1 (SAMHD1) and the apolipoprotein B mRNA editing enzyme catalytic subunit 3G (APOBEC3G), which deplete the pool of cellular deoxynucleotide triphosphate necessary for reverse transcription and hypermutate nascent viral genomes, respectively[173–178].

Aside from viral transfer of *de novo* synthesized particles, DCs transmit HIV-1 to target $CD4^+$ T cells in the absence of productive replication, a mechanism known as *trans*-infection[88,179] (**Figure 6B**). Initially, HIV-1 *trans*-infection was attributed to the capacity of the CLR DC-SIGN to bind viral envelope glycoproteins[179]. However, a number of studies indicated that other receptors were involved in this process of cell-to-cell viral transfer[161,180–186]. For example, anti-DC-SIGN antibodies did not have a blocking effect on viral *trans*-infection[182]. In addition, DC maturation greatly increased their *trans*-infection capacity although it decreased DC-SIGN expression levels[186]. Almost a decade ago, two independent groups demonstrated that DC-mediated HIV-1 *trans*-infection relies on the I-type lectin Siglec-1[70,187], which binds sialylated gangliosides on the viral membrane and whose expression is enhanced upon cell activation (**Figure 6B**).

HIV-1 *trans*-infection is a dynamic process that involves viral attachment or binding, internalization within a non-classical compartment connected to the extracellular space, and viral release in the cellular contact between a DC and a target $CD4^+$ T cell, which is termed 'infectious synapse'[166,188,189] (**Figure 6B**). Following binding, intact HIV-1 particles are transported and concentrate at the surface of DCs[189,190], leading to the formation of a non-classical and non-acidic endosomal compartment enriched in tetraspanins, MHC-II and Siglec-1[188,191,192]. Although this virus-containing compartment (VCC) is connected to the extracellular milieu[189–191], internalized HIV-1 particles remain inaccessible to heavy molecules such as neutralizing antibodies[193]. The original function of this compartment is related to a mechanism of antigen dissemination, as it also accumulates antigen-containing extracellular vesicles that are able to prime adaptive immune responses[67,73]. Thus, it appears that HIV-1 has evolved a strategy to subvert Siglec-1 immune function to gain access to target $CD4^+$ T cells.

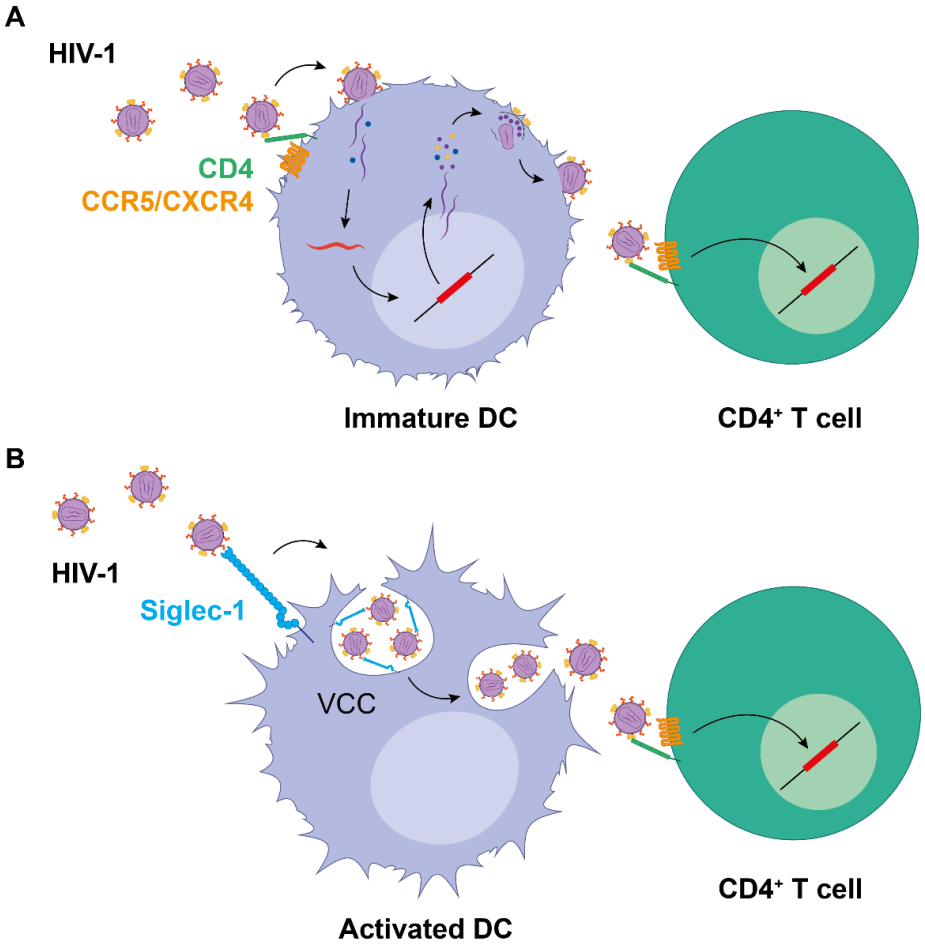

Figure 6. Routes of HIV-1 transmission mediated by DCs. A. DCs are susceptible to productive HIV-1 infection or *cis*-infection due to the expression of HIV-1 receptor and co-receptors such as CCR5. *De novo* synthesized HIV-1 particles infect CD4⁺ T cells upon the formation of DC:CD4⁺ T cell contacts. **B.** Activated DCs mediate viral transmission to target CD4⁺ T cells via *trans*-infection, a mechanism that relies on Siglec-1-mediated capture of HIV-1 particles, which are stored and transmitted to CD4⁺ T cells through an infectious synapse. VCC: virus-containing compartment.

Overall, two distinct routes of HIV-1 transmission to CD4⁺ T cells have been described, involving either productive DC infection (*cis*-infection) or viral capture by DCs and transmission in the absence of synthesis of new viral particles (*trans*-infection). A model has been proposed in which viral transmission can occur in a two-phase process, with viral *trans*-infection within the first 24 hours post-HIV-1 exposure followed by transmission of *de novo* synthesized particles at later timepoints (72 hours post-HIV-1 exposure)[171]. However, it has also been reported that the transmission mode importantly depends on the maturation status of the cell. Indeed, mature DCs are 10 to 100-fold less infective than iDCs[168,194,195] while they have a superior *trans*-infection capacity[186], which is explained by the higher Siglec-1 expression in these cells[70].

2.6 Siglec-1 in HIV-1 *trans*-infection

Siglec-1, also termed sialoadhesin (Sn) or CD169, is the central molecule of DC-mediated HIV-1 *trans*-infection[70,187]. As an I-type lectin, it is composed by different Ig-like domains (i.e. two β-sheets cross-linked by a disulphide bond) that are classified in three 'sets': V-set, C1-set and C2-set[196]. Siglec-1 displays an N-terminal V-set domain that binds sialic acid and 16 C2-set Ig-like domains, all of them extracellular[26,197,198] (**Figure 7**). Among Siglecs, the most similar members to Siglec-1 are Siglec-5 and Siglec-14, which share 100% homology in the V-set domain. Siglec-1 is also conserved among different mammalian species, with human Siglec-1 sharing an overall 72% homology its murine counterpart. Moreover, homology with murine Siglec-1 is complete in the N-terminal amino acids critical for sialic acid binding[197,199]. These critical amino acids include an arginine at position 116 (R116) as well as tryptophans 21 and 125 (Q21, Q125)[197,199,200].

Siglec-1 binds N-acetylneraminic acid (Neu5Ac) in both N- and O-glycans and with a preference for an α2-3 linkage[201]. These sugars are present in different macromolecules such as gangliosides, which are glycosphingolipids composed by a lipidic ceramide portion and a variable glycan polar head group that might contain sialic acid[202]. Importantly, these gangliosides are present on the plasma membrane on cholesterol-enriched domains from which multiple enveloped viruses bud, including HIV-1[203–206]. Hence, Siglec-1 mediates HIV-1 binding via recognition of sialylated gangliosides anchored to the viral membrane, in particular sialyllactose-containing gangliosides such as GM1a and GM3[70,187,207,208] (**Figure 7**).

Although Siglec-1 affinity for sialylated ligands is in the micromolar range, high-avidity binding can be achieved upon clustering of thousands of gangliosides in the viral membrane with their receptors on the cellular membrane[26,209,210]. Moreover, as Siglec-1 contains 16 Ig-like C2-type extracellular domains that separate the ligand-binding site from the cell surface, it is available for interaction with external ligands and not bound in *cis* to cell-surface molecules, what usually happens with shorter Siglecs that are also expressed by DCs[26,197,201,211]. The cytoplasmic tail of Siglec-1 is also particular, as in contrast to almost all other Siglecs, it is a short domain without signaling modules such as the inhibitory tyrosine-based motif (ITIM) present in other family members[26].

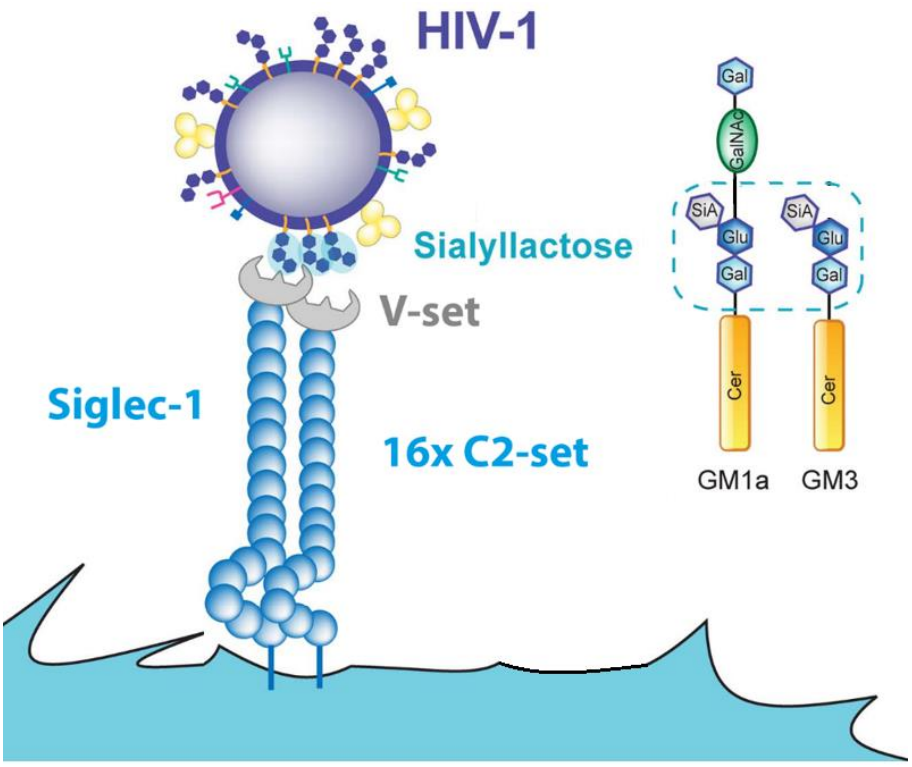

Figure 7. Siglec-1 structure and HIV-1 recognition. Siglec-1 includes 17 domains, an N-terminal V-set domain with sialic acid binding capacity, and 16 C2-set Ig-like domains that project the V-set from the cell surface. HIV-1 is recognized by Siglec-1, in particular through binding of sialyllactose-containing gangliosides such as GM1a and GM3 that are present on the viral membrane. Cer: ceramide; Gal: galactose; GalNAc: N-acetylgalactosamine; SiA: sialic acid; Glu: glucose. Adapted from ref.[98].

Siglec-1 is expressed by myeloid cells such as DCs, macrophages and monocytes[70,187,192,212,213], and its expression *in vivo* is associated with an immune activation status, like the one found during autoimmune diseases and viral infections[201,214–217]. In particular, Siglec-1 is up-regulated in environments in which type I IFNs are present[214,215,217]. *In vitro*, Siglec-1 expression is induced on DCs, monocytes and macrophages by IFNα[187,192,213,218], and thus it is considered an IFN-stimulated gene. Nonetheless, it can also be up-regulated in different myeloid cells upon exposure to rhinovirus[219] and following treatment with tumour necrosis factor (TNF) and LPS[70,216].

In line with their capacity to up-regulate Siglec-1 on DCs, stimulation with either IFNα or LPS boosts the capacity of DCs to mediate HIV-1 *trans*-infection[70,186,187]. Importantly, both immune activating factors are present during the course of HIV-1 infection, suggesting a role for Siglec-1 in HIV-1 cell-to-cell transmission *in vivo*. IFNα levels are potently boosted during acute infection, and sustained – although to a lower extent – throughout the chronic stage, which is characterized by a persistent immune activation associated with poor

prognosis[35,147,220–223]. Several cell types have been identified as the sources of IFNα production during the course of HIV-1 infection, and therefore all of them contribute to Siglec-1 induction. The capacity of pDCs to secrete IFNα in response to HIV-1 sensing has been demonstrated *in vitro*[36,37,224–226] and *in vivo*[227–229], both during the acute and chronic phases of the disease[35,227,228]. Noteworthy, pDC activation in response to HIV-1 sensing induces IFNα secretion through TLR7 and TLR9 signalling[34–37] and maturation of bystander DCs[230]. However, whether secretion of this cytokine by pDCs can directly up-regulate Siglec-1 expression on DCs remains unknown.

In addition to pDCs, myeloid DCs also secrete type I IFNs, although this is mostly and indirectly triggered by immune activating signals present throughout the course of HIV-1 infection, which can induce the expression of IFN-stimulated genes on DCs in an autocrine manner[231–235]. One of those factors is bacterial LPS, which is increased in the plasma of HIV-1-infected individuals due to the bacterial translocation that takes place in the GALT as a consequence of the gut epithelial barrier disruption occurring early after HIV-1 infection[147,148,236]. Yet, the contribution of autocrine type I IFNs in Siglec-1 up-regulation on DCs upon LPS treatment has not been assessed yet.

The role of Siglec-1 in HIV-1 *trans*-infection has been well-studied using *in vitro* settings, and a report also revealed that this mechanism mediates dissemination of a murine retrovirus and HIV-1 in secondary lymphoid tissues of living mice[237]. However, an important question is in which anatomical locations Siglec-1 could mediate HIV-1 transmission in *trans* during viral infection in humans. As this receptor is an IFN-stimulated gene whose expression on DCs is importantly up-regulated by IFNα and also by bacterial LPS[70,187], HIV-1 *trans*-infection might be relevant for viral dissemination in anatomical tissues where these immune activation factors are present.

HIV-1 is mostly acquired by sexual transmission[108], and in the cervical mucosa there are two major sources of antiviral type I IFN responses after retroviral infection: resident myeloid cells[238] and pDCs, which are soon recruited to the cervix along with $CD4^+$ T cells[239,240]. Although increased antiviral IFNα secretion could limit initial viral infection, it could promote viral capture on cervical myeloid cells via Siglec-1 induction as well. Several cervical DC subtypes have been found to mediate HIV-1 *trans*-infection *ex vivo*[241–244]. However, whether DCs at the cervix express Siglec-1 and can mediate *trans*-infection via this receptor remains unexplored. DCs transfer viruses to bystander $CD4^+$ T cells in the mucosa, but also favor a systemic viral dissemination upon DC migration to lymphoid

tissues (**Figure 8**). Indeed, DCs bearing retroviruses are found in the draining lymph nodes of distinct animal models as soon as 24 h after vaginal challenge[89,132–134], and these findings originally led to formulate the Trojan Horse hypothesis, which states that DCs can serve as vehicles transporting the virus from the entry sites to distant tissues[88,90]. Thus, it would be of great interest to assess the contribution of Siglec-1 in viral cell-to-cell transmission in this critical anatomical compartment for HIV-1 acquisition.

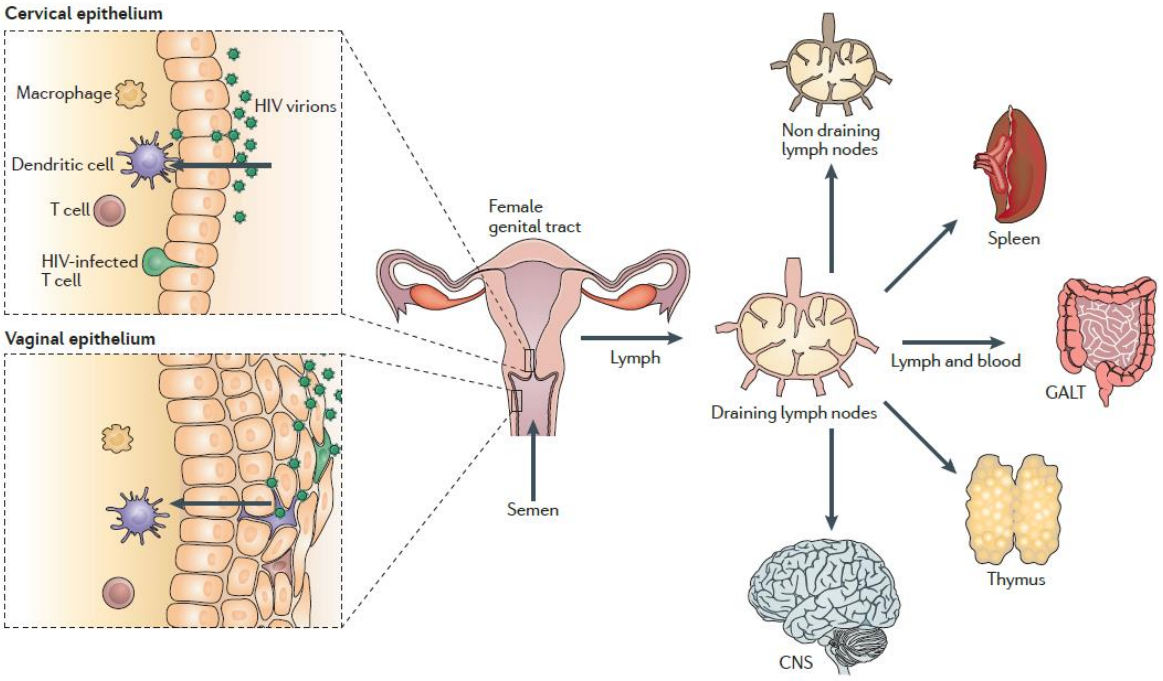

Figure 8. HIV-1 dissemination from the female reproductive tract. DCs participate in systemic HIV-1 dissemination, transporting the virus from entry sites to distant tissues. DCs are found in the cervicovaginal mucosa, where they are among the first cells to encounter HIV-1. Of note, two different types of mucosal surfaces are found in the female reproductive tract. The mucosa of vagina and ectocervix consists of a stratified epithelial layer and the underlying submucosa, while the submucosa of endocervix and uterus is lined by a monolayer of columnar epithelium. Upon interaction with HIV-1, DCs migrate to the genital draining lymph nodes, where the establishment of a self-propagating infection might spread the infection to other organs and tissues. From ref.[245].

Aside from HIV-1, other viruses also exploit DCs as Trojan Horses for viral dissemination from the entry sites[91–97,246]. In particular, this mechanism of viral spread might play a crucial role in the dissemination of EBOV filovirus, which employs DCs to spread systemically[91].

3. Ebola and Marburg filoviruses

Filoviruses such as EBOV and MARV viruses are the aetiological agents of filovirus disease (FVD), a severe acute condition that is associated with high percentages of lethality and for which no approved specific treatments are currently available.

3.1 History and epidemiology

In 1967, laboratory workers from Marburg and Frankfurt were infected while manipulating tissues from *Cercopithecus aethiops* monkeys imported from Uganda[247,248]. The cause of infection was a novel virus, which was named 'Marburg virus' and is now classified as a filovirus[249]. In 1976, an outbreak causing acute hemorrhagic fever occurred in Zaire, now the Democratic Republic of the Congo, and the cause was attributed to another filovirus, named 'Ebola virus' after the river Ebola in the north of the country[250]. The same year, a second outbreak burst in Sudan, and the new pathogen was named 'Sudan virus'[251]. Subsequent filoviral outbreaks occurred in Africa and occasionally in other geographical localizations, which led to the discovery of additional filoviruses, such as Reston virus, Taï Forest virus and Bundibugyo virus[248].

Until 2014, there had been 22 epidemics caused by filoviruses[252], with mortality rates of EBOV and Sudan viruses, the most lethal species, ranging between 40-90%[248]. During 2014-2016, the largest EBOV outbreak ever recorded occurred in West-Africa, with 28,616 infected patients and 11,310 reported deaths[253]. Since August 2018, an ongoing EBOV outbreak affects the Democratic Republic of the Congo, with 3313 reported cases and 2203 deaths[254].

3.2 Classification and viral structure

The *Filoviridae* family of the order *Mononegavirales* is composed by the genus *Ebolavirus*, *Marburgvirus* and *Cuevavirus*, each divided in different species[249]. The genus *Ebolavirus* includes five species: *Zaire ebolavirus* (Ebola virus, EBOV), *Sudan ebolavirus* (Sudan virus, SUDV), *Reston ebolavirus* (Reston virus, RESTV), *Taï Forest ebolavirus* (Taï Forest virus, TAFV) and *Bundibugyo ebolavirus* (Bundibugyo virus, BDBV). In addition, there are multiple EBOV isolates, such as EBOV-Mayinga, the strain derived from the 1976 outbreak, and EBOV-Makona, from West-Africa 2014-2016[252]. The genus *Marburgvirus* is composed by a single species, *Marburg marburgvirus*, which includes the two closely related virus types Marburg virus (MARV) and Ravn virus (RAVV). Finally, the recently

discovered genus *Cuevavirus* contains a single species, *Lloviu cuevavirus* (Lloviu virus, LLOV). Among these species, EBOV, SUDV, TAFV, BDBV, MARV and RAVV are pathogenic in humans[249].

EBOV genome is a non-segmented ssRNA chain of approximately 19 kb and negative polarity. The genome includes 3'- leader and 5'-trailer sequences, and each particular gene is flanked by 3' and 5' untranslated regions (UTRs). Viral genome encodes 7 viral proteins: NP, VP35, VP40, GP, VP30, VP24 and L[248,252,255,256] (**Figure 9A**). The nucleoprotein (NP) encapsidates the genome, protecting RNA from degradation. Viral protein 40 (VP40) is the structural monomer of the viral matrix[257]. L gene encodes the RNA-dependent RNA polymerase necessary for replication of the viral genome, with viral protein 35 (VP35) acting as a cofactor[258]. Viral protein 30 (VP30) functions as a transcriptional activator that supports primary transcription and also RNA editing, while viral protein 24 (VP24) participates in nucleocapsid assembly and might also be a minor matrix protein. The gene encoding the viral glycoprotein (GP) encodes actually three different proteins[255,259,260]. The primary product of this gene is soluble GP (sGP), but RNA editing leads to expression of a second small soluble glycoprotein (ssGP) or the type I transmembrane protein that mediates recognition of viral receptor and fusion with target cells. Initially expressed as GP0, this protein is cleaved by a cellular protease to give rise to the heavily glycosylated GP1 and the transmembrane protein GP2, which function similarly to gp120 and gp41 in HIV-1, respectively[261]. Aside from the roles previously indicated, VP35 and VP24 counteract host production and signalling of type I IFNs[262,263].

Structurally, EBOV virions display a uniform diameter of around 80 nm, but greatly vary in length (up to 14 μm) and in shape, with the filamentous form being the most characteristic[252,255] (**Figure 9B**). Filoviruses are enveloped viruses with a lipoprotein membrane derived from the productively infected cell, and GP is the only viral protein exposed on the virion surface, where it forms an homotrimer of GP1/GP2 dimers[252,255]. The VP40 matrix protein is in contact with the membrane and forms the filamentous structure of viral particles[257]. Inside the matrix, the viral core is composed by the viral RNA and the NP nucleocapsid, along with VP35, VP30 and L[252,255] (**Figure 9B**).

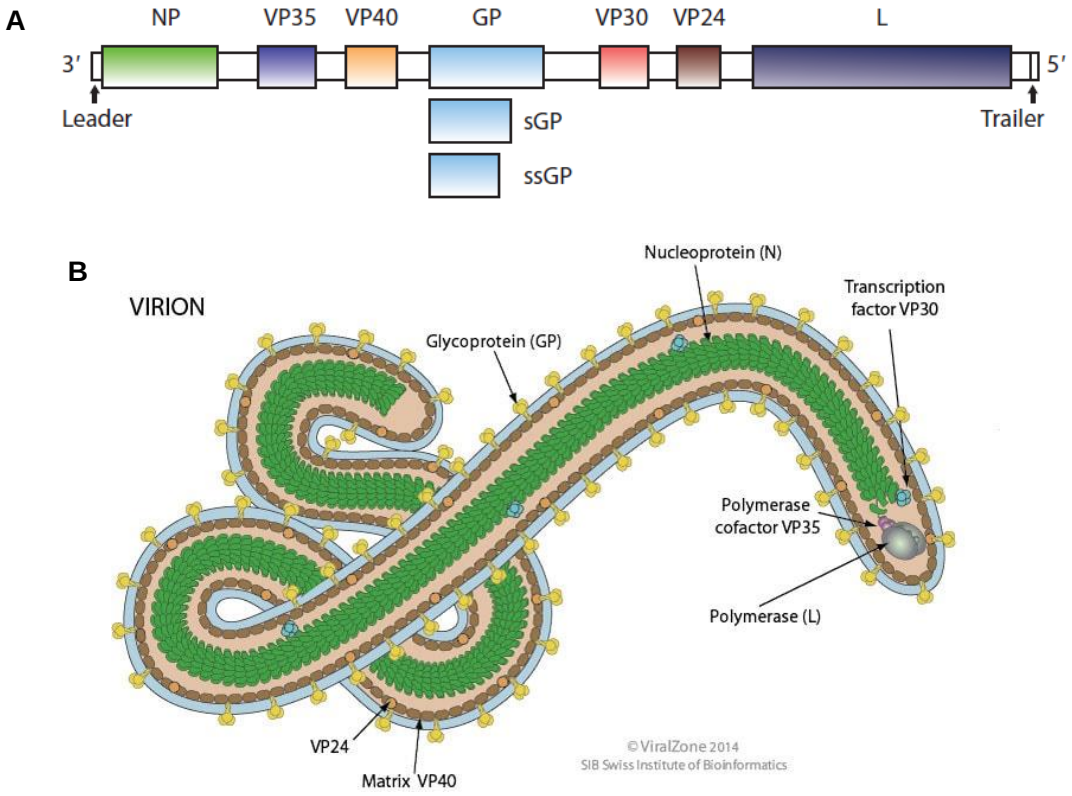

Figure 9. EBOV genome and viral structure. A. EBOV ssRNA genome encodes seven viral proteins, with three alternative forms of the glycoprotein. From ref.[252]. **B.** EBOV enveloped virions are filamentous particles with a diameter of 80 nm and variable length containing different structural proteins and enzymes. From ref.[264].

3.3 Tropism and replication cycle

Filoviruses display a broad cell tropism, including DCs, macrophages, monocytes, hepatocytes, adrenocortical cells, endothelial cells and fibroblasts[91,265,266]. The process of viral entry into these cells is complex, perhaps as complex as any mechanism of viral entry identified to date, involving a number of viral and host factors interactions[267,268]. In this section, we will describe the steps of viral entry into filoviral cellular targets, focusing on what is currently known about viral entry into myeloid cells.

Initial EBOV attachment to the cell surface is mediated by particular host receptors that recognize the viral glycoprotein or specific lipids present on the viral membrane. EBOV glycoprotein is recognized by different host cell receptors (**Figure 10A**), which were first identified as attachment factors for other viruses. Almost two decades ago, landmark studies in the HIV-1 field indicated that several CLRs expressed on myeloid cells - such as DC-SIGN (CD209) or L-SIGN (CD209L) - specifically interacted with glycans present on the HIV-1 glycoprotein[269]. Although these CLRs are pathogen recognition receptors that

should favour antigen presentation, in the case of HIV-1 interaction, they were also found to promote viral uptake on DCs, and subsequent viral dispersion that leads to productive infection of bystander target cells[179,270]. Similarly to HIV-1, EBOV binds to mannose-specific CLRs like DC-SIGN (**Figure 10A, first panel**) through the recognition of equivalent glycans exposed on filoviral glycoproteins[271]. In addition, blockade of LSECtin (**Figure 10A, first panel**) partially reduced EBOV glycoprotein binding to DCs[272], highlighting the need to further explore its role in viral attachment and entry. Aside from CLRs, several glycosaminoglycans interact with EBOV and MARV glycoproteins, as is the case of heparin (**Figure 10A, first panel**), heparan sulphate or chondroitin sulphate[273–275]. Since several myeloid cells express heparan sulphate and chondroitin sulphate[276–279] these are good candidates to mediate viral attachment into myeloid cells. Of note, the role of heparin has already been tested, but it has only shown a modest impact on EBOV and MARV entry into macrophages[273].

Beyond the viral glycoproteins exposed on their surface, EBOV and MARV viruses also drag on their envelope different lipid molecules that serve as ligands for particular surface receptors on target cells. In particular, phosphatidylserine has been identified as a viral component mediating viral attachment to myeloid cells[280] (**Figure 10A, second panel**). This lipid is enriched in the cellular membranes of dying cells, and is also incorporated on apoptotic bodies, where it acts as an 'eat-me' signal for phagocytes[281]. Myeloid cells can therefore bind and internalize apoptotic bodies through particular receptors that recognize phosphatidylserine, and this mechanism of apoptotic clearance is exploited by EBOV[280].

At least two families of phosphatidylserine recognizing-receptors have been implicated on this mechanism of EBOV attachment: the T-cell immunoglobulin and mucin domain (TIM) and the Tyro-Axl-Mer (TAM) group of receptors, as reviewed in ref.[280]. Although the overall role of phosphatidylserine interacting-receptors on EBOV entry has been confirmed in primary myeloid cells[282], the relative contribution of each family and their particular members on distinct myeloid cells is not clearly delineated yet. TIM-1 and TIM-4 mediate viral attachment and entry into several non-phagocytic cell lines[282–284]. However, TIM-1 is dispensable for viral entry into macrophages[285]. Thus, given that phosphatidylserine modulates viral interaction with myeloid cells, future works should address the role of TIM-4 receptor (**Figure 10A, second panel**). Among TAM receptors, Tyro3, Axl and Mer contribute to EBOV attachment and entry into several non-phagocytic cell types[286,287]. Mer also mediates viral entry into macrophages (**Figure 10A, second panel**), although Axl does not[285]. Overall, evidence gathered so far indicates that Mer and possibly TIM-4 are the

phosphatidylserine interacting-receptors with greater contribution to viral attachment to myeloid cells. Intriguingly, both EBOV and MARV incorporate sialylated ganglioside GM1a when they bud from producing cells[288]. Thus, Siglec-1 might acts as an attachment factor mediating viral entry into these cells through a glycoprotein-independent mechanism as well.

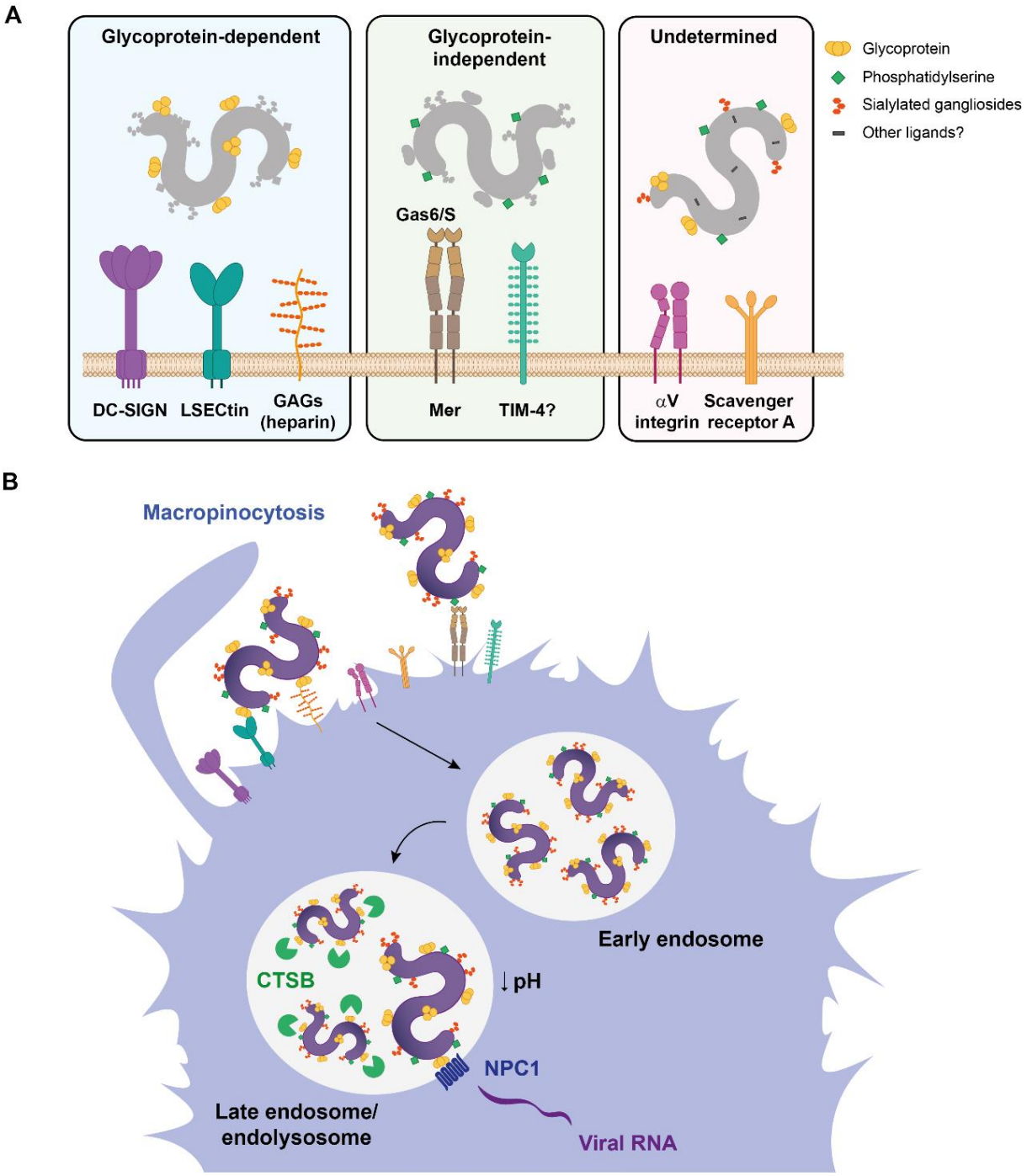

Figure 10. Viral entry into myeloid cells. A. Viral attachment via glycoprotein-dependent, glycoprotein-independent or unidentified mechanisms. **B**. Viral internalization begins when viruses enter early endosomes through macropinocytosis. Viral cargo of early endosomes is

transferred to late endosomes, where cathepsin B cleaves viral glycoprotein to allow for NPC1 interaction and viral RNA entry into the cytoplasm. CTSB: cathepsin B; NPC1: Niemann-Pick receptor C1. Adapted from ref.[289].

Other receptors have also been implicated in EBOV entry into myeloid cells, but their ligands on the viral particle remain unidentified. Such is the case of integrin alpha V and the scavenger receptor A, which facilitate viral entry into macrophages[285,290] (**Figure 10A, third panel**). Key comprehensive knowledge is still missing, and given the complexity of EBOV attachment, extensive research is needed to decipher the distinct and alternative receptors that facilitate viral attachment to myeloid cells.

All the distinct viral attachment mechanisms discussed (**Figure 10A**) are key to trigger a series of post-attachment steps that culminate with viral cytoplasmic entry (**Figure 10B**). Once attached to the cell surface, EBOV enters myeloid cells through a macropinocytic mechanism (**Figure 10B**) that relies on dynamin and the signalling molecules PIKfyve and AMP-activated protein kinase (AMPK)[291–293]. Upon internalization, viruses enter early endosomes, whose maturation leads EBOV to accumulate into LAMP1 positive late endosomes or endolysosomes[294–296] (**Figure 10B**). Maturation of EBOV-containing endosomes is mediated by the homotypic fusion and vacuole protein-sorting (HOPS) complex[297] and TPC 1 and 2[298] (**Figure 10B**). Viral cytoplasmic entry from late endosomes is favoured by the low pH of these compartments[299,300], which allows for optimal activity of cathepsins, the cysteine-proteases that cleave the viral glycoproteins (**Figure 10B**). Of note, only cathepsin B (CTSB) is necessary for EBOV entry into DCs[301], but requirements in other myeloid cells remain unknown. Once cleaved by cathepsins (**Figure 10B**), viral glycoproteins interact with the endosomal Niemann-Pick receptor C1 (NPC1) that is required for filoviral entry into target cells[297,302]. This interaction mediates fusion of the viral and endosome membranes, allowing the entry of the viral genome into the cytoplasm, where replication occurs (**Figure 10B**).

Upon cytoplasmic entry, viral replication takes place and newly generated virions bud from the infected cell, closing the viral cycle (**Figure 11**). Once the negative-stranded viral RNA genome reaches the cytosol, it serves as a template to generate mRNAs of the individual viral genes, a process requires the activity of the polymerase L and also VP30, VP35 and NP[248] (**Figure 11**). Viral proteins are synthesized with the host cell translation machinery. In addition, RNA genome is also copied into a full-length positive RNA complement that serves as a template for the synthesis of new negative-sense RNA genomes, a step that

relies on proteins L, VP35 and NP (**Figure 11**). Newly synthesized viral proteins accumulate in below the cell membrane, where they assemble. The matrix protein VP40 directs the budding process from specialized cholesterol-enriched domains[288], which requires interaction with the host ESCRT machinery[257,303,304] (**Figure 11**). Of note, and similarly to HIV-1 Gag, expression of EBOV VP40 alone is sufficient to generate non-infectious VLPs with the same morphology as real filoviral particles[257,303]. These VLPs are useful tools for studying different aspects of filoviral behaviour without the requirement of high biosafety laboratory containment to handle infectious EBOV and MARV.

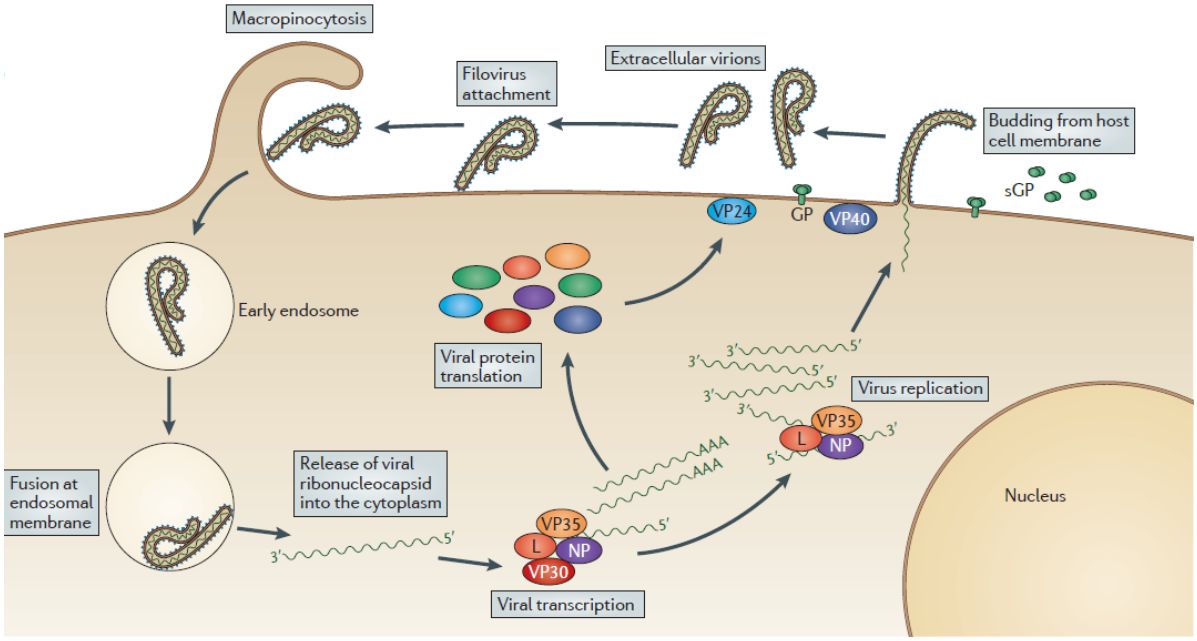

Figure 11. EBOV replicative cycle. Following entry of the viral genome into the cytoplasm, L polymerase and other viral proteins synthesize viral mRNAs and new viral genomes. The host cell translation machinery synthesizes viral proteins, that assemble around a viral genome below the cell surface. Viral VP40 governs the budding from cholesterol-enriched plasma membrane domains, that culminates with the release of newly synthesized virions. Of note, the soluble forms of viral glycoprotein are directly secreted to the extracellular media. From ref.[248].

3.4 Natural course of filoviral infection and treatment

Filoviruses can replicate in human and other animal cells, and outbreaks are originated by zoonosis from an unidentified natural reservoir in which rodents, bats and even non-human primate species could be involved[305,306]. However, once the outbreak is ongoing viral transmission occurs in a human-to-human fashion, and several transmission routes have been described, such as direct blood inoculation from contaminated material or direct contact with infected individuals and with corpses during burial practices[252,307–310]. The risk of transmission is highly increased upon contact of infectious body fluids or tissues with mucosal surfaces or nonintact skin[252], and upon viral acquisition the natural course of the disease includes these phases: primary infection, incubation, early illness, peak illness and in some cases, recovery (**Figure 12**).

The incubation stage (1 week before symptom onset) occurs upon initial viral exposure, during which viruses infect DCs and other myeloid cells present in the mucosal tissues or nonintact skin. Noteworthy, these cells act as early filoviral targets and also participate in viral dissemination from the entry sites[91,311,312]. During the incubation phase patients remain asymptomatic and are able to carry on with their normal activities. However, they become quickly incapacitated upon progression of the illness.

During the early illness stage (1 week after symptoms onset), non-specific symptoms such as neuromuscular weakness, myalgia, diarrhea and fever appear, and viral RNA is detected in blood[252] (**Figure 12**). Viral load increases and reaches its peak at the illness stage (2-3 weeks after symptoms onset) (**Figure 12**). This phase is characterized by stable declining of viral RNA in blood, but paradoxically, also with a maximal organ injury and risk of death[313]. As the infection progresses, the clinical symptomatology persists and respiratory and renal functions might be compromised[314,315], accompanied by central nervous system dysfunction[313] (**Figure 12**). Patients surviving the peak illness phase enter the recovery phase (week 4 after symptom onset) (**Figure 12**). During this phase plasma viremia is resolved, but the virus can persist in certain anatomical compartments and cause long-term sequelae, including cardiac dysfunction[316] and uveitis[317]. Of note, infectious EBOV particles have been isolated from semen from convalescent individuals up to 101 days after symptom onset[318–321], and a case of sexually transmitted EBOV infection from a male survivor from the 2014-16 outbreak was reported[322].

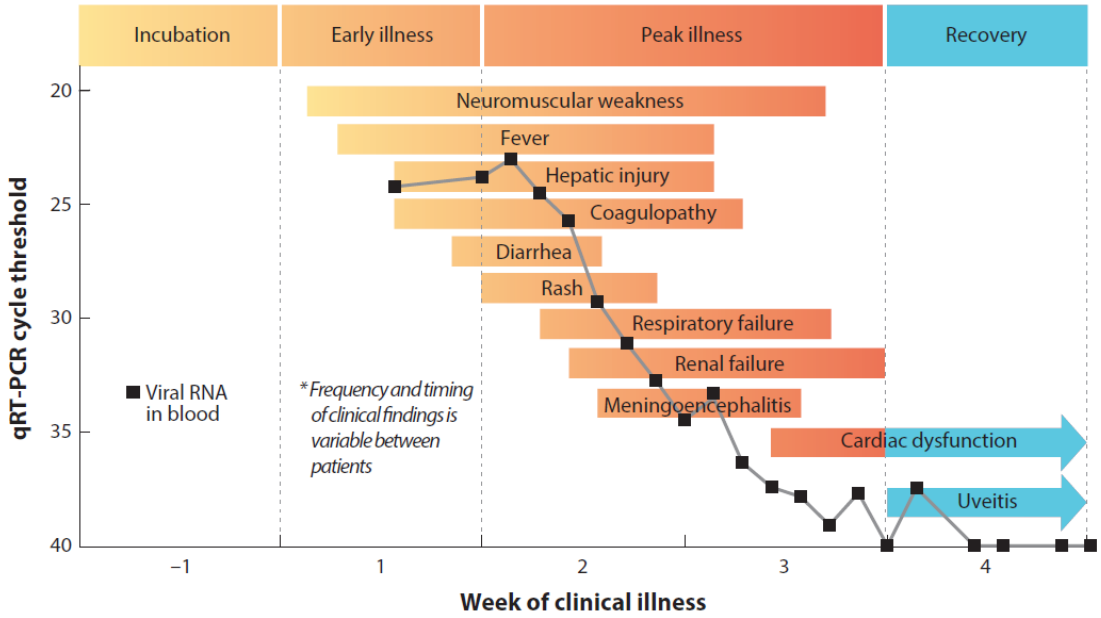

Figure 12. Natural course of EBOV infection. Upon viral acquisition, EBOV infection rapidly progresses to a severe disease characterized by the presence of unspecific symptomatology and the affectation of multiple organs, with detectable viremia that progressively decreases until the recovery phase. From ref.[252].

In spite of the efforts carried out during the past decades, there are currently no approved drugs specifically directed against any filovirus, and the treatment is limited to supportive care[252]. The antivirals that are under development and that are being tested in the ongoing EBOV outbreak in the Democratic Republic of the Congo[323] target viral components such as the glycoprotein, and thus only tackle the *Zaire ebolavirus* species. However, other filoviruses with equal outbreak potential remain uncovered by these strategies. The efficacy of these antivirals could be increased by targeting host factors in cells that are relevant in filoviral pathogenesis, such as DCs and other myeloid APCs.

3.5 DCs and other myeloid cells in filoviral pathogenesis

Given the main route of viral transmission through exposed mucosal surfaces and nonintact skin, both EBOV and MARV target DCs and macrophages at the entry sites[91,266,311,312]. Here, they become productively infected and are thought to importantly contribute to viral systemic dissemination upon migration to the secondary lymphoid tissues (**Figure 13**). In agreement with this hypothesis, myeloid cells were the first infected cells detected in entry tissues from EBOV-infected non-human primates[312] and in a MARV-infected individual[311], and infected DCs were found in lymphoid tissues of animal models early upon viral challenge[91]. Importantly, the colonization of secondary lymphoid tissues by infected

myeloid cells induces apoptosis of by-stander lymphocytes, impairing the induction of adaptive immune responses[324] (**Figure 13**). Initial viral replication in the lymphoid tissues leads to the increase of plasma viremia, which is further boosted by the infection of activated circulating monocytes[325]. In turn, high plasma viremia facilitates infection of other cells such as hepatocytes and adrenocortical cells[324,326,327] (**Figure 13**).

In addition to contribute to dissemination of infection, myeloid APCs participate in EBOV pathogenesis through alternative mechanisms (**Figure 13**). Once infected, the immune activity of these cells is dysregulated, which impairs their capacity to initiate efficient innate and adaptive immune responses[328–332]. Moreover, viral sensing leads to a potent activation state characterized by secretion of pro-inflammatory cytokines[333–336], a 'cytokine storm' that results in the recruitment of more potential viral targets to the entry sites and is an important cause of organ injury during EBOV infection[337–343] (**Figure 13**). Thus, DCs and other myeloid APCs are early targets of filoviral infection and contribute to viral spread to lymphoid tissues, and also to viral pathogenesis through the induction of potent pro-inflammatory responses, which makes them critical players during the course of EBOV infection.

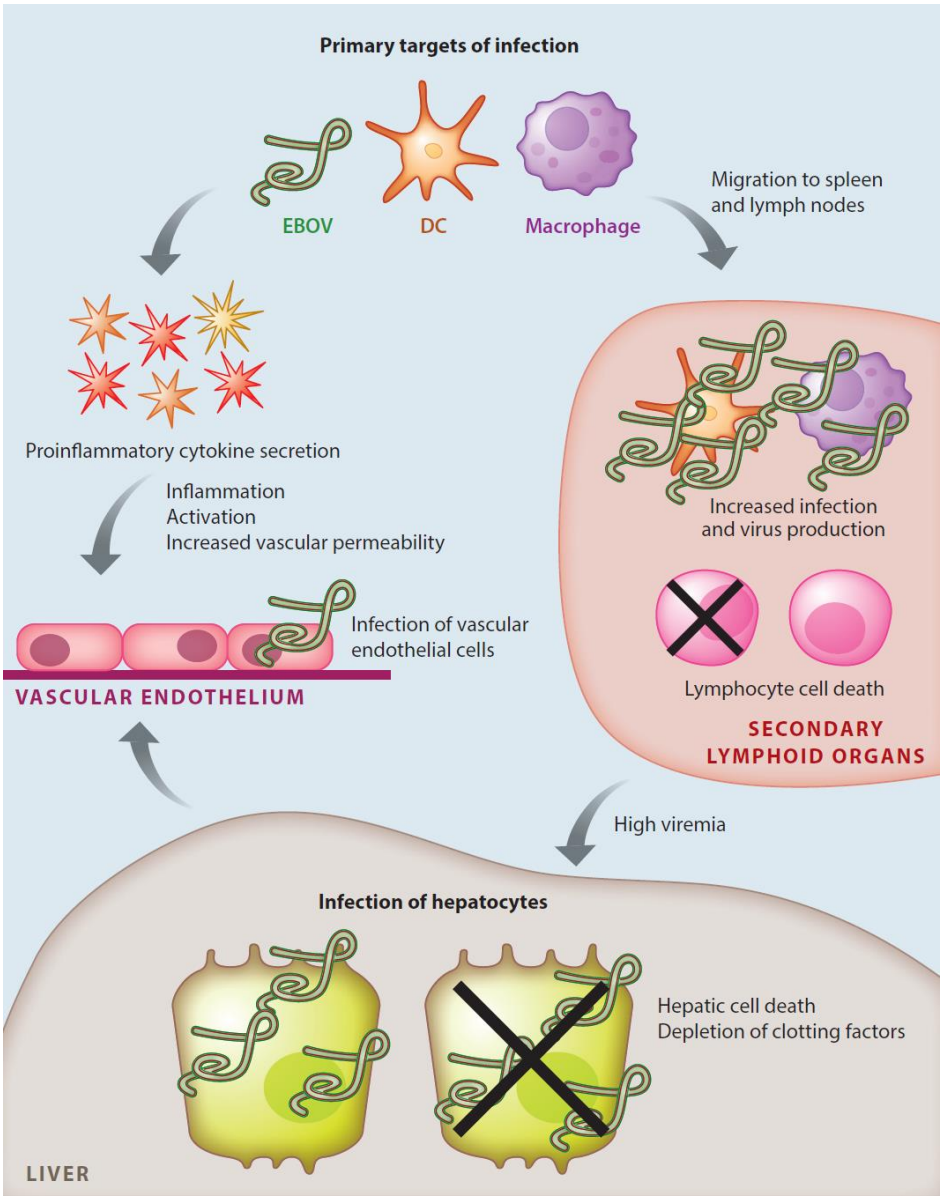

Figure 13. The role of myeloid APCs in EBOV pathogenesis. Myeloid APCs such as DCs and macrophages are early EBOV targets that become infected in the viral entry sites, contributing to viral systemic dissemination and also to viral pathogenesis through the secretion of pro-inflammatory cytokines. From ref.[344].

While the secretion of pro-inflammatory cytokines during EBOV infection is well established, the presence of type I IFNs has been a matter of debate, as reviewed in ref.[345]. Despite the capacity of some filoviral proteins to interfere with type I IFN secretion or signalling *in vitro*[328,330–332,346–349], it has been observed that IFNα is produced *in vivo* during filoviral infection. IFNα is detected in the plasma of EBOV-infected individuals, especially in fatality cases[350], and also in the plasma of non-human primates challenged both with EBOV and MARV[351,352]. Moreover, IFN-stimulated genes are up-regulated during EBOV infection in peripheral blood mononuclear cells[352–355]. LPS, which induces type I IFN

secretion by myeloid cells, was also found in the blood of an EBOV-infected patient that had a gram-negative septicemia[356].

Taken together, DCs and other myeloid APCs have a crucial role in the establishment and pathogenesis of filoviral infection. Moreover, a type I IFN response has been detected during filoviral infection and has been associated with a poor outcome of the disease. This, along with the fact that filoviral membrane includes sialylated gangliosides, suggests that the IFN-stimulated gene Siglec-1 expressed by DCs might have a role in viral entry into these cells.

Chapter 2

HYPOTHESIS & AIMS

DCs are among the first cells to encounter viruses and other pathogens at the portals of infection. Upon viral capture, these cells migrate to regional lymphoid tissues to initiate adaptive immune responses against them. However, DCs also mediate HIV-1 cell-to-cell transmission through a mechanism known as *trans*-infection. Siglec-1, the key molecule for HIV-1 *trans*-infection, recognizes sialylated gangliosides present on the lipidic membrane of HIV-1, which is a component shared by all enveloped viruses. Considering all this, our **hypothesis** is that different enveloped viruses hijack the immune function of DCs to disseminate systemically from the entry sites, and that Siglec-1 expressed on these cells plays a key role in this pathogenic strategy. Hence, the particular aims of this thesis are the following:

- **Aim 1:** To determine the physiological mechanisms leading to Siglec-1 up-regulation on DCs in the context of HIV-1 infection, determining the natural sources of IFNα enhancing Siglec-1 expression on these cells.
- **Aim 2:** To assess whether myeloid cells from cervical tissues, a key anatomical location for HIV-1 acquisition, are able to capture and *trans*-infect HIV-1 in a Siglec-1-dependent manner.
- **Aim 3:** To generate a set of new anti-Siglec-1 monoclonal antibodies (mAbs) with the capacity to block HIV-1 capture and *trans*-infection mediated by DCs.
- **Aim 4:** To determine the role of Siglec-1 in Ebola virus binding and capture by DCs in an HIV-1 comparative manner, and Siglec-1 contribution to viral cytoplasmic entry into DCs.
- **Aim 5:** To test the capacity of new anti-Siglec-1 mAbs to block filoviral capture and cytoplasmic entry into myeloid cells.

Chapter 3

RESULTS I

Siglec-1 is up-regulated on DCs by paracrine and autocrine secretion of type I IFNs

Part of the results included in this chapter are from:

Perez-Zsolt, D.*, Cantero-Pérez, J.*, Erkizia, I., Benet, S., Pino, M., Serra-Peinado, C., Hernández-Gallego, A., Castellví, J., Tapia, G., Arnau-Saz, V., Garrido, J., Tarrats, A., Buzón, M.J., Martinez-Picado, J., Izquierdo-Useros, N.† and Genescà, M.† (2019). **Dendritic cells from the cervical mucosa capture and transfer HIV-1 via Siglec-1**. *Front Immunol*. 10:825. doi: 10.3389/fimmu.2019.00825.

*Equal author contribution; †Last authors.

1. Introduction

DCs are key inducers of adaptive immune responses against infectious agents. As sentinels of the immune system, they line the mucosal surfaces and are among the first cells to interact with invading pathogens such as HIV-1. These antigen-presenting cells are refractory to HIV-1 infection due to the expression of restriction factors such as SAMHD1 and APOBEC3G[173–178]. However, DCs vigorously transmit HIV-1 to target $CD4^+$ T cells via *trans*-infection[88,179]. This mechanism of viral cell-to-cell transmission relies on Siglec-1, a receptor expressed on DCs that recognizes sialylated gangliosides anchored to the viral membrane[70,187] that is potently up-regulated in the presence of IFNα[187,213]. Accordingly, stimulation with IFNα of MDDCs and myeloid cells directly isolated from lymphoid tissues increases their capacity to capture and transmit HIV-1 to target $CD4^+$ T cells[187,192].

As a member of the type I IFN family, IFNα is a potent antiviral cytokine secreted in response to different types of viruses[38,357]. In the case of HIV-1, acute infection induces a cytokine storm that increases IFNα levels[220,221], while the chronic stage of the disease is characterized by a persistent immune activation state in which IFNα is also present[147,220]. Several cell types have been identified as the sources of IFNα production during the course of HIV-1 infection. pDCs are considered the most potent type I IFN producers in blood[33], and in the context of HIV-1 infection, their capacity to secrete IFNα in response to viral sensing has been demonstrated *in vitro*[36,37,224–226] and *in vivo*[227–229], contributing to type I IFN production during both acute and chronic phases of the disease[35,227,228]. Of note, pDC activation in response to HIV-1 sensing induces IFNα secretion and maturation of bystander myeloid DCs[230]. However, whether IFNα secreted by HIV-1-exposed pDCs can up-regulate Siglec-1 on these cells, which could contribute to viral dissemination via *trans*-infection, has not been addressed yet. Aside from pDCs, myeloid DCs have been reported to secrete IFNα in SIV-infected rhesus macaques, substantially contributing to the plasma levels of this cytokine[238]. In humans, DCs secrete type I IFNs in response to immune activating signals, which can in turn stimulate gene expression on these cells in an autocrine manner[231,233–235]. One of such factors is bacterial LPS, that is increased during HIV-1 infection due to bacterial translocation in the GALT, as a consequence of the gut epithelial barrier disruption that occurs early upon HIV-1 infection and persist chronically[147,148,236]. Intriguingly, LPS up-regulates Siglec-1 on DCs, boosting their ability to capture and transfer HIV-1 to target cells[70]. However, whether Siglec-1 up-regulation on LPS-treated DCs is mediated by the effect of autocrine type I IFN secretion is yet to be determined.

Here, we sought to identify the natural sources of type I IFNs that up-regulate Siglec-1 on DCs during HIV-1 infection, assessing in the first place the contribution of HIV-1-exposed pDCs. We confirmed that HIV-1 sensing triggers IFNα secretion by pDCs inducing Siglec-1 expression on bystander DCs, a mechanism highly accentuated in women that might have an impact on early HIV-1 dissemination. Moreover, we determined that LPS exposure triggers an autocrine production of IFNα that mediates Siglec-1 up-regulation on DCs.

2. Material & Methods

2.1 Ethics statement

This study was approved by the institutional review board on biomedical research from Hospital Universitari Germans Trias i Pujol (HUGTiP, Badalona, Spain). All individuals involved in this study gave their written informed consent to donate blood for research.

2.2 Primary cells

Peripheral blood mononuclear cells from HIV-1-seronegative donors obtained throughout the Banc de Sang i Teixits (Barcelona) were separated by Ficoll-Hypaque gradient (Alere Technologies AS). pDCs were negatively isolated using magnetic beads from the Plasmacytoid DC isolation kit (Miltenyi Biotec; purity >70%) and immediately used for experiments. Monocytes were purified by CD14-positive selection magnetic beads (Miltenyi Biotec; purity >97% $CD14^+$). MDDCs were obtained culturing monocytes in the presence of 1,000 International Units (IU)/ml of GM-CSF and IL-4 (both from R&D) during 7 days, replacing medium with fresh cytokines every 2 days. DCs were either left untreated as iDCs or stimulated at day 5 for 48 h with 1,000 IU/ml of IFNα or 100 ng/ml of LPS (both from Sigma-Aldrich) with or without 2 μg/ml of the carrier-free recombinant B18R protein (eBioscience). All primary cells were maintained in Roswell Park Memorial Institute medium-1640 (RPMI) supplemented with 10% fetal bovine serum (FBS), 100 IU/ml of penicillin and 100 μg/ml of streptomycin (all from Invitrogen).

2.3 Cell lines

Uninfected and HIV-1_{BAL}-infected human MOLT-4 cells[358] were maintained in RPMI (Invitrogen). HEK-293T cells (CRL-11268; obtained from the ATCC repository) were maintained in Dulbecco's Modified Eagle's Medium (DMEM; Invitrogen). All media

contained 10% FBS, 100 IU/ml of penicillin and 100 µg/ml of streptomycin (all from Invitrogen).

2.4 IFNα measurement in supernatants from pDCs and DC stimulation assays

$0.1x10^6$ primary pDCs and $0.1x10^6$ HIV-1_{BAL}-infected or uninfected MOLT-4 cells were co-cultured for 24 h at 37ºC. Prior to co-culture, pDCs were treated for 10 min at room temperature (RT) with 10 µg/ml of an anti-CD4 RPA T-4 mAb to avoid viral fusion, an isotype control (both from BD), or left untreated. After co-culture, IFNα in the supernatants was quantified with a Verikine Human IFN Alpha Elisa Kit (pbl Assay Science). Alternatively, supernatants were transferred to $0.2x10^6$ DCs. After 24 h incubation, DCs were labelled with an anti-Siglec-1 7-239 PE mAb or a matched isotype PE control (both from AbD Serotec), and assessed for Siglec-1 expression with a FACSCalibur (Becton Dickinson). Supernatants were also added to DCs previously treated with 2 mg/ml of carrier-free recombinant B18R (eBioscience) to block signalling through the type I IFN receptor. Aside from supernatants, DCs were exposed to RPMI supplemented with 10% FBS, 100 IU/ml of penicillin and 100 µg/ml of streptomycin (all from Invitrogen) with or without 1,000 IU/ml of recombinant IFNα (Sigma-Aldrich).

For IFNα-treated DCs, the mean number of Siglec-1 antibody binding sites per cell was determined using a Quantibrite kit (BD) following the manufacturer's instructions. Rainbow calibration beads (BD) were employed before quantification to ensure that the fluorescence intensity measurements were consistent along the experiments.

2.5 Immunophenotyping

Distinctly treated DCs were blocked with 1 mg/ml of human IgGs (Baxter, Hyland) and labelled for 30 min at 4ºC with the following mAbs: anti-CD83 HB15e FITC, anti-CD86 2331 FITC, anti-HLA-DR L243 PerCP, anti-DC-SIGN DCN46 PE, anti-CD14-PerCP MφP9 (all from BD Biosciences), anti-Siglec-1 7-239 PE (AbD Serotec). Mouse IgG1 PE (AbD Serotec) and IgG2b PE (BD Biosciences) mAbs were included as isotype controls. Labelled cells were acquired using a FACSCalibur flow cytometer (BD) and collected data was analysed using CellQuest (BD) and FlowJo (TreeStar) softwares. Adequate differentiation from monocytes to DCs was monitored by the loss of CD14 and the acquisition of DC-SIGN.

2.6 HIV-$1_{Gag\text{-}eGFP}$ VLP generation and capture assay

HIV-$1_{Gag\text{-}eGFP}$ VLP stocks were generated by transfection of HEK-293T cells with the molecular clone pGag-eGFP obtained from the US National Institutes of Health (NIH) AIDS Research and Reference Reagent Program. HEK-293T cells were transfected in T75 flasks with 30 µg of plasmid DNA using calcium phosphate (CalPhos; Clontech) and incubated during 48 h at 37ºC. Supernatants containing HIV-$1_{Gag\text{-}eGFP}$ VLPs were harvested, filtered (Millex HIV, 0.45 µm; Millipore) and frozen at -80ºC until use. The $p24^{Gag}$ content of viral and VLP stocks was determined by enzyme-linked immunosorbent assay (ELISA) (Perkin-Elmer).

For capture experiments, distinctly treated DCs were pulsed with a constant rate of 0.4 ng p24 of HIV-$1_{Gag\text{-}eGFP}$ VLPs per 10^5 cells for 2 h at 37ºC. After extensive washing, cells were acquired with a FACSCalibur flow cytometer (BD) and the percentage of positive cells was determined using FlowJo software (TreeStar).

2.7 Statistical analyses

Data are reported as the mean and the standard error of the mean (SEM) for each condition. Mean changes were assessed by paired *t* test, Wilcoxon matched-pairs signed rank test, and Mann-Whitney test (all two-sided), which were considered significant at $P<0.05$. Sex main effect inference across multiple experiments was assessed using the Prentice Rank Sum Test, a generalized Friedman rank sum test with replicated blocked data. All analyses and figures were generated with the GraphPad Prism v7.0d software.

3. Results

3.1 IFNα secreted by pDCs exposed to HIV-1 induces Siglec-1 expression on bystander DCs

We hypothesize that type I IFNs secreted by pDC might contribute to Siglec-1 up-regulation on bystander DCs in the context of an HIV-1 infection. It has been reported that pDCs elicit a potent type I IFN response upon HIV-1 recognition[224,359]. HIV-1 binds to CD4 receptors on the surface of pDCs, and subsequent viral internalization allows for HIV-1 sensing through endosomal TLR7 and TLR9, activating the production and release of large amounts of type I IFNs[34–36]. Thus, we assessed whether the type I IFN response elicited by pDCs exposed to HIV-1 induced Siglec-1 up-regulation on bystander DCs.

We cultured primary pDCs with an uninfected or an HIV-1_{BAL}-infected MOLT-4 cell line and quantified IFNα levels in the supernatants after 24 h of co-culture. IFNα secretion was higher in pDCs exposed to HIV-1 compared to non-exposed cells, and levels of secreted IFNα were reduced when an anti-CD4 antibody was included to avoid viral internalization and signalling (**Figure 14A**). Hence, IFNα is produced by pDCs in response to HIV-1 exposure, as previously reported[224]. Then, we added these supernatants to MDDCs and, after 24 h, we determined Siglec-1 levels on these cells by flow cytometry. Concurrently with their levels of FNα, supernatants derived from HIV-1-exposed pDCs induced higher Siglec-1 levels on DCs than those from non-exposed pDCs, and Siglec-1 up-regulation was blocked when the anti-CD4 antibody had been present during the co-culture (**Figure 14B**). These results show that paracrine secretion of type I IFNs by pDCs in response to HIV-1 infection induce Siglec-1 up-regulation on bystander DCs. To further confirm the role of type I IFNs, we added B18R to the supernatant of HIV-1-exposed pDCs. This soluble recombinant receptor with high affinity for type I IFNs completely abrogated the capacity of the supernatant to up-regulate Siglec-1 on DCs (**Figure 15**, purple histograms). Of note, the effect of IFNα secreted by pDCs exposed to HIV-1 could be reproduced using recombinant IFNα, which up-regulated Siglec-1 on DCs to a similar extent (**Figure 15**, orange histogram).

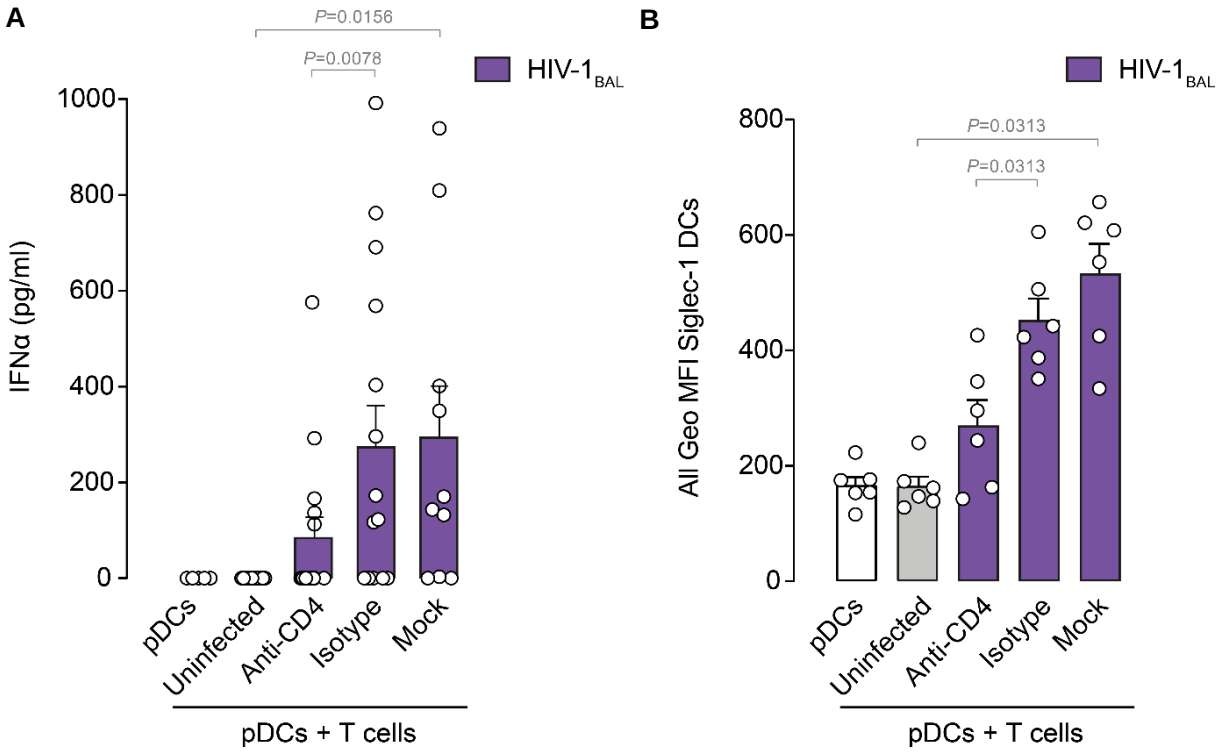

Figure 14 (caption overleaf)

Figure 14. IFNα secreted by HIV-1-exposed pDCs induces Siglec-1 expression on bystander myeloid DCs. A. IFNα release quantified by ELISA in supernatants from pDCs co-cultured for 24 h with an HIV-1_{BAL} infected or uninfected MOLT $CD4^+$ T cell line in the presence or absence of 10 µg/ml of an anti-CD4 or an isotype antibody. **B.** Siglec-1 levels determined by fluorescence-activated cell sorting (FACS) in MDDCs exposed to supernatants from panel **A** for 24 h. Data show mean values and SEM from three independent experiments including cells from at least six donors. Statistical differences were assessed with a two-sided Wilcoxon matched-pairs signed rank test.

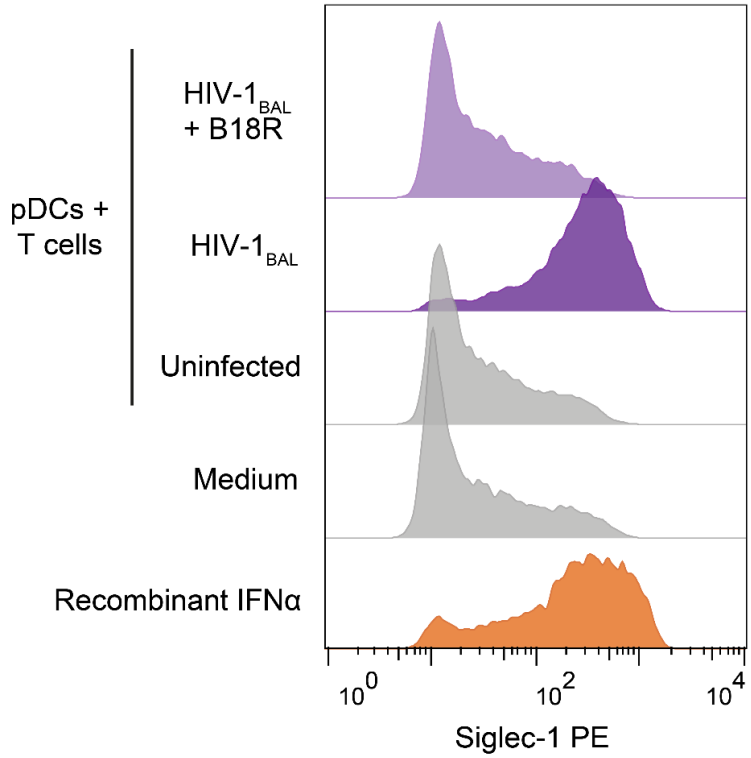

Figure 15. Type I IFNs secreted by pDCs and recombinant IFNα induce Siglec-1 on DCs. Representative FACS histograms showing Siglec-1 expression on MDDCs treated during 48 h with supernatants from HIV-1_{BAL}-exposed pDCs in the presence or absence of B18R, HIV-1_{BAL}-unexposed pDCs, R10 medium alone or R10 with 1,000 IU/ml of recombinant IFNα.

It has been reported that in response to HIV-1, a higher frequency of pDCs from women secrete IFNα when compared to those derived from men, which could account for the increased expression of IFN-stimulated genes in HIV-1-infected women as compared to men[360]. In agreement with these data, we also found that pDCs from pre-menopause women secreted higher levels of IFNα than those from men when co-cultured with the HIV-1_{BAL}-infected MOLT-4 cell line (**Figure 16A**). To rule out the possibility that the higher IFNα secretion in woman could be compensated with a lower capacity of this cytokine to induce Siglec-1 expression on female DCs, equivalent amounts of recombinant IFNα were added

to DCs as a way to mimic the type I IFN response elicited by HIV-1-exposed pDCs (**Figure 15**). Noteworthy, no differences were found between the absolute Siglec-1 expression levels on DCs from women or men (**Figure 16B**).

Taken together, these results indicate that Siglec-1 is up-regulated on DCs by paracrine type I IFNs secreted by pDCs in response to HIV-1. However, alternative sources of type I IFNs might also fuel this process upon HIV-1 infection. Indeed, DCs have been proposed to contribute to the overall type I IFN production in response to HIV-1, as they maintained IFNα production in a SIV-infected non-human primate model devoid of pDC activity[238].

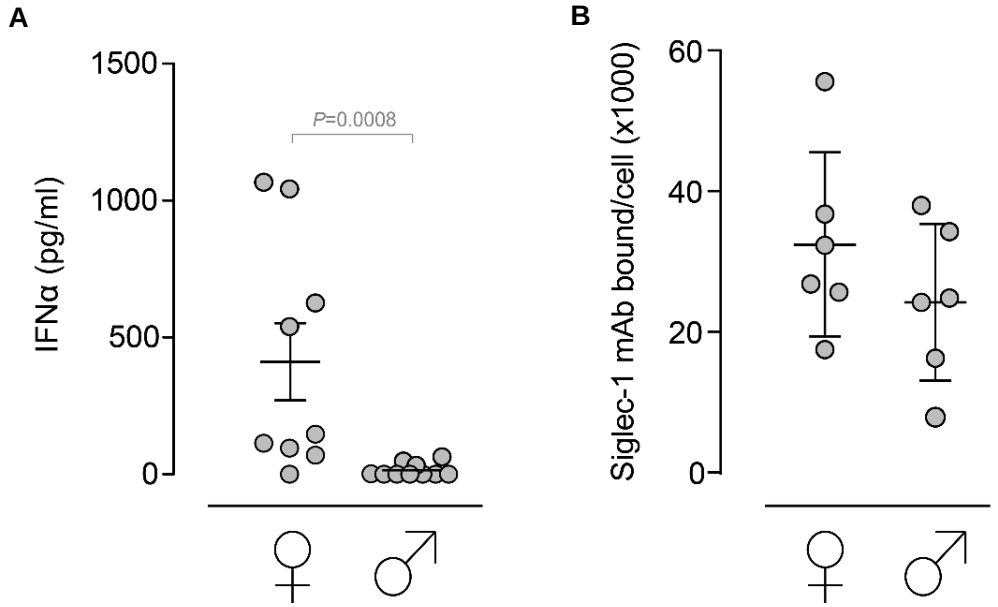

Figure 16. IFNα secretion by HIV-1-exposed pDCs is higher in women than in men. A. IFNα release quantified by ELISA in supernatants of pDCs from women and men co-cultured for 24 h with HIV-1_{BAL}-infected MOLT-4 T cells. Data show mean values and SEM from four independent experiments and cells from nine female and ten male donors. **B.** Siglec-1 quantification on the surface of DCs exposed for 48 h to 1,000 IU/ml of IFNα. Data show mean values and SEM from three independent experiments and cells from six female and six male donors. In all cases, statistical differences were assessed with a two-sided Mann-Whitney test.

3.2 Autocrine type I IFNs induce Siglec-1 expression on LPS-treated DCs

In contrast to pDCs, which elicit a potent type I IFN response upon HIV-1 recognition[224,359], the ability of DCs to secrete type I IFNs in response to HIV-1 sensing is unclear as some viral components antagonize with the type I IFN secretory pathway *in vitro*[361,362]. However, DCs respond to immune activating factors such as bacterial LPS with IFNα secretion, which exerts its effects in an autocrine manner[231,234,235]. Given the increase of LPS in the

plasma of HIV-1 infected individuals[147], we next assessed the contribution of autocrine type I IFNs released by DCs upon LPS sensing on the induction of Siglec-1 expression.

We measured Siglec-1 levels on human MDDCs stimulated with IFNα and LPS, but also in the presence of the type I IFN antagonist B18R (**Figure 17**). As compared to iDCs, treatment with both IFNα and LPS up-regulated Siglec-1 on DCs, which is consistent with previous reports[70,187] (**Figure 17**). Interestingly, Siglec-1 up-regulation on LPS-treated DCs was completely abrogated in the presence of B18R, yielding Siglec-1 levels comparable to those of iDCs (**Figure 17**). Thus, Siglec-1 expression is enhanced on LPS-treated DCs via activation of the type I IFN receptor, indicating that DCs respond to LPS by secreting type I IFNs, which in turn induce Siglec-1 expression through an autocrine loop.

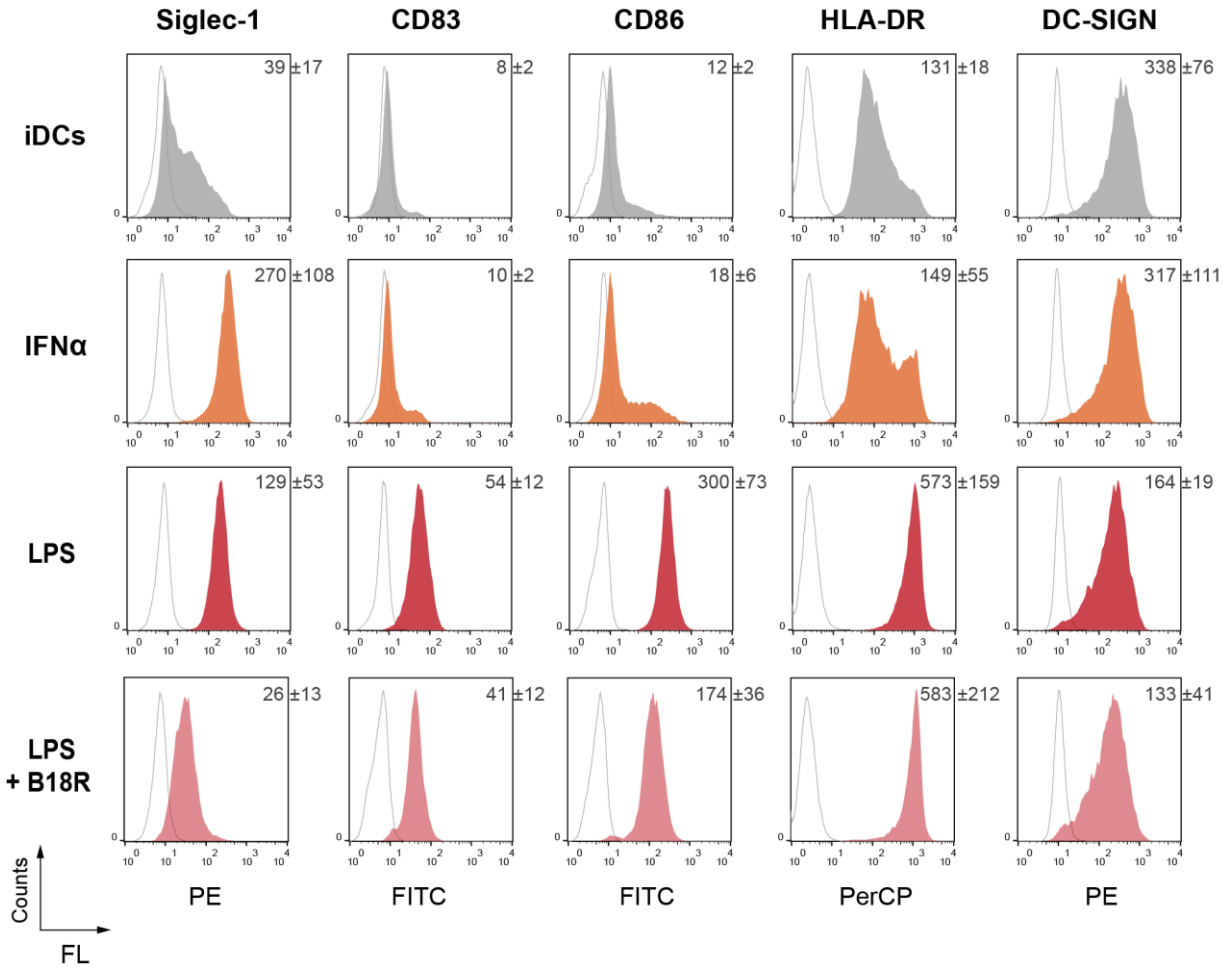

Figure 17. Autocrine type I IFNs induce Siglec-1 expression on LPS-treated DCs. Representative flow cytometry histograms for Siglec-1, CD83, CD86, HLA-DR and DC-SIGN surface staining on iDCs and DCs treated for 48 h with 1,000 IU/ml IFNα or 100 ng/ml of LPS in the presence or absence of 2 µg/ml B18R. Top-right values indicate the geometric mean fluorescence intensity (MFI) and standard deviation (SD) from five biological replicates or donors and four independent experiments.

Since both IFNα and LPS are factors that modulate the activation status of DCs[363–365], we also measured the expression of classical maturation markers such as CD83, CD86 and HLA-DR, as well as the CLR DC-SIGN. In line with previous reports[187,231,366], IFNα did not increase maturation markers as compared to iDCs (**Figure 17**). In contrast, and also consistent with previous data[365,367,368], all maturation markers increased upon LPS treatment as compared to iDCs, while DC-SIGN levels decreased (**Figure 17**). Of note, when DCs were treated with LPS in the presence of the type I IFN receptor antagonist B18R, no major changes were observed in any of the maturation markers or DC-SIGN as compared to the stimulation with LPS alone (**Figure 17**). Thus, expression these receptors under LPS activation indicates that induction of Siglec-1 is mediated by autocrine type I IFN production, and that Siglec-1 up-regulation is independent of the maturation status of the cells, as observed upon Siglec-1 induction via IFNα.

Siglec-1 up-regulation on DCs exerted by LPS increases the capacity of these cells to capture HIV-1 particles, enhancing viral transmission to target $CD4^+$ T cells via *trans*-infection[70]. Thus, we next assessed the effect of autocrine type I IFNs on the capacity of LPS-treated DCs to capture HIV-1 particles. For this purpose, we generated fluorescent HIV-$1_{Gag\text{-}eGFP}$ VLPs[369–372], which lack HIV-1 envelope glycoprotein but carry sialyllactose-containing gangliosides recognized by Siglec-1, recapitulating wild-type HIV-1 capture by DCs[70,187]. We pulsed iDCs and DCs treated with either recombinant IFNα or LPS with or without B18R with equal amounts of HIV-$1_{Gag\text{-}eGFP}$ VLPs, and after extensive washing, viral capture was assessed by flow cytometry. As compared to iDCs, both IFNα- and LPS-treated DCs captured higher levels of HIV-$1_{Gag\text{-}eGFP}$ VLPs (**Figure 18**), which is concurrent with their Siglec-1 levels (**Figure 17**) and in line with previous reports[70,186,187]. However, when cells were stimulated with LPS in the presence of B18R, the capacity of LPS to induce viral capture by DCs was completely lost (**Figure 18**). Thus, autocrine type I IFNs secreted by DCs in response to LPS treatment are necessary to boost Siglec-1-mediated viral capture by LPS-treated DCs. Overall, these results indicate that LPS signalling on DCs induces the secretion of type I IFNs, which in turn up-regulates Siglec-1 through an autocrine loop. This natural source of type I IFNs could fuel HIV-1 cell-to-cell transmission via Siglec-1 in the context of HIV-1 infection, characterized by an early onset of bacterial translocation in the gut and a persistent activation exerted by bacterial products such as LPS[147,148,236].

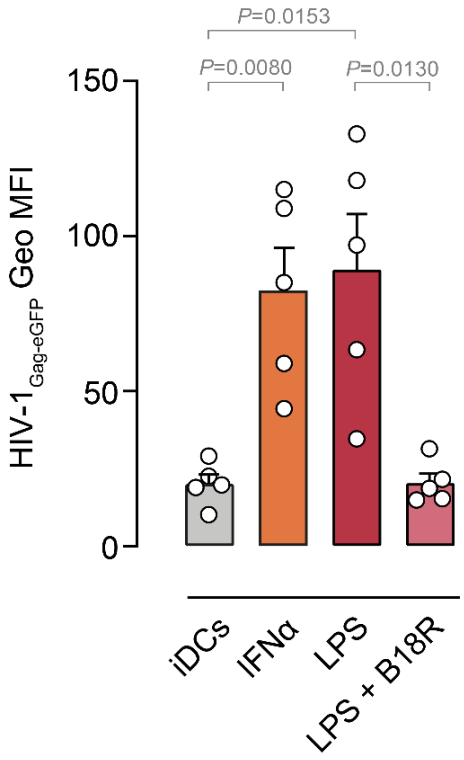

Figure 18. Autocrine type I IFNs produced by myeloid DCs in response to LPS boost HIV-1$_{Gag\text{-}eGFP}$ VLP capture. Viral uptake by iDCs and DCs treated with IFNα, LPS or LPS with B18R pulsed with HIV-1$_{Gag\text{-}eGFP}$ VLPs for 2 h at 37ºC and assessed by flow cytometry. Data show mean values and SEM from five donors and four independent experiments. Statistical differences were assessed using a two-sided paired *t* test.

Taken together, the results in this chapter indicate that Siglec-1 is up-regulated on DCs by paracrine type I IFNs secreted by pDCs in response to HIV-1, but also by autocrine type I IFNs produced in response to LPS. Hence, we identified two complementary sources of type I IFNs that can operate in the context of HIV-1 infection fuelling Siglec-1 expression and therefore DC-to-T-cell viral transmission. Moreover, we confirmed that sex influences the secretion of paracrine IFNα, with women-derived pDCs responding more potently to HIV-1 than those derived from men. In the light of these results, we hypothesize that the contribution of Siglec-1-mediated HIV-1 *trans*-infection can be particularly relevant in women, and especially in those tissues where pDCs accumulate during HIV-1 infection. Intriguingly, vaginal administration of SIV to non-human primates resulted in a rapid accumulation of pDCs in the cervical mucosa, where they induced an inflammatory milieu characterized by the presence of IFNα[239,373]. Thus, cervical tissues arise as a potential anatomical location in which HIV-1 *trans*-infection mediated by Siglec-1 on DCs could take place, aiding HIV-1 cell-to-cell transmission in the early stages of HIV-1 infection.

Chapter 4

RESULTS II

DCs from the cervical mucosa capture and transfer HIV-1 via Siglec-1

The results included in this chapter are part of:

Perez-Zsolt, D.*, Cantero-Pérez, J*., Erkizia, I., Benet, S., Pino, M., Serra-Peinado, C., Hernández-Gallego, A., Castellví, J., Tapia, G., Arnau-Saz, V., Garrido, J., Tarrats, A., Buzón, M.J., Martinez-Picado, J., Izquierdo-Useros, N.† and Genescà, M.† (2019). **Dendritic cells from the cervical mucosa capture and transfer HIV-1 via Siglec-1**. *Front Immunol*. 10:825. doi: 10.3389/fimmu.2019.00825.

*Equal author contribution; †Last authors.

1. Introduction

Women account for 51% of people living with HIV worldwide, and in 2018 this represented 19.1 million females[374]. Since HIV-1 infection is mostly acquired by sexual transmission[375], understanding the female genital tract immunobiology is imperative not only to halt novel infections, but also to design strategies that will limit HIV-1 spread within the mucosa and contain the virus during the early stages of infection. HIV-1 acquisition relies on a series of orchestrated events that lead to systemic infection, beginning with viral entry through the genital epithelium and followed by the productive infection of distinct $CD4^+$ target cells that reside within the mucosa. Local infection is early disseminated to draining lymph nodes, aiding to spread HIV-1 systemically and boost viral replication[132]. While current antiviral agents are potent inhibitors of viral infection in the mucosa, efficacy of preventive methods is also critically dependent on effective blockade of all potential receptors involved in HIV-1 dissemination from the genital mucosa to the lymphoid tissues[131,376,377]. Yet, the precise molecular mechanisms underlying viral dissemination routes from the genital mucosa that boost systemic HIV-1 infection remain unknown.

Although productive infection during the first days after vaginal SIV exposure is low and mainly restricted to the cervicovaginal tissues[132], evidence for rapid dissemination to the draining lymph nodes has been demonstrated as soon as 24 h post-infection[89,133,134]. These studies suggest a critical role for cervical myeloid cells and, particularly, DCs in early dissemination of mucosal viruses to lymphoid tissues. Importantly, viral spread does not only rely on *de novo* productive infection of myeloid cells[88,171,179], but can be triggered upon activation of mucosal myeloid cells via the capture and storage of large amounts of HIV-1 particles that are later transferred to target cells, as previously reported for MDDCs[185,186,378]. Once mucosal myeloid cells migrate to secondary lymphoid tissues for induction of antiviral immune responses, trapped viruses can be efficiently transferred to $CD4^+$ T cells[88,179], which become productively infected and fuel systemic viral dispersion. This highly infectious process is known as *trans*-infection, and pioneering work already identified that migratory HLA-DR^+ $CD3^-$ cervical cells efficiently captured and transmitted HIV-1 in *trans*[376]. Recent data also demonstrated that among all myeloid cell subsets, vaginal and cervical DCs capture and transport transmitted/founder viruses through the cervicovaginal mucosa and facilitate infection of target cells[243,244].

Even though *trans*-infection was initially attributed to the capacity of CLRs such as DC-SIGN to specifically bind to the viral envelope glycoprotein of HIV-1[179], viral capture in

the female genital mucosa is independent of this particular receptor, as the majority of cervical DCs capturing HIV-1 do not express DC-SIGN[379] and neutralizing mAbs against DC-SIGN cannot block viral transmission[376]. In addition to CLRs, HIV-1 capture by myeloid cells is mediated by Siglec-1[70,187,213]. This receptor potently enhances HIV-1 capture and storage in VCCs[189], that are later released from DCs to infect target cells via virological synapse formation[188]. Siglec-1 expression is potently enhanced by type I IFN signalling[213,380], which is triggered by viral immune sensing by pDCs and bacterial LPS exposure, as we have commented in the previous chapter. *In vivo*, Siglec-1 is required for robust infection and early dissemination of a retrovirus within the lymphoid tissue of a murine model[237]. However, its potential role during HIV-1 infection in the female genital tract remains unexplored.

Here, we sought to clarify whether Siglec-1-mediated viral *trans*-infection could impact the early stages of HIV-1 infection in women, and performed a comprehensive analysis of Siglec-1 expression on human cervical anatomical compartments. In all samples studied, we identified mucosal DCs expressing this receptor, whose expression was boosted by IFNα antiviral signalling. Moreover, we found that cervical DCs enhanced viral capture and *trans*-infection, and that this mechanism is effectively blocked with mAbs against Siglec-1 receptor.

2. Material & Methods

2.1 Ethics statement

This study was approved by the institutional review board on biomedical research from HUGTiP (Badalona, Spain) and Hospital Universitari Vall d'Hebron (HUVH, Barcelona, Spain), reference numbers PI-14-070 and PR (IR)294/2017. A written informed consent was obtained from all the participants. The study was performed in accordance with the Declaration of Helsinki and the requirements of Good Clinical Practice.

2.2 Cervical tissue digestion and immunophenotyping

Human cervical tissues were obtained from women (age range 39-82 years) undergoing hysterectomies for non-neoplasic indication at either HUGTiP and Hospital Municipal de Badalona, and the healthy tissue status was confirmed by the Pathology Service. A piece from ectocervix and endocervix was separated by anatomical localization was delivered to

the laboratory in RPMI supplemented with 15% FBS, 500 U/ml penicillin, 500 µg/ml streptomycin, 50 µg/ml gentamicin, 2.5 µg/ml Fungizone (Life Technologies), minimum essential medium (MEM) non-essential aminoacids and 1 mM MEM-sodium pyruvate (both from Invitrogen). All tissues were processed within 24 h after surgery. The mucosal epithelium and the underlying stroma of ectocervix and endocervix were separated from muscular tissue and dissected into approximately 8 mm^3 blocks. Depending on the assay, tissue blocks were either cultured at 37ºC and 5% CO_2, digested or included in optimal cutting temperature compound for immunofluorescence as previously described[381].

For digestion, five to eight pieces from ectocervix or endocervix were placed in 1.5 ml tubes containing RPMI supplemented with 5% FBS in the presence of 5 mg/ml collagenase IV (all from Invitrogen). Tubes were shaken for 30 min at 400 rpm and 37ºC. After enzymatic digestion, tissue blocks were manually dissociated with a disposable pellet pestle following two series of 20 rotations pulling it up and down. The obtained suspension was filtered using a 70 µm cell strainer (SPL Life Sciences) and cells were collected at 16ºC after a phosphate-buffered saline (PBS) wash. After staining the cells with Live/Dead Aqua (Invitrogen) for 30 min at RT, they were suspended in staining buffer (PBS with 1% mouse serum and 1% goat serum) and stained with the following mAbs: anti-CD14 MφP9 V450, anti-CD11c B-ly6 PE-Cy7, anti-HLA-DR G46-6 PerCP-Cy5.5 (all from BD Biosciences), anti-CD3 OKT3 eVolve 655 (eBiosciences), anti-CD45 Hl30 Alexa Fluor 700, anti-CD11b M1/70 FITC, anti-Siglec-1 7-239 PE (all from BioLegend). Mouse IgG1-PE (BioLegend) was included as an isotype control. Labelled cells were acquired using an LSRFortessa SORP flow cytometer (BD) (Flow Cytometry Platform, IGTP) and collected data was analysed using FlowJo vX.0.7 software (TreeStar).

2.3 Immunofluorescence

Cervical 5 µm cryosections were dried at RT, fixed in 3.7% formaldehyde (Sigma-Aldrich) diluted in PHEM buffer as previously described[381], permeated with 0.2% Triton X-100 (Sigma-Aldrich) in PHEM buffer, and blocked with 0.2% cold fish gelatin, 0.1% Triton X-100 (both from Sigma-Aldrich) and 10% normal goat serum (Gibco) in PBS. Sections were first incubated in presence of the following primary mAbs: mouse anti-Siglec-1 7-239, rabbit anti-CD11c EP1347Y or rabbit anti-CD14 EPR3653 (all from Abcam). After extensive PBS washing, samples were incubated with the following secondary mAbs: donkey anti-rabbit IgG Alexa Fluor 488 or donkey anti-mouse IgG Alexa Fluor 647 (both from Jackson ImmunoResearch). Sections were covered with 4',6-diamidino-2-

phenylindole (DAPI)-containing mounting medium (ProLong Gold Antifade Mountant; Life Technologies, Invitrogen) and a coverslip. Confocal microscopy images were obtained with a Zeiss LSM 710 microscope and the Zen Blue Image acquisition software.

2.4 Immunohistochemistry

Ten cervical formalin-fixed, paraffin-embedded samples from the Pathology Department (HUGTiP) were analysed. Of note, we chose samples from five HIV-1-infected and five seronegative women, but results were equivalent regardless of the serological status. Immunohistochemical staining was performed using a Ventana Benchmark Ultra (Ventana Medical Systems) in accordance with the manufacturer's protocol, with standard antigen retrieval (pH 9.0; Ventana) and the anti-Siglec-1 SP213 mAb (LSBio) added at a 1/100 dilution for 12 min. A blind quantification of Siglec-1^+ cells was carried by a pathologist, and images were captured using a DP71 digital camera (Olympus, Center Valley, PA, USA) attached to a BX41 microscope (Olympus). Siglec-1^+ cells were counted in five consecutive fields in the subepithelial area of ectocervix or endocervix. Tissues in which a significant inflammatory infiltrate was detected were considered as highly inflamed.

2.5 Generation of HIV-$1_{Gag\text{-}eGFP}$ VLP and HIV-1 stocks

Fluorescent HIV-$1_{Gag\text{-}eGFP}$ VLPs were generated as previously described (**Chapter 3, Material & Methods 2.6**). The replication-competent HIV-1 stock was generated by transfecting HEK-293T cells with the proviral construct NFN-SX, an HIV-$1_{NL4.3}$ provirus that expresses the HIV-1_{JRFL} envelope glycoprotein (kindly provided by W. O'Brien). 30 µg of plasmid DNA were added to cells in T75 flasks, and transfection was performed using a calcium phosphate kit (Calphos; Clontech). Supernatants were harvested 48 h post-transfection, filtered (Millex-HV, 0.45µm; Millipore) and frozen at -80ºC until use. The $p24^{Gag}$ content of VLP and HIV-1 stocks was determined by ELISA (Perkin-Elmer). The median tissue culture infectious dose ($TCID_{50}$) or 50% tissue culture infective doses of HIV-$1_{NFN\text{-}SX}$-infection employed in *trans*-infection assays were determined by end-point dilution culture on the TZM-bl cell line (from the NIH AIDS Research and Reference Reagent Program, from J.C. Kappes, X. Wu, and Tranzyme Inc.), that contains an HIV long terminal repeat linked to a luciferase reporter gene[382] and were maintained in DMEM (Invitrogen). All media contained 10% FBS, 100 IU/ml of penicillin and 100 µg/ml of streptomycin (all from Invitrogen).

2.6 HIV-$1_{Gag\text{-}eGFP}$ VLP uptake assays

$1x10^6$ digested ectocervical and endocervical cells were pre-incubated for 15 min at RT with 20 µg/ml of anti-Siglec-1 7D2 mAb (Abcam), a murine IgG1 κ isotype control (BD) or left untreated. Cells were pulsed overnight with 2.7-20 ng of $p24^{Gag}$ HIV-$1_{Gag\text{-}eGFP}$ VLP at 37ºC in a 5% CO_2 incubator in the presence or absence of 1,000 IU/ml of recombinant IFN-2α (Sigma-Aldrich) in RPMI medium supplemented with 10% FBS, 100 IU/ml of penicillin and 100 µg/ml of streptomycin (all from Invitrogen). After extensive washing, cells were stained as previously described (**Chapter 4, Material & Methods 2.2**), acquired using an LSRFortessa SORP flow cytometer (BD) (Flow Cytometry Platform, IGTP) and analysed with FlowJo v10.3 software (TreeStar).

For imaging flow cytometer analyses, $1x10^6$ digested ectocervical and endocervical cells were pulsed with HIV-$1_{Gag\text{-}eGFP}$ VLPs as previously described in this section. After extensive washing, cells were resuspended in PBS with 1:250 Live/Dead Aqua staining (Invitrogen) and incubated for 30 min at RT. Cells were then fixed and permeabilized (Fix & Perm; Invitrogen), and stained with an anti-Siglec-1 7-239 PE mAb (BioLegend). Cells were acquired with an Amnis ImageStreamX imaging flow cytometer (Merck), and analysed using IDEAS v6.1 software. A gradient root mean square (RMS) value >40 was established as the best focus threshold, and single cells were selected in the Area vs. Aspect Ratio dot plot of the brightfield channel.

2.7 HIV-1 p24 immunostaining

A cervical formalin-fixed, paraffin-embedded sample from a viremic patient diagnosed with sexually transmitted HIV-1 infection a decade ago was obtained from the Pathology Department of the HUVH. At the time of sample collection, the patient had between 5,160 and 10,400 HIV-1 RNA copies/ml in blood. Samples were dewaxed and placed in decreasing ethanol concentrations. Heat-induced epitope retrieval was performed in ethylenediaminetetraacetic acid (EDTA) buffer pH 9.0 (Abcam) in a water bath at 100ºC for 10 min. Slides were permeabilized in Tris-buffered saline 1x (TBS) (Fisher Scientific) with 0.1% Triton X-100 and 1% bovine serum albumin (BSA; both from Sigma-Aldrich). Then, a blocking step was performed with TBS 1x supplemented with 10% donkey serum (Jackson ImmunoResearch) and 1% BSA for 2 h. Samples were incubated with mouse anti-p24 Kal-1 mAb (Dako-Agilent) overnight at 4ºC. Later, rabbit anti-Siglec-1 SP213 mAb (LSBio) was added for 15 min at RT. Samples were then stained with the secondary

antibodies donkey anti-mouse Alexa Fluor 647 and donkey anti-rabbit Alexa Fluor 488 (both from Invitrogen), counterstained with DAPI (Thermo Fisher Scientific) and mounted with Fluoromount G (eBioscience). Images were obtained with an Olympus Spectral Confocal Microscope FV1000 using a 20x and 60x phase objective and sequential mode to separately capture the fluorescence at an image resolution of 800 x 800 pixels. Image J software was employed for image processing. Alternatively, samples were acquired in z-stacks every 0.2 µm on a Zeiss LSM 780 confocal inverted microscope with an apochromatic 63x oil (NA = 1.4) and processed with Volocity software (Perkin-Elmer) using the 3D Opacity module for reconstruction.

2.8 Stimulation of cervical tissues with IFNα

After dissection of the tissue as previously described (**Chapter 4, Material & Methods 2.2**), five pieces from ectocervix or endocervix were separately placed into a 12 well plate containing 1 ml of tissue culture medium. Recombinant IFN-2α was added to the medium at 1,000; 10,000 or 100,000 IU/ml. After 24 h at 37ºC and 5% CO_2, tissue was digested and the remaining culture plate was treated with accutase (Thermo Fisher Scientific) for 30 min at 37ºC to detach adherent cells. Finally, tissue and adherent cells were pooled together and stained for flow cytometry analysis as previously described (**Chapter 4, Material & Methods 2.2**).

2.9 *Trans*-infection assays

Ectocervical and endocervical blocks from HIV-1 non-infected donors were left untreated or incubated overnight with 10,000 IU/ml of IFNα and 100 ng/ml of CCL19 (MIP-3β). Tissue was then digested, pooled together and stained with mAbs as previously described (**Chapter 4, Material & Methods 2.2**) to sort single $CD45^+$ $CD3^-$ $CD19^-$ $HLA\text{-}DR^+$ live cells by FACS. Sorted cells were pre-incubated with anti-Siglec-1 7D2 or isotype control mAbs for 10 min at RT. Cells were subsequently incubated with 185 ng of p24/ml of an R5-tropic HIV-$1_{NFN\text{-}SX}$ virus (with an estimated $TCID_{50}$ of 116.824 ng/ml) in the presence of 20 µg/ml of the indicated mAbs for 4 h at 37ºC. After extensive washing, myeloid cells were co-cultured with the reporter TZM-bl cell line at a 1:1 ratio for 48 h. Finally, luciferase activity was measured with Britelite plus (Perkin-Elmer) in a Synergy MX luminometer (Biotek).

2.10 Statistical analyses

Data are reported as the mean and the SEM for each condition. Mean changes were assessed by Mann-Whitney test, Wilcoxon matched-pairs signed rank test, paired *t* test, one-way repeated measures analysis of variance (ANOVA) test and one-sample *t* test, which were considered significant at $P<0.05$. All analyses and figures were generated with the GraphPad Prism v7.0d software and R v3.5.

3. Results

3.1 Myeloid cells derived from human cervical tissues express Siglec-1

We first measured Siglec-1 expression by flow cytometry on human cervical cells derived from tissues from benign hysterectomies processed immediately after prescribed surgery. Gating on hematopoietic $CD45^+$, single and viable cells (**Figure 19A**) allowed identifying a population of HLA-DR^+ $CD3^-$ myeloid cells that represented a mean of 6 and 7.5% of cells derived from ectocervix and endocervix, respectively (**Figure 19B**, red gate and bar graph). While HLA-DR^- cells (**Figure 19B**, grey and brown gates) did not express Siglec-1 (**Figure 19C**), we found a mean of 24.5 and 11.5% of cells expressing Siglec-1 among the HLA-DR^+ fraction at the ectocervix and endocervix, respectively (**Figure 19D**, blue gate and bar graph). These cells predominantly expressed CD11c, CD14 (**Figure 19E**, pink gate and bar graph) and CD11b (**Figure 19F**, orange gate). By contrast, HLA-DR^+ cells lacking Siglec-1 expression (**Figure 19D**, yellow gate) distributed in three different subpopulations: $CD11c^+$ $CD14^+$, $CD11c^+$ $CD14^-$ and $CD11c^-$ $CD14^-$ (**Figure 19G**). Thus, we identified a subpopulation of Siglec-1^+ myeloid DCs in human cervical tissues that expresses typical interstitial DC markers such as HLA-DR, CD11b, CD11c and CD14[383].

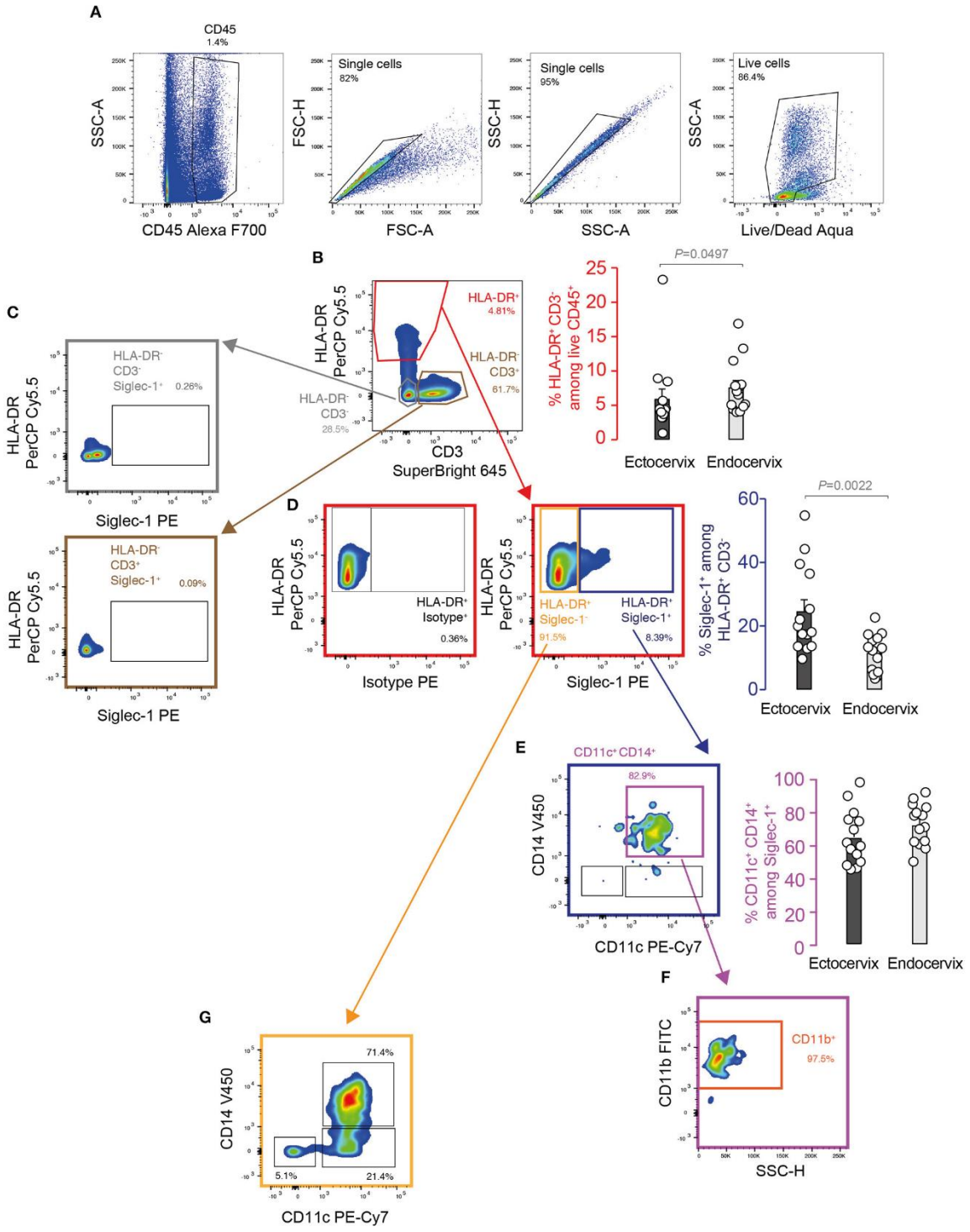

Figure 19. Siglec-1 is expressed on myeloid cells from the human cervical mucosa. Representative FACS analysis depicting the gating strategy employed to identify and characterize Siglec-1-positive cells in human cervix. Colored gates, arrows and dot plot frames indicate the analyzed populations, and color-matched bar graphs indicate the frequencies of those populations. **A.** Hematopoietic cells were identified by the expression of the common leukocyte antigen CD45, single cells were selected by doublet discrimination and viable cells identified using a live/dead Aqua staining. **B.** Representative dot plot showing distinct

populations of hematopoietic cells based on HLA-DR and CD3 staining, and bar graph representing frequencies of HLA-DR$^+$ CD3$^-$ myeloid cells. **C.** Representative dot plot illustrating the absence of Siglec-1-positive cells within the HLA-DR$^-$ fraction. **D.** Representative dot plot and frequency of Siglec-1 expression compared to a matched isotype control analyzed in the myeloid HLA-DR$^+$ fraction. **E.** Representative dot plot and frequency of CD11c/CD14 expression in myeloid HLA-DR$^+$ cells that express Siglec-1. **F.** Representative dot plot of CD11b expression in cells expressing CD11c, CD14 and Siglec-1. **G.** Representative dot plot of CD11c and CD14 expression within the HLA-DR$^+$ myeloid cells that do not express Siglec-1, indicating the presence of CD11c$^+$ CD14$^+$, CD11c$^-$ CD14$^-$ and CD11c$^+$ CD14$^-$ subpopulations. Data show mean values and SEM from 14 donors. Statistical differences were assessed using a Mann-Whitney test.

As Siglec-1 is an inducible receptor up-regulated in the presence of immune activating factors that can lead to myeloid cell maturation[70,213] (**Figure 17**), we also assessed whether Siglec-1 is preferentially expressed on mature cervical cells, which up-regulate HLA-DR[363,365]. We found that HLA-DR expression was lower in Siglec-1$^-$ cells as compared to Siglec-1$^+$ cells in both ectocervical and endocervical tissues (**Figure 20**). Thus, the activation status that leads to Siglec-1 up-regulation on cervical myeloid cells is accompanied by the maturation of these cells.

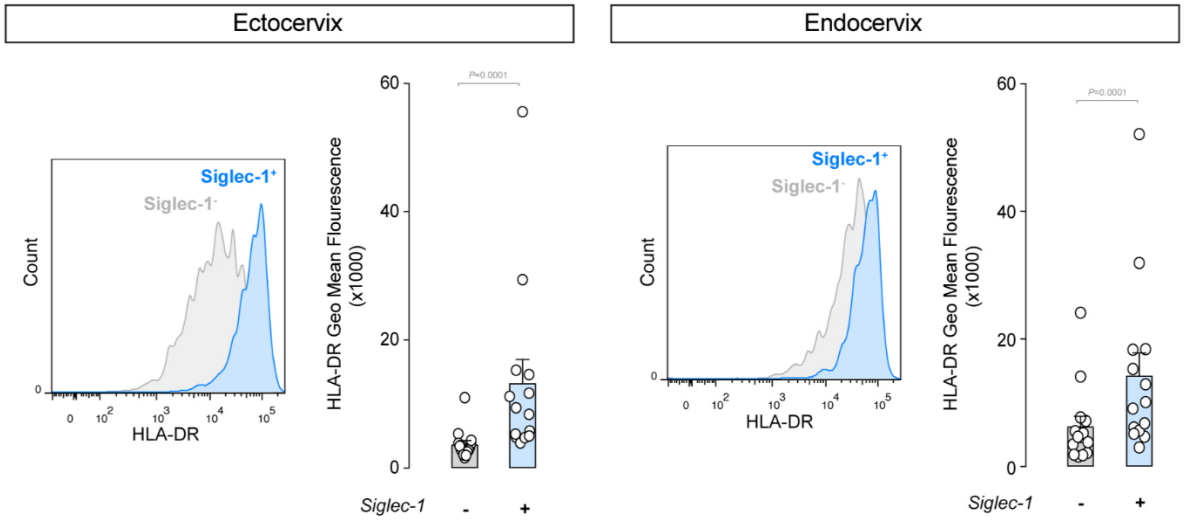

Figure 20. Siglec-1 is preferentially expressed on cervical cells with high levels of HLA-DR. Representative histograms showing HLA-DR expression on Siglec-1+ and Siglec-1- populations of CD3$^-$ CD11c$^+$ CD14$^+$ myeloid cells from ectocervical and endocervical tissues. Bar graphs show the geometric MFI and SEM of HLA-DR expression from 14 donors. Statistical differences were assessed using a Wilcoxon matched-pairs signed rank test.

3.2 Siglec-1$^+$ cells accumulate in ectocervical and endocervical submucosa

We next aimed to determine the localization of Siglec-1$^+$ cells within the cervix. For this purpose, we analyzed ectocervical and endocervical tissues from benign hysterectomies by immunofluorescence staining. Siglec-1$^+$ cells were predominantly found at the lamina propria and submucosa of both ectocervix and endocervix (**Figure 21**). Moreover, and in agreement with flow cytometry data, they were also positive for CD14 and CD11c (**Figure 21**). Of note, no Siglec-1$^+$ cells were found in the lower region of the epithelium, where Langerhans (langerin/CD207$^+$) cells usually accumulate[384].

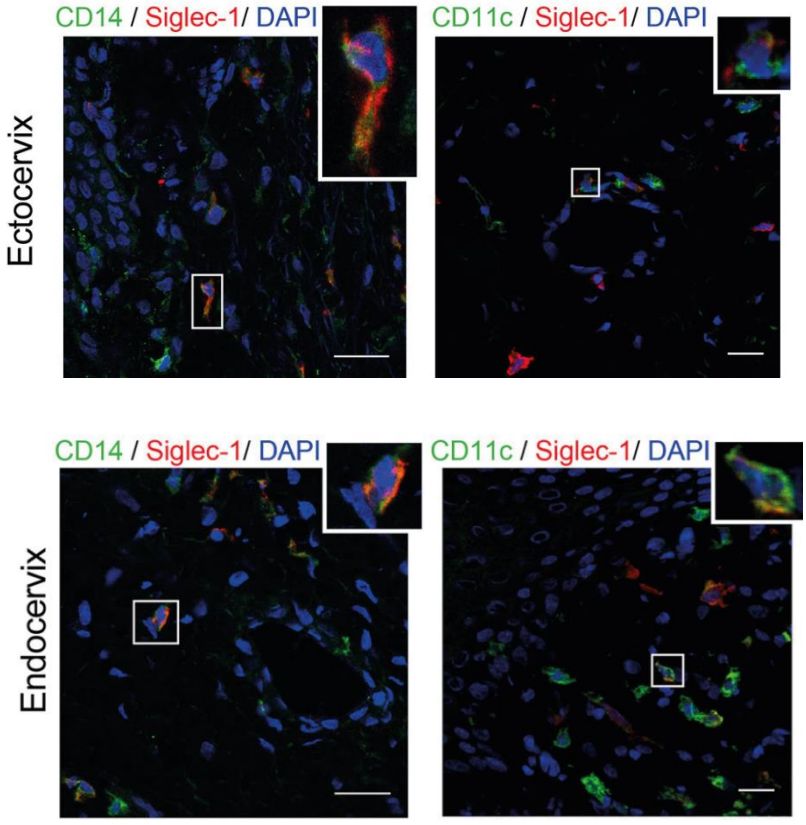

Figure 21. Siglec-1$^+$ cells locate in the submucosa of human cervical tissues. Immunofluorescent staining of Siglec-1 (Alexa Fluor 647, red) in combination with CD14 or CD11c (Alexa Fluor 488, green) in ectocervical and endocervical tissues. DAPI staining (blue) reveals the cellular nuclei. Top-right inset panels show a magnification of selected cells. Scale bars: 20 µm.

We also analyzed Siglec-1 expression on endocervix and ectocervix by immunohistochemistry, which allowed us to identify Siglec-1$^+$ cells displaying a myeloid cell morphology (**Figure 22**). These cells accumulated within the submucosa of the ectocervix, which is lined by a stratified squamous epithelium (**Figure 22A**, left panel). Similar Siglec-1$^+$ cells were found in the endocervix, which is covered by a single layer of

columnar epithelium (**Figure 22A**, right panel), albeit they were found at lower frequencies than in the ectocervix. However, those endocervical samples classified as highly inflamed based on the histopathological detection of inflammatory infiltrates displayed higher frequencies of Siglec-1$^+$ cells (**Figure 22B**), that were comparable to those observed at the ectocervix (**Figure 22A**, left panel). Of note, the higher inflammation status could not be attributed to age, particular clinical indications for surgery, HIV-1 infection or viral load (**Table 2**).

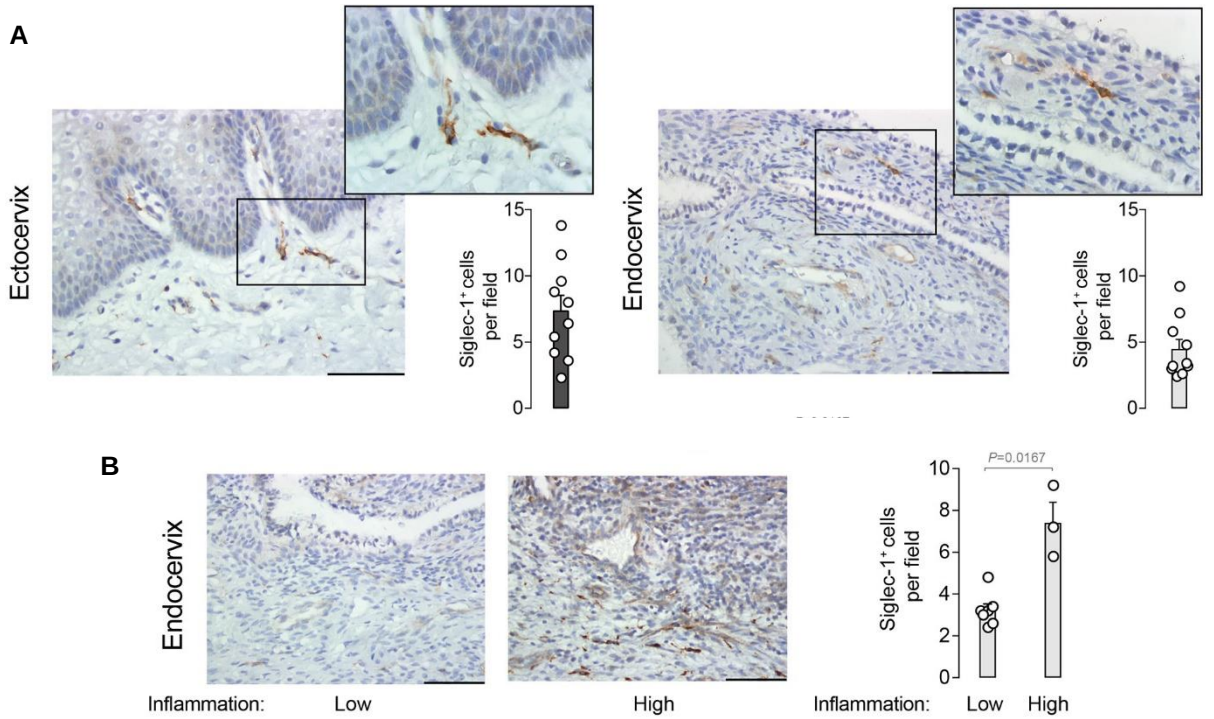

Figure 22. Siglec-1$^+$ cell frequency in endocervix depends on the inflammation status of the tissue. A. Representative images of Siglec-1 immunohistochemical staining (40x) on ten ectocervix and endocervix samples. Scale bars: 100 µm. Insets depict an amplification (100x) of the selected regions. Bar graphs show the mean values and SEM of the number of Siglec-1$^+$ cells per field counted in five consecutive fields. **B.** Representative images of Siglec-1 immunohistochemical staining (40x) of 10 endocervical tissues with different inflammation status (High/Low). Scale bars: 100 µm. Bar graph shows the mean values and SEM of the number of Siglec-1$^+$ cells per field counted in five consecutive fields of ten endocervix samples with different inflammation grades. Statistical differences were assessed using a Mann-Whitney test.

Table 2. Clinical data associated to cervical tissues where Siglec-1 was quantified by immunohistochemistry.

Patient	Siglec-1 $^{+}$ cells per field at the Ectocervix	Siglec-1 $^{+}$ cells per field at the Endocervix	Age (yr)	Indication for surgery	HIV status	Viral Load (copies /ml)
1	9,6	2,6	52	Prolapse	-	NA
2	2,3	3,4	53	Prolapse	-	NA
3	4,2	7,2*	45	Prolapse	-	NA
4	13,8	9,2*	52	Prolapse	-	NA
5	3,6	5,8*	60	Prolapse	-	NA
6	8,8	4,8	59	Unknown	+	< 50 (ART)
7	6,4	2,4	45	Prolapse	+	< 50 (ART)
8	11,6	3,2	57	Cystocele	+	140 (ART)
9	5,4	3	41	Uterine fibroids	+	400 Controller (naïve)
10	8	3,2	52	Prolapse + Cystocele	+	1.164 (naïve)

Higher levels of inflammation were observed in these tissues*

Taken together, these results demonstrate the presence of Siglec-1$^+$ cells in the steady state beneath the mucosa of ectocervix and endocervix, where cervical DCs are usually found[243].

3.3 DCs from cervical mucosa capture HIV-1 via Siglec-1 and are detected *in vivo*

In order to assess if Siglec-1$^+$ myeloid cells from cervical tissues capture and store HIV-1 via Siglec-1, we pulsed cellular suspensions processed immediately after prescribed surgery with fluorescent HIV-1$_{Gag\text{-}eGFP}$ VLPs[369–372]. After extensive washing, viral capture by cervical cells was assessed by flow cytometry. Among the single-live CD45$^+$ myeloid HLA-DR$^+$ fraction, a mean of 11.8 and 3.6% of cells expressed Siglec-1 in ectocervix and endocervix, respectively (**Figure 23A**, blue gate and bar graph), and a mean of 14.1 and 7% of cells captured HIV-1$_{Gag\text{-}eGFP}$ VLPs (**Figure 23B**, green gate and bar graph). Of note, HLA-DR$^+$ cells that did not capture HIV-1$_{Gag\text{-}eGFP}$ VLPs lacked Siglec-1 expression (**Figure 23C**), and cells that captured viral particles were predominantly Siglec-1$^+$ in most of the tissues (**Figure 23D**, purple gate and bar graph).

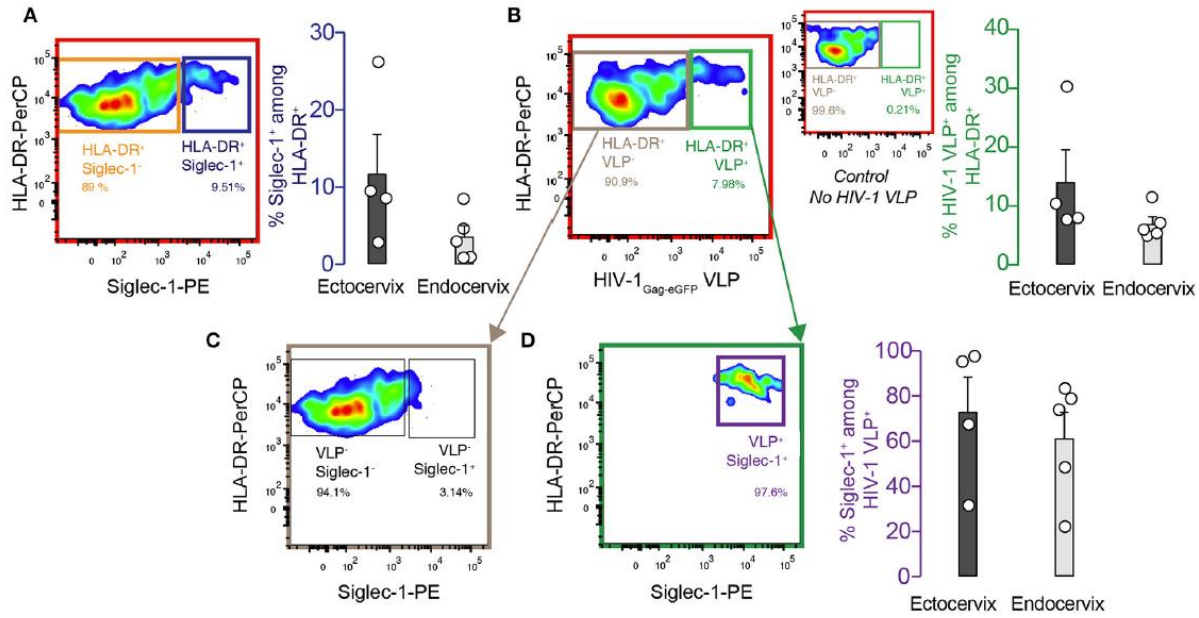

Figure 23. Myeloid cells from human cervical tissues capture HIV-1 VLPs. Ectocervical and endocervical cells were obtained from benign hysterectomies, pulsed with HIV-1$_{Gag\text{-}eGFP}$ VLPs for 18 h at 37ºC, extensively washed, labeled with the indicated antibodies and assessed by FACS. Colored gates, arrows and dot plot frames indicate the analyzed populations, and color-matched bar graphs indicate the frequencies of those populations. **A.** Representative dot plot and frequency of Siglec-1 expression in the HLA-DR$^+$ fraction of single-viable hematopoietic cells from cervical tissues. Single and viable cells were identified using the same gating strategy as in **Figure 19A**. **B.** Representative dot plot and frequency of cells capturing HIV-1$_{Gag\text{-}eGFP}$ VLPs among the HLA-DR$^+$ fraction. Smaller dot plot depicts the control

without VLPs. **C.** Representative dot plot showing reduced Siglec-1 expression on HLA-DR$^+$ cells that do not capture HIV-1$_{Gag\text{-}eGFP}$ VLPs. **D.** Representative dot plot and frequency of Siglec-1$^+$ cells among myeloid HLA-DR$^+$ cells capturing HIV-1$_{Gag\text{-}eGFP}$ VLPs. Data show mean values and SEM from ectocervical and endocervical cells from four to five donors.

Viral capture by Siglec-1$^+$ cervical cells was further confirmed by Amnis-imaging technology, which combines flow cytometry and fluorescence microscopy allowing direct visualization of acquired cells. This revealed that HIV-1$_{Gag\text{-}eGFP}$ VLPs and Siglec-1 localize within a VCC **(Figure 24)**, resembling to the sac-like structures that have been described in HIV-1-capturing MDDCs and activated tonsillar myeloid cells[70,192].

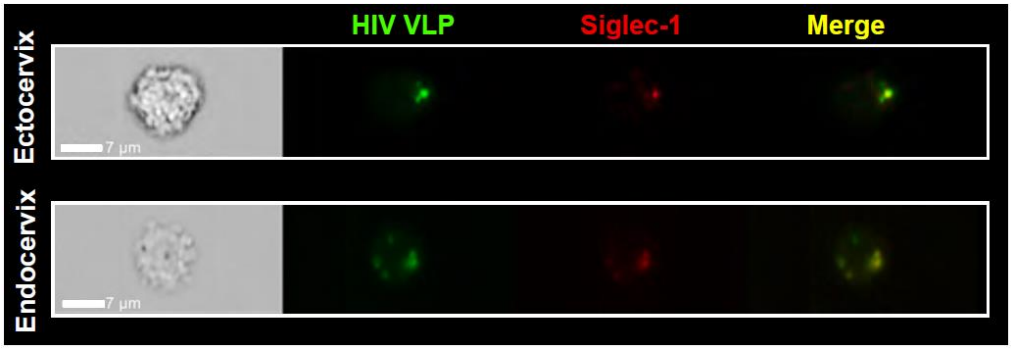

Figure 24. HIV-1 VLPs and Siglec-1 closely localize in cervical cells. Images of cervical cells derived from benign hysterectomies, pulsed with HIV-1$_{Gag\text{-}eGFP}$ VLPs for 12 h at 37ºC, extensively washed, stained with an anti-Siglec-1 mAb and acquired by Amnis-imaging FACS. Green fluorescent HIV-1$_{Gag\text{-}eGFP}$ VLPs accumulate in a sac-like VCC enriched in Siglec-1, labelled in red.

Since HIV-1$_{Gag\text{-}eGFP}$ VLPs lack the envelope glycoprotein, observed capture could only rely on Siglec-1 recognition of gangliosides that are present on the viral membranes[207,208]. Thus, Siglec-1$^+$ myeloid cells from ectocervical and endocervical tissues accumulate captured HIV-1$_{Gag\text{-}eGFP}$ VLPs within a sac-like VCC via Siglec-1 recognition of viral membrane gangliosides.

To determine if Siglec-1$^+$ cells from cervical tissues are capable of capturing wild-type HIV-1 during the natural course of HIV-1 infection, we next studied the cervical biopsy of a viremic HIV-1-infected patient by immunostaining. Confocal microscopy revealed the presence of Siglec-1$^+$ cells harboring HIV-1 p24 antigens within the cervical submucosa (**Figure 25A**). Moreover, three-dimensional z-stack reconstructions of Siglec-1$^+$ cells showed p24 accumulation within VCCs that differed from the p24 staining of productively

infected cells lacking Siglec-1 expression (**Figure 25B** and **Movie 1**). Thus, Siglec-1$^+$ cervical cells can trap HIV-1 particles throughout the course of HIV-1 infection *in vivo*.

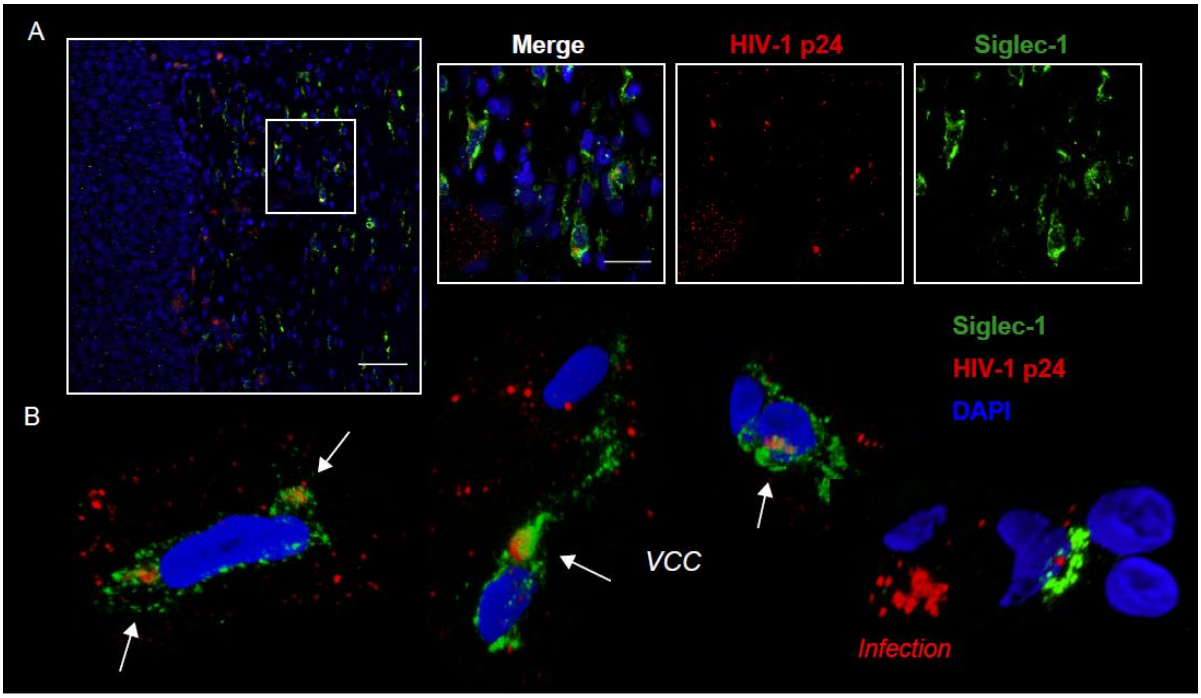

Figure 25. *In vivo*, Siglec-1$^+$ cervical cells accumulate HIV-1 within VCCs. A. Immunofluorescent staining of paraffin-embedded cervical tissue from a viremic HIV-1-infected woman labeling HIV-1 p24 antigen (red), Siglec-1 (green) and cell nucleus (blue). Scale bar: 50 µm. Inset panels zoom in the squared region showing different fluorescences. Scale bar: 20 µm. **B.** Three-dimensional volumetric x-y-z data field reconstruction of Siglec-1$^+$ cells from four different areas of the cervical tissue of the viremic HIV-1-infected individual. Opacity representation of DAPI-stained nuclei and fluorescence of the virus-containing compartment (VCC; white arrows), where HIV-1 p24 accumulation differs from the scattered pattern associated to productive viral replication shown in the right bottom image (Infection).

3.4 IFNα enhances Siglec-1 and HIV-1 capture on cervical DCs

Previous results indicated that the basal expression of Siglec-1 is sufficient to promote viral capture by myeloid cells from the cervix. However, this receptor is potently up-regulated on myeloid cells by type I IFNs such as IFNα[187,192,213] (**Figure 17**). In the cervical mucosa, resident myeloid cells readily produce type I IFNs in response to SIV/HIV infection[385]. Thus, we next investigated whether IFNα could trigger Siglec-1 expression on cervical myeloid cells and enhance Siglec-1-depedent HIV-1 capture. For this purpose, we cultured small pieces of ectocervix and endocervix[381] in the presence or absence of increasing concentrations of recombinant IFNα. After enzymatic digestion, cells were analysed by FACS. The percentage of Siglec-1$^+$ cells among the myeloid HLA-DR$^+$ CD11c$^+$ CD14$^+$

DC fraction increased with IFNα concentration in a dose-dependent manner (**Figure 26**). Thus, IFNα up-regulates Siglec-1 on cervical DCs, as it does on MDDCs and tonsillar myeloid cells[187,192].

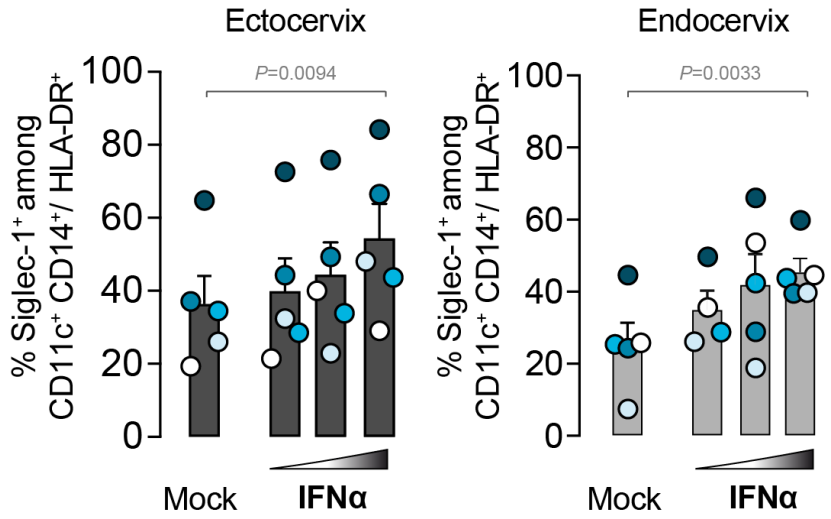

Figure 26. IFNα induces Siglec-1 expression on cervical DCs. Frequency of Siglec-1$^+$ cells among the myeloid HLA-DR$^+$ CD11c$^+$ CD14$^+$ fraction from small pieces of ectocervical and endocervical tissues cultured in the presence or absence of increasing concentrations of IFNα (1,000; 10,000 and 100,000 IU/ml) and assessed by FACS as in **Figure 19**. Data show mean values and SEM from four independent experiments and include cells from ectocervix and endocervix of five donors. Colors depict each particular donor. Statistical differences were assessed using a one-way repeated measures ANOVA test.

We next determined if IFNα enhances the capacity of cervical DCs to capture HIV-1 particles. In this case, cervical tissue pieces were digested and cell suspensions were pulsed with HIV-1$_{Gag\text{-}eGFP}$ VLPs in the presence or absence of IFNα. FACS analysis revealed that, under these conditions, IFNα treatment also increased the frequency of Siglec-1$^+$ cells (**Figure 27A**). This effect that was more prominent in the endocervix, where basal Siglec-1 expression was lower (**Figures 19D** and **27A**). Accordingly, IFNα treatment increased the percentage of myeloid HLA-DR$^+$ CD11c$^+$ CD14$^+$ DCs capturing HIV-1$_{Gag\text{-}eGFP}$ VLPs, especially at the endocervix (**Figure 27B**). This indicates that endocervical DCs might acquire a higher capacity to *trans*-infect HIV-1 once the antiviral type I IFN response is mounted and Siglec-1 expression is triggered on DCs.

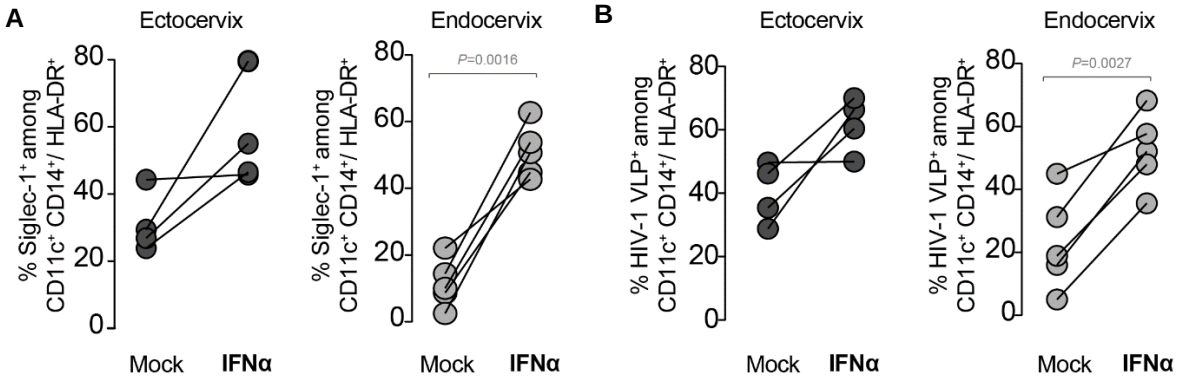

Figure 27. IFNα enhances HIV-1 VLP capture by cervical DCs. A. Frequency of Siglec-1$^+$ cells among the myeloid HLA-DR$^+$ CD11c$^+$ CD14$^+$ fraction of cervical suspensions obtained by tissue digestion and cultured in the presence or absence of IFNα. Statistical differences were assessed using a paired *t* test. **B.** Percentage of cells capturing HIV-1$_{Gag\text{-}eGFP}$ VLPs among the myeloid HLA-DR$^+$ CD11c$^+$ CD14$^+$ fraction of cervical suspensions obtained by cervical tissue digestion and cultured in the presence or absence of IFNα. Statistical differences were assessed using a paired *t* test.

3.5 Anti-Siglec-1 mAbs block HIV-1 capture and *trans*-infection mediated by cervical DCs

Our results suggested that anti-Siglec-1 mAbs, which block HIV-1 *trans*-infection mediated by MDDCs[70,187], could offer protection against HIV-1 uptake and prevent dissemination mediated by cervical cells. Thus, we pre-incubated cell suspensions from the ectocervix and endocervix with an anti-Siglec-1 mAb or an isotype control before HIV-1$_{Gag\text{-}eGFP}$ VLP exposure. While the isotype control had no blocking effect, pre-treatment with the anti-Siglec-1 mAb led to a reduction of HIV-1$_{Gag\text{-}eGFP}$ VLP uptake by DCs even after IFNα treatment (**Figure 28**).

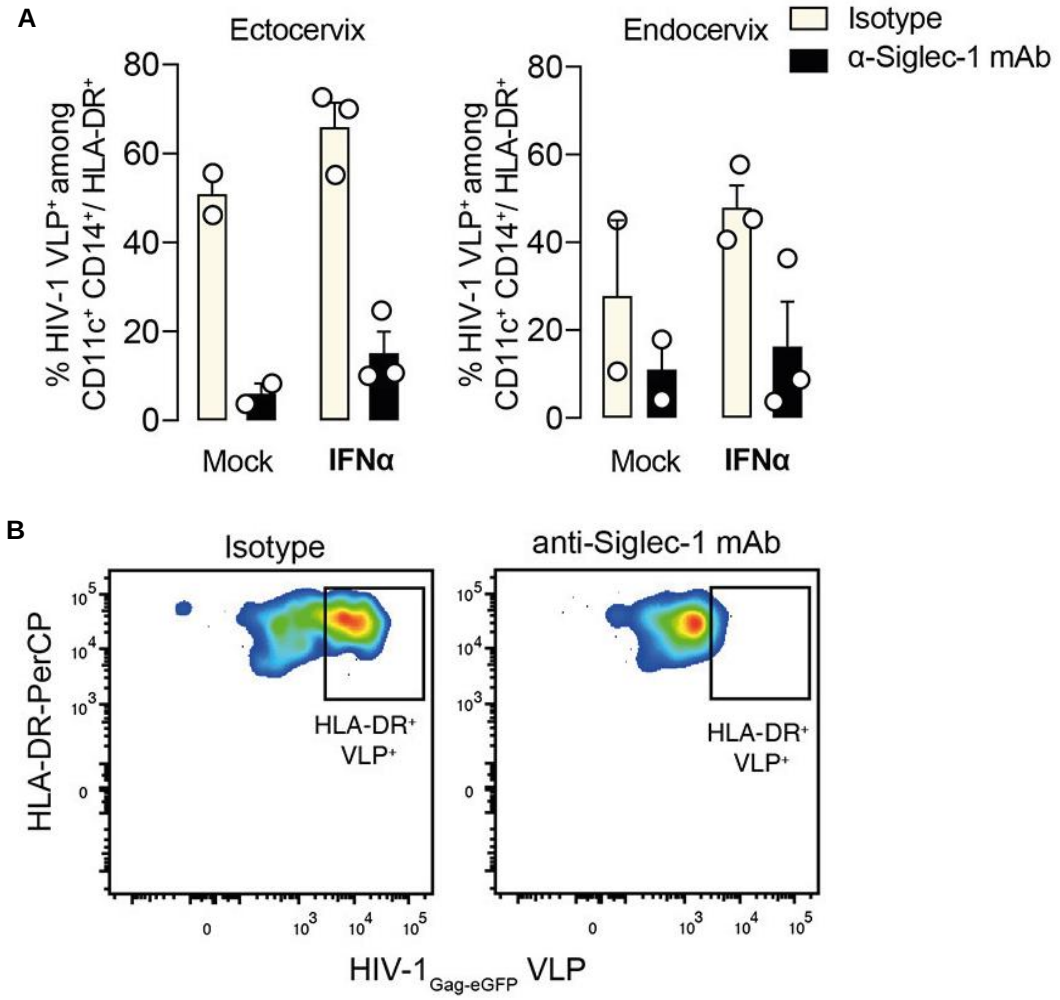

Figure 28. Anti-Siglec-1 mAbs impair HIV-1 capture by cervical DCs. A. Frequency of cells capturing HIV-$1_{Gag\text{-}eGFP}$ VLPs among the myeloid HLA-DR$^+$ CD11c$^+$ CD14$^+$ fraction of cervical cell suspensions cultured in the presence or absence of IFNα and pre-incubated with 20 µg/ml of anti-Siglec-1 7D2 mAb or an isotype control. Bar graphs show mean values and SEM from two to three donors. **B.** Representative inhibition of HIV-$1_{Gag\text{-}eGFP}$ VLP capture by anti-Siglec-1 7D2 mAb.

Next, we addressed whether blocking Siglec-1 reduced the capacity of myeloid cervical DCs to transmit HIV-1 to target cells via *trans*-infection. For this purpose, mock- or IFNα-treated HLA-DR$^+$ CD3$^-$ cervical DCs were sorted and pulsed with wild-type R5-tropic HIV-$1_{NFN\text{-}SX}$ in the presence of an anti-Siglec-1 mAb or an isotype control. After extensive washing, cells were co-cultured with a reporter CD4$^+$ cell line to measure viral *trans*-infection (**Figure 29**). Of note, the expression of Siglec-1 on these cells at the steady state is shown in **Figure 19D**. In seven independent cervicovaginal tissues, we consistently observed a reduction in HIV-1 transmission levels by cells treated with the anti-Siglec-1 mAb as compared to the isotype control, with a mean of 70% of reduction in viral

transmission (**Figure 29**). These results confirm the contribution of Siglec-1 on viral *trans*-infection mediated by cervical DCs and highlight the potential use of anti-Siglec-1 mAbs to block this mechanism of viral cell-to-cell transmission.

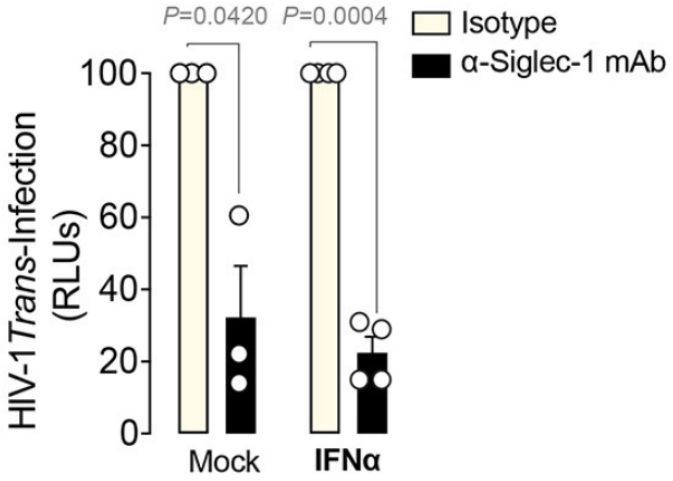

Figure 29. Anti-Siglec-1 mAbs block HIV-1 *trans*-infection mediated by cervical DCs. Relative transmission of the R5-tropic HIV-1_{NFN-SX} to $CD4^+$ target cells by cervical $CD45^+$ HLA-DR^+ $CD3^-$ $CD19^-$ sorted cells in the presence or absence of IFNα and pre-incubated with 20 µg/ml of isotype or anti-Siglec-1 7D2 mAbs before viral exposure. Values are normalized to those of isotype-treated cells, which are set as 100%. Data show mean values and SEM from two independent experiments and include cells from three-four donors. Statistical differences were assessed using a one-sample *t* test.

Overall, the results of this chapter identify the presence of Siglec-1-expressing cells in cervical tissues in the basal state that are capable of capturing HIV-1 and mediate viral transmission to target $CD4^+$ cells. Moreover, Siglec-1 is up-regulated on cervical DCs upon IFNα exposure, an effect that is more remarkable in the endocervix, where basal Siglec-1 expression is lower than in the ectocervix. Thus, we propose that Siglec-1^+ cervical DCs might facilitate HIV-1 *trans*-infection within the cervical tissues and favour the nascent infection, as well as viral dissemination to the secondary lymphoid tissues, even in the presence of the antiviral IFNα environment. These findings highlight the importance of including Siglec-1 inhibitors along with antiretroviral agents in forthcoming microbicidal strategies, to stop not only the productive cellular infection in the cervix, but also the systemic viral dissemination from the female genital tract. As anti-Siglec-1 mAbs efficiently block HIV-1 *trans*-infection mediated by cervical DCs, we propose to include them in strategies aimed at blocking DC-mediated viral dissemination.

Chapter 5

RESULTS III

New anti-Siglec-1 mAbs block HIV-1 capture and *trans*-infection mediated by DCs

The results included in this chapter are part of:

Perez-Zsolt, D., Erkizia, I., Pino, M., García-Gallo, M., Martín, M.T., Benet, S., Chojnacki, J., Fernández-Figueras, M.T., Guerrero, D., Urrea, V., Muñiz-Trabudua, X., Kremer, L., Martinez-Picado, J.* and Izquierdo-Useros, N.* (2019). **Anti-Siglec-1 antibodies block Ebola viral uptake and decrease cytoplasmic viral entry**. *Nat Microbiol*. 4(9):1558-1570. doi: 10.1038/s41564-019-0453-2.

*Last authors.

1. Introduction

Preventing new HIV-1 infections is one of the strategies adopted by the World Health Organization to control the HIV-1 epidemic[386]. Sexual transmission is the main cause of HIV-1 acquisition[375], with young women in Sub-Saharan Africa being at particular risk of acquiring HIV-1 through sexual intercourse[108]. Current microbicidal strategies aimed at preventing sexual HIV-1 acquisition by women are based on antiretroviral drugs that block different steps of the viral cycle, as reviewed in ref.[156]. These agents efficiently hamper productive infection of target cells, preventing generation of *de novo* synthesized viral particles. However, HIV-1 can also be transferred to $CD4^+$ T cells by DCs via *trans*-infection, a cell-to-cell viral transmission mechanism that does not rely on productive infection of DCs[88,179]. Instead, this process depends on the capacity of DCs to capture and store large amounts of viruses and to transfer them to target $CD4^+$ T cells upon the formation of infectious synapses[188]. This mechanism has been proposed to occur locally in HIV-1 entry sites, such as the cervicovaginal mucosa[98]. Moreover, evidence suggests that cervical HIV-1-bearing DCs migrate to the regional lymph nodes, spreading the infection systemically[89,133,134,380]. Thus, an effective strategy aimed at preventing HIV-1 sexual transmission in women should include antiretrovirals to block productive viral replication at the cervicovaginal mucosa, but also tackle DC-mediated viral dissemination via *trans*-infection.

Siglec-1 is the key molecule for HIV-1 *trans*-infection[70,187]. In the previous chapter, we showed that *trans*-infection mediated by cervical DCs can be blocked using mAbs against Siglec-1. Therefore, we propose the use of anti-Siglec-1 mAbs in combination with antiretroviral drugs to improve the efficacy of forthcoming microbicides. Although murine anti-Siglec-1 clones are commercially available, the clinical use of these mAbs would require a process of humanization. However, this strategy is out of our reach, as we have no access to the original hybridomes producing these mAbs and we lack critical information about them, including their aminoacidic sequences, which are needed for adequate humanization. Thus, here we aimed to generate a set of new anti-Siglec-1 mAbs with the capacity to block DC-mediated HIV-1 capture and *trans*-infection, which could eventually be humanized for their clinical use.

In this chapter we explain how we selected and produced five new anti-Siglec-1 clones with high affinity for Siglec-1 that bind to different epitopes on the N-terminal region of the receptor, while comparing their activity to commercially available clones such as 7-239

and 7D2. Moreover, we show that new clones efficiently block HIV-1 capture and *trans*-infection mediated by DCs. Thus, the newly generated anti-Siglec-1 mAbs could be promising tools to combine with antiretroviral agents and generate efficient microbicides to combat HIV-1 sexual transmission in women.

2. Material & Methods

2.1 Ethics statement

This study was approved by the institutional review board on biomedical research from HUGTiP (Badalona, Spain). All individuals involved in this study gave their written informed consent to participate. Animal care and treatment was carried out at Centro Nacional de Biotecnología/Centro Superior de Investigaciones Científicas (CNB/CSIC, Madrid, Spain) in accordance with Spanish and EU laws. The CSIC Ethics Committee approved the experiments and the Agriculture Department of the Community of Madrid approved the use of experimental animals (reference numbers PROEX 18/4 and PROEX 121/16).

2.2 Cells and viral stocks

MDDCs were obtained and activated as previously described (**Chapter 3**, **Material & Methods 2.2**).

HEK-293T cells and TZM-bl cell lines were cultured as previously described (**Chapter 3**, **Material & Methods 2.3** and **Chapter 4**, **Material & Methods 2.5**, respectively). Raji B-lymphocyte cell line (kindly provided by Dr. Y. van Kooyke) were maintained in RPMI supplemented 10% FBS, 100 IU/ml of penicillin and 100 µg/ml of streptomycin (all from Invitrogen).

Murine cells stably expressing human Siglec-1 were generated by electroporation of pCMV6-Entry comprising the coding region of human Siglec-1 (OriGene) followed by selection in blasticidine-containing media (InvivoGen). HEK-293T cells were transfected with 30 µg of pCMV6-Entry containing coding regions of human Siglec-1, Siglec-5 or Siglec-7 (all from OriGene) using calcium phosphate (Calphos; Clontech). Cells were stained with anti-Siglec-1 7-239 PE, anti-Siglec-5/14 1A5 PE (both from BioLegend) or Siglec-7 5-386 PE mAbs (AbD Serotec) to determine surface expression of all receptors. Of note, Siglec-14 shares 100% of amino acid homology with Siglec-5 in the V-set domain,

and thus mAbs recognizing Siglec-5 cross-react with Siglec-14. Raji cells were used to develop a stable cell line expressing Siglec-1 (Raji Siglec-1). Cells were transfected with Siglec-1 plasmid by using Amaxa nucleofector (Lonza) following manufacturer's instructions. Transfected cells were sorted and cloned in a FACSVantage SE and maintained in RPMI with 1 mg/ml of geneticin for selection of a stable clone with high Siglec-1 expression, which was assessed staining with anti-Siglec-1 7-239 PE (BioLegend).

HIV-$1_{Gag\text{-}eGFP}$ VLP and HIV-$1_{NL4.3}$ stocks were obtained, quantified and titrated as previously described (**Chapter 4**, **Material & Methods 2.5**). For HIV-$1_{NL4.3}$ stock, a pNL4-3 plasmid from the NIH AIDS Research and Reference Reagent Program was employed.

2.4 Mice immunization and generation of new anti-Siglec-1 mAbs

Three groups of five female BALB/c mice (Envigo) were immunized three times with either $8x10^6$ IFNα-treated human DCs or $20x10^6$ 300.19 murine cells stably expressing human Siglec-1. One group of five female C57BL/6J mice (Envigo) were immunized 3 times with $20x10^6$ L1.2 C57BL/6J murine cells stably expressing human Siglec-1 with or without 10 µg of CpG ODN 1826 adjuvant (InvivoGen). Mice received 3 dorsal subcutaneous injections in a 28-day interval with immunogens diluted in Freund's adjuvant (300 µl). At days 68-72, blood was extracted to analyse serum responses. All sera derived from immunizations with Siglec-1-positive cells had blocking activity, and were further assessed by ELISA and FACS.

An ELISA plate covered with 1 µg/ml of recombinant human Siglec-1 (R&D Systems) was used to detect sera containing Siglec-1-specific mAbs, including 1 µg/ml of the commercial clones 7D2 and 7-239 as positive controls. In addition, sera were employed to label Raji Siglec-1 cells with a secondary anti-mouse IgGs labelled in PE (Invitrogen) and assessed by FACS. Best antibody-producing mice were identified based on the capacity of their sera to yield positive ELISA and FACS results at lower dilutions. Splenocytes from those mice were employed to produce hybridomas, and the secreted mAbs were tested for Siglec-1 recognition using Raji Siglec-1 cells. Best hybridomas were cloned twice and further analysed in HIV-$1_{Gag\text{-}eGFP}$ VLP capture assays. Five hybridomas generating five new anti-Siglec-1 mAbs (namely 3F1, 5B10, 1F5, 6G5 and 4E8) were selected based on their ability to recognize Siglec-1 and block HIV-$1_{Gag\text{-}eGFP}$ VLP uptake. DNA from hybridomas was

sequenced following the standard operating procedure from GenScript. mAbs were purified by protein A or protein G affinity chromatography using HiTrap columns (GE Healthcare).

Specificity of purified anti-Siglec-1 mAbs was assessed against HEK-293T cells transfected with Siglec-1, -5 and -7 revealed with DyLight 649 secondary IgG mAb (Invitrogen). The same secondary mAb was employed to confirm recognition of Raji Siglec-1 cells by new anti-Siglec-1 mAbs. Isotypes were determined by ELISA using peroxidase-conjugated antibodies with specificity for the heavy chain of murine IgG1, IgG2a, IgG2b, IgG3 or IgM (Southern Biotech).

2.5 Siglec-1 mini-protein ELISA

Siglec-1 mini-protein was constructed by inserting the XbaI restriction fragment from the OriGene Siglec-1 plasmid (including the V-set domain and 3 Ig-like domains of the receptor) into the XbaI restriction fragment of the pcDNA3-human constant antibody fragment (Fc) plasmid (kindly provided by Dr. Javier Dominguez). The plasmid was sequenced and transfected into HEK-293T cells with calcium phosphate (CalPhos; Clontech), and secreted protein was harvested 48-72 h post-transfection and detected by Western blot using the anti-Siglec-1 7D2 mAb. Siglec-1 mini-protein was added to Nunc MaxiSorp ELISA plates (Invitrogen) coated with 5µg/ml of goat anti-human Fc and employed for detection of new and commercial mAbs with a horseradish peroxidase (HRP)-labelled goat anti-mouse IgG $F(ab')_2$ (Jackson ImmunoResearch). Murine IgG2b (eBioscience) or IgG1 (BD) isotype mAbs were used as negative controls.

2.6 Surface Plasmon Resonance (SPR) analyses of anti-Siglec-1 mAbs

SPR analyses were carried out with a Biacore 3000 (GE Healthcare). Human Siglec-1 recombinant protein was immobilized at 10 µg/ml in sodium acetate 10 mM pH 5.0 onto a CM5 sensor chip using an amine coupling method as indicated by the supplier. Hepes-buffered saline (HBS)-EP (Biacore; GE Healthcare) was used as running buffer. Kinetic assays to estimate the equilibrium dissociation constant (K_{D1}) were performed using different concentrations of mAbs (1,23-100 nM) at a flow rate of 30 µl/min, an association time of 2 min and a dissociation time of 5 min. Competition binding assays were performed as previously described[387], with anti-Siglec-1 specific mAbs (100 nM) injected at a flow rate of 30 µl/min. Two mAbs were sequentially injected in a single cycle (co-inject option) for 2 min. Three control analyses were used: i) injection of first mAb followed by running

buffer, ii) co-injection of first mAb, and iii) injection of running buffer followed by second mAb. The chip surface was regenerated with a single pulse of 10 mM Glycine-HCl 10 mM pH 1.7 for 10 sec at the same flow rate.

Sensograms were analysed using the BIAevaluation software 4.1 and resonance data were overlaid, aligned and fitted to a bivalent model. All data sets were processed using a double-referencing method[388]. Percentage of binding inhibition to Siglec-1 of the second mAb by the first mAb was carried out according to ref.[389] by the following calculation: 100 – [(second mAb binding in the presence of first mAb)/(second mAb binding in the absence of the first mAb)] x 100.

2.7 Competition between new anti-Siglec-1 mAbs and HIV-$1_{Gag\text{-}eGFP}$ VLPs in Raji Siglec-1 cells

A constant amount of 150 ng of HIV-$1_{Gag\text{-}eGFP}$ VLP p24 was mixed in parallel with increasing concentrations of commercial anti-Siglec-1 mAbs (clones 7-239 and 7D2), new anti-Siglec-1 mAbs (clones 3F1, 5B10, 1F5, 6G5 and 4E8) and IgG1 isotype control. $2x10^5$ Raji Siglec-1 cells were pulsed with these mixes for 1 h at 37ºC, washed and assessed by FACS. Equivalent quantities of two mAbs were mixed to achieve the same concentrations used for single-mAb experiments. Of note, concentration of all mAbs employed (included commercial ones) was confirmed using a sandwich ELISA revealed with goat HRP-conjugated polyclonal anti-mouse Igs antibodies (Dako). An IgG2b mAb (BD Biosciences) was included as standard for quantification.

2.8 HIV-$1_{NL4\text{-}3}$ uptake and *trans*-infection assays

$2x10^5$ DCs were incubated with 80 ng of HIV-$1_{NL4\text{-}3}$ p24 for 3 h at 37ºC. For blockade, cells were pre-incubated for 15 min at RT with 10 µg/ml of anti-Siglec-1 mAbs 7D2, 7-239 (both from Abcam), new anti-Siglec-1 mAbs, an IgG1 isotype control (BD Biosciences) or left untreated before viral exposure. After extensive washing, part of the cells was lysed with 0.5% Triton X-100 (Sigma-Aldrich) to measure $p24^{Gag}$ content by ELISA (Perkin-Elmer). Remaining DCs were co-cultured with the reporter cell line TZM-bl at a 1:1 ratio to measure *trans*-infection. Co-cultures were assayed for luciferase activity 48 h later (BrightGlo luciferase system; Promega) using a Fluoroskan Ascent FL luminometer (Thermo Labsystems). Background values from non-HIV-1 pulsed co-cultures were substracted for each experiment.

2.9 Statistical analyses

Data are reported as the mean and the SEM for each condition. Mean changes were assessed by a paired *t* test, considered significant at $P<0.05$. Mean changes from 100% normalized values were assessed with a one-sample *t* test, considered significant at $P<0.05$. Response curves of mAbs were adjusted to a non-linear fit regression model (calculated with a four-parameter logistic curve with variable slope) and the associated extra sum-of-squares F tests were used to compare significant differences between the $logIC_{50}$ of mAbs. All analyses and figures were generated using GraphPad Prism v7.0d software and R v3.5.

3. Results

3.1 Generation and characterization of new anti-Siglec-1 mAbs

Given the potential therapeutic benefit of blocking Siglec-1 to control HIV-1 dissemination, we began a screening for identifying new anti-Siglec-1 mAbs with the capacity to interfere with DC-mediated viral *trans*-infection. We first attempted to generate anti-human-Siglec-1 murine mAbs immunizing mice with peptides from the Siglec-1 V-set domain that directly interact with sialylated ligands[26]. However, although the generated polyclonal antibodies recognized those peptides, they failed to bind to the native receptor, suggesting the requirement of a three-dimensional immunogen to generate receptor-binding mAbs[390]. Thus, we next immunized mice with murine and human cells expressing high levels of the native human Siglec-1 receptor. After screening over a thousand hybridomas from these immunizations, five new clones (3F1, 5B10, 1F5, 4E8 and 6G5) were selected for their capacity to produce mAbs recognizing both cellular Siglec-1 receptor and a recombinant Siglec-1 protein. Upon purification, mAb specificity was demonstrated by their binding capacity to HEK-293T cells transfected with a plasmid coding for human Siglec-1, which was absent in Siglec-5 or Siglec-7 transfected cells (**Figure 30A-B**). Moreover, all new mAbs bound to Raji B-lymphocytes expressing human Siglec-1, similarly to commercial clones such as 7-239 and 7D2 (**Figure 30C**).

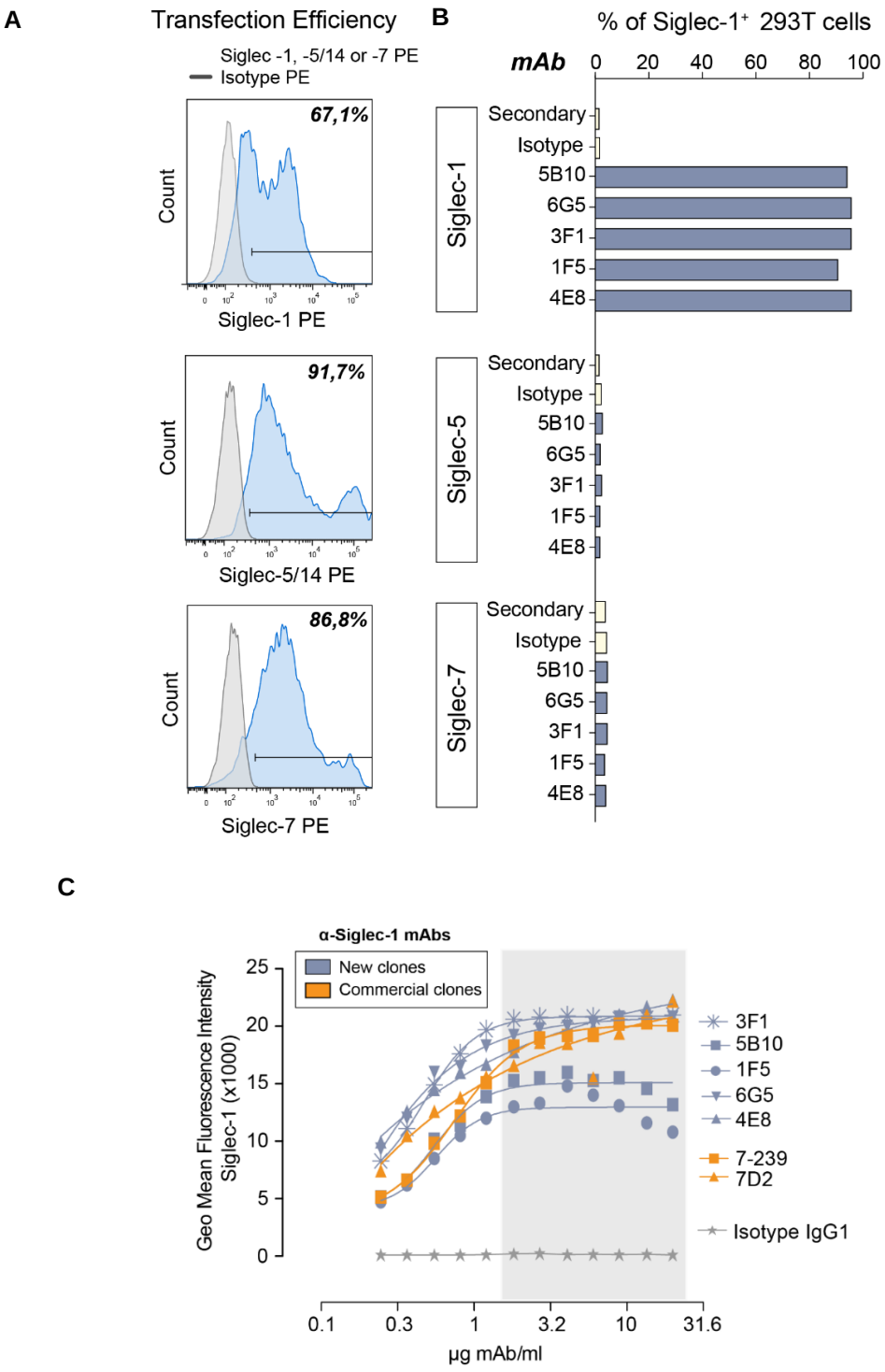

Figure 30. New mAbs produced upon mice immunization with Siglec-1-expressing cells recognize native Siglec-1 receptor. A. Transfection efficiency percentages of HEK-293T cells assessed by cell surface staining of Siglec-1, Siglec-5/14 and Siglec-7 (blue lines) as compared to an isotype control (grey lines). Of note, Siglec-14 shares 100% of amino acid homology with Siglec-5 in the V-set domain, and thus mAbs recognizing Siglec-5 cross-react with Siglec-14. Data from one experiment. **B.** Staining of HEK-293T cells transfected with human Siglec-1 plasmid using new anti-Siglec-1 mAbs and assessed by FACS, and lack of recognition of Siglec-5 and Siglec-7 transfected cells. A DyLight 649 secondary IgG mAb was

employed to reveal the assay. Siglec-5 plasmid was chosen because it displays the highest sequence homology to the V-set domain of Siglec-1. Data from one experiment. **C.** Representative Siglec-1 staining of Raji Siglec-1 cells labelled with increasing concentrations of new anti-Siglec-1 mAbs (3F1, 5B10, 1F5, 6G5, 4E8; shown in blue), commercial anti-Siglec-1 mAbs (7D2, 7-239; shown in orange) and an isotype control (shown in grey) revealed with a DyLight 649 secondary IgG mAb. Non-linear fit to a variable response curve is depicted for each mAb, and the shadowed area indicates saturating concentrations. Data from one experiment.

New mAbs were further characterized to determine gene usage, sequence identity, isotype and affinity for Siglec-1 (**Figure 31**). Sequence analysis revealed that new mAbs share 93 to 98% germline identity for heavy chains and 95 to 98% for light chains, with a distinctive germline gene usage indicative of their unique B cell lineage origin (**Figure 31A**). Moreover, they displayed two distinct isotypes, IgG1 and IgG2b (**Figure 31A**). Apparent affinity of new and commercial anti-Siglec-1 mAbs was estimated by SPR, where the full human Siglec-1 protein was covalently immobilized to a sensor chip. Determination of K_{D1} for Siglec-1 of each mAb revealed that all displayed high affinities below the nanomolar range (**Figure 31B**).

A

mAb	VH	Identity (%)	VL	Identity (%)	IgG
3F1	V1S34*01 F	97.69	V8-27*01 F	97.98	IgG1
5B10	V1-59*01 F	93.75	V8-24*01 F	95.62	IgG2b
1F5	V1-76*01 F	93.06	V8-21*01 F	97.31	IgG2b
4E8	V3-8*02 F	97.54	V6-15*01 F	98.21	IgG1
6G5	V1-72*01 F	93.75	V4-57-1*01F	97.16	IgG1

B

mAb	K_{D1} (M^{-1})
3F1	5.7×10^{-10}
5B10	3.9×10^{-10}
1F5	2.9×10^{-10}
4E8	6×10^{-10}
6G5	2.9×10^{-10}
7-239	3.1×10^{-10}
7D2	9.7×10^{-10}

Figure 31. Characterization of new anti-Siglec-1 mAbs. A. Variable heavy (VH) and variable light (VL) chains-gene usage, sequence analysis, and IgG subclass determined by ELISA for new anti-Siglec-1 mAbs. **B.** Equilibrium dissociation constants (K_{D1}) of new and commercial mAbs calculated by fitting to a bivalent model the kinetic parameters obtained by SPR analysis, where recombinant human Siglec-1 was covalently immobilized to a sensor chip.

3.2 New anti-Siglec-1 mAbs bind to different epitopes

To further define the Siglec-1 binding region of new mAbs, we employed a recombinant Siglec-1 mini-protein that expresses the V-set domain plus three Ig-like domains fused to a human Fc domain bound to an ELISA plate. Siglec-1 mini-protein was effectively

detected by new and commercial mAbs (**Figure 32**). Thus, all binding epitopes are located in these four N-terminal domains.

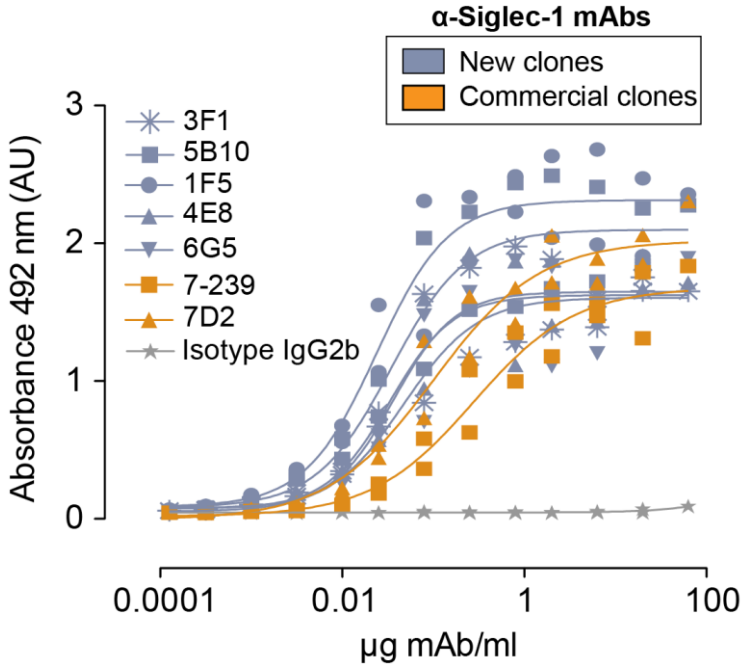

Figure 32. Epitopes recognized by new anti-Siglec-1 mAbs locate within the four N-terminal domains of the receptor. Binding of the indicated anti-Siglec-1 mAbs to immobilized Siglec-1 mini-proteins (V-set plus three Ig-like domains) detected by ELISA.

We next analyzed relative competition for binding to Siglec-1 between all possible mAb pairs using SPR. Two representative experiments are shown in **Figure 33**. We sequentially injected two mAbs in a single cycle (**Figure 33**, blue lines). Competition of the second mAb with the first mAb (**Figure 33**, left graph) was observed when after adding the second mAb, we retrieved a similar signal as controls in which after the first mAb we injected buffer or the first mAb again (**Figure 33**, grey lines). In contrast, no competition was observed (**Figure 33**, right graph) when signal obtained after sequentially injecting the first and second mAbs was similar to that of injecting the second mAb after buffer (**Figure 33**, red lines).

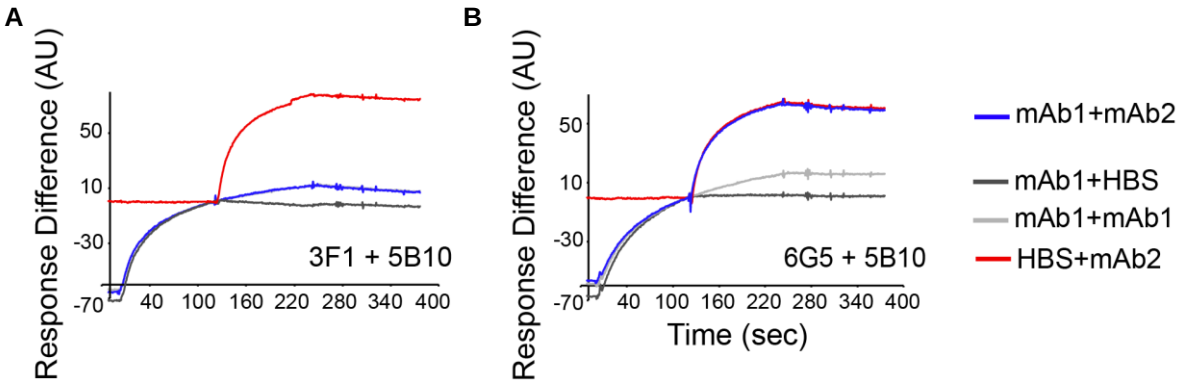

Figure 33. Representative SPR competition assays. Competitive Siglec-1 binding assays of mAb pairs assessed by surface plasmon resonance, where a recombinant human Siglec-1 protein was covalently immobilized in a sensor chip. Graphs show response difference (arbitrary units; AU) over time (sec) of sequentially co-injected mAb pairs in a single cycle. **A.** Example of competition for Siglec-1 binding between the first and second mAbs (3F1 and 5B10), where co-injection (blue line) retrieved the same signal as controls in which we injected buffer after the first mAb (dark grey line) or we co-injected the first mAb (light grey line). **B.** Example of lack of competition between the first and second mAbs (6G5 and 5B10), where the signal retrieved by co-injection (blue line) was similar to that obtained when buffer was injected before the second mAb (red line). Association-dissociation curves of all individual competition experiments are shown in **Figure 34**. HBS: hepes-buffered saline.

All cross-competition analyses (**Figure 34**) allowed calculation of the percentage of inhibition of the second mAb binding exerted by the first mAb (**Figure 35A**). New mAbs 5B10 and 1F5, on the one hand, and 4E8 on the other competed with commercial mAbs 7-239 and 7D2, respectively, while 3F1 competed with both 5B10 and 1F5 (**Figures 34, 35A**). This is likely due to steric hindrance caused by mAbs binding to the same epitope or in close proximity, although conformational changes induced by the first mAb could also difficult the access to the epitope recognized by the second mAb. Through combinatorial competition and calculation of the inhibitory activity, we defined a relative antigenic binding map, where overlap represents a high degree of competition between tested mAbs (**Figure 35B**). As we found mAbs that bound to Siglec-1 in the presence of others, they might be recognizing distinct epitopes and therefore could be used as a combination therapy to maximize efficacy.

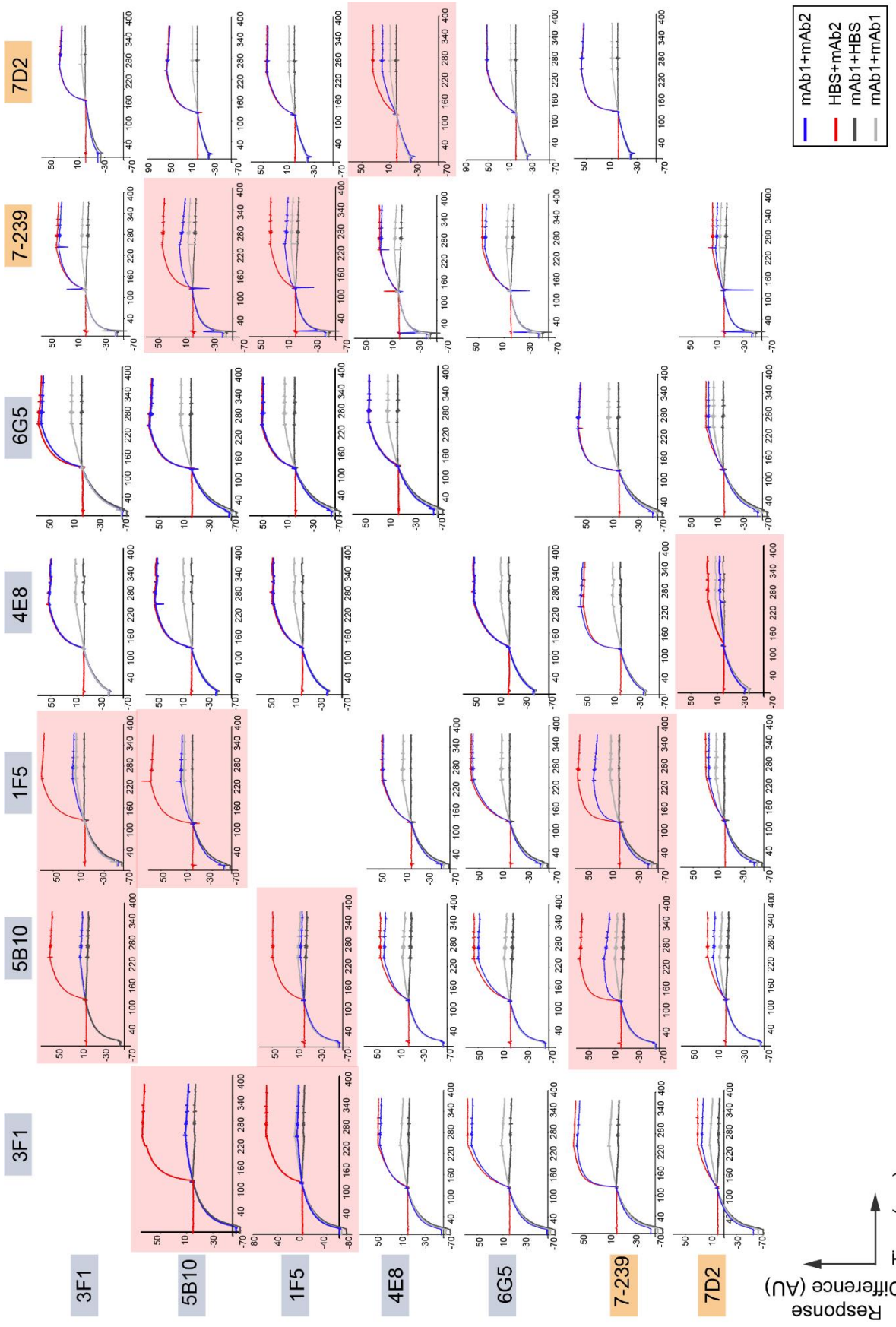

Figure 34 (caption overleaf).

Figure 34. SPR competition assays. Graphs showing all competition assays performed as in **Figure 33**. Red shadowed areas indicate a high degree of competition. Competition graphs of each mAb with itself are not shown, but are included as controls in each of the experiments (light grey lines).

A

Second mAb

First mAb	3F1	5B10	1F5	4E8	6G5	7-239	7D2
3F1	84.1	85	86.7	4.9	9.1	7	18.5
5B10	85.5	82.9	88.9	11.9	11.9	58.5	29.2
1F5	71.5	71	76.3	3.5	5.1	37.2	12.5
4E8	0.9	2.9	3.6	72.2	2.8	-6.9	79.1
6G5	6.8	1.9	2.3	-0.04	76.8	-2.8	12
7-239	7.9	56.5	56.6	3.8	8.7	87.1	27.3
7D2	1.8	2.0	3.0	40.2	2.2	0.1	55.2

% of binding inhibition of second mAb

B

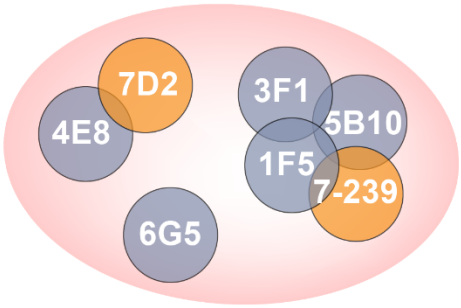

Relative Antigenic Map

Figure 35. Competition between mAbs and relative antigenic map. A. Percentage of binding inhibition calculated for each mAb competition assay. Red color intensities indicate the extent of competition as compared to the inhibition of an antibody with itself. **B.** Relative antigenic map derived from all combinatorial cross-competition analyses performed, where overlapping represents high degree of competition between mAbs recognizing proximal epitopes.

3.3 New anti-Siglec-1 mAbs block HIV-1 capture

We next assessed if new anti-Siglec-1 mAbs could halt HIV-1 viral uptake. For this purpose, we made use of fluorescent HIV-$1_{Gag\text{-}eGFP}$ VLPs[369–372] lacking the envelope glycoprotein. A constant amount of these VLPs was mixed with increasing concentrations of new or commercial anti-Siglec-1 mAbs before they were added in combination to Raji Siglec-1 cells. In these competition assays, only the commercial mAb 7-239 and new mAbs 1F5, 5B10 and 3F1 were able to completely block HIV-$1_{Gag\text{-}eGFP}$ VLP uptake (**Figure 36A**). Moreover, the concentration of new mAb 3F1 that inhibited viral uptake by 50% (IC_{50} value) was significantly lower than that of the commercial 7-239 mAb (**Figure 36B-C**).

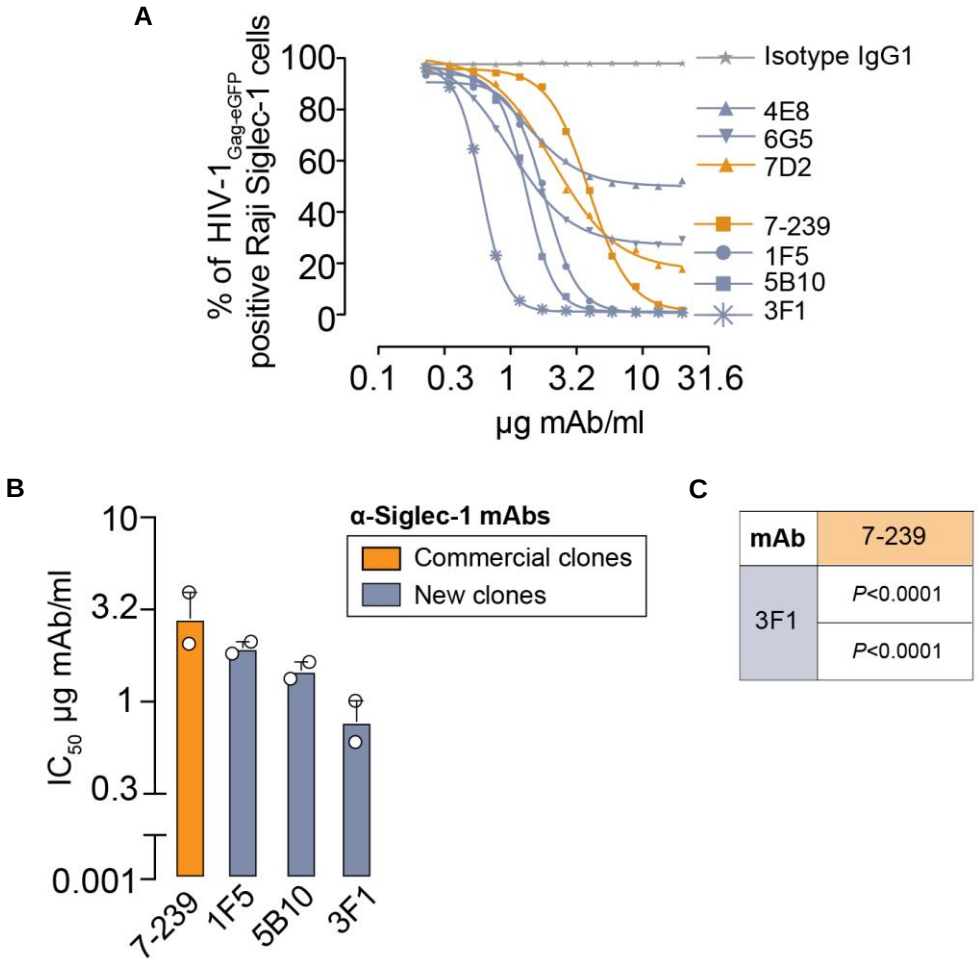

Figure 36. New anti-Siglec-1 mAbs block HIV-1 uptake by Raji Siglec-1 cells. A. Competition between HIV-$1_{Gag\text{-}eGFP}$ VLPs and anti-Siglec-1 mAbs for Raji Siglec-1 binding upon incubation for 1 h at 37ºC. Representative non-linear fit to a variable response curves based on 12 *xy* values from one experiment out of two are shown. **B.** IC_{50} values of particular mAbs that completely blocked HIV-$1_{Gag\text{-}eGFP}$ VLP uptake. Data show mean values and SEM from two independent experiments. **C.** *P*-values comparing the adjusted models for competitive HIV-$1_{Gag\text{-}eGFP}$ VLP uptake inhibition ($logIC_{50}$) of 3F1 and 7-239. Non-linear dose-response curve models were fitted based on 12 *xy* values from two independent experiments. Comparisons were inferred with an extra sum-of-squares F test.

We also tested if combining more than one new mAbs could increase their individual blocking efficacy. Combinations of mAbs 3F1, 5B10 and 1F5 were not able to improve the blocking effect of each single mAb (**Figure 37A**). These results are in line with the capacity of these particular mAbs to compete with each other (**Figure 35**). However, new mAbs 4E8 and 6G5, which displayed an incomplete blocking capacity (**Figure 36A**) achieved a full blockade when applied in combination (**Figure 37B**). These data concur with the inability of these mAbs to compete with each other or with any other new mAb (**Figure 35**), suggesting that they bind further from the viral binding epitope than other mAbs do.

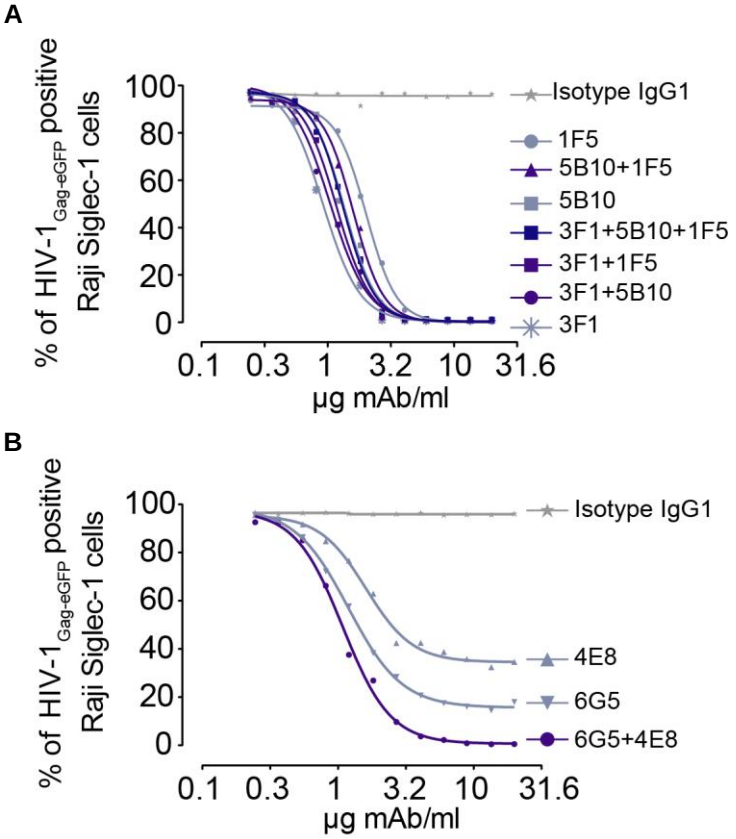

Figure 37. Particular mAb combinations can increase their capacity to block HIV-1 uptake. Competition between HIV-$1_{Gag\text{-}eGFP}$ VLPs and mixes of anti-Siglec-1 mAbs for Raji Siglec-1 binding. **A.** Mixes of mAbs that fully block HIV-$1_{Gag\text{-}eGFP}$ when added separately. **B.** Combination of 4E8 and 6G5 mAbs, which show an incomplete blockade when applied alone.

We next assessed if new mAbs block DC-mediated HIV-1 uptake and *trans*-infection of target cells. First, we determined that capture of wild-type HIV-$1_{NL\text{-}4.3}$ by primary MDDCs was higher upon LPS and IFNα treatment as compared to untreated iDCs (**Figure 38A**), which is consistent with previous reports[186,187]. Pre-treatment with new anti-Siglec-1 mAbs inhibited DC capture of HIV-$1_{NL4.3}$, especially on activated DCs (**Figure 38B**).

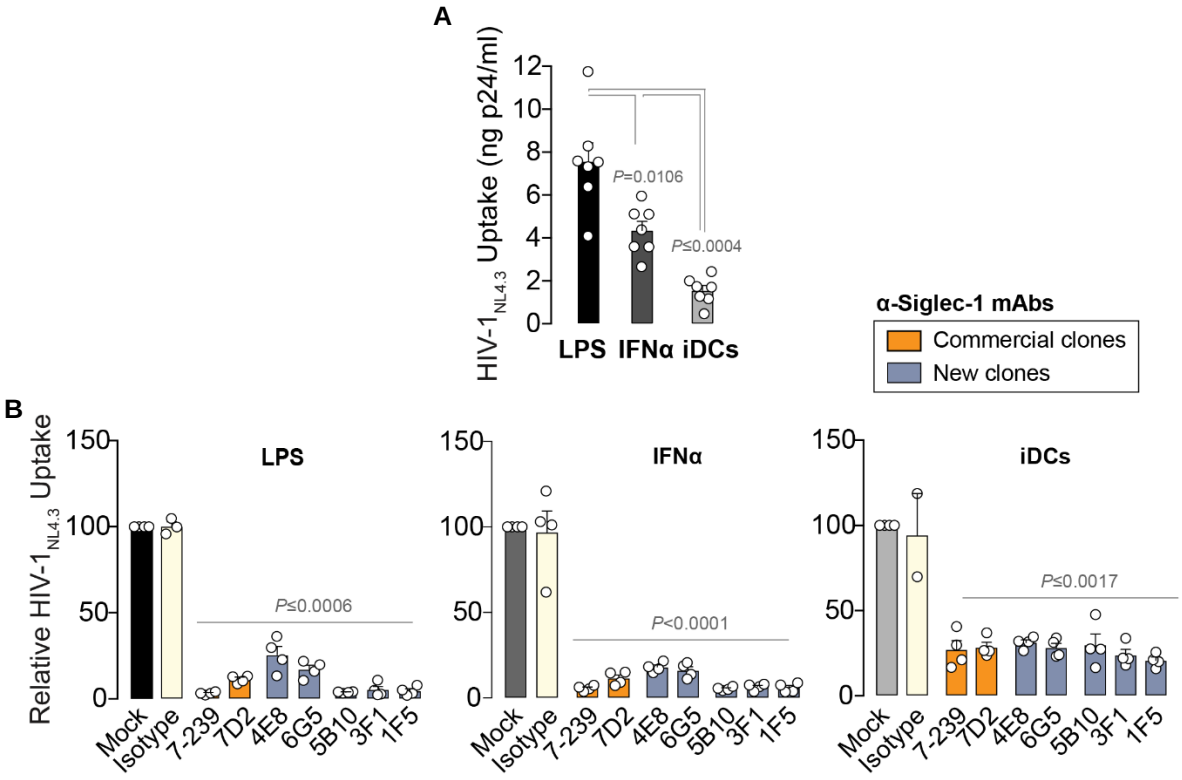

Figure 38. New anti-Siglec-1 mAbs block HIV-1 uptake by DCs. **A.** Comparative HIV-$1_{NL4.3}$ uptake by DCs pulsed with the virus for 3 h at 37ºC, washed and lysed to measure cell-associated $p24^{Gag}$ content by ELISA. Data show mean values and SEM from three independent experiments including cells from seven donors. Statistical differences were assessed using a paired *t* test. **B.** Relative HIV-$1_{NL-4.3}$ uptake by distinctly treated DCs pre-incubated with the indicated mAbs measured by $p24^{Gag}$ ELISA. Values are normalized to those of Mock-treated cells, shown in panel **A** and set at 100%. Data show mean values and SEM from two independent experiments and cells from two-four donors. Statistical differences were assessed with a one-sample *t* test.

3.4 New anti-Siglec-1 mAbs block HIV-1 *trans*-infection mediated by DCs

Finally, we tested the capacity of new anti-Siglec-1 mAbs to block HIV-1 *trans*-infection. Distinctly treated DCs were pre-incubated with or without anti-Siglec-1 mAbs or an isotype control and pulsed with equivalent amounts of HIV-$1_{NL4.3}$. After extensive washing, DCs were co-cultured with the $CD4^+$ reporter TZM-bl cell line, and luciferase induction on these cells by HIV-$1_{NL4.3}$ was measured to assess *trans*-infection. Concurring with previous reports[186,187], activated DCs had the highest capacity to *trans*-infect HIV-$1_{NL4.3}$ (**Figure 39A**). As expected by their capacity to block viral capture by activated DCs (**Figure 38B**), new anti-Siglec-1 mAbs efficiently blocked HIV-1 *trans*-infection (**Figure 39B**).

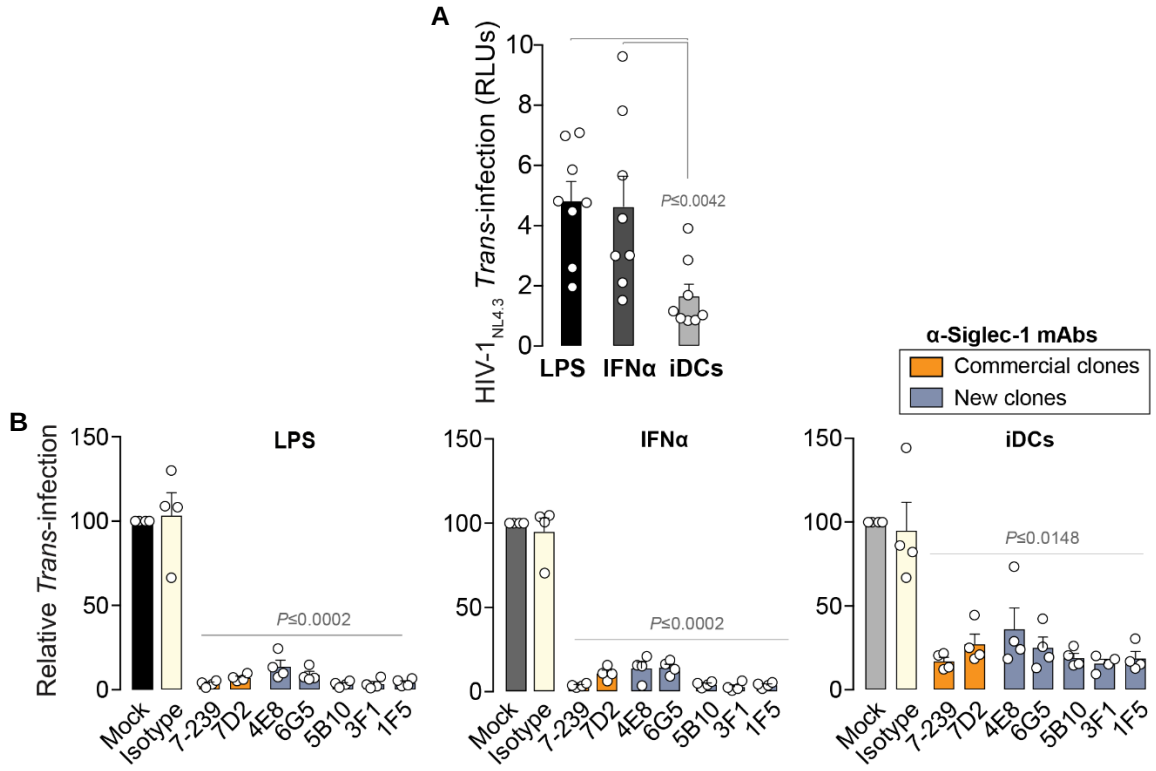

Figure 39. New anti-Siglec-1 mAbs block DC-mediated HIV-1 *trans*-infection. Comparative HIV-$1_{NL4.3}$ *trans*-infection of a reporter $CD4^+$ cell line mediated by distinctly treated DCs. Cells were pulsed with HIV-$1_{NL4.3}$ for 3 h at 37ºC, and after extensive washing co-cultured during 2 days with the reporter cell line, to determine the induced luciferase activity in relative light units (RLUs). Data show mean values and SEM from three independent experiments and include cells from eight donors in duplicates. Statistical differences were assessed with a paired *t* test. **B.** Relative HIV-$1_{NL4.3}$ trans-infection mediated by distinctly treated DCs pre-incubated with the indicated mAbs. Values are normalized to those of Mock-treated cells, shown in panel **A** and set at 100%. Data show mean values and SEM from two independent experiments and include cells from four donors. Statistical differences were assessed using a one-sample *t* test.

Collectively, results in this chapter indicate that the set of newly generated anti-Siglec-1 mAbs recognize Siglec-1 with high affinity and can be employed alone or in combination to efficiently block HIV-1 capture by Siglec-1-expressing cells. Their capacity to abrogate DC-mediated HIV-1 *trans*-infection suggests their potential use in microbicidal strategies in combination with antiretrovirals, which inhibit viral productive replication but do not limit viral dissemination mediated by DCs. Moreover, and considering that Siglec-1 recognizes sialylated gangliosides anchored to the viral membrane, new mAbs could also impair Siglec-1 interaction with other sialylated pathogens aside from HIV-1.

Chapter 6

RESULTS IV

Siglec-1 mediates Ebola viral uptake and cytoplasmic entry into DCs

The results included in this chapter are part of:

Perez-Zsolt, D., Erkizia, I., Pino, M., García-Gallo, M., Martín, M.T., Benet, S., Chojnacki, J., Fernández-Figueras, M.T., Guerrero, D., Urrea, V., Muñiz-Trabudua, X., Kremer, L., Martinez-Picado, J.* and Izquierdo-Useros, N.* (2019). **Anti-Siglec-1 antibodies block Ebola viral uptake and decrease cytoplasmic viral entry**. *Nat Microbiol*. 4(9):1558-1570. doi: 10.1038/s41564-019-0453-2.

*Last authors.

1. Introduction

In the previous chapters, we have addressed the contribution of Siglec-1 on DCs during HIV-1 infection, a context in which this receptor mediates viral capture, accumulation in a cellular VCC and, ultimately, facilitates viral transfer to target $CD4^+$ T cells. Siglec-1 exerts its activity by binding sialylated gangliosides that are present on the HIV-1 membrane[70,187], which derives from the plasma membrane of virus-producing cells. As all enveloped viruses drag host cell membranes during their budding process, we hypothesize that Siglec-1 could recognize sialylated gangliosides from other viruses aside from HIV-1, and that this recognition could also influence the outcome of other viral infections.

Distinct filoviruses such as EBOV and MARV incorporate sialylated gangliosides on their viral membranes[288] and could therefore interact with Siglec-1. These filoviruses cause sporadic outbreaks of the highly lethal FVD in humans[391]. Intriguingly, DCs and other myeloid cells that up-regulate Siglec-1 upon activation, such as macrophages[192] or monocytes[213], are susceptible to EBOV productive infection[265,312,328]. Due to their location at portals of viral entry, myeloid cells become productively infected at the early stages of the disease, and aid for systemic dissemination as they migrate to the secondary lymphoid tissues[91]. Following myeloid infection and, filoviruses infect a number of different cell types, and this leads to the severe symptomatology of FVD[344]. Thus, understanding the mechanisms that govern viral entry into myeloid cells is crucial to develop therapeutic strategies aimed at blocking viral infection at the early stages.

EBOV entry into myeloid cells entails a sequence of events involving a number of viral and host factors, that begins with the attachment of the virus to the cell surface through distinct mechanisms[268]. CLRs such as DC-SIGN mediate the attachment of Ebola virus via glycoprotein recognition[392–394]. In sharp contrast, the TIM/TAM receptors bind EBOV by recognizing lipids such as phosphatidylserine on the viral membrane[282,285]. After attachment, viruses are internalized through macropinocytosis and directed to late endosomes, where EBOV glycoprotein is cleaved by cellular proteases such as CTSB in DCs[301]. This allows glycoprotein interaction with the endosomal receptor NPC1[297,302], which triggers viral fusion and release of the viral genome into the cytoplasm that orchestrates viral replication.

As we have previously shown in this thesis, immune activating signals such as LPS and IFNα potently enhance Siglec-1 expression on myeloid cells, and this boosts their ability to internalize HIV-1 in a Siglec-1-dependent manner. Of note, both LPS and IFNα are also

present during the course of EBOV disease[333,350,356]. LPS was detected in a case of EBOV infection complicated with septicemia[356], and IFNα has been found in plasma from EBOV-infected individuals[333,350]. Moreover, both EBOV and MARV infection of non-human primates results in the up-regulation of IFN-stimulated genes, indicating that type I IFNs are released in response to filoviral challenge[351,352,395]. Thus, FVD is characterized by an immune-activating environment that can up-regulate Siglec-1 expression. However, whether Siglec-1 is a factor mediating EBOV internalization on DCs remains largely unexplored.

Here, we report that Siglec-1 acts as an attachment factor for EBOV, that mediates viral binding and capture by activated DCs, and directs captured viral particles into the same VCC previously described for HIV-1. Moreover, Siglec-1-mediated capture contributes to viral cytoplasmic entry, indicating that EBOV also exploits this receptor as a way to infect DCs.

2. Material & Methods

2.1 Ethics statement

This study was approved by the institutional review board on biomedical research from HUGTiP (Badalona, Spain), and all individuals involved gave their written informed consent to participate.

2.2 Primary cells and cell lines

MDDCs were obtained and activated as previously described (**Chapter 3**, **Material & Methods 2.2**).

HEK-293T cells were maintained as previously described (**Chapter 3**, **Material & Methods 2.3**). Raji B-lymphocyte and Raji DC-SIGN cell lines (kindly provided by Dr. Y. van Kooyke) were maintained in RPMI medium (Invitrogen) or RPMI plus 1 mg/ml of geneticin (Invitrogen). Vero E6 cells (CRL-1586; ATCC) were maintained in Eagle's Minimum Essential Medium (EMEM; ATCC) supplemented with 10% FBS, 100 IU/ml of penicillin and 100 µg/ml of streptomycin (all from Invitrogen).

Siglec-1-expressing HEK-293T cells were transfected with X-tremeGENE 9 DNA Transfection Reagent (Merck) in T75 flasks with 30 µg of a pCMV6-Entry backbone

(OriGene) comprising the coding region of human Siglec-1 or a point mutation generated by changing (Arg→Ala) at position 116 (R116A) by Blue Heron Biotech. Raji cells were used to develop stable cell lines expressing Siglec-1 (Raji Siglec-1) or Siglec-5 (Raji Siglec-5). Cells were transfected with pCMV6-Entry comprising the coding region of human Siglec-1 or Siglec-5 (OriGene) by using Amaxa nucleofector (Lonza) following manufacturer's instructions. Transfected cells were sorted and cloned in a FACSVantage SE and maintained in RPMI with 1 mg/ml of geneticin for selection of stable clone with high Siglec expression. Cells were stained with anti-Siglec-1 7-239 PE mAb (BioLegend), anti-DC-SIGN DCN46 PE mAb (BD Biosciences), and anti-Siglec-5/14 1A5 PE (BioLegend) to assess surface expression of all receptors.

2.3 Generation of viral stocks

$Ebo_{VP40\text{-}eGFP}$ VLPs were generated transfecting HEK-293T cells with the molecular clone CAGGS-eGFP-VP40 (kindly provided by Dr. Bieniasz). For $Ebo_{VP40\text{-}NanoLuc}$ VLPs[396], cells were transfected with the molecular clone VP40-NanoLuc (kindly provided by Dr. Pekarik). For Ebo-$GP_{VP40\text{-}eGFP}$ VLPs, cells were transfected with CAGGS-eGFP-VP40 plasmid along with pcDNA3.1-Zaire GP (BEI Resources). For Ebo-$GP_{VP40\text{-}BlaM}$ VLPs, cells were transfected with molecular clones pcDNA3.1-BlaM-VP40, pcDNA3-Zaire NP and pcDNA3.1-Zaire GP (all from BEI Resources). HEK-293T cells were transfected with calcium phosphate (CalPhos; Clontech) or X-tremeGENE 9 DNA Transfection Reagent (Merck) in T75 flasks using a total of 20-30 µg of plasmid DNA at equimolar ratios. $2x10^6$ primary monocytes isolated by CD14-negative selection (Miltenyi Biotec) were labelled with rabbit polyclonal anti-GM1 antibodies (Abcam), nucleofected with Amaxa and the recommended kit (Lonza) using 2 µg of $VP40_{NanoLuc}$ and 2 µg of pcDNA3.1-Zaire GP to counteract tetherin activity[397] to produce Ebo-$GP_{VP40\text{-}NanoLuc}$ VLPs. Supernatants were harvested 72 h post-transfection, cleared of cellular debris by centrifugation and frozen at -80ºC until use. The VP40 content of VLP stocks was determined by a home-made sandwich ELISA using mouse IgG1 anti-VP40 mAbs to coat Nunc MaxiSorp plates (Invitrogen) and a mouse IgG2a anti-VP40 mAb to detect bound protein (both from Fitzgerald). Goat anti-mouse IgG2a HRP (Jackson ImmunoResearch) was employed to reveal the assay. Purified VP40 protein (IT Bioservices) was used as a standard for quantification. Alternatively, monocyte-derived $EboGP_{VP40\text{-}NanoLuc}$ VLPs were quantified using the Nano-Glo Luciferase Assay System (Promega) and assessed on an EnSight Multimode Plate Reader (Perkin-Elmer).

HIV-$1_{mCherry}$, HIV-1_{NFN-SX}, HIV-$1_{Gag-eGFP}$ and HIV-$1_{NL4.3}$ were obtained, quantified and titrated as previously described in refs.[186,192].

2.4 Ebola VLP binding and uptake assays

Binding and uptake experiments with $Ebo_{VP40-eGFP}$ were performed pulsing $1x10^5$ DCs with a constant amount of 80 ng of VP40 for the indicated time-points at 4ºC or 37ºC. For blockade, cells were pre-incubated for 15 min at RT with 10 µg/ml of anti-Siglec-1 mAbs 7D2, 7-239 (both from Abcam), a 1/100 dilution of anti-DC-SIGN mAb MR1 (kindly provided by Dr. A. Corbí), 500 µg/ml of mannan from *Saccharomyces cerevisiae* (Sigma-Aldrich), an IgG1 isotype control (BD Biosciences) or left untreated before viral exposure. After extensive washing, cells were acquired with a FACSCelesta or Calibur (BD) and the frequency of positive cells was determined using the FlowJo software (TreeStar). Forward-angle and side-scatter light gating were employed to exclude dead cells and debris from all the analyses.

Alternatively, $5x10^5$ HEK-293T cells transfected with wild-type or R116 Siglec-1 encoding plasmids were pulsed with 800 ng of VP40 for 3 h at 37ºC. After extensive washing, cells were labelled with anti-Siglec-1 7-239 PE mAb (BioLegend) or an isotype control and assessed by FACS. Non-transfected cells were used to place the positivity marker and only assess Siglec-1-dependent viral uptake.

2.5 Ganglioside detection on Ebola VLPs

$Ebo_{VP40-eGFP}$ VLPs were adhered to poly-L coated coverslips, fixed in 3% paraformaldehyde (PFA), permeabilised and blocked using 0.1% saponin and 0.5% BSA. VLPs were immunostained with rabbit anti-GM1 polyclonal antibody and detected by anti-rabbit IgG Fab fragments (Jackson ImmunoResearch) coupled to Star Red dye (KK114; Abberior) by n-hydroxysuccinimide chemistry. Samples were acquired in a Zeiss LSM 710 confocal microscope with a 63x/1.4 NA oil objective and processed using ImageJ Fiji software.

2.6 Siglec-1 mini-protein ELISA

A Siglec-1 mini-protein containing the V-set domain and 3 Ig-like domains of the receptor was produced as previously described (**Chapter 5**, **Material & Methods 2.5**). The mini-protein was incubated with 10 µg/ml of anti-Siglec-1 7-239 mAb or IgG1 isotype control for 30 min at RT. Mixes were then added to Ebo-$GP_{VP40-NanoLuc}$ VLPs produced on HEK-

293T cells or primary monocytes for 1 h at RT. Combinations were applied for 1.5 to a Nunc MaxiSorp plate (Invitrogen) coated with 5 µg/ml of goat anti-human Fc (Jackson ImmunoResearch) and blocked with BSA, extensively washed, lysed with Nano-Glo Luciferase Assay System (Promega) and assessed on an EnSight luminometer (Perkin-Elmer).

2.7 Uptake of Ebola VLPs displaying envelope glycoproteins

Uptake experiments using Ebo-$GP_{VP40\text{-}eGFP}$ VLPs were performed pulsing $1x10^5$ DCs with 600 ng of VP40 for 3 h at 37ºC. Alternatively, $2x10^5$ Raji cells were pulsed with 600-900 ng of VP40 for 3 h at 37ºC. For blockade, cells were pre-incubated as previously described (**Chapter 6**, **Material & Methods 2.4**). Uptake of two different monocyte-derived Ebo-$GP_{VP40\text{-}NanoLuc}$ VLP stocks was tested by pulsing $5x10^5$ Raji Siglec-1 cells for 12 h at 37ºC. Cells were extensively washed, lysed with Nano-Glo Luciferase Assay System and assessed on an EnSight luminometer (Perkin-Elmer).

2.8 DC transduction

Lentiviral particles coding for different shRNAs were co-infected along with a vpx-expressing lentivirus to counteract restriction by SAMHD1 and facilitate monocyte infection, as previously described[70]. Briefly, VSV-G-pseudotyped SIV3 lentivector (kindly provided by Dr. A. Cimarelli) was produced as previously described[398]. $5x10^6$ isolated monocytes were infected with SIV3 particles and transduced with two different SIGLEC1-specific or one non-targeted short hairpin RNA (shRNA) control MISSION Lentiviral Transduction Particles (Sigma-Aldrich) at a multiplicity of infection (MOI) = 50. Transduced monocytes were differentiated into LPS-treated DCs (**Chapter 3**, **Material & Methods 2.2**), labelled with anti-Siglec-1 7-239 PE mAb (BioLegend) and assessed for Ebo-$GP_{VP40\text{-}eGFP}$ VLP capture as previously described (**Chapter 6**, **Material & Methods 2.7**).

2.9 Microscopy analysis

$2.5x10^5$ DCs were pulsed with 780 ng of Ebo-$GP_{VP40\text{-}eGFP}$ VP40 for 4 h at 37ºC. After extensive washing, cells were fixed and permeabilized (Fix & Perm; Invitrogen) and stained with anti-Siglec-1 7-239 PE mAb (BioLegend). Alternatively, cells were cultured for 12 h with 390 ng of Ebo-$GP_{VP40\text{-}eGFP}$ VP40, washed, fixed, permeabilized and stained

with anti-Siglec-1 7-239 Alexa Fluor 647 mAb (BioLegend). Cells were cytospun onto coverslips, covered with DAPI-containing Fluoroshield mounting media (Sigma-Aldrich) and analysed with an Ultraview ERS Spinning Disk System (Perkin-Elmer) mounted on a Zeiss Axiovert 200 M inverted microscope. For deconvolved images we used a confocal LSM Zeiss780 equipped with an apochromatic 63x oil (NA = 1.4) objective. Pinhole aperture was set to 1 and sampling conditions adjusted to nyquist (voxel size = 54.9x54.9x200 nm) Stacks were deconvolved using Huygens Pro and applying a Point Spread Function obtained by recording Tetraspeck Microspheres of 0.1 µm (Molecular Probes) with the same microscopic parameters as our samples. Volocity software (Perkin-Elmer) was used to analyse microscopy images as previously described[207].

For electron microscopy analysis, $5x10^6$ LPS-treated DCs were pulsed for 12 h with 3,700 ng of VP40 from Ebo-$GP_{VP40\text{-}eGFP}$ VLPs, incubated 4 h more with 1,150 ng of p24 from HIV-$1_{NFN\text{-}SX}$, extensively washed in PBS and fixed in 2.5% glutaraldehyde for 3 h at 4ºC. Cells were then processed by the Electron Microscopy Platform of HUGTiP as described elsewhere[358], for analysis of ultra-thin sections with a JEOL JEM 1010 electron microscope.

2.10 Super-resolution microscopy analysis of VCCs

$1x10^6$ LPS-treated DCs were pulsed with 400 ng of VP40 from Ebo-$GP_{VP40\text{-}NanoLuc}$ VLPs and 200 ng of p24 from a 1:1 mixture of HIV-$1_{Gag\text{-}eGFP}$ and HIV-$1_{NL4.3}$ for 12 h at 37ºC. This mixture was employed to reduce the amount of fluorescent signal in VCCs and aid in distinguishing individual particles. Cells were washed, adhered to poly-L coated coverslips, fixed in 3% PFA, and permeabilised and blocked using 0.1% saponin and 0.5% BSA plus 100 µg/ml of human IgGs. Cells were stained with mouse IgG2a anti-VP40 mAb (Fitzgerald) and anti-mouse Fab fragments (Jackson ImmunoResearch) coupled to Star Red followed by staining with anti-Siglec-1 6H9 mAb detected with anti-mouse Fabs coupled to Star 580 (Abberior). Of note, 6H9 clone was selected throughout our anti-Siglec-1 mAb screening for its capacity to recognize Siglec-1 by FACS while not blocking HIV-$1_{Gag\text{-}eGFP}$ VLP uptake. Following immunostaining, samples were post-fixed, overlaid with SlowFade Diamond mounting medium (ThermoFisher Scientific) and imaged using confocal or STED microscopy.

Super-resolution analysis was performed using Leica SP8 STED 3x microscope equipped with a 100x/1.4 NA oil STED objective. 3D STED images were acquired sequentially using

637 nm, 587 nm and 498 nm lines from the white light laser. STAR signals were depleted with a donut-shaped 755-nm pulsed STED laser, while eGFP signal was depleted with a donut-shaped 592-nm pulsed STED laser. Approximately 120 nm lateral and 300 nm axial resolution (full-width-at-half-maximum) was achieved in all three-acquisition channels representing 2-fold resolution improvement with respect to confocal images in all directions (estimated from fluorescent bead and single fluorescent antibody molecule measurements. 3D STED images were deconvoluted with Huygens Professional software using theoretical PSF parameters corresponding to the system's effective observation spot or point-spread-function. Image analyses were performed using ImageJ Fiji or Imaris software.

2.11 Ebola VLP cytoplasmic entry assays

DCs or distinct Raji cell lines were pre-incubated or not with blocking reagents as previously described (**Chapter 6, Material & Methods 2.4**). An equivalent fusogenic amount of Ebo-$GP_{VP40\text{-}BlaM}$ VLPs (ranging from 15-55 ng of VP40) was added to $2.5x10^5$ cells and incubated for 12 h at 37ºC. The CCF2-AM substrate (Invitrogen) was added to cells following manufacturer's indications to identify cells in which Ebo-$GP_{VP40\text{-}BlaM}$ VLP cytoplasmic entry occurred. Cells were acquired with an LSRII flow cytometer (BD) and the percentage of positive cells was determined using the FlowJo software (TreeStar).

DCs derived from blood donors were regularly stained with an anti-Siglec-1 7-239 PE mAb, allowing us to identify Siglec-1 null individuals by FACS. Direct genotyping of rs150358287G4T by Taqman allelic discrimination from Applied Biosystems (No. AHKAY5K) confirmed the null status of the indicated donor. To use equivalent numbers of fusogenic viral particles in all entry assays, Ebo-$GP_{VP40\text{-}BlaM}$ stocks were titrated in duplicate by serial ½ dilutions in $3x10^4$ Vero E6 cells/well seeded in 96-well plates, loaded with CCF2-AM substrate and assessed by FACS. Fusogenicity was compared in the highest non-saturated well, where cytoplasmic entry on Vero E6 cells ranged from 26 to 47% of cells.

2.12 Statistical analyses

Data are reported as the mean and the SEM for each condition. Mean changes were assessed by a paired *t* test and a Mann-Whitney test, considered significant at $P<0.05$. Mean changes from 100% normalized values were assessed with a one-sample *t* test, considered

significant at $P<0.05$. All analyses and figures were generated with the GraphPad Prism v7.0d software.

3. Results

3.1 DC activation enhances Ebola viral binding and uptake via Siglec-1 recognition of sialylated gangliosides

DCs respond to activating signals triggered by infection to initiate antiviral responses, but these cells are also primary targets of filoviruses. Activating immune signals such as IFNα and LPS potently up-regulate Siglec-1 expression[70,187] (**Figure 17**) and are augmented throughout EBOV infection[333,350,356]. To test the capacity of distinctly activated MDDCs to recognize EBOV, we pulsed distinctly treated DCs with equivalent amounts of fluorescent Ebola VLPs lacking the envelope glycoprotein, which were produced by transfection of a plasmid coding for EBOV VP40 matrix protein fused to a reporter ($Ebo_{VP40\text{-}eGFP}$ VLPs)[399]. After extensive washing, we measured the fold-change over time in geometric MFI by FACS, comparing nonexposed cells versus cells pulsed with the virus (**Figure 40**). Active viral uptake at 37ºC was higher than when temperature was arrested for endocytosis to only allow viral binding (4ºC), and these differences increased over time on activated DCs (**Figure 40A**). The percentage of eGFP-positive was also determined by FACs, showing that activated DCs have a higher $Ebo_{VP40\text{-}eGFP}$ VLP binding capacity (**Figure 40B**) and increased uptake ability than iDCs (**Figure 40C**). Hence, the activation status induced on DCs by IFNα and LPS (**Figure 17**) promotes EBOV viral particle binding and uptake by these cells.

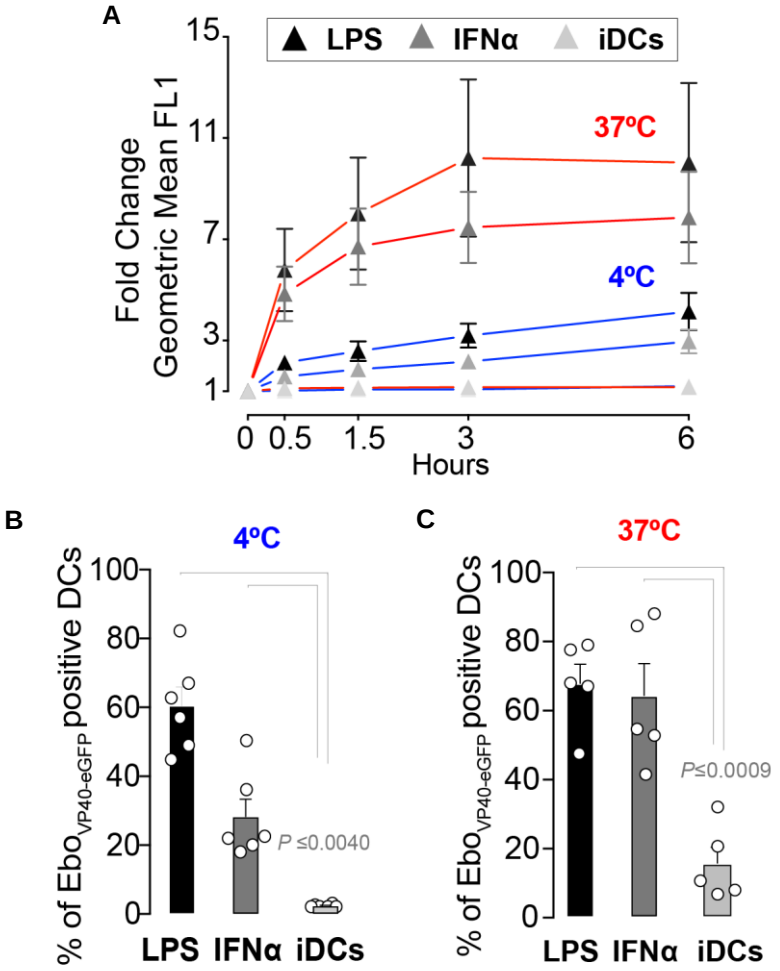

Figure 40. Ebola viral binding and uptake by DCs is enhanced upon cell activation. A. Fold-change in the geometric MFI of distinctly treated DCs incubated with $Ebo_{VP40\text{-}eGFP}$ VLPs at 4ºC or 37ºC for the indicated hours, washed and assessed by FACS, as compared to non-pulsed DCs. Data show mean values and SEM from one experiment and include cells from three donors. **B.** Comparative binding of $Ebo_{VP40\text{-}eGFP}$ VLPs to DCs, which were pulsed for 6 h at 4ºC with viral particles, washed and assessed by FACS. Graphs show mean and SEM from two independent experiments and include cells from six donors. **C.** Comparative $Ebo_{VP40\text{-}eGFP}$ VLP uptake by DCs treated as in **B**. Graphs show mean and SEM from two independent experiments and include cells from five donors. Statistical differences in **B** and **C** were assessed with a paired *t* test.

These results suggested the activity of a viral endocytic receptor whose expression is elicited upon DC activation. $Ebo_{VP40\text{-}eGFP}$ VLPs lack the viral glycoprotein required for CLR recognition[400], but carry sialyllactose-containing gangliosides such as GM1[288,401,402] that were detected by confocal microscopy on the viral membrane employing specific antibodies (**Figure 41**).

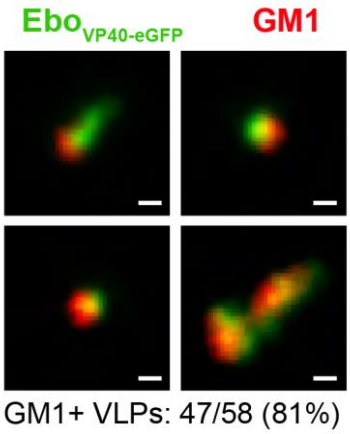

Figure 41. Ebola VLPs display GM1 sialylated ganglioside. Confocal microscopy of $Ebo_{VP40\text{-}eGFP}$ VLPs stained with anti-GM1 antibodies (in red) and percentage of co-staining.

Sialylated gangliosides such as GM1 are recognized by Siglec-1[70]. Thus, we next confirmed the specificity of $Ebo_{VP40\text{-}eGFP}$ VLPs for this receptor by two complementary approaches. First, we produced a recombinant Siglec-1 mini-protein expressing the V-set plus three Ig-like domains fused to a human Fc. We pre-incubated this mini-protein in the presence or absence of an isotype control or anti-Siglec-1 7-239 mAb. These mixes were further incubated with an Ebola VLP stock produced transfecting a plasmid coding for VP40 protein fused to NanoLuciferase ($Ebo_{VP40\text{-}NanoLuc}$ VLP)[396]. When we applied these mixtures to an anti-human Fc-coated ELISA plate, only the untreated mini-protein or that treated with an isotype mAb effectively bound to the plate, and $Ebo_{VP40\text{-}NanoLuc}$ signal could be detected by luminescence (**Figure 42A**). Second, we transfected HEK-293T cells, which do not express Siglec-1, with plasmids containing human Siglec-1 with or without a mutation (R116A) that abrogates sialic acid recognition[201] and HIV-1 binding[187]. Each plasmid yielded a similar transfection efficiency (**Figure 42B**, left graph), but expression of the mutated protein led to the loss of $Ebo_{VP40\text{-}eGFP}$ VLP recognition by transfected cells as compared to cells expressing the wild-type receptor (**Figure 42B**, right graph). Taken together, these results demonstrate that Siglec-1 directly interacts with Ebola VLPs bearing gangliosides but lacking the viral glycoprotein, and that sialylated viral residues are critical for this interaction.

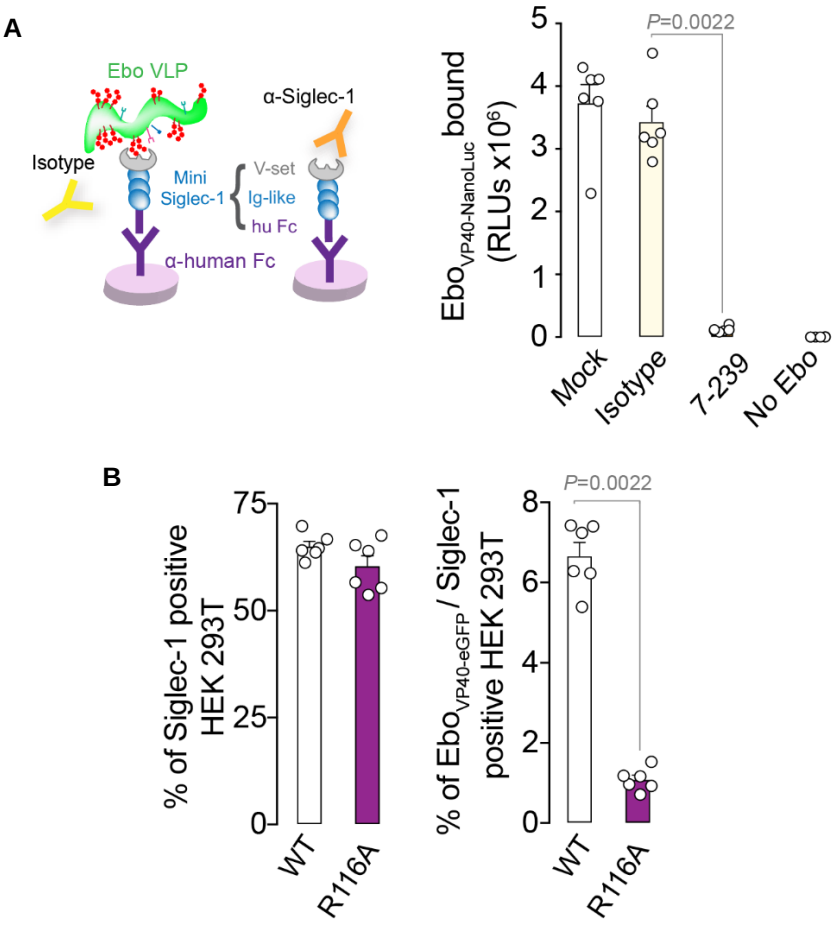

Figure 42. Siglec-1 interacts with Ebola VLPs through recognition of sialylated gangliosides. A. Siglec-1 mini-proteins containing human Fc were left untreated or incubated with an isotype or anti-Siglec-1 7-239 mAb, and then exposed to $Ebo_{VP40\text{-}NanoLuc}$ VLPs as illustrated. Binding of these VLPs to an ELISA plate coated with anti-human Fc allowed for detection of $Ebo_{VP40\text{-}NanoLuc}$ VLPs bound to mini-Siglec-1 by NanoLuciferase activity in RLUs. Data show mean values and SEM from two experiments with triplicates. **B.** (Left graph) Siglec-1 expression on HEK-293T cells transfected with a plasmid encoding Siglec-1 or an R116A mutated plasmid that abrogates sialic acid recognition. (Right graph) $Ebo_{VP40\text{-}eGFP}$ VLP uptake by transfected HEK-293T cells that were positive for an anti-Siglec-1 PE mAb labelling. Non-transfected cells were employed as internal controls to subtract Siglec-1-independent viral uptake. Statistical differences in **A** and **B** were assessed using a Mann-Whitney test.

We next investigated whether the observed Ebola viral binding and uptake on activated DCs was mediated by Siglec-1 (**Figure 43**). For this purpose, DCs were pre-treated with the commercial anti-Siglec-1 mAb clones 7D2 and 7-239. While isotype control had no inhibitory effect, pre-treatment with anti-Siglec-1 mAbs resulted in a reduction of $Ebo_{VP40\text{-}eGFP}$ VLP binding (**Figure 43A**) and uptake (**Figure 43B**) by DCs. As Ebola VLPs did not contain viral glycoproteins, pre-treatment with the anti-DC-SIGN MR1 mAb or with the

broad CLR competitor inhibitor mannan had no effect on viral binding or uptake (**Figure 43A-B**). Representative flow cytometry dot plots showing the gating strategy followed in uptake assays are depicted in **Figure 44**. These results indicate that Siglec-1 mediates Ebola VLP binding and capture through the recognition of sialylated gangliosides present on viral membranes.

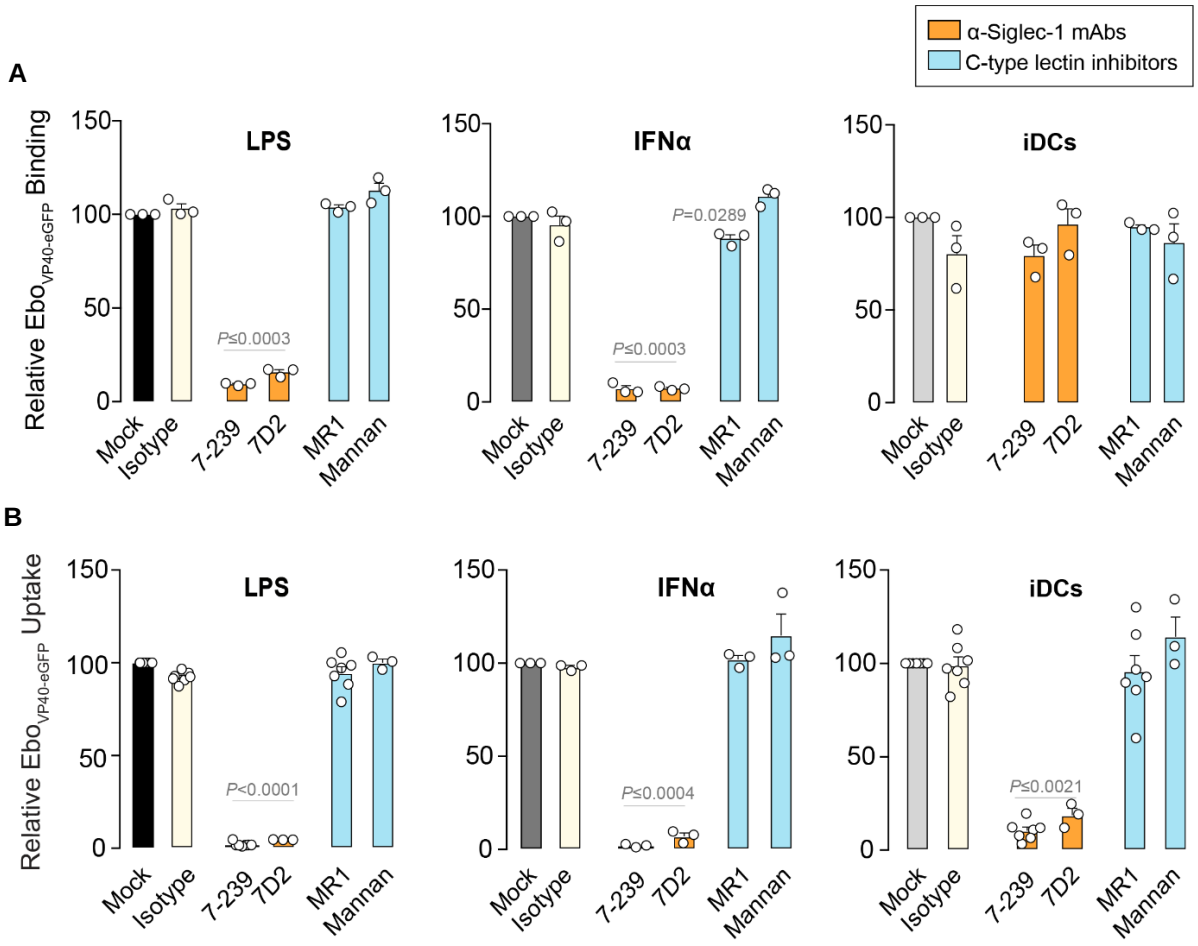

Figure 43. Siglec-1 mediates Ebola VLP binding and uptake on DCs. A. Relative $Ebo_{VP40\text{-}eGFP}$ VLP binding to distinct DCs pre-incubated with an isotype control (yellow bars), anti-Siglec-1 mAbs (orange bars), or CLR inhibitors (blue bars). For comparative purposes, values are normalized to levels of $Ebo_{VP40\text{-}eGFP}$ VLP uptake by Mock-treated cells, shown in **Figure 40B** and set as 100% (dark bars). Graphs show mean values and SEM from one experiment and cells from three donors. **B.** Relative $Ebo_{VP40\text{-}eGFP}$ VLP uptake of DCs treated as in **A**. Data show mean values and SEM from three independent experiments and include cells from three-seven donors. Representative dot plots are shown in **Figure 44**. Statistical differences in **A** and **B** were assessed using a one-sample *t* test.

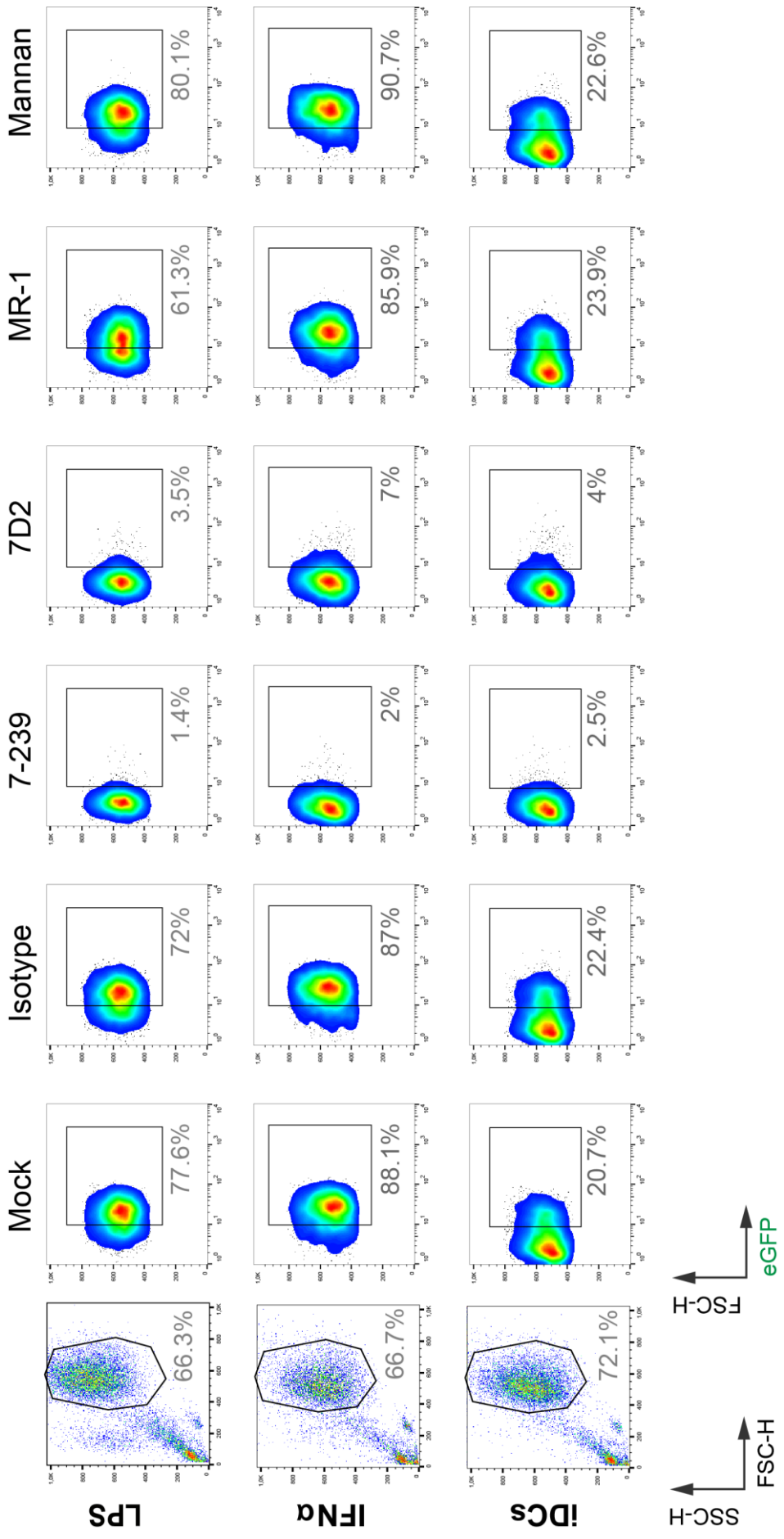

Figure 44 (caption overleaf).

Figure 44. Representative gating strategy employed in Ebola VLP uptake assays. FACS analysis of $Ebo_{VP40\text{-}eGFP}$ VLP uptake by distinctly treated DCs from one donor pre-incubated with the indicated mAbs and inhibitors. Data are representative from three independent experiments and cells from at least three donors.

3.2 Siglec-1 facilitates DC uptake of Ebola viruses bearing envelope glycoproteins

We next tested Siglec-1 capacity to bind gangliosides on Ebola VLPs in the presence of the native glycoproteins exposed on infectious Ebola viruses, which are recognized by C-type lectins[400]. Ebola VLPs were pseudotyped with the native Zaire ebolavirus envelope GP to generate Ebo-$GP_{VP40\text{-}eGFP}$ VLPs, which recapitulate wild-type Ebola virus results and can be handled without the need for high-level biosafety containment. Distinctly treated DCs were pulsed with equal amounts of Ebo-$GP_{VP40\text{-}eGFP}$ VLPs, and after extensive washing, cells were assessed by FACS. Again, DC activation with either IFNα or LPS boosted the capacity of DCs to capture Ebo-$GP_{VP40\text{-}eGFP}$ VLPs (**Figure 45A**). Pre-treatment with anti-Siglec-1 mAbs inhibited retention of viruses containing the Zaire envelope glycoprotein (**Figure 45B**). In contrast, pre-incubation with andi-DC-SIGN MR1 mAb or mannan did not significantly reduce viral uptake by activated DCs (**Figure 45B**). However, on iDCs, which express high levels of DC-SIGN (**Figure 17**), MR1 and mannan had a similar inhibitory effect on viral capture as anti-Siglec-1 mAbs (**Figure 45B**). These results strongly suggest that on activated DCs, alternative receptors beyond DC-SIGN contribute to Ebola viral uptake.

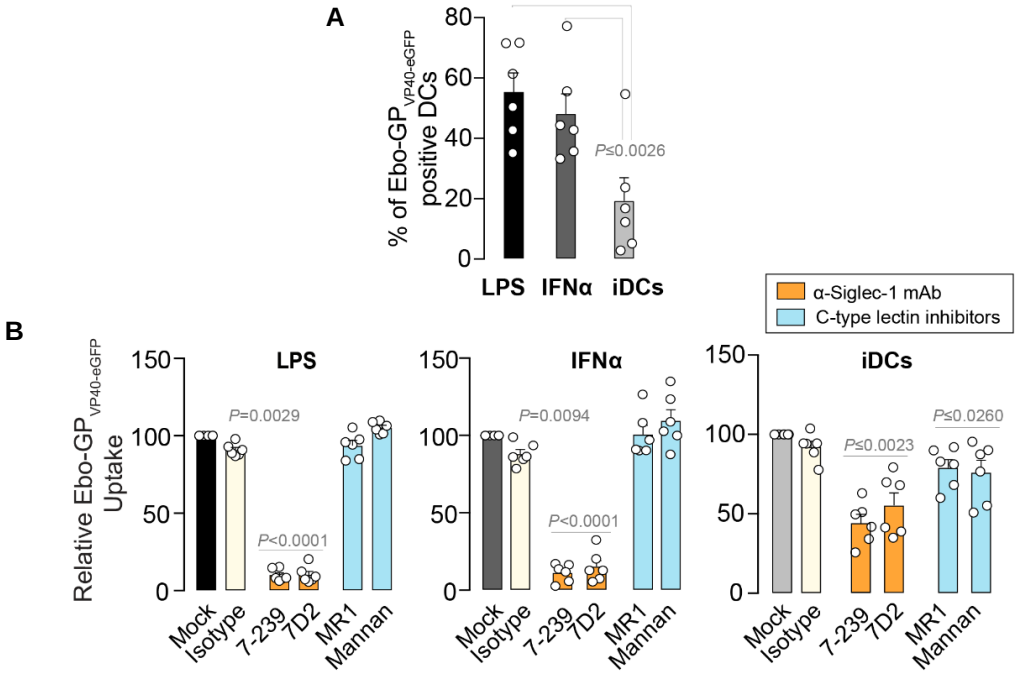

Figure 45. DCs capture Ebola VLPs displaying envelope GP via Siglec-1. A. Comparative uptake of Ebo-GP$_{VP40\text{-}eGFP}$ VLPs by different DCs pulsed with VLPs for 3 h at 37ºC, washed and assessed by FACS. Data show mean values and SEM from two independent experiments and cells from six donors. Statistical differences were assessed with a paired *t* test. **B.** Relative Ebo-GP$_{VP40\text{-}eGFP}$ VLPs uptake by distinctly treated DCs pre-incubated with the indicated mAbs and inhibitors. Values are normalized to Ebo-GP$_{VP40\text{-}eGFP}$ VLP levels captured by Mock-treated DCs, shown in panel **A** and set as 100%. Graphs include mean values and SEM from two independent experiments and cells from six donors. Statistical differences were assessed using a one-sample *t* test.

To further confirm the essential contribution of Siglec-1 in Ebola viral recognition, we employed two complementary strategies. First, we used plasmids coding for Siglec-1 and other lectins to transfect a cell line devoid of these receptors. We chose a Raji B-lymphocyte line because it lacks endogenous expression of these lectins, and transfection does not induce unspecific Siglec-1 up-regulation as it happens when monocytic cell lines are employed[70]. Raji cells expressed Siglec-1, DC-SIGN, Siglec-5 or none of these lectins (**Figure 46A**), and were assessed for their ability to capture Ebo-GP$_{VP40\text{-}eGFP}$ VLPs (**Figure 46B**). Raji Siglec-1 efficiently captured Ebo-GP$_{VP40\text{-}eGFP}$ VLPs (**Figure 46B**), and this capacity was abolished by pre-treatment with anti-Siglec-1 7-239 mAb (**Figure 46B**). Raji DC-SIGN cells also captured Ebo-GP$_{VP40\text{-}eGFP}$ VLPs, which was blocked by anti-DC-SIGN MR1 mAb (**Figure 46B**). In contrast, no viral capture was observed in Raji Siglec-5 cells nor the parental Raji B-cell line (**Figure 46B**). Of note, Siglec-5 molecule is shorter than Siglec-1 and binds sialylated ligands on the surface of the same cell expressing it,

interacting in *cis* with them[26]. This masks Siglec-5 potential viral binding moieties in spite of displaying a high homology with the V-set domain of Siglec-1. As a second approach to confirm the role of Siglec-1 in Ebola viral capture, we transduced LPS-treated DCs with two lentiviruses coding for different SIGLEC1-specific shRNAs[70]. These shRNAs reduced Siglec-1 expression on DCs (**Figure 46C**, left panel) leading to a concurrent loss of Ebo-$GP_{VP40\text{-}eGFP}$ VLP capture (**Figure 46C**, right panel). In contrast, no effects were observed when a non-targeted shRNAs control lentivirus was employed (**Figure 46C**). The complementary strategies of Siglec-1 *de novo* expression on heterologous cells and Siglec-1 silencing on DCs further confirm that this receptor plays a central role in Ebola viral capture.

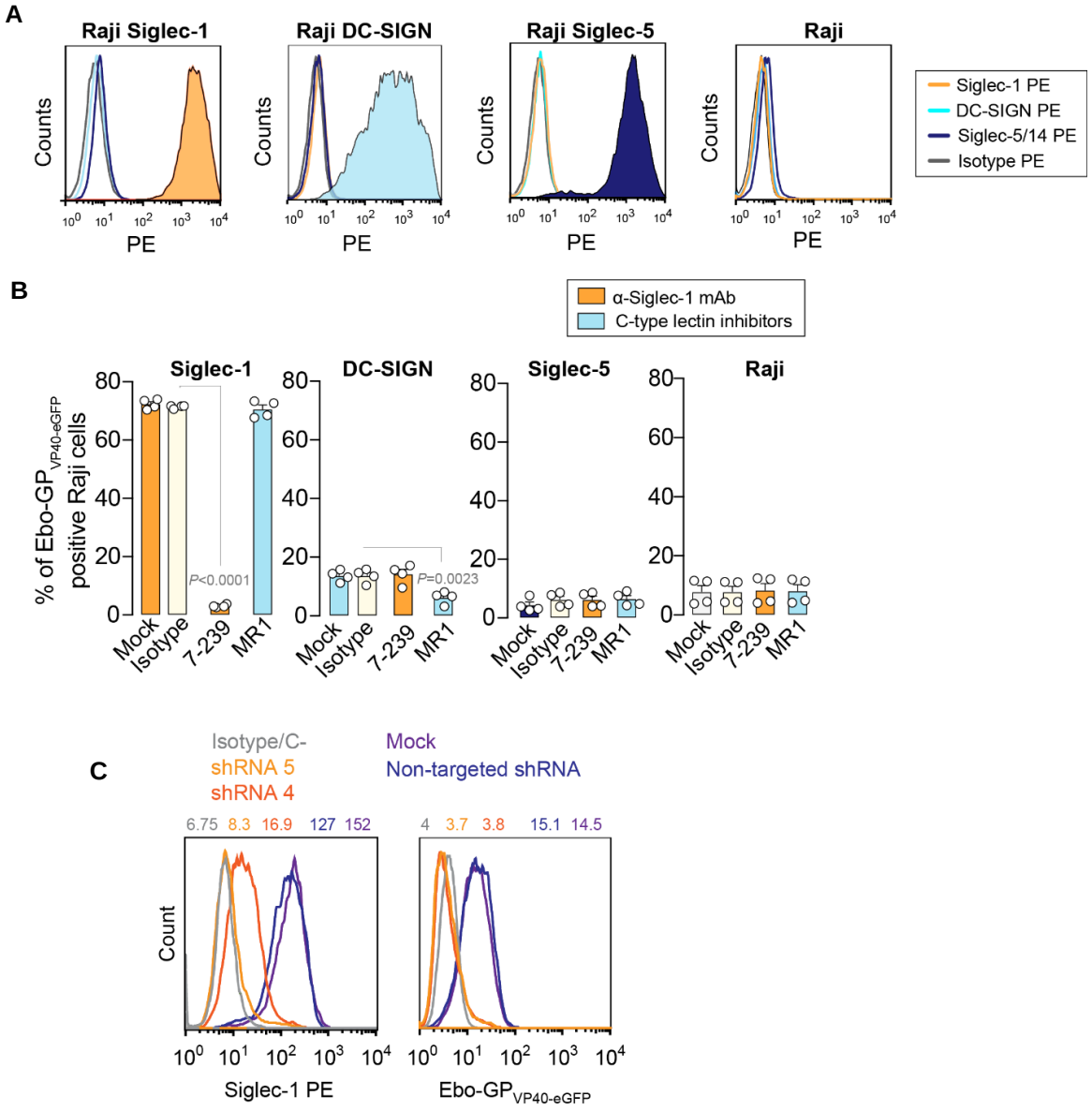

Figure 46. Confirmation that Siglec-1 mediates capture of Ebola VLPs displaying envelope GP. A. Expression of Siglec-1, DC-SIGN and Siglec-5 by Raji B-lymphocytes

transfected with plasmids encoding for the indicated receptors and assessed by FACS. Representative histograms from two independent experiments with four replicas. **B.** Comparative Ebo-$GP_{VP40\text{-}eGFP}$ VLP uptake by Raji B-lymphocytes expressing the indicated receptors incubated with VLPs for 6 h at 37ºC and pre-incubated with the indicated mAbs. Data show mean values and SEM from two independent experiments including four replicas. Statistical differences were assessed with a paired *t* test. **C.** Siglec-1 expression (left panel) and Ebo-$GP_{VP40\text{-}eGFP}$ VLP capture (right panel) by LPS-DCs transduced with Siglec-1-specific or non-targeted shRNAs and incubated with VLPs for 3 h at 37ºC. Representative frequencies of positive cells from two donors and one experiment are shown.

To determine if Ebola VLPs produced by early cellular filoviral targets can also incorporate sialylated gangliosides and interact with Siglec-1, we produced Ebo-$GP_{VP40\text{-}NanoLuc}$ VLPs on primary monocytes. Staining of monocytes producing Ebo-$GP_{VP40\text{-}NanoLuc}$ VLPs with an anti-GM1 mAb revealed the presence of this ganglioside on these cells (**Figure 47A**). We next employed the Siglec-1 mini-protein assay to test Siglec-1 capacity to recognize monocyte-derived Ebo-$GP_{VP40\text{-}NanoLuc}$ VLPs. Pre-incubation of mini-Siglec-1 protein with an isotype mAb had no effect on VLP detection on an anti-human Fc-coated plate as compared to mock-treated protein. In contrast, Ebo-$GP_{VP40\text{-}NanoLuc}$ VLP signal was reduced when the mini-protein was pre-incubated with anti-Siglec-1 7-239 mAb (**Figure 47B**). Moreover, Ebo-$GP_{VP40\text{-}NanoLuc}$ VLP capture by Raji Siglec-1 cells was reduced in the presence of anti-Siglec-1 7-239 mAb as compared to an isotype control (**Figure 47C**). Thus, Ebola viral particles produced by primary filoviral targets such as monocytes are recognized by Siglec-1-expressing cells.

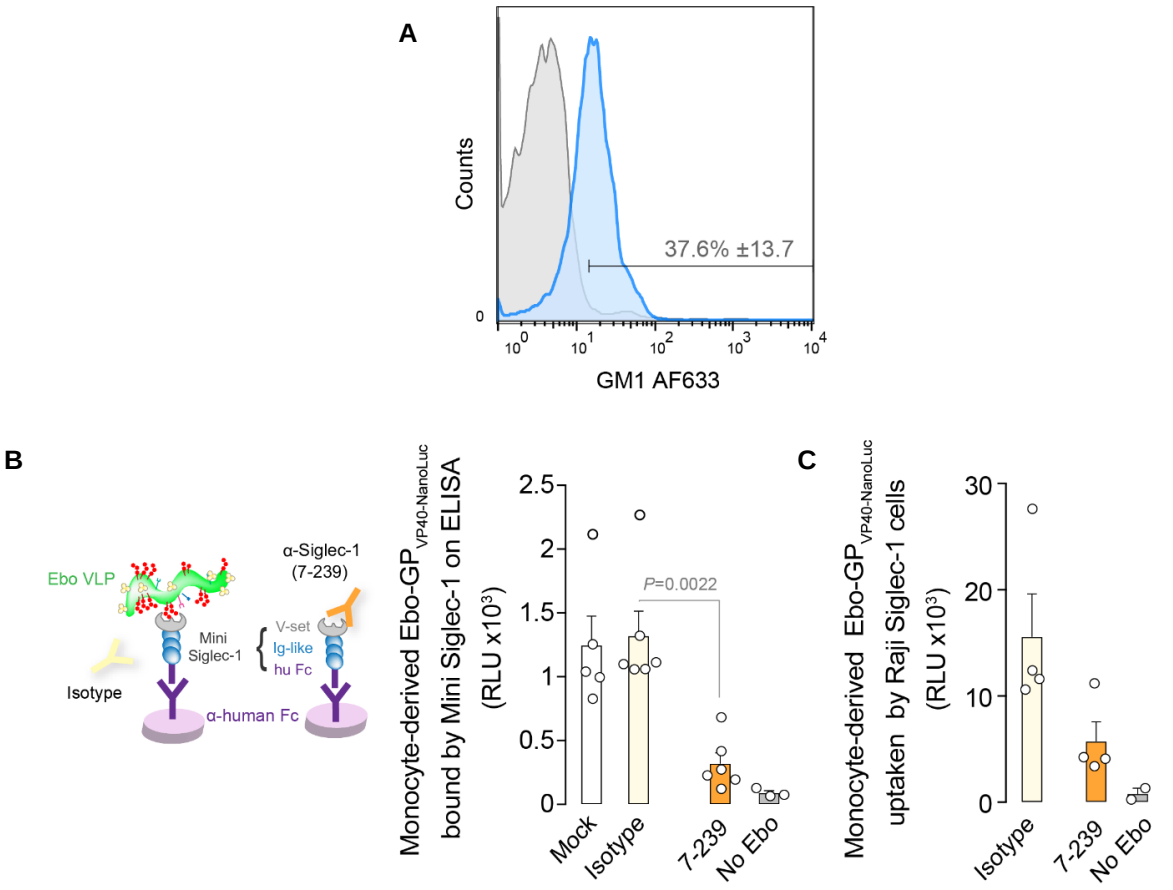

Figure 47. Monocytes display GM1 on their membrane and produce Ebola VLPs recognized by Siglec-1. A. Histograms showing surface staining of GM1 ganglioside on primary monocytes. The mean percentage and SD of GM1-positive cells from three donors and two independent experiments are also indicated. **B.** Monocyte-derived Ebo-GP$_{VP40\text{-}NanoLuc}$ VLPs binding to a human Fc-coated ELISA plate as in **Figure 42A** and assessed by NanoLuciferase activity in RLUs. Graph shows mean values and SEM from one experiment analysing two different monocyte-derived VLP stocks in triplicate. Statistical differences were assessed using a Mann-Whitney test. **C.** Uptake of monocyte-derived Ebo-GP$_{VP40\text{-}NanoLuc}$ VLPs by Raji Siglec-1 cells pulsed for 12 h at 37ºC and pre-incubated with the indicated mAbs. Data show mean values and SEM from two experiments analysing two different monocyte-derived VLP stocks. AF633: Alexa Fluor 633.

Taken together, these results indicate that Ebola viral particles bearing envelope glycoproteins are captured by Siglec-1-expressing cells via recognition of sialylated gangliosides anchored to the viral membrane. Thus, Siglec-1 acts as an attachment factor for Ebola virus, and this interaction could mediate viral internalization into DCs.

3.3 Siglec-1 traffics captured Ebola VLPs to the same VCC where HIV-1 is retained

To determine the role of Siglec-1 in EBOV internalization by DCs, we investigated the fate of captured Ebola viral particles by confocal microscopy. Distinctly treated DCs were pulsed with fluorescent Ebo-GP$_{VP40\text{-}eGFP}$ VLPs and subsequently stained with an anti-Siglec-1 mAb and DAPI to visualize the cell nucleus (**Figure 48**). The majority of viral particles captured by LPS-treated DCs accumulated within a sac-like VCC enriched in Siglec-1; IFNα-treated DCs polarized captured viruses towards one cell pole, and most iDCs displayed a random distribution of Ebo-GP$_{VP40\text{-}eGFP}$ VLPs throughout the cell surface (**Figure 48**). These distribution patterns had been previously described for HIV-1 upon DC capture[189,190]. Moreover, we observed HIV-1 accumulation within virus-containing structures in Siglec-1-expressing cells from cervical tissues (**Figures 24** and **25B**).

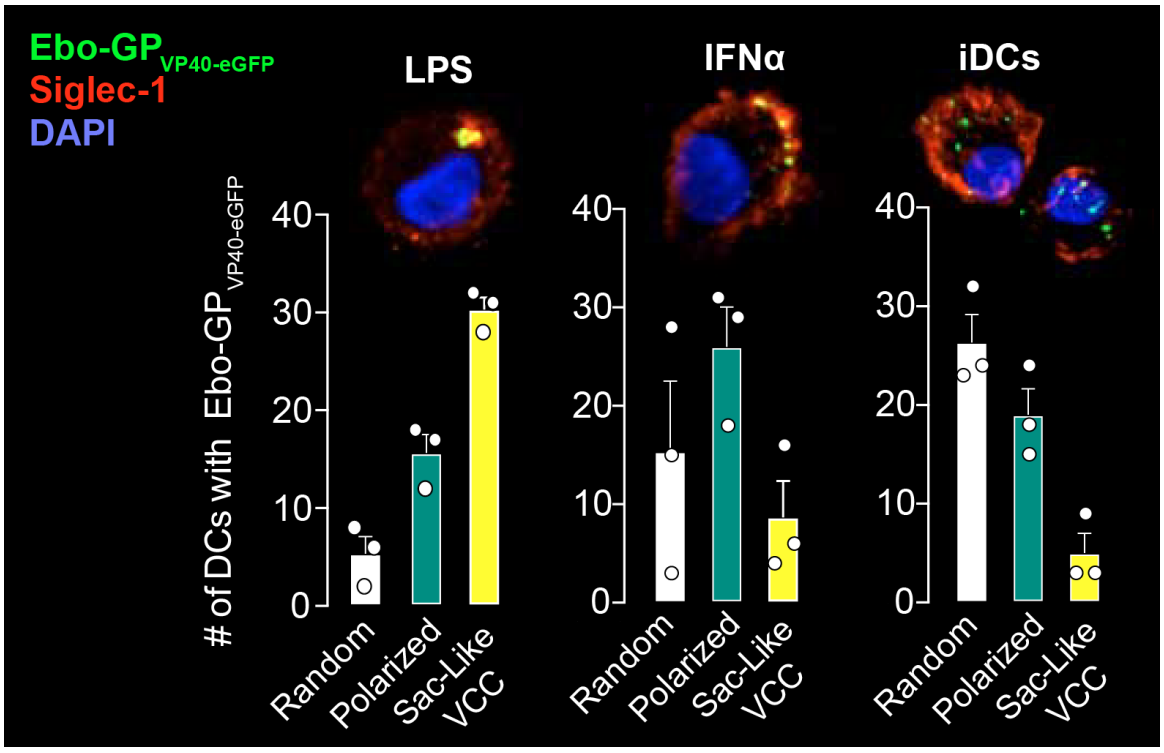

Figure 48. Distribution patterns of Ebola VLPs captured by DCs. Confocal microscopy analysis of different DCs pulsed with Ebo-GP$_{VP40\text{-}eGFP}$ VLPs for 4 h at 37ºC and stained with an anti-Siglec-1 PE mAb (red) and DAPI (blue). (Images) Representative viral distribution pattern for each type of DC analysed. Merge of z-planes showing maximum fluorescence intensity of the three channels. (Bar graphs) Number of DCs displaying each of the viral patterns. Data show mean values and SEM of fifty cells from three different donors.

To confirm that captured Ebola VLPs and HIV-1 are internalized through the same entry mechanism, we added red fluorescent HIV-1 to LPS-treated DCs that had previously been

pulsed with Ebo-$GP_{VP40\text{-}eGFP}$ VLPs. Confocal microscopy revealed that most of the Siglec-1-enriched sac-like compartments where Ebo-$GP_{VP40\text{-}eGFP}$ VLPs accumulated also contained HIV-1 particles (**Figure 49A** and **Movies 2** and **3**). Ultrastructure analysis by transmission electron microscopy (**Figure 49B**) and super-resolution microscopy (**Figure 49C** and **Movies 4 and 5**) also confirmed the presence of sac-like structures containing both Ebola and HIV-1 viral particles in LPS-treated DCs. Moreover, super-resolution microscopy revealed proximity between Siglec-1 and captured Ebo-$GP_{VP40\text{-}eGFP}$ VLPs (**Figure 49C** and **Movies 4** and **5**). Thus, data from confocal, electron and super-resolution microscopy further indicated that Siglec-1 is critical for EBOV and HIV-1 accumulation within VCCs in activated DCs.

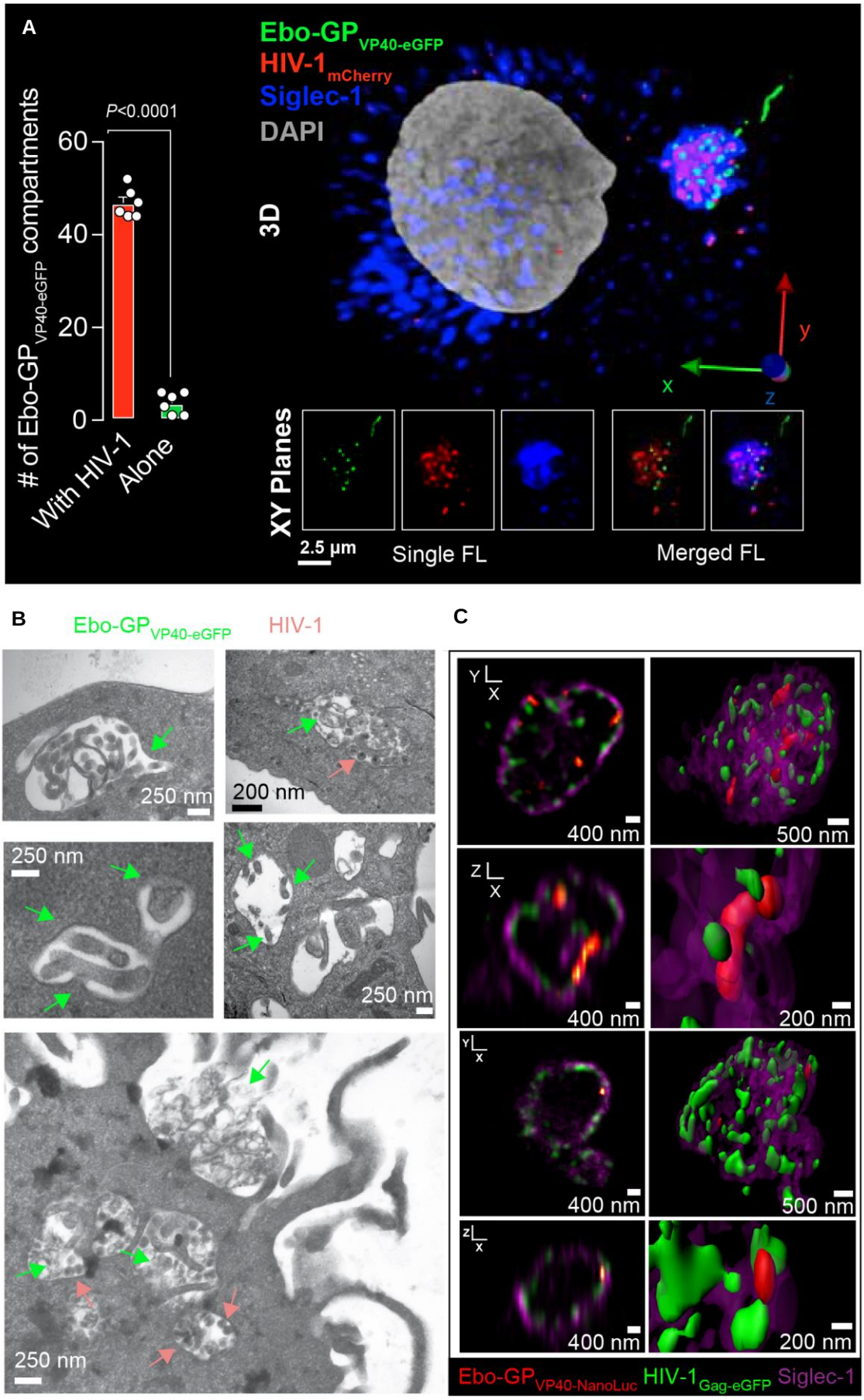

Figure 49 (caption overleaf).

Figure 49. DCs accumulate captured Ebola VLPs in the same Siglec-1-positive VCC as HIV-1. A. Confocal analysis of LPS-treated DCs pulsed with Ebo-$GP_{VP40\text{-}eGFP}$ VLPs and subsequently incubated with red fluorescent HIV-$1_{mCherry}$, extensively washed and stained with anti-Siglec-1 Alexa Fluor 647 (blue) and DAPI (grey). (Bar graph) Number of Ebola VCCs where red HIV-$1_{mCherry}$ signal was found along with eGFP signal or where eGFP signal was found alone. Data show mean values and SEM from fifty compartments in cells from six different donors and two independent experiments. Statistical differences were assessed with a paired *t* test. (3D reconstruction) Representative image of a single cell with a sac-like VCC (as in **Movies 2** and **3**). Images were collected every 0.2 μm. Deconvolved reconstruction shows the fluorescence of the grey channel and maximum intensity of the other channels within a 3D volumetric x-y-z data field. XY planes show magnification of the VCC with single or merged fluorescence channels. Scale bar: 2.5 μm. **B.** Electron micrographs of LPS-DCs exposed to Ebo-$GP_{VP40\text{-}eGFP}$ VLPs followed by a pulse with HIV-$1_{NFN\text{-}SX}$. Colored arrows indicate distinct viral particles captured within VCCs. Scale bars: 200-250 nm. **C.** Super-resolution microscopy showing the architecture of VCCs within LPS-treated DCs exposed to Ebo-$GP_{VP40\text{-}NanoLuc}$ VLPs (red) and HIV-$1_{Gag\text{-}eGFP}$ VLPs (green) mixed with HIV-$1_{NL4.3}$. Siglec-1 is colored in magenta. Left columns show volume slices while right columns depict an isosurface rendering of representative VCC (as in **Movies 4** and **5**) from the left images.

3.4 Ebola viral capture by Siglec-1 contributes to cytoplasmic entry into activated DCs

As DCs are primary filoviral targets that become productively infected early upon viral exposure[91], we next investigated if EBOV uptake via Siglec-1 enhances the capacity of the virus to fuse and enter the cytoplasm of activated DCs. This mechanism would resemble to that of phosphatidylserine receptors, which display a V-set domain as Siglec-1 does[403]. For this purpose, we employed a viral cytoplasmic entry assay that relies on the incorporation of a β-lactamase (BlaM)-VP40 chimera into Ebola VLPs bearing the Zaire envelope glycoprotein (Ebo-$GP_{VP40\text{-}BlaM}$ VLPs)[404] to recapitulate EBOV entry. When non-infectious Ebo-$GP_{VP40\text{-}BlaM}$ VLPs fuse with cellular membranes, BlaM released into the cytoplasm cleaves a CCF2-AM dye loaded into DCs and changes its fluorescence emission from fluorescein green to coumarin blue. As opposed to the system previously employed to determine viral uptake, this assay selectively detects Ebola virions entering the cell cytoplasm by fusion.

Distinctly treated DCs were pulsed with equivalent amounts of Ebo-$GP_{VP40\text{-}BlaM}$ VLPs, and after extensive washing, the percentage of cells cleaving CCF2-AM dye as a result of Ebola VLP cytoplasmic entry was analysed by FACS. Entry of Ebo-$GP_{VP40\text{-}BlaM}$ VLPs into LPS-treated DCs was lower than in iDCs, while stimulation with IFNα did not reduce viral fusion (**Figure 50A**). Thus, as opposed to what we observed for viral binding and uptake

(**Figure 40B-C**), cytoplasmic viral entry does not correlate with the levels of Siglec-1 expression on DCs (**Figure 17**). To investigate the relative contribution of Siglec-1 and CLRs on Ebola VLP cytoplasmic entry, cells were pre-treated with specific inhibitors before viral exposure (**Figure 50B**). While isotype control had no inhibitory effect, addition of 7-239 or 7D2 anti-Siglec-1 mAbs reduced Ebo-$GP_{VP40\text{-}BlaM}$ VLP entry into activated DCs (**Figure 50B**). Pre-treatment with anti-DC-SIGN MR1 mAb had no significant effect on cytoplasmic entry in any of the tested DCs, even though the employed Ebola VLPs displayed the envelope glycoprotein required for CLR recognition[400]. Combination of anti-DC-SIGN and anti-Siglec-1 mAbs had no further inhibitory capacity than the anti-Siglec-1 mAb alone (**Figure 50B**). Pre-treatment with the broad CLR inhibitor mannan did not reduce cytoplasmic entry in LPS-DCs, but significantly reduced fusion on IFNα-treated DCs and most prominently on iDCs (**Figure 50B**). Combination of mannan and anti-Siglec-1 mAbs had no further inhibitory capacity than mannan on iDCs, but reached higher inhibition levels on IFNα-treated DCs (**Figure 50B**). Representative flow cytometry dot plots showing the gating strategy followed in cytoplasmic entry assays are depicted in **Figure 51**.

Thus, while CLRs partially mediate Ebola VLP cytoplasmic entry into iDCs and IFNα-treated DCs, blockade of Siglec-1 reduced viral entry into LPS-DCs (62.6±17.5%) and IFNα-treated DCs (42±18.4%). Nevertheless, the inhibition levels were lower than those observed for viral uptake (**Figure 45B**), Hence, Siglec-1-independent viral binding also facilitates cytoplasmic entry, highlighting the need to combine inhibitors with different specificities to achieve full blockade.

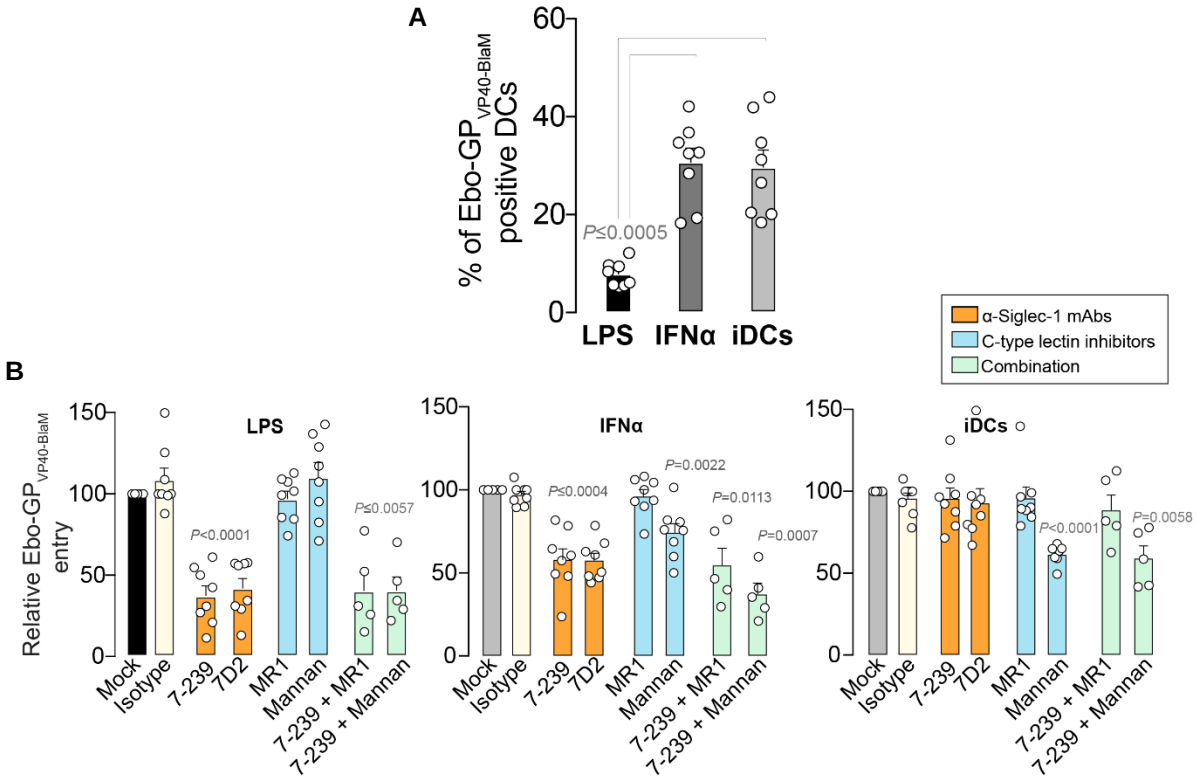

Figure 50. Siglec-1 contributes to Ebola VLP cytoplasmic viral entry into activated DCs. **A.** Comparative cytoplasmic entry of Ebo-$GP_{VP40\text{-}BlaM}$ VLPs added for 12 h at 37ºC to distinctly treated DCs and assessed by FACS using a CCF2-AM dye. Data show mean values and SEM from three independent experiments and include cells from eight donors. Statistical differences were assessed with a paired *t* test. **B.** Relative Ebo-$GP_{VP40\text{-}BlaM}$ VLP cytoplasmic entry into DCs pre-incubated with the indicated mAbs and inhibitors. Values are normalized to the levels of Ebo-$GP_{VP40\text{-}BlaM}$ entry into mock-treated cells, shown in panel **A** and set as 100%. Data show mean values and SEM from three experiments including cells from five-eight donors. Representative dot plots are shown in **Figure 51**. Statistical differences were assessed using a one-sample *t* test.

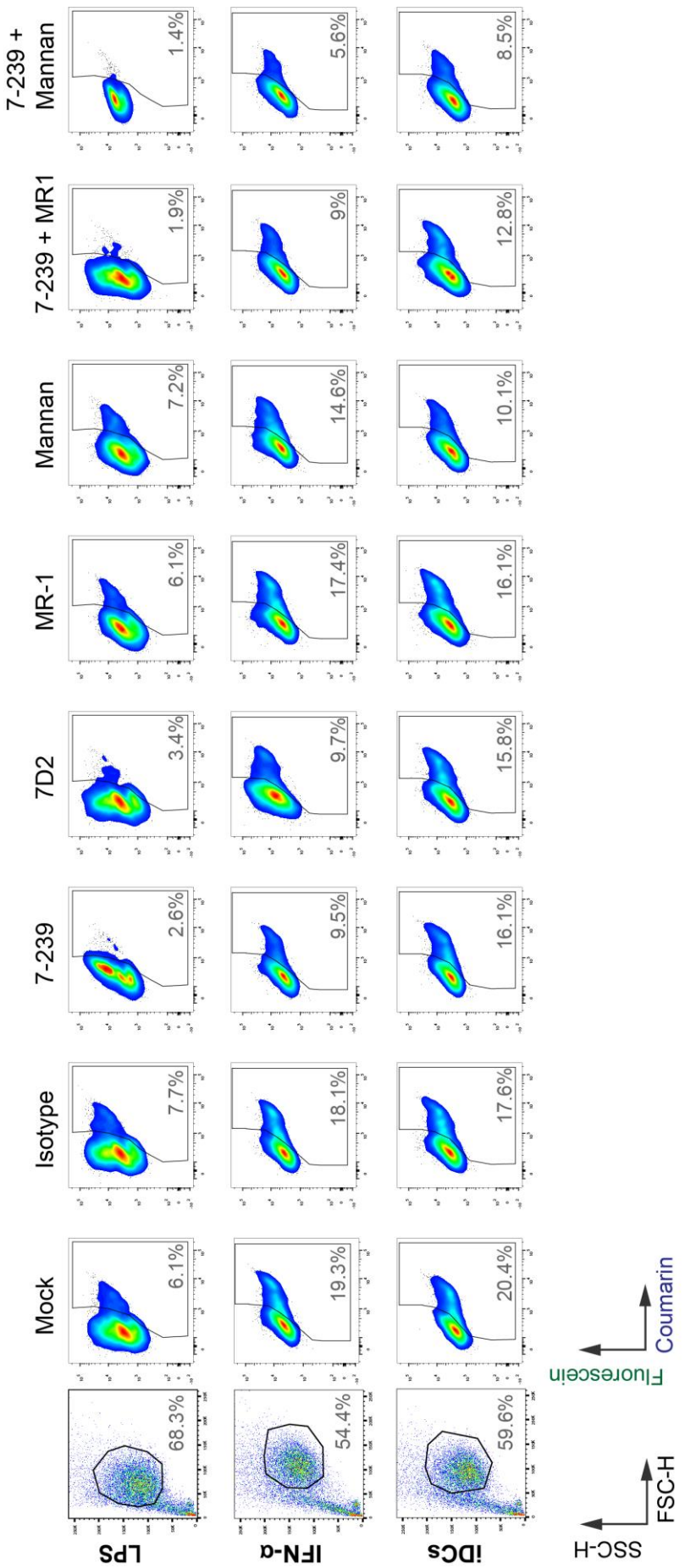

Figure 51 (caption overleaf).

Figure 51. Representative gating strategy employed in Ebola VLP cytoplasmic entry assays. FACS analysis of $Ebo_{VP40\text{-}BlaM}$ VLP cytoplasmic entry into distinctly treated DCs from one donor pre-incubated with the indicated mAbs and inhibitors. Data are representative from three independent experiments and cells from at least five donors.

To further confirm the role of Siglec-1 in Ebola VLP cytoplasmic entry, we assessed Ebo-$GP_{VP40\text{-}BlaM}$ VLP entry into Raji cells, but no fusion was detected regardless of the levels of Siglec-1 expression (**Figures 52** and **46A**). Thus, the already described resistance of Raji cells to Ebola viral entry[285] is not overcome by the capacity of Siglec-1 to enhance viral capture. However, we found that cytoplasmic Ebo-$GP_{VP40\text{-}BlaM}$ VLP entry was reduced on permissive primary DCs derived from a Siglec-1 null individual which naturally lack expression of Siglec-1 receptor[405], an effect that was more prominent upon DC activation (**Figure 53**). This observation further confirms Siglec-1 contribution to Ebola VLP cytoplasmic entry into activated DCs.

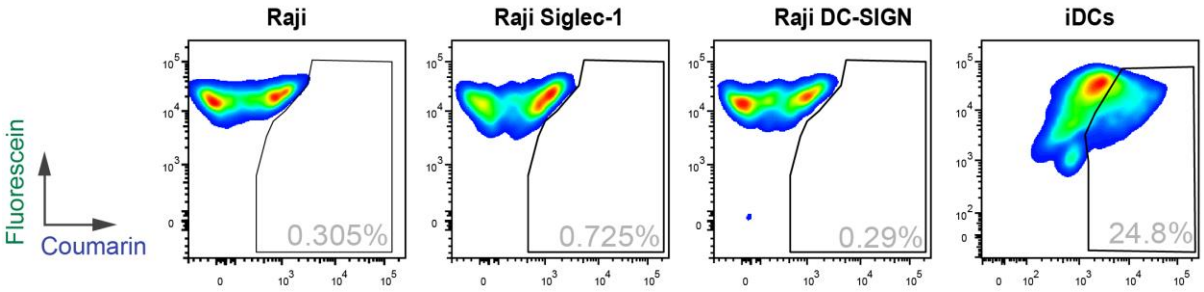

Figure 52. Siglec-1 expression does not confer permissiveness to Ebola VLP entry into Raji cells. Representative dot plots from two independent experiments showing cytoplasmic viral entry of Ebo-$GP_{VP40\text{-}BlaM}$ VLP pulsed with distinct Raji cells or iDCs for 12 h at 37ºC, exposed to CCF2-AM and assessed by FACS.

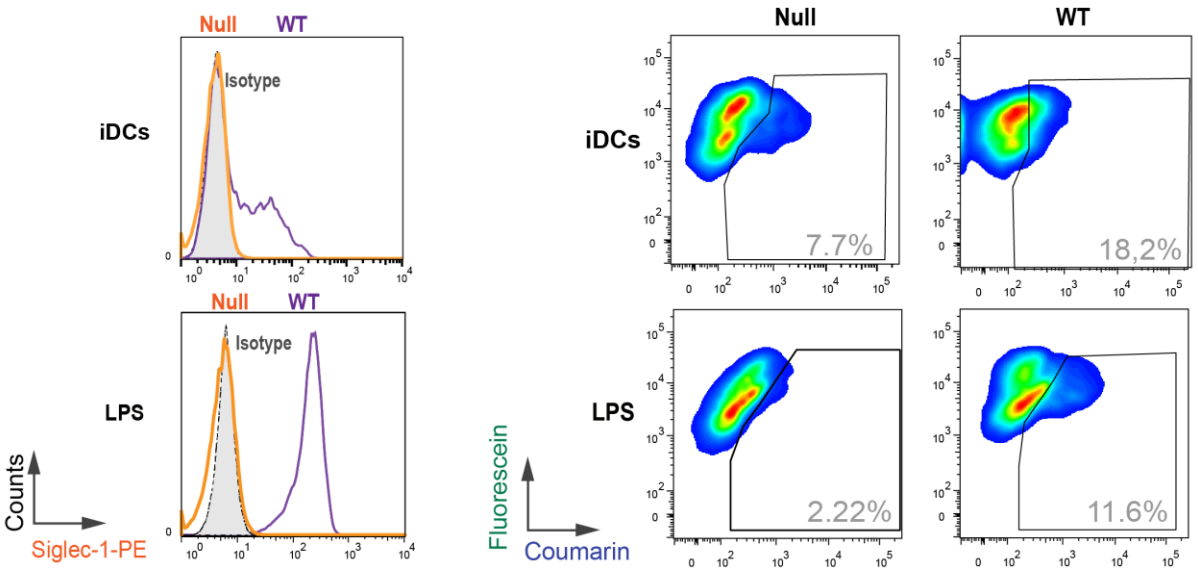

Figure 53. Confirmation that Siglec-1 contributes to Ebola VLP cytoplasmic entry into activated DCs. Histograms showing Siglec-1 expression levels on iDCs and LPS-treated DCs derived from a wild-type and a Siglec-1 null individual. Dot plots compare cytoplasmic viral entry of Ebo-$GP_{VP40\text{-}BlaM}$ VLPs into iDCs and LPS-treated DCs from a wild-type and a Siglec-1 null individual. WT: wild-type.

Taken together, results from this chapter show a role for Siglec-1 as an attachment factor that mediates both binding and uptake of Ebola VLPs by activated DCs. Importantly, Siglec-1-mediated viral attachment is one of the host-viral interactions that eventually lead to viral cytoplasmic entry. Thus, blocking Siglec-1 poses an interesting option to hamper EBOV entry into DCs, which are primary targets for this filovirus[91]. This novel mechanism for EBOV mimics that reported for HIV-1, which also exploits Siglec-1 recognition to gain access into DCs[70,187]. However, as opposed to HIV-1, which is *trans*-infected but does not productively infect DCs, in the case of EBOV, Siglec-1 interaction facilitates viral fusion and cytoplasmic entry on DCs. Given that new anti-Siglec-1 mAbs efficiently block HIV-1 capture and *trans*-infection (**Chapter 5**), we next aimed to test their potential to block Ebola viral attachment and cytoplasmic entry into DCs.

Chapter 7

RESULTS V

New anti-Siglec-1 mAbs block Ebola viral uptake and decrease cytoplasmic viral entry into myeloid cells

The results included in this chapter are part of:

Perez-Zsolt, D., Erkizia, I., Pino, M., García-Gallo, M., Martín, M.T., Benet, S., Chojnacki, J., Fernández-Figueras, M.T., Guerrero, D., Urrea, V., Muñiz-Trabudua, X., Kremer, L., Martinez-Picado, J.* and Izquierdo-Useros, N.* (2019). **Anti-Siglec-1 antibodies block Ebola viral uptake and decrease cytoplasmic viral entry**. *Nat Microbiol*. 4(9):1558-1570. doi: 10.1038/s41564-019-0453-2.

*Last authors.

1. Introduction

EBOV and MARV filoviruses cause intermittent outbreaks of FVD in humans, a deadly condition with great sanitary and socio-economic impact, as underscored by the recent EBOV outbreaks in West Africa (2014-2016) and the Democratic Republic of the Congo (ongoing since August 2018). Although significant progress in specific antiviral drugs has been achieved in the last years[389,406], no anti-filoviral agents are currently available. Moreover, therapies that are currently being evaluated only tackle *Zaire ebolavirus* species, while other ebolavirus and marburgvirus species with similar outbreak potential are not covered by these antiviral strategies and will require future treatments.

Infection of myeloid cells such as DCs is a strategy co-opted by different filoviruses to establish initial replication and facilitate filoviral systemic dissemination[91,266,311,312]. In the previous chapter, we showed that Siglec-1 expressed by activated DCs is an attachment factor that contributes to Ebola VLP entry into these cells through recognition of sialylated gangliosides (**Chapter 6**). In addition, we also produced a set of new anti-Siglec-1 mAbs (3F1, 5B10, 1F5, 4E8 and 6G5) with high affinity for Siglec-1 and efficiently blocked the capacity of DCs to capture of HIV-1, a sialylated virus that follows the same internalization pathway as Ebola VLPs into DCs (**Chapters 5** and **6**).

Here, we assessed the capacity of new anti-Siglec-1 mAbs to inhibit Ebola viral capture and entry into activated DCs. All new mAbs fully blocked Ebola viral uptake and significantly reduced viral cytoplasmic entry into these cells. New mAbs also exerted their blocking activity on myeloid cells directly isolated from lymphoid tissues or activated monocytes. Moreover, they proved effective against entry of Ebola VLPs pseudotyped with MARV glycoproteins. Hence, new anti-Siglec-1 mAbs arise as potential pan-filoviral agents that could be further developed to improve clinical prophylaxis in forthcoming outbreaks.

2. Material & Methods

2.1 Ethics statement

This study was approved by the institutional review board on biomedical research from HUGTiP (Badalona, Spain), and all donors gave their written informed consent to participate.

2.2 Primary cell cultures

MDDCs were obtained and activated as previously described (**Chapter 3**, **Material & Methods 2.2**).

Human tonsils were obtained from individuals undergoing prescribed tonsillectomies at the HUGTiP. After mechanical disruption, tonsillar mononuclear cells were isolated by Ficoll-Hypaque gradient centrifugation (Alere Technologies AS). B-lymphocytes were subsequently depleted with magnetic beads targeting CD19 while blocking Fc receptors (Miltenyi Biotec). Myeloid cells were further enriched by blood dendritic cell antigen 1 (BDCA1)-positive selection and cells were stimulated with 1,000 IU/ml of IFNα for 24-48 h as previously described[192]. Obtained cell suspensions were maintained in RPMI supplemented with 10% FBS, 100 IU/ml of penicillin and 100 µg/ml of streptomycin (all from Invitrogen).

2.3 Cell lines, plasmids and viral stocks

HEK-293T, Raji and Vero E6 cell lines were maintained as previously described (**Chapter 3**, **Material & Methods 2.3**, **Chapter 5**, **Material & Methods 2.2** and **Chapter 6**, **Material & Methods 2.2**). Raji B cells were employed to develop a stable line expressing Siglec-1 as previously described (**Chapter 5**, **Material & Methods 2.2**).

Ebo-$GP_{VP40\text{-}eGFP}$ VLPs were generated transfecting HEK-293T cells with the molecular clones CAGGS-eGFP-VP40 (kindly provided by Dr. Bieniasz) and pcDNA3.1-Zaire GP (BEI Resources). For Ebo-$GP_{VP40\text{-}BlaM}$ VLPs, cells were transfected with molecular clones pcDNA3.1-BlaM-VP40, pcDNA3-Zaire NP and pcDNA3.1-Zaire GP or pCAGGS-Marburg Musoke GP (all from BEI Resources). HEK-293T cells were transfected with calcium phosphate (CalPhos; Clontech) or X-tremeGENE 9 DNA Transfection Reagent (Merck) in T75 flasks using a total of 20-30 µg of plasmid DNA at equimolar ratios. Supernatants were harvested 72 h post-transfection, cleared of cellular debris by centrifugation and frozen at -80ºC until use. Stocks were quantified for their VP40 content and titrated as previously described (**Chapter 6**, **Material & Methods 2.3** and **2.11**).

2.4 Competition between new anti-Siglec-1 mAbs and Ebola VLPs in Raji Siglec-1 cells

200-500 ng of Ebo-$GP_{VP40\text{-}eGFP}$ VLP VP40 were mixed in parallel with increasing concentrations of commercial anti-Siglec-1 mAbs (clones 7D2 and 7-239), new anti-Siglec-1 mAbs (clones 3F1, 5B10, 1F5, 6G5 and 4E8) and IgG1 isotype control. $2x10^5$ Raji Siglec-1 cells were pulsed with these mixes for 3 h at 37ºC, washed and assessed by FACS. Of note, concentration of all mAbs employed (included commercial ones) was confirmed using a sandwich ELISA revealed with goat HRP-conjugated polyclonal anti-mouse Igs antibodies (Dako), and an IgG2b mAb (BD Biosciences) was included as standard for quantification.

2.5 Ebola VLP uptake and cytoplasmic entry assays

For uptake experiments, $1x10^5$ DCs were incubated with 600 ng of Ebo-$GP_{VP40\text{-}eGFP}$ VLP VP40 for 3 h at 37ºC. For blockade, cells were pre-incubated for 15 min at RT with 10 µg/ml of anti-Siglec-1 mAbs 7D2, 7-239 (both from Abcam), new anti-Siglec-1 mAbs, an IgG1 isotype control (BD Biosciences) or left untreated before viral exposure. After extensive washing, cells were assessed by FACS. Alternatively, IFNα-treated BDCA1-positive myeloid cells directly isolated from lymphoid tissues were pulsed with 770 ng of Ebo-$GP_{VP40\text{-}eGFP}$ VLP VP40 for 12 h at 37ºC per $1.3\text{-}3x10^6$ cells and treated as described for DCs.

For cytoplasmic entry assays, $1.5\text{-}3x10^5$ DCs or IFNα-treated monocytes were pre-treated with 10 µg/ml of anti-Siglec-1 mAbs 7D2, 7-239 (both from Abcam), new anti-Siglec-1 mAbs, an IgG1 isotype control (BD Biosciences), the CTSB inhibitor CA-074 Me at 50 µM (Enzo Life Sciences) or left untreated before viral exposure with equivalent fusogenic amounts of Ebo-$GP_{VP40\text{-}BlaM}$ VLPs (30 ng of VP40). After a 12 h incubation at 37ºC, cells were washed and assessed by FACS. Alternatively, IFNα-treated BDCA1-positive myeloid cells directly isolated from lymphoid tissues were pulsed with 75 ng of Ebo-$GP_{VP40\text{-}eGFP}$ VLP VP40 for 12 h at 37ºC per $0.6\text{-}1.5x10^5$ cells and treated as described for DCs. Cytoplasmic entry assays with Ebo-Marburg $GP_{VP40\text{-}BlaM}$ VLPs containing the MARV glycoprotein was carried out adding 40 ng of VLPs to $2.5x10^5$ activated DCs and IFNα-treated monocytes, but entry was only detected on activated monocytes[335]. Of note, none of the commercial or new anti-Siglec-1 mAbs employed displayed unspecific antiviral

effects, since none of them reduced Ebo-$GP_{VP40\text{-}BlaM}$ VLP entry into Vero E6 cells as compared to an isotype control mAb.

2.6 Statistical analyses

Data are reported as the mean and the SEM for each condition. Mean changes from 100% normalized values were assessed with a one-sample *t* test, considered significant at $P<0.05$. Response curves of mAbs were adjusted to a non-linear fit regression model (calculated with a four-parameter logistic curve with variable slope) and the associated extra sum-of-squares F tests were used to compare significant differences between the $logIC_{50}$ of mAbs. All analyses and figures were generated using GraphPad Prism v7.0d software and R v3.5.

3. Results

3.1 New anti-Siglec-1 mAbs block Ebola viral uptake by Siglec-1-expressing cells

To assess the capacity of new anti-Siglec-1 mAbs to halt Ebola viral uptake, we employed fluorescent Ebola VLPs bearing EBOV GP (Ebo-$GP_{VP40\text{-}eGFP}$ VLPs). First, we determined the capacity of anti-Siglec-1 mAbs and to block Ebola VLP capture by Raji B-lymphocytes stably expressing human Siglec-1 (Raji Siglec-1 cells), while comparing it to commercially available anti-Siglec-1 mAb clones 7-239 and 7D2. A constant amount of Ebo-$GP_{VP40\text{-}eGFP}$ VLPs was mixed with increasing concentration of new and commercial anti-Siglec-1 mAbs and then added in combination to Raji Siglec-1 cells, and viral uptake was assessed by FACS (**Figure 54**). In contrast to the results obtained for HIV-1, in which 6G5 and 4E8 mAbs did not achieve full blockade (**Figure 36A**), all new anti-Siglec-1 mAbs completely inhibited Ebo-$GP_{VP40\text{-}eGFP}$ VLP uptake by Raji Siglec-1 cells (**Figure 54A**). Since EBOV is approximately sixfold larger than HIV-1 the individual binding of 4E8 and 6G5 mAbs might be sufficient to cause steric hindrance to virus binding. Again, 3F1 mAb inhibited Ebo-$GP_{VP40\text{-}eGFP}$ VLP uptake more potently than commercial mAbs (**Figure 54B-C**).

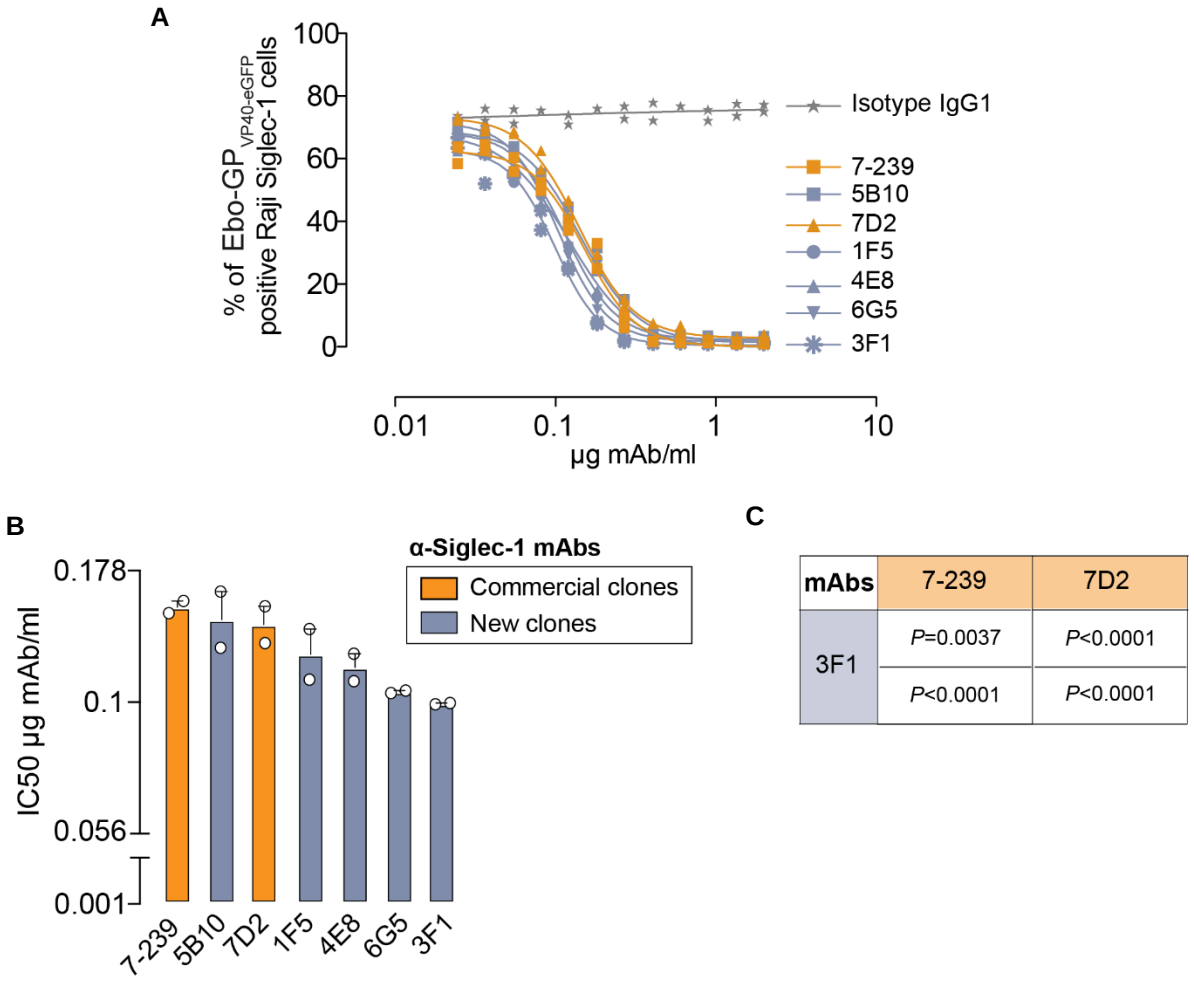

Figure 54. New mAbs block Ebola viral uptake by Raji Siglec-1 cells. A. Competition between Ebo-$GP_{VP40\text{-}eGFP}$ VLPs and anti-Siglec-1 mAbs for Raji Siglec-1 binding upon incubation for 3 h at 37ºC. Non-linear fit to a variable response curves based on 12 *xy* values are shown. **B.** IC_{50} values of all mAbs. Data show mean values and SEM from two independent experiments. **C.** *P*-values comparing the adjusted models for competitive Ebo-$GP_{VP40\text{-}eGFP}$ VLP uptake inhibition ($logIC_{50}$) of 3F1 commercial mAbs 7-239 and 7D2. Non-linear dose-response curve models were fitted based on 12 *xy* values from two independent experiments. Comparisons were inferred with an extra sum-of-squares F test.

Next, we determined the capacity of new anti-Siglec-1 mAbs to block viral capture by primary DCs. Pre-treatment of distinctly treated DCs with new anti-Siglec-1 mAbs significantly blocked Ebo-$GP_{VP40\text{-}eGFP}$ VLP uptake, especially on activated DCs (**Figure 55A**). Moreover, new mAb 1F5 reduced Ebola VLP capture by IFNα-treated BDCA1-positive myeloid cells directly isolated from lymphoid tissues (**Figure 55B**), which have been shown to capture HIV-1 in a Siglec-1-dependent manner[192]. These results indicate that new anti-Siglec-1 mAbs efficiently interfere with Ebola viral capture by activated DCs.

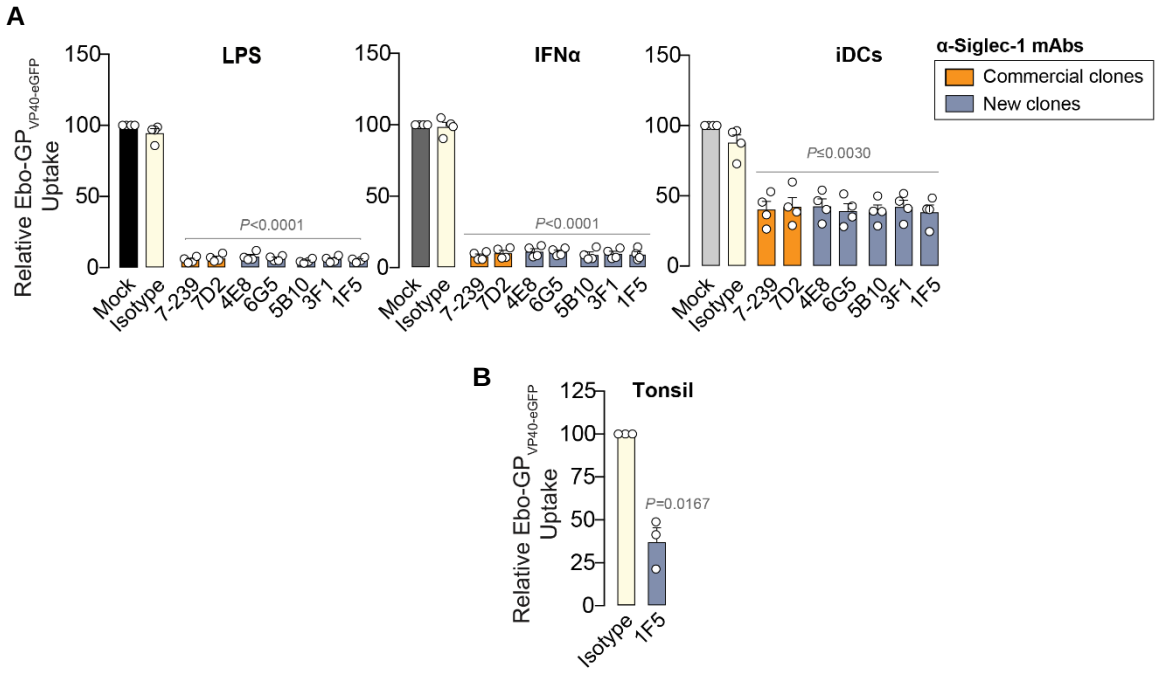

Figure 55. New mAbs block Ebola VLP uptake by activated DCs and myeloid cells from lymphoid tissues. A. Relative Ebo-$GP_{VP40\text{-}eGFP}$ VLP uptake for 3 h at 37ºC by distinctly treated DCs pre-incubated with the indicated mAbs and assessed by FACS. Values are normalized to those of Mock-treated cells, shown in **Figure 45A** and set as 100%. Data show mean values and SEM from two independent experiments and include cells from four donors. Statistical differences were assessed using a one-sample *t* test. **B.** Relative Ebo-$GP_{VP40\text{-}eGFP}$ VLP uptake for 12 h at 37ºC by IFNα-treated BDCA1-positive myeloid cells directly isolated from lymphoid tissues. Values are normalized to those of Isotype-treated cells, with a mean uptake of 15 ± 8% (SD), set as 100%. Data show mean values and SEM from one experiment that includes cells from three donors.

3.2 New anti-Siglec-1 mAbs reduce filoviral cytoplasmic entry into activated myeloid cells

To assess if new anti-Siglec-1 mAbs could impact on cytoplasmic viral entry into activated DCs, we employed Ebola VLPs bearing the BlaM-VP40 chimeric protein and EBOV GP (Ebo-$GP_{VP40\text{-}BlaM}$ VLPs). Activated DCs pre-incubated with new and commercial anti-Siglec-1 mAbs were pulsed with equivalent amounts of Ebo-$GP_{VP40\text{-}BlaM}$ VLPs, and cells treated with the CTSB inhibitor CA-074 Me, a potent cytoplasmic viral entry inhibitor[301], were included as a control. New anti-Siglec-1 mAbs effectively reduced Ebo-$GP_{VP40\text{-}BlaM}$ VLP cytoplasmic entry into both LPS- and IFNα-treated DCs (**Figure 56A**). In addition, new clone 1F5 reduced Ebo-$GP_{VP40\text{-}BlaM}$ VLP entry into IFNα-treated BDCA1-positive cells directly isolated from lymphoid tissues (**Figure 56B**).

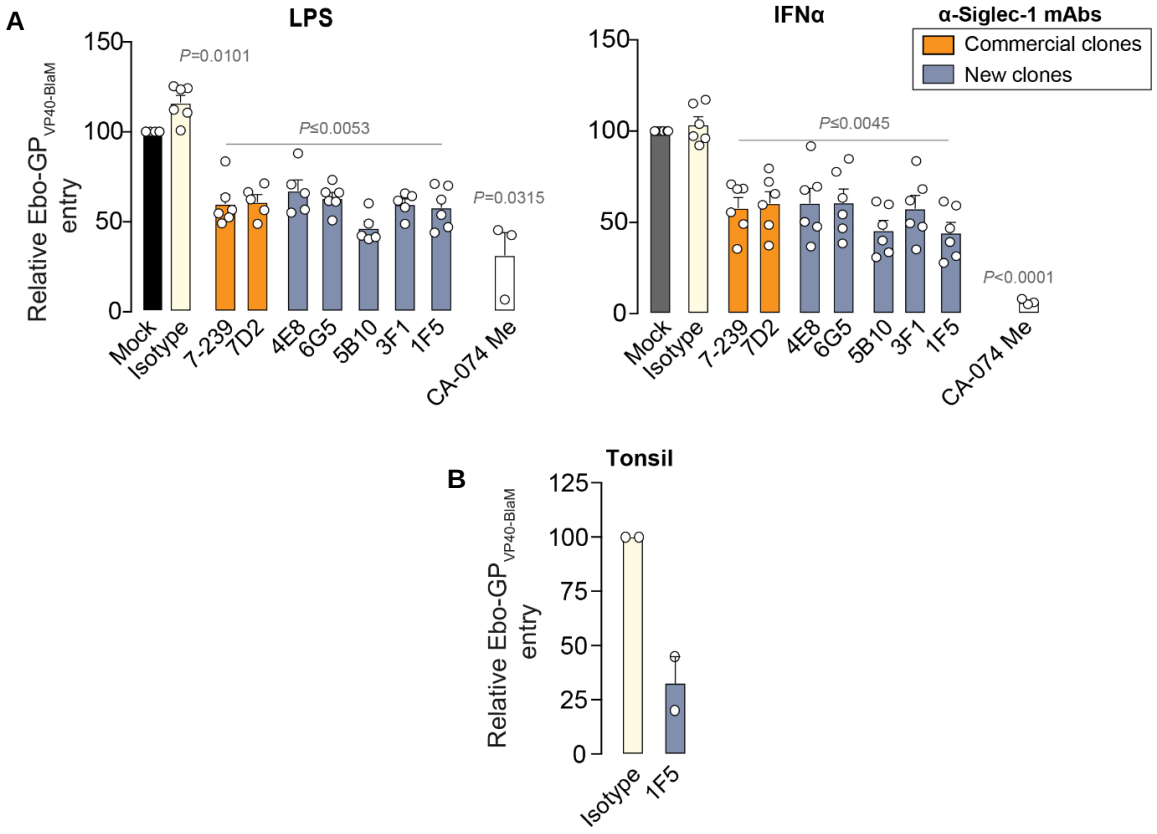

Figure 56. New mAbs reduce Ebola VLP cytoplasmic entry into activated myeloid cells. **A.** Relative Ebo-GP$_{VP40\text{-}BlaM}$ VLP cytoplasmic viral entry upon incubation for 12 h at 37ºC with distinctly treated DCs pre-incubated with the indicated mAbs. CTSB inhibitor CA-074 Me was included as a control. Values are normalized to those of Mock-treated cells, shown in **Figure 50A** and set as 100%. Data show mean values and SEM from two independent experiments including cells from three-six donors. Statistical differences were assessed with a one-sample *t* test. **B.** Relative cytoplasmic Ebo-GP$_{VP40\text{-}BlaM}$ VLP entry upon incubation for 12 h at 37ºC with IFNα-treated BDCA1-positive myeloid cells directly isolated from lymphoid tissues pre-incubated with novel mAb 1F5. Values are normalized to those of Isotype-treated cells, with a mean entry of 5 ± 4% (SD), set as 100%. Data show mean values and SEM from one experiment and cells from two donors.

Finally, we assessed the role of Siglec-1 in cytoplasmic viral entry into other myeloid cells that act as early filoviral targets[407] and express Siglec-1[213], such as IFNα-treated monocytes (**Figure 57**). Ebo-GP$_{VP40\text{-}BlaM}$ VLP cytoplasmic entry into IFNα-treated monocytes was reduced in the presence of new anti-Siglec-1 mAbs (**Figure 57A**). Moreover, cytoplasmic entry of Ebola VLPs containing the MARV glycoprotein was also inhibited by new anti-Siglec-1 mAbs (**Figure 57B**), as expected by the glycoprotein-independent recognition mechanism of this receptor, which relies on recognition of viral membrane gangliosides.

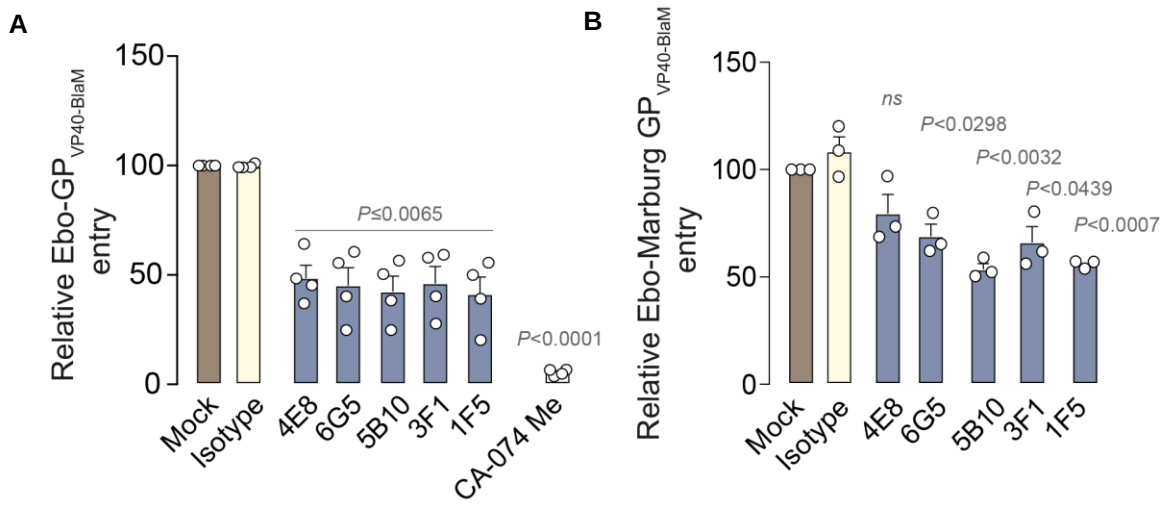

Figure 57. New mAbs reduce Ebola and Marburg cytoplasmic viral entry into activated monocytes. A. Relative cytoplasmic entry of Ebo-$GP_{VP40\text{-}BlaM}$ VLP pulsed for 12 h at 37ºC with IFNα-treated monocytes pre-incubated with new mAbs. Values are normalized to Mock-treated cells, with a mean entry of 41 ± 20% (SD) and set as 100%. Data show mean values and SEM from one experiment and include cells from four donors. **B.** Relative cytoplasmic entry of Ebo-Marburg $GP_{VP40\text{-}BlaM}$ VLPs (containing the MARV glycoprotein) pulsed for 12 h at 37ºC with IFNα-treated monocytes pre-incubated with new mAbs. Values are normalized to those of Mock-treated cells, with a mean entry of 20 ± 5% (SD) and set as 100%. Data show mean values and SEM from one experiment including cells from three donors. Statistical differences in **A** and **B** were assessed with a one-sample *t* test.

Collectively, this chapter shows that new anti-Siglec-1 mAbs efficiently block Ebola VLP capture by Siglec-1-expressing cells, which leads to a reduction in cytoplasmic viral entry into activated myeloid cells such as DCs and monocytes. Importantly, this effect is extended to VLPs bearing MARV glycoprotein, indicating their potential cross-protection against different filoviruses. Moreover, since the capture of a distant lentivirus such as HIV-1 is also reduced by Siglec-1 blockade, it is likely that other enveloped viruses exploit Siglec-1 on myeloid cells to gain access to target cells, and that anti-Siglec-1 mAbs might represent broad-spectrum inhibitors for enveloped viruses that deserve further characterization.

Chapter 8

DISCUSSION

DCs are the most potent APCs[1,2] and their immune function is key to initiate immunity against viruses[3–5]. However, DC migratory function can be subverted by some viruses to disseminate systemically[88–97]. In this thesis we explored how Siglec-1 expression on DCs might contribute to the viral pathogenesis of two different enveloped viruses such as HIV-1 and EBOV. Based on the results obtained throughout this thesis, here we discuss the role of Siglec-1 in HIV-1 and EBOV infection, highlighting the pathways that trigger Siglec-1 up-regulation during the course of both types of viral-associated diseases. We also address the capacity of this receptor to mediate initial events of the pathogenesis by both viruses, aiding systemic dissemination from the entry sites upon viral encounter. Moreover, we propose the use of newly generated anti-Siglec-1 mAbs as a way to combat DC-mediated dissemination of both pathogens.

1. Mechanisms of Siglec-1 up-regulation by type I IFNs during HIV-1 and EBOV infection

Siglec-1 is a receptor potently up-regulated on distinct human DCs upon stimulation with type I IFNs such as IFNα[187]. The presence of IFNα during HIV-1 infection has been extensively reported[147,220,221], and several cell types have been identified as the sources of IFNα production. pDCs are known for their capacity to secrete IFNα in response to HIV-1[36,37,224–229] upon sensing of HIV-1 genome through TLR7 and TLR9[34–36]. Moreover, IFNα secreted by HIV-1-exposed DCs induces maturation of bystander myeloid DCs[230]. Here, we confirmed that pDCs exposed to HIV-1 produce IFNα (**Figure 14A**), and found that secretion of this cytokine up-regulates Siglec-1 expression on DCs (**Figure 14B**). Thus, we identified mechanism of paracrine Siglec-1 up-regulation on myeloid DCs during HIV-1 infection (**Figure 58A**). Aside from pDCs, type I IFNs can also be secreted in an autocrine manner by myeloid DCs[231,233–235] activated by factors such as LPS, which is found in plasma upon HIV-1 infection due to the bacterial translocation that occurs in the GALT[147,148,236] (**Figure 58A**). Here, we determined that Siglec-1 up-regulation on LPS-treated DCs[70] is mediated by the effect of type I IFNs secreted by these cells upon LPS sensing (**Figure 17**) (**Figure 58A**). Thus, we identified two alternative sources of type I IFNs (i.e. paracrine and autocrine) that can up-regulate Siglec-1 expression on DCs during HIV-1 infection (**Figure 58A**). Of note, plasma from HIV-1-infected individuals also stimulates Siglec-1 expression on DCs signaling via type I IFN receptor[192]. This explains why on circulating monocytes of HIV-1 infected individuals, Siglec-1 expression correlates *in vivo* with the levels of plasma viremia, and why these levels only diminish after introduction of ART[192].

Aside from HIV-1, IFNα is also present throughout the course of EBOV infections. Secretion of IFNα has been detected in humans and non-human primate models[350,352], especially in fatality cases[350], while asymptomatic EBOV infections are characterized by the absence of this cytokine[408]. Thus, IFNα might mediate Siglec-1 up-regulation on DCs during EBOV infection as well (**Figure 58B**). Although *in vitro* pDCs exposed to EBOV do not secrete IFNα[409], activated pDCs have been found in EBOV-infected non-human primates, suggesting that these cells might produce IFNα *in vivo*[395] (**Figure 58B**). Aside from pDCs, myeloid cells could contribute to IFNα secretion during EBOV infection, as EBOV-like particles induce IFNα production by murine bone marrow-derived DCs through TLR signaling[410]. EBOV glycoprotein interaction with human monocyte-derived macrophages induced TLR4-dependent IFNα secretion by these cells[411]. Moreover, a secreted or shed form of EBOV glycoprotein signals through TLR4[336], although IFNα secretion in response to these secreted glycoproteins remains unexplored (**Figure 58B**). Noteworthy, LPS was also found in a case of EBOV infection complicated with septicemia, possibly due to bacterial translocation[356], which might account for indirect IFNα secretion during EBOV infection as described for HIV-1 (**Figure 58B**).

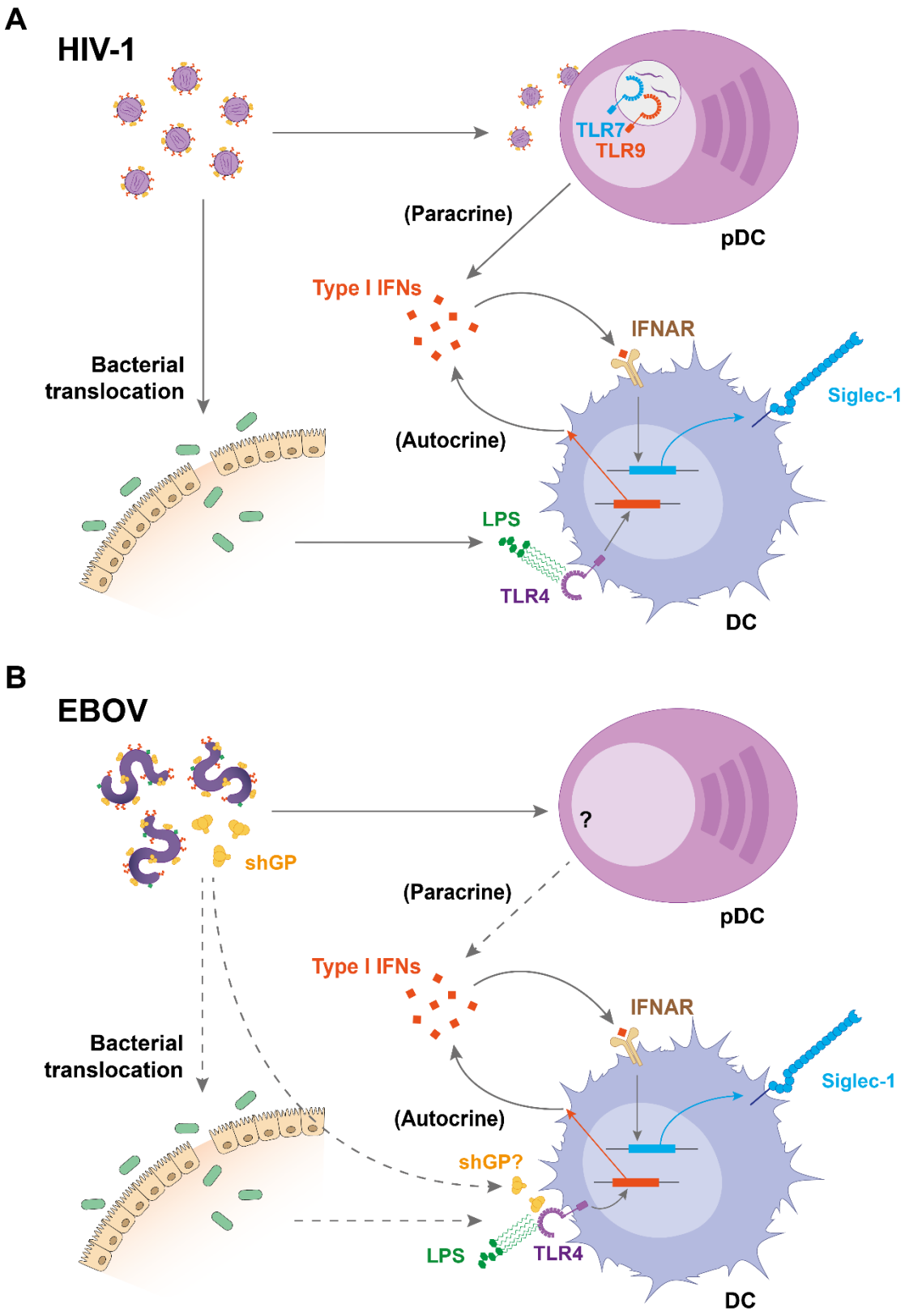

Figure 58. Mechanisms of Siglec-1 up-regulation during HIV-1 and EBOV infections. A. HIV-1 induces secretion of type I IFNs by pDCs through TLR7 and TLR9 sensing, which up-regulates Siglec-1 on DCs in a paracrine manner. Moreover, LPS from bacterial translocation up-regulates Siglec-1 on DCs via TLR4 and autocrine type I IFNs. **B.** During EBOV infection,

type I IFNs might also have a central role enhancing Siglec-1 expression on DCs, although this needs further investigation. pDCs may produce type I IFNs in response to EBOV infection *in vivo*, while bacterial translocation was suspected during a case of gram-negative septicemia in an EBOV-infected patient. In addition, viral components such as secreted or shed EBOV glycoproteins may induce activation of myeloid cells through TLR4 signaling, providing an alternative stimulus of autocrine type I IFNs during EBOV infection. IFNAR: IFNα/β receptor; shGP: shed glycoprotein. Adapted from ref.[412].

Taken together, the presence of type I IFNs throughout the course of these viral infections is well-established, although both HIV-1 and EBOV have evolved particular molecular mechanisms via viral antagonistic proteins that aid to evade cellular immune sensing[248,345,413,414]. Intriguingly, the protective role of type I IFNs responses is controversial, since the apparent antiviral function during the earliest stages of infection may, in turn, fuel pathogenesis during the later stages of viral disease. That seems to be the case not only for HIV-1[147], but also for EBOV[345], where clinical data collected during human outbreaks has indicated that elevated levels of circulating IFNα, as well as upregulation of IFN-inducible genes, correlates with fatal disease outcome[350,353–355]. Thus, HIV-1 and EBOV infections trigger an immune activation state that up-regulates Siglec-1 expression on DCs, a situation that might favor early viral dissemination events in an otherwise antiviral environment[415].

2. Siglec-1 expressed on cervical DCs mediates HIV-1 *trans*-infection

Intriguingly, these early viral dissemination events can take place in the cervical mucosa in the case of HIV-1 infection. HIV-1 is mostly acquired by sexual transmission[108], and in the cervical mucosa, IFNα-producing pDCs are soon recruited to the cervix upon viral acquisition[239]. Although increased antiviral IFNα secretion could limit initial viral infection[416–419], it could promote viral capture on cervical myeloid cells via Siglec-1 induction as well. Of note, we found that HIV-1-exposed pDCs from women secrete higher levels of IFNα than those from men (**Figure 16A**), which is in line with previous results[360]. Conversely, sex did not affect Siglec-1 expression in response to IFNα, as it had been reported for other IFN-stimulated genes during chronic HIV-1 infection[420] (**Figure 16B**). These results suggest that the paracrine induction of Siglec-1 expression might occur in the female reproductive mucosa, a key anatomical compartment for HIV-1 acquisition in women.

APCs from the female reproductive tract may not only boost the productive infection of primary target cells, but also the viral dissemination towards distal tissues[89,134,242,380] (**Figure 59**). DC-T cell conjugates represent an optimal milieu for productive HIV-1 infection, which may boost initial viral replication of $CD4^+$ T cells[88,421]. Moreover, uninfected DCs could promote HIV-1 dissemination to draining lymph nodes after mucosal challenge[89,133] (**Figure 59**). Yet, the precise molecular mechanism mediating these processes remained unexplored in the cervicovaginal tissue. Here, we detected Siglec-1 expression on a population of cervical myeloid cells expressing HLA-DR, CD11c, CD14, and CD11b (**Figure 19**), all classical markers known to be present on DCs of the submucosa at the lower female genital tract[379,383,384,422]. Moreover, these cells were able to mediate viral capture and transmission to target cells (**Figures 23, 29**).

Our findings concur with prior studies where the migratory $CD3^-$ $HLA\text{-}DR^+$ fraction or the cervicovaginal $CD11c^+$ DCs were found to be the myeloid cell subset that preferentially captured and transported HIV-1 out of the cervicovaginal mucosa[243,244,376]. Nevertheless, we now show that on DCs of the ectocervix and endocervix, alternative receptors beyond DC-SIGN operate in HIV-1 viral uptake and transfer, as previously reported for MDDCs[161,180–184,186,368]. Our results provide a plausible mechanism for previous reports where the predominant cervical myeloid cell population that captured HIV-1 was found to be DC-SIGN negative[379], or where there was a lack of inhibition of neutralizing mAbs against DC-SIGN on viral transmission mediated by cervical myeloid cells[376]. The discovery of Siglec-1 expression on myeloid cervical DCs (**Figure 19**) and the capacity of Siglec-1^+ cells to capture viruses *in vivo* (**Figure 25**) help to understand how this particular receptor can facilitate boosting of HIV-1 replication and dissemination from the genital mucosa to the corresponding draining lymph nodes in the absence of DC productive infection.

Baseline levels of Siglec-1 on myeloid cells in the lamina propria of all cervical tissues examined herein already allowed viral uptake (**Figure 19**), demonstrating that Siglec-1 could act as a viral attachment factor even in the absence of prior viral infection. However, as tissues with a high level of inflammatory infiltrate showed an increased number in Siglec-1^+ cells (**Figure 22**), ongoing inflammatory events triggered upon infection could magnify Siglec-1 mediated HIV-1 uptake and *trans*-infection. Indeed, in a cervical biopsy of an HIV-1 viremic woman, we found Siglec-1^+ cells with HIV-1-containing compartments, demonstrating that these cells actually trap viruses and form these compartments *in vivo* **(Figure 25)**. Interestingly, similar VCC-like structures have been

detected in urethral macrophages of HIV-1-infected individuals under suppressive ART[423], but it remains to be determined if Siglec-1 is implicated in the formation of these particular structures.

Further, we demonstrated that $CD14^+$ $CD11c^+$ DCs up-regulate Siglec-1 expression in a dose response manner after IFNα stimulation of the cervical tissue, especially at the endocervix (**Figure 27**). In contrast, higher basal expression of Siglec-1 was found on ectocervical myeloid cells at the steady state (**Figure 27**). These data suggest that while pre-existing basal immune activation at the ectocervix could already favour Siglec-1 capture of early invading viruses, endocervical cells will most likely mediate viral uptake at later time points, once antiviral type I IFN responses are mounted and Siglec-1 expression is boosted on DCs (**Figure 59**). Indeed, this could explain why we only observed an increased number of Siglec-1^+ cells on biopsies from the endocervix that had a high inflammatory score. Overall, detection of Siglec-1 on cervical DCs contributes to understand why the IFN system is not more effective against HIV-1 despite its substantial up-regulation early upon infection[239,373,377]. Similarly, it may also explain why treatments inducing pDC recruitment[424] and a strong type I IFN response [425] before vaginal challenge in macaques are incapable of limiting viral infection beyond the infected mucosa and can even enhance viral replication.

As other sexually transmitted infections such as herpes virus or chlamydia infection trigger type I IFN responses in mucosal tissues via pDC recruitment and/or bacterial LPS exposure[426,427], it would be important to explore the role of Siglec-1 in favouring HIV-1 acquisition, replication and dissemination in women with pre-existing sexually transmitted infections[375]. Moreover, since inflammatory $CD14^+$ $CD11c^+$ DCs are known to induce Th17 T-cell differentiation[428], and these are the preferential targets of viral infection in the cervix right after retroviral invasion[429], it would also be critical to evaluate the role of this Siglec-1^+ DC subset on susceptibility to HIV-1 infection.

In addition to facilitate local HIV-1 cell-to-cell transmission in the cervical mucosa via *trans*-infection, Siglec-1 could allow systemic viral dissemination upon DC migration to lymphoid tissues (**Figure 59**). Indeed, DCs bearing retroviruses are found in the draining lymph nodes of distinct animal models as soon as 24 h after vaginal challenge[89,132–134] and these findings originally led to formulate the Trojan Horse hypothesis, which states that DCs can serve as vehicles transporting the virus from the entry sites to distant tissues[88,90]. According to this hypothesis, Siglec-1^+ cervical DCs might contribute to viral

dissemination from the entry sites, transporting captured HIV-1 to the regional lymph nodes, where efficient transfer to target CD4$^+$ T cells could take place (**Figure 59**).

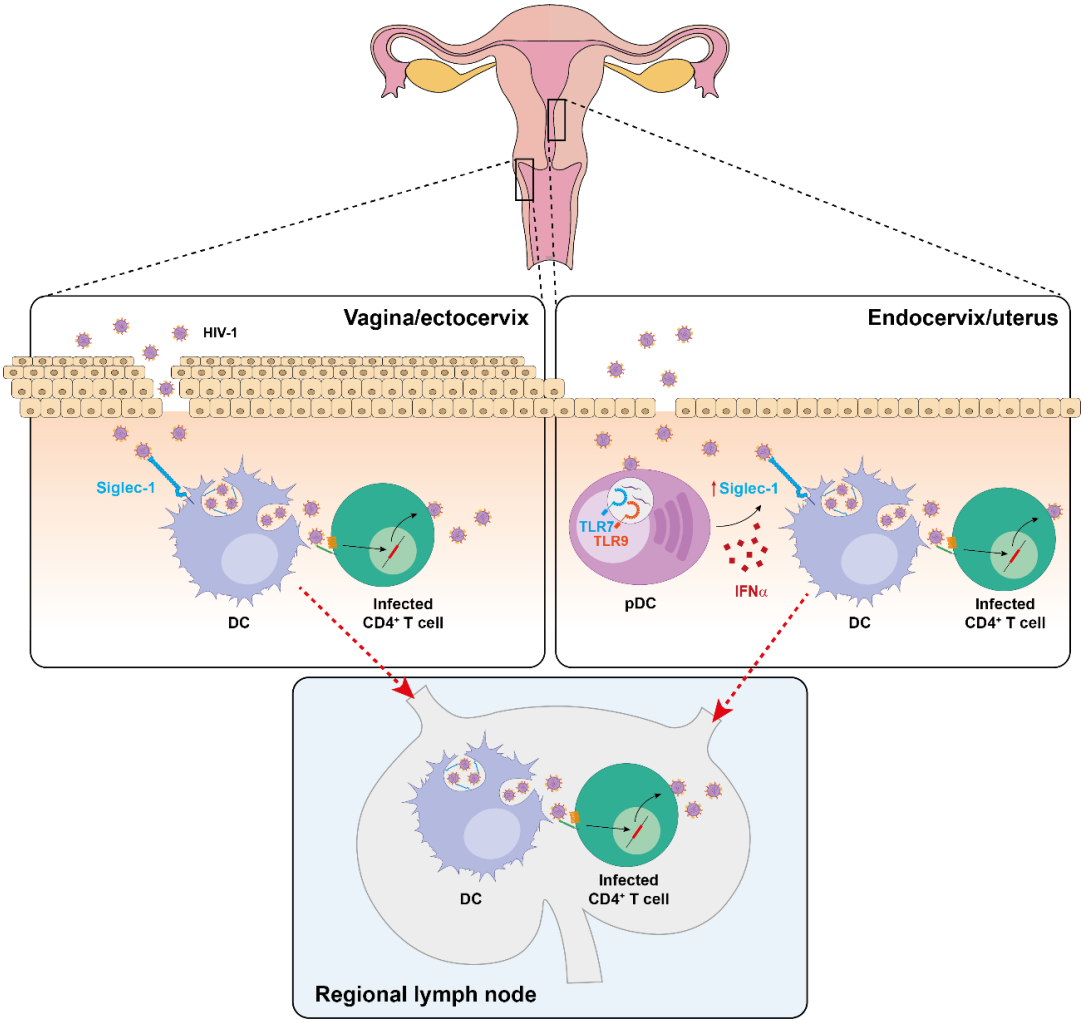

Figure 59. Proposed mechanism of HIV-1 dissemination from the female reproductive tract. In the vaginal/ectocervical mucosa, basal Siglec-1 DCs may mediate local HIV-1 *trans*-infection to target CD4$^+$ T cells. At the endocervical mucosa, lower Siglec-1 expression is boosted in response to IFNα released by recruited pDCs sensing HIV-1. DCs may also contribute to systemic HIV-1 spread due to their ability to migrate to secondary lymphoid tissues, where CD4$^+$ T cells accumulate. While a similar mechanism could be exploited by EBOV, further work needs to address this possibility. From ref.[412].

In summary, myeloid DCs expressing Siglec-1 are found in the cervical tissues of women in the basal state. IFNα-treated myeloid DCs up-regulate Siglec-1 expression, which increases viral capture and *trans*-infection, providing an explanation of how the virus may succeed in an otherwise antiviral environment. We propose that Siglec-1$^+$ cervical DCs may facilitate HIV-1 transfer to bystander CD4$^+$ T cells through recognition of sialylated

gangliosides, thus favouring the nascent infection within the cervical mucosa, but also prompting early dissemination to secondary lymphoid tissues.

3. Siglec-1 is a common factor mediating access of EBOV and HIV-1 into DCs

Gangliosides are ubiquitous molecules present in the cell plasma membrane, and thus it is likely that other enveloped viruses aside from HIV-1 also incorporate these molecules during budding processes. Indeed, the presence of sialylated gangliosides has been detected on both EBOV and MARV viral particles[288]. Here, we confirmed that Ebola VLPs incorporate GM1 ganglioside (**Figure 41**) and that capture of these VLPs was higher following activation with LPS and IFNα (**Figure 40**), concurrent with higher Siglec-1 levels on activated cells (**Figure 17**). Moreover, we demonstrated that this capture is mediated by Siglec-1 using alternative approaches, including capture inhibition with anti-Siglec-1 mAbs and Siglec-1 silencing (**Figures 45, 46**). Hence, we identified Siglec-1 as a novel factor mediating Ebola VLP attachment in activated DCs.

Upon viral capture, Siglec-1 directed Ebola VLPs to a VCC that also accumulated captured HIV-1 particles (**Figure 49**), and that is similar to those that we observed in the cervical biopsy of a viremic HIV-1-infected patient (**Figure 25**). This compartment was previously described as a tetraspanin-enriched VCC that accumulates HIV-1[189–191] and that is the same compartment where extracellular vesicles are trapped within activated DCs[70,73]. Extracellular vesicles assemble and bud from cell plasma membranes as viruses do[430,431], and thus incorporate sialylated gangliosides recognized by Siglec-1[69]. Upon Siglec-1 binding, captured nanovesicles are directed towards a compartment[70–72] that has been proposed to function as a depot involved in antigen dissemination[66–68]. Indeed, extracellular vesicles displaying processed MHC:peptide complexes on their surface can be captured by DCs, stored and transferred DCs to antigen-specific $CD4^+$ T cells[67] (**Figure 60, top**). Thus, it appears that both HIV-1 and EBOV exploit a pre-existing pathway of extracellular vesicle internalization to gain access into DCs, which could aid viral pathogenesis (**Figure 60**).

In the context of HIV-1 infection, DCs capture viral particles via Siglec-1 and stored them in VCCs[70], where they remain protected from neutralizing antibodies[193]. Upon the formation of DC-$CD4^+$ T cell contacts, trapped viruses are efficiently transmitted across infectious synapses to susceptible lymphocytes via *trans*-infection[88,179,188,432] (**Figure 60, bottom left**). This mechanism was previously demonstrated on activated MDDCs, monocytes, blood conventional DCs, pre-DCs, and primary myeloid cells isolated from

lymphoid tissues[70,187,192,213,433], and now also on DCs isolated from cervical tissues (**Figure 29**).

Filoviral *trans*-infection from DCs to CD4$^+$ T cells is improbable as lymphocytes are largely resistant to EBOV infection[434]. Nonetheless, filoviruses display a broad cell tropism, infecting hepatocytes, adrenal cortical cells and endothelial cells, among other cellular targets[265,266,311,435]. Thus, aside from lymphocytes, other cellular targets could be *trans*-infected (**Figure 60, bottom right**), as it was previously shown for a human cell line binding EBOV that *trans*-infected HeLa cells[436]. However, further research will be required to determine in which anatomical context DCs trapping EBOV via Siglec-1 could transfer that infectivity to susceptible cellular targets *in vivo*.

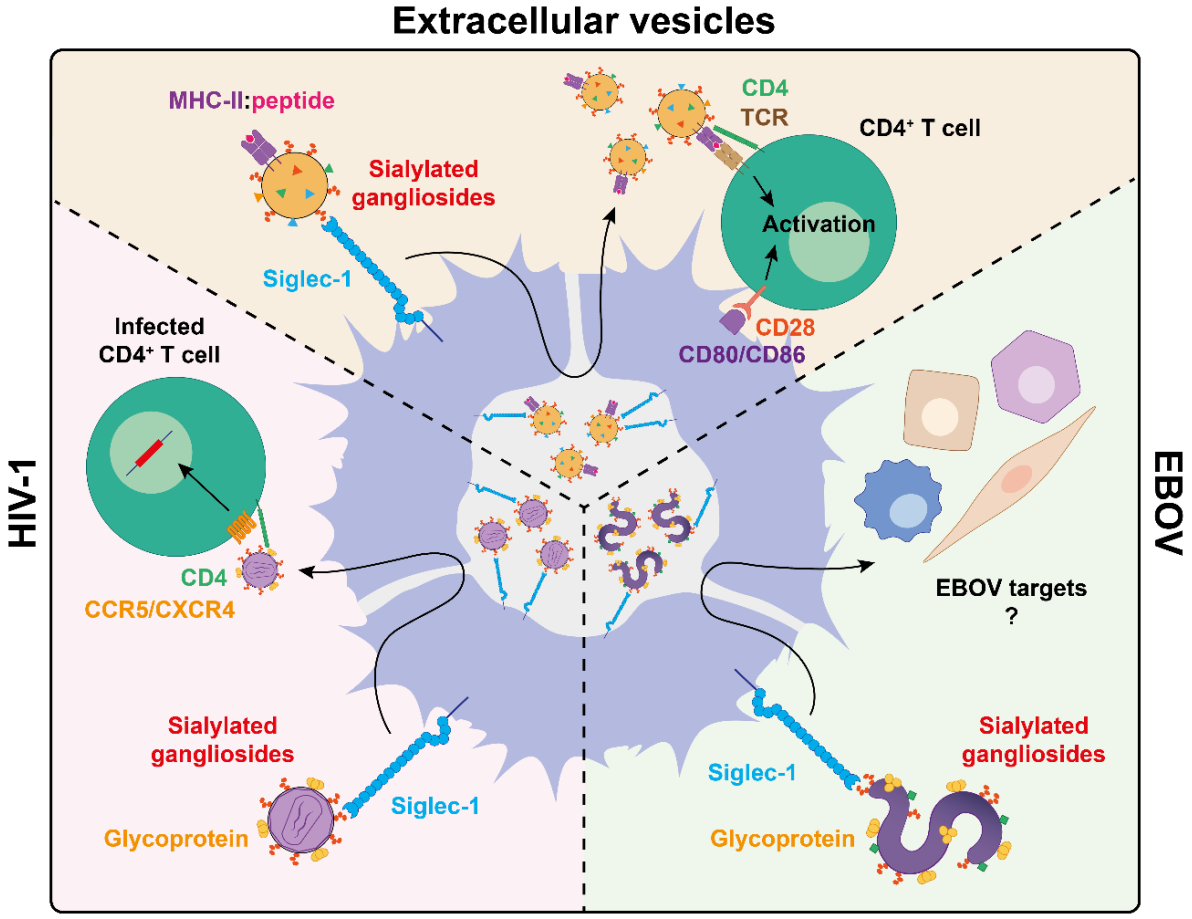

Figure 60. Viral subversion of Siglec-1-mediated extracellular vesicle dissemination. DCs capture extracellular vesicles bearing MHC:peptide complexes or distinct enveloped viruses such as HIV-1 or EBOV through Siglec-1 recognition of sialylated gangliosides, and are then trafficked and stored within a sac-like compartment. While captured extracellular vesicles exit this compartment to present antigens to T cells via immune synapse formation complemented by the co-stimulatory signals provided by the activated DC, the exit of HIV-1 leads to the *trans*-infection of CD4$^+$ T cells, and in the case of EBOV, viral dissemination to

other target cells need further investigation. MHC-II: major histocompatibility complex class II; TCR: T cell receptor. From ref.[412].

4. Siglec-1 is an attachment factor on DCs that contributes to EBOV cytoplasmic entry

Aside from the potential role in EBOV *trans*-infection, the formation of this VCC via Siglec-1 might culminate with viral entry into the cell cytoplasm, as DCs are highly susceptible to EBOV productive infection[91,328]. EBOV entry into DCs is governed by multiple interactions between the virus and distinct host factors, which drive a complex series of events that eventually lead to viral internalization, as reviewed in refs.[267,268] (**Figure 61**). Initial viral attachment to the cellular surface is mediated either by the recognition of particular host receptors through the viral glycoprotein or by specific viral lipids or glycolipids embedded on the envelope that can interact with other type of receptors. Attachment favors viral internalization within endosomes, where EBOV glycoprotein is cleaved by cellular proteases such as B cathepsins[301,437,438]. This leads to glycoprotein recognition by the endosomal receptor NPC1[297,302], which along the TPCs[298], facilitates viral fusion, release of viral RNA into the cytoplasm and productive replication[267,268] (**Figure 61**).

Among viral attachment factors, the CLRs DC-SIGN[393] and LSECtin[272], as well as the glycosaminoglycan heparin[273], have been proposed to mediate viral attachment to DCs and other myeloid cells via recognition of the viral glycoprotein (**Figure 61A**). In addition, TIM/TAM receptors such as Mer and possibly TIM-4 mediate viral entry into DCs through binding to phosphatidylserine on the viral membrane[282,285], while the alpha V integrin and the scavenger receptor A trigger viral entry through unidentified receptors[285,290] (**Figure 61A**). Here, we found that Ebola VLP attachment to activated DCs via Siglec-1 contributes to the overall process of cytoplasmic entry into these cells (**Figures 50** and **53**), thus identifying a new glycoprotein-independent factor that resembles that of TIM/TAM receptors[282,284] (**Figure 61**). However, in this case it is mediated by recognition of sialylated gangliosides instead of phosphatidylserine anchored to the viral membrane (**Figure 61**). Conversely, and despite we found that DC-SIGN mediates viral attachment to iDCs (**Figure 45**), blockade of this receptor did not impair cytoplasmic viral entry into these cells (**Figure 50**). In contrast, treatment with the competitive inhibitor mannan, which broadly interacts with distinct mannose-binding lectins, partially reduced EBOV attachment and entry into distinctly treated DCs (**Figures 50**), which is in line with previous reports[439]. Thus, alternative CLRs to DC-SIGN and LSECtin, which is insensitive to mannan[272,440],

also contribute to Ebola VLP entry into DCs and further research will be needed to identify them.

Siglec-1 recognition of sialylated gangliosides on EBOV modulates the binding, uptake and trafficking of filoviral particles into a sac-like VCC continuous with the plasma membrane (**Figure 61B**). Here we show that viruses stored in this compartment can be re-directed into the classical endosomal pathway and facilitate viral entry into the cytoplasm. However, future research should address how EBOV accumulation into VCCs converges with the endosomal trafficking pathway, and how Siglec-1 mediated attachment facilitates viral cytoplasmic entry (**Figure 61B**).

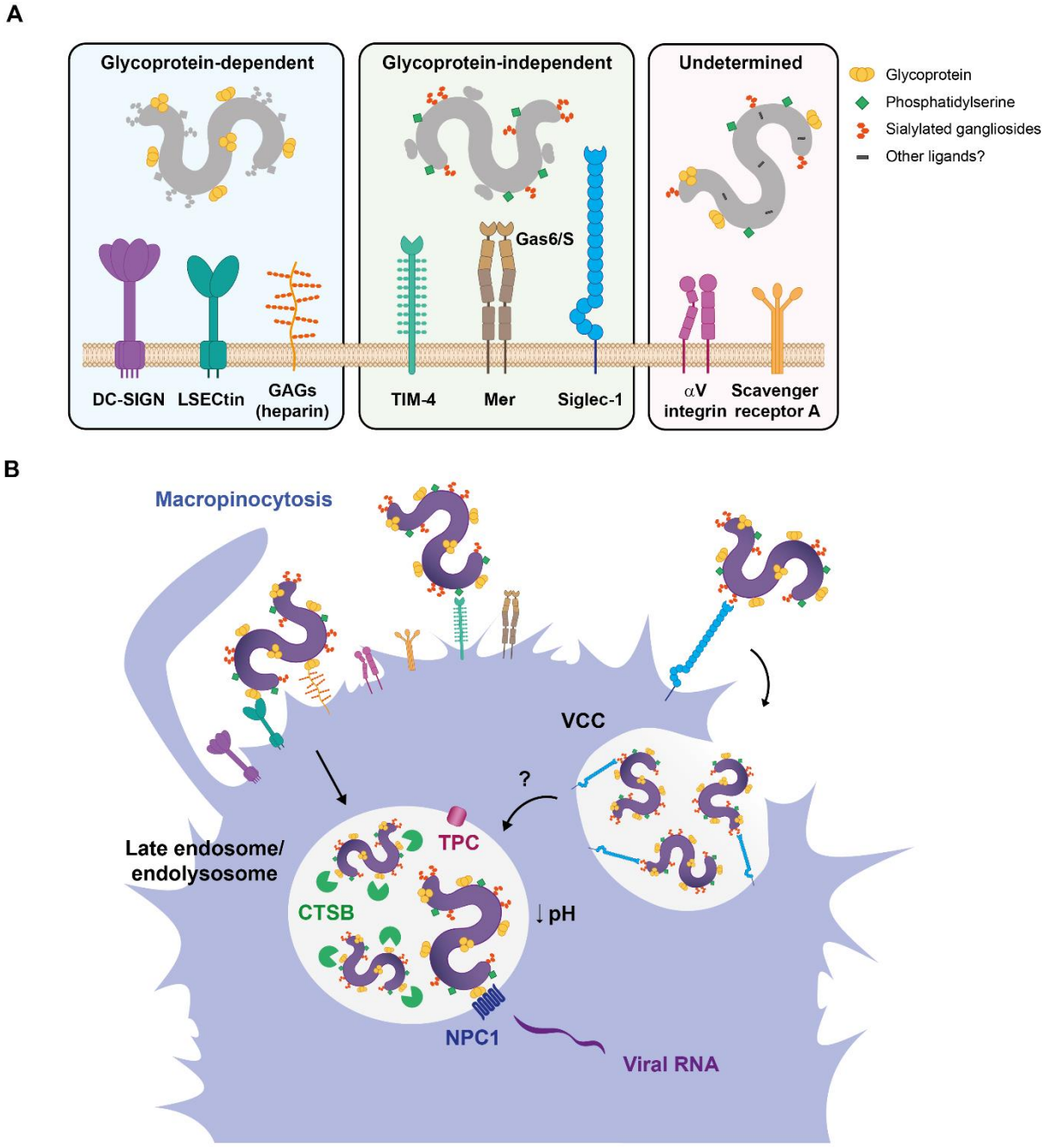

Figure 61. Siglec-1 is an attachment factor mediating EBOV entry into myeloid cells. A. Viral attachment via glycoprotein-dependent, glycoprotein-independent or unidentified mechanisms. **B**. Viral internalization begins when viruses enter early endosomes through macropinocytosis. Viral cargo of early endosomes is transferred to late endosomes, where CTSB cleaves viral glycoprotein to allow for NPC1 interaction and viral RNA entry into the cytoplasm. Viral particles captured by Siglec-1 are directed towards a VCC, that eventually converges with the endosome trafficking pathway through an unidentified mechanism. VCC: virus-containing-compartment; TPC: two-pore channel; CTSB: cathepsin B; NPC1: Niemann-Pick receptor C1. From ref.[289].

While Siglec-1 contributes to EBOV entry into DCs, filoviral replication within these cells compromises immune function and prevents adaptive immune responses by limiting cytokine secretion, down-regulating the expression of MHC and costimulatory molecules and also by reducing the ability of DCs to stimulate T-cell proliferation[328,329,441,442]. These results suggested that EBOV suppression of DC function prevents initiation of adaptive immune responses and facilitates uncontrolled systemic virus replication[441,442] through a viral evasion mechanism that is enhanced by Siglec-1 activity. However, clinical data gathered during the West African 2014–2016 outbreak showed a strong and sustained T-cell activation[443], challenging the *in vivo* relevance of this viral DC-escape mechanism[345]. Nonetheless, productive infection of DCs facilitates viral dissemination from the entry sites, as DCs are early filoviral targets that migrate to lymphoid tissues upon viral acquisition[91]. Thus, Siglec-1 could participate in viral dissemination facilitating viral entry into primary targets, a mechanism that should be further evaluated using relevant *in vivo* models.

Sexual transmission is not considered a major route of EBOV infection. However, a case of sexually transmitted EBOV has been well documented[322]. Moreover, a recent mathematical model is consistent with a significant contribution of sexual EBOV transmission during the 2014-2016 outbreak in West-Africa[444]. Importantly, infectious viral particles are found in semen of EBOV convalescent individuals several months following symptoms onset[318–321], and seminal fluid amyloids may enhance EBOV infection[445]. As the cytokine TGF-β1 is abundant in semen, and it also up-regulates Siglec-1 expression on DCs[446], the role of this receptor should be further assessed in the context of EBOV sexual transmission. Moreover, DCs are early and sustained targets of EBOV that can disseminate infection from the portals of viral entry to the regional lymph nodes, spleen and liver[91]. Since Siglec-1 is expressed in all these EBOV replicating-tissues[201,447] this receptor could also boost systemic viral spread as previously suggested for HIV-1[91,311,312,344,448].

Taken together, Siglec-1 facilitates HIV-1 and EBOV access into DCs, boosting viral cell-to-cell transmission via *trans*-infection and aiding viral cytoplasmic entry, respectively. In both cases, DC invasion has been proposed to contribute to viral systemic dissemination from the entry sites. Thus, targeting Siglec-1 poses an attractive option to combat HIV-1 and EBOV at the early stages of infection.

5. New anti-Siglec-1 mAbs as potential therapeutic agents against HIV-1 and EBOV

In the context of HIV-1 infection, current ART efficiently blocks HIV-1 productive replication in target cells, and therefore microbicidal strategies aimed at preventing novel sexually transmitted infections in women include such antiretroviral drugs[156]. However, our findings highlight the importance of including Siglec-1 inhibitors along with these treatments, to tackle not only the productive cellular infection in the cervix, but also the systemic viral dissemination from the female genital tract. As we found that an anti-Siglec-1 mAb efficiently reduced HIV-1 capture and *trans*-infection mediated by cervical DCs (**Figures 29**), we propose the use of anti-Siglec-1 mAbs in combination with ART as a microbicidal strategy to combat sexual HIV-1 transmission.

Although murine anti-Siglec-1 mAbs are commercially available, here we generated a set of new anti-Siglec-1 mAbs that can be eventually humanized for their use in clinical settings. The newly generated anti-Siglec-1 mAbs displayed high affinity and specificity for Siglec-1 (**Figures 30** and **31**). Moreover, these mAbs bound to different epitopes present on the N-terminal region of Siglec-1 (**Figures 35**), so full efficacy could be achieved by using some of these mAbs alone and others in combination (**Figures 37**). When we assessed the capacity of new mAbs against HIV-1 cell-to-cell transmission, all the clones efficiently blocked HIV-1 capture (**Figure 38**) and *trans*-infection mediated by DCs (**Figure 39**). Hence, we propose to combine these new anti-Siglec-1 mAbs with antiretroviral drugs in microbicidal strategies to prevent HIV-1 sexual transmission.

Aside from HIV-1, these mAbs could have efficacy against filoviruses such as EBOV as well. Here we show that mAbs directed against Siglec-1 partially blocked Ebola VLP entry into activated DCs, monocytes and myeloid cells directly isolated from lymphoid tissues (**Figures 56** and **57**). Moreover, we found that cytoplasmic entry of Ebola VLPs bearing the MARV glycoprotein into activated monocytes is also efficiently blocked by new anti-Siglec-1 mAbs (**Figure 57**). Hence, these mAbs can offer cross-protection against different ganglioside-containing filoviruses, and targeting Siglec-1 on myeloid cells pose an attractive option to limit viral spread from the initial site of infection, while protecting these APCs from infection for effective induction of immune responses. However, effective antifiloviral therapies targeting cellular host factors such as Siglec-1 will only reach their full clinical potential if specific compounds are available to block all the possible viral entry pathways with a well-tolerated and potent pharmacological activity.

Past decades have brought the development of a number of drugs to combat EBOV infection, and some of them halt viral entry by tackling both viral and host factors involved in this process (**Figure 62**). ZMapp is a cocktail of three mAbs that targets EBOV glycoprotein (**Figure 62A**) that protected non-human primates[449] and was administered during the 2014-2016 EBOV outbreak in West-Africa[406]. However, in the current outbreak at the Democratic Republic of Congo, a new clinical trial has demonstrated that both a mAb cocktail (REGN-EB3) and a mAb monotherapy (mAb114) have higher efficacy than ZMapp[323,450]. These mAbs, which previously demonstrated efficacy in non-human primate models[389,451], are now available to EBOV-infected individuals. However, a major limitation of these therapies is that they only tackle EBOV glycoprotein and therefore cannot protect against other filoviruses. To face this potential problem, several neutralizing mAbs have been selected for their capacity to broadly cross-react with glycoproteins from multiple ebolavirus species[452–454]. However, all of these mAbs failed to recognize MARV glycoprotein, presumably due to the genetic heterogenicity between filoviruses from the *Ebolavirus* and *Marburgvirus* genus[249]. Moreover, targeting the viral glycoprotein has additional drawbacks. Upon EBOV infection, the viral glycoprotein is secreted in soluble forms, and therefore may act as a decoy factor, reducing efficacy of anti-glycoprotein agents[260,455]. In addition, due to the high mutation rates experienced by RNA viruses, the efficacy and recognition capacity of these mAbs could be hampered by the appearance and selection of resistant variants[454,456]. Several mAbs and inhibitors have also been developed against host factors that recognize the viral glycoprotein, and among those, the globular multivalent glycofullerenes (**Figure 62A**) that target DC-SIGN are of special interest due to their high inhibitory capacity at sub-nanomolar doses[457]. However, glycoprotein variability could also diminish the activity of those compounds targeting CLRs or glycosaminoglycans, such as the heparin inhibitor suramin (**Figure 62A**), that reduces EBOV entry into cell lines[458]. Thus, these antivirals could be used in combined therapies to avoid the emergence of resistant viruses.

The appearance of resistant variants could be further limited by using pharmacological agents that target the universal lipid components present on the envelope of different viruses. CLR01 is a tweezer molecule that disrupts the viral lipid envelope without affecting the integrity of cellular plasma membranes (**Figure 62A**), and has demonstrated a broad antiviral effect against different enveloped viruses including EBOV[459,460]. However, CLR01 is inhibited by human serum and therefore its clinical potential is limited to topical applications[460]. An alternative approach is the use of inhibitors against host

factors that recognize lipids on the viral envelope, which are ubiquitously incorporated during the viral budding process and could therefore cross-protect against several filoviruses. In this line, phosphatidylserine-containing liposomes that interact with TIM/TAM receptors reduce EBOV entry into murine peritoneal macrophages[282], while here we show that anti-Siglec-1 mAbs reduce Ebola VLP entry into activated DCs and monocytes (**Figure 62A**). Thus, anti-Siglec-1 mAbs could boost the safety and effectiveness of combined antifiloviral therapies and offer broad-spectrum activity to tackle different filoviruses. Moreover, since previous studies have shown that HIV-1 and henipaviruses also interact with Siglec-1[70,187,461], this strategy could be valuable for other enveloped viruses.

Alternative targets of this combined therapy could also include inhibitors of attachment factors with unidentified viral ligands. Such is the case of tannic acid (**Figure 62A**), a scavenger receptor A inhibitor, which reduced EBOV entry into macrophages[285]. Moreover, post-attachment factors could also provide additional candidates, but their role on relevant cellular functions could complicate their clinical use. Although the macropinocytic inhibitors dynasore (which blocks dynamin), apilimod (which inhibits PIKfyve) and compound C (which is active against AMPK) all reduced EBOV entry into myeloid cells[291–293] (**Figure 62B**), the feasibility and safety of applying these compounds *in vivo* needs further studies. Tetrandrine, a potent inhibitor of the TCP1 and TCP2 found on the membranes of acidic organelles such as endosomes and lysosomes (**Figure 62B**), blocked EBOV entry into macrophages, and protected a mouse model upon lethal EBOV challenge[298]. In addition, anti-malarials that accumulate in endolysosomes, such as chloroquine (**Figure 62B**), protected mice against EBOV challenge[462], although in subsequent studies failed to protect guinea pigs, mice and hamsters[463–465]. Artesunate-amodiaquine (**Figure 62B**) is another antimalarial that was used for protection against EBOV during the 2014-2016 West-African outbreak[466]. Interference of endosomal acidification with diphyllin derivatives reduced EBOV entry into macrophages[467], while the modulators of estrogen receptor clomiphene and tomerifene protected mice against EBOV by blocking the viral glycoprotein interaction with NPC1[468] (**Figure 62B**). Although NPC1 inhibitors, such as U18666 (**Figure 62B**), reduce EBOV and MARV entry into target cells[297], the lack of activity of this particular receptor leads to Niemann Pick C1 disease, a severe neurodegenerative lysosomal storage disorder[469–471]. Thus, studies assessing toxicity are still needed.

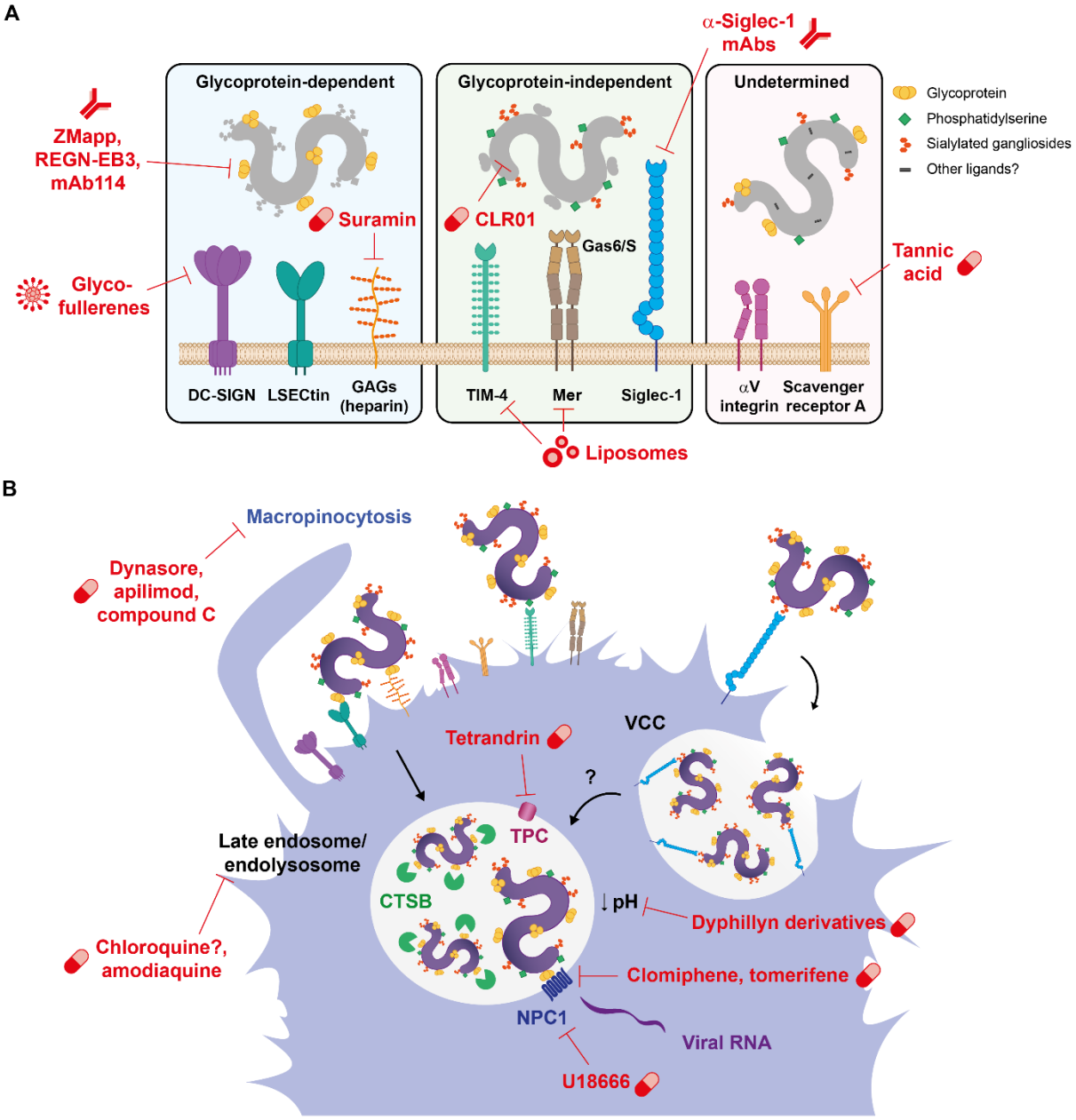

Figure 62. Strategies aimed at blocking EBOV entry into myeloid cells. **A**. Potential therapeutic agents targeting different host and viral factors involved in viral attachment. **B.** Other potential treatments to halt viral internalization at different steps of the entry cycle. VCC: virus-containing compartment; TPC: two-pore channel; CTSB: cathepsin B; NPC1: Niemann-Pick receptor C1. From ref.[289].

The clinical applicability of entry blockers looks promising for combating early events of infection. However, in most of the patients, systemic viral dissemination has already occurred when they seek for treatment. Thus, in these clinical settings, entry blockers could be combined with other antiviral drugs acting at later stages of the life cycle of EBOV to maximize efficacy. Such is the case of the nucleoside analogue favipiravir (T-705), that

protected non-human primates[472], or remdesivir (GS-5734)[473], that is currently being tested on a clinical trial at the Democratic Republic of the Congo[323].

The general complexity that governs viral attachment to the cellular surface and the number of host factors implicated in downstream events highlights the need to accurately dissect the contribution of each of these candidates in animal models. In turn, this basic knowledge gathered studying current animal models[474,475] will be key to have a rational and systematic approach to test the activity and safety of all potential inhibitors, select the most promising ones and design a new generation of antivirals whose combination could increase efficacy of individual treatments, as previously shown[476,477].

Taken together, we generated a set of new anti-Siglec-1 mAbs that reduce HIV-1 *trans*-infection and also filoviral entry into activated myeloid cells. We propose that these new mAbs might be employed in combined strategies with either antiretroviral drugs or filoviral entry inhibitors to block the early dissemination events of HIV-1 and filoviral infection, respectively. Noteworthy, the identification of Siglec-1 null adult individuals without any associated health condition[405] demonstrates that this receptor is dispensable and its therapeutic blockade is not expected to cause serious side effects. Moreover, since Siglec-1 participates in viral capture of two distant viruses such as HIV-1 and EBOV, it is likely that other enveloped viruses exploit Siglec-1 on myeloid cells to infect or *trans*-infect target cells, and that anti-Siglec-1 mAbs might represent broad-spectrum inhibitors for enveloped viruses.

Chapter 9

CONCLUSIONS

Aim 1: To determine the physiological mechanisms leading to Siglec-1 up-regulation on DCs in the context of HIV-1 infection, determining the natural sources of IFNα enhancing Siglec-1 expression on these cells.

- IFNα secreted by pDCs exposed to HIV-1-infected cells induces Siglec-1 expression on bystander DCs.
- Type I IFNs secreted by DCs in response to LPS induce Siglec-1 expression in an autocrine manner.

Aim 2: To assess whether myeloid cells from cervical tissues, a key anatomical location for HIV-1 acquisition, are able to capture and *trans*-infect HIV-1 in a Siglec-1-dependent manner.

- Myeloid cells derived from cervical tissues express Siglec-1 and capture HIV-1 particles, a capacity that is enhanced upon IFNα stimulation.
- *In vivo*, cervical myeloid cells accumulate HIV-1 in a sac-like VCC enriched in Siglec-1.
- Myeloid cells derived from cervical tissues mediate HIV-1 *trans*-infection in a Siglec-1-dependent manner.

Aim 3: To generate a set of new anti-Siglec-1 mAbs with the capacity to block HIV-1 capture and *trans*-infection mediated by DCs.

- New anti-Siglec-1 mAbs with high affinity for Siglec-1 bind to different epitopes located in the N-terminal region of Siglec-1.
- New anti-Siglec-1 mAbs block HIV-1 capture and *trans*-infection mediated by DCs.

Aim 4: To determine the role of Siglec-1 in Ebola virus binding and capture by DCs in an HIV-1 comparative manner, and Siglec-1 contribution to viral cytoplasmic entry into DCs.

- Siglec-1 mediates binding and capture of Ebola viral particles by DCs.
- Ebola viral particles captured by activated DCs accumulate in the same VCC as HIV-1.
- Siglec-1 participates in cytoplasmic entry of Ebola viral particles into activated DCs.

Aim 5: To test the capacity of new anti-Siglec-1 mAbs to block filoviral capture and cytoplasmic entry into myeloid cells.

- New anti-Siglec-1 mAbs block capture of Ebola viral particles into activated DCs and myeloid cells directly isolated from lymphoid tissues.
- New anti-Siglec-1 mAbs block cytoplasmic entry of Ebola viral particles into activated DCs and myeloid cells directly isolated from lymphoid tissues, and of Marburg vial particles into activated monocytes.

Chapter 10

REFERENCES

1. Steinman RM. The dendritic cell system and its role in immunogenicity. *Annu Rev Immunol*. 1991;**9**:271–96.

2. Banchereau J, Steinman RM. Dendritic cells and the control of immunity. *Nature*. 1998;**392**(6673):245–52.

3. Norbury CC, Malide D, Gibbs JS, Bennink JR, Yewdell JW. Visualizing priming of virus-specific CD8+ T cells by infected dendritic cells in vivo. *Nat Immunol*. 2002;**3**(3):265–71.

4. Paludan C, Schmid D, Landthaler M, Vockerodt M, Kube D, Tuschl T, et al. Endogenous MHC class II processing of a viral nuclear antigen after autophagy. *Science (80-)*. 2005;**307**(5709):593–6.

5. Wilson NS, Behrens GMN, Lundie RJ, Smith CM, Waithman J, Young L, et al. Systemic activation of dendritic cells by Toll-like receptor ligands or malaria infection impairs cross-presentation and antiviral immunity. *Nat Immunol*. 2006;**7**(2):165–72.

6. Janeway CA, Medzhitov R. Innate Immune Recognition. *Annu Rev Immunol*. 2002;**20**:197–216.

7. Riera Romo M, Pérez-Martínez D, Castillo Ferrer C. Innate immunity in vertebrates: An overview. *Immunology*. 2016;**148**(2):125–39.

8. Cui J, Chen Y, Wang HY, Wang RF. Mechanisms and pathways of innate immune activation and regulation in health and cancer. *Hum Vaccines Immunother*. 2014;**10**(11):3270–85.

9. Janeway CA. Approaching the asymptote? Evolution and revolution in immunology. *Cold Spring Harb Symp Quant Biol*. 1989;**54**:1–13.

10. Medzhitov R, Preston-Hurlburt P, Janeway CA. A human homologue of the Drosophila Toll protein signals activation of adaptive immunity. *Nature*. 1997;**388**(6640):394–7.

11. Poltorak A, Smirnova I, He X, Liu MY, Van Huffel C, Birdwell D, et al. Genetic and physical mapping of the Lps locus: Identification of the Toll-4 receptor as a candidate gene in the critical region. *Blood Cells, Mol Dis*. 1998;**24**(3):340–55.

12. Poltorak A, He X, Smirnova I, Liu MY, Van Huffel C, Du X, et al. Defective LPS signaling in C3H/HeJ and C57BL/10ScCr mice: Mutations in Tlr4 gene. *Science (80-)*. 1998;**282**(5396):2085–8.

13. Kawai T, Akira S. The role of pattern-recognition receptors in innate immunity: Update on Toll-like receptors. *Nat Immunol*. 2010;**11**(5):373–84.

14. O'Neill LAJ, Golenbock D, Bowie AG. The history of Toll-like receptors - redefining innate immunity. *Nat Rev Immunol*. 2013;**13**(6):453–60.

15. Takeda K, Akira S. Toll-like receptors in innate immunity. *Int Immunol*. 2005;**17**(1):1–14.

16. Kawai T, Akira S. Toll-like receptors and their crosstalk with other innate receptors in infection and immunity. *Immunity*. 2011;**34**(5):637–50.

17. Harman AN, Bye CR, Nasr N, Sandgren KJ, Kim M, Mercier SK, et al. Identification of lineage relationships and novel markers of blood and skin human dendritic cells. *J Immunol*. 2013;**190**(1):66–79.

18. Geijtenbeek TBH, Tornsma R, van Vliet SJ, van Duijnhoven GCF, Adema GJ, van Kooyk Y, et al. Identification of DC-SIGN, a novel dendritic cell-specific ICAM-3 receptor that supports primary immune responses. *Cell*. 2000;**100**(5):575–85.

19. Zhang F, Ren S, Zuo Y. DC-SIGN, DC-SIGNR and LSECtin: C-type lectins for infection. *Int Rev Immunol*. 2014;**33**(1):54–66.

20. Powell LD, Varki A. I-type lectins. Vol. 270, Journal of Biological Chemistry. 1995. p. 14243–6.

21. Angata T, Brinkman-Van der Linden ECM. I-type lectins. *Biochim Biophys Acta*. 2002;**1572**(2–3):294–316.

22. Kelm S, Pelz A, Schauer R, Filbin MT, Tang S, Bellard ME de, et al. Sialoadhesin, myelin-associated glycoprotein and CD22 define a new family of sialic acid-dependent adhesion molecules of the immunoglobulin superfamily. *Curr Biol*. 1994;**4**(11):965–72.

23. Crocker PR, Varki A. Siglecs, sialic acids and innate immunity. *Trends Immunol*. 2001;**22**(6):337–42.

24. Crocker PR. Siglecs: Sialic-acid-binding immunoglobulin-like lectins in cell-cell interactions and signalling. *Curr Opin Struct Biol*. 2002;**12**(5):609–15.

25. Crocker PR. Siglecs in innate immunity. *Curr Opin Pharmacol*. 2005;**5**(4):431–7.

26. Crocker PR, Paulson JC, Varki A. Siglecs and their roles in the immune system. *Nat Rev Immunol*. 2007;**7**(4):255–66.

27. Varki A, Angata T. Siglecs - The major subfamily of I-type lectins. *Glycobiology*. 2006;**16**(1):1–27.

28. Manel N, Hogstad B, Wang Y, Levy DE, Unutmaz D, Littman DR. A cryptic sensor for HIV-1 activates antiviral innate immunity in dendritic cells. *Nature*. 2010;**467**(7312):214–7.

29. Lahaye X, Satoh T, Gentili M, Cerboni S, Conrad C, Hurbain I, et al. The capsids of HIV-1 and HIV-2 determine immune detection of the viral cDNA by the innate sensor cGAS in dendritic cells. *Immunity*. 2013;**39**(6):1132–42.

30. Ori D, Murase M, Kawai T. Cytosolic nucleic acid sensors and innate immune regulation. *Int Rev Immunol*. 2017;**36**(2):74–88.

31. Collin M, Bigley V. Human dendritic cell subsets: An update. *Immunology*. 2018;**154**(1):3–20.

32. Rhodes JW, Tong O, Harman AN, Turville SG. Human dendritic cell subsets, ontogeny, and impact on HIV infection. *Front Immunol*. 2019;**10**:1088.

33. Siegal FP, Kadowaki N, Shodell M, Fitzgerald-Bocarsly PA, Shah K, Ho S, et al. The nature of the principal type 1 interferon-producing cells in human blood. *Science (80-)*. 1999;**284**(5421):1835–7.

34. Ju X, Zenke M, Hart DNJ, Clark GJ. CD300a/c regulate type I interferon and TNF-α secretion by human plasmacytoid dendritic cells stimulated with TLR7 and TLR9 ligands. *Blood*. 2008;**112**(4):1184–94.

35. Mandl JN, Barry AP, Vanderford TH, Kozyr N, Chavan R, Klucking S, et al. Divergent

TLR7 and TLR9 signaling and type I interferon production distinguish pathogenic and nonpathogenic AIDS virus infections. *Nat Med*. 2008;**14**(10):1077–87.

36. Beignon AS, McKenna K, Skoberne M, Manches O, DaSilva I, Kavanagh DG, et al. Endocytosis of HIV-1 activates plasmacytoid dendritic cells via Toll-like receptor-viral RNA interactions. *J Clin Invest*. 2005;**115**(11):3265–75.

37. Meier A, Alter G, Frahm N, Sidhu H, Li B, Bagchi A, et al. MyD88-dependent immune activation mediated by human immunodeficiency virus type 1-encoded Toll-like receptor Ligands. *J Virol*. 2007;**81**(15):8180–91.

38. McNab F, Mayer-Barber K, Sher A, Wack A, O'Garra A. Type I interferons in infectious disease. *Nat Rev Immunol*. 2015;**15**(2):87–103.

39. Worbs T, Hammerschmidt SI, Förster R. Dendritic cell migration in health and disease. *Nat Rev Immunol*. 2017;**17**(1):30–48.

40. Trombetta ES, Mellman I. Cell Biology of antigen processing in vitro and in vivo. *Annu Rev Immunol*. 2005;**23**:975–1028.

41. Fujii SI, Liu K, Smith C, Bonito AJ, Steinman RM. The linkage of innate to adaptive immunity via maturing dendritic cells in vivo requires CD40 ligation in addition to antigen presentation and CD80/86 costimulation. *J Exp Med*. 2004;**199**(12):1607–18.

42. Spörri R, Reis e Sousa C. Inflammatory mediators are insufficient for full dendritic cell activation and promote expansion of CD4+ T cell populations lacking helper function. *Nat Immunol*. 2005;**6**(2):163–70.

43. Steinman RM, Banchereau J. Taking dendritic cells into medicine. *Nature*. 2007;**449**(7161):419–26.

44. Dustin ML, Chakraborty AK, Shaw AS. Understanding the structure and function of the immunological synapse. *Cold Spring Harb Perspect Biol*. 2010;**2**(10):a002311.

45. Basu R, Huse M. Mechanical communication at the immunological synapse. *Trends Cell Biol*. 2017;**27**(4):241–54.

46. Santana MA, Esquivel-Guadarrama F. Cell biology of T cell activation and differentiation. *Int Rev Cytol*. 2006;**250**:217–74.

47. Wilson NS, Villadangos JA. Regulation of antigen presentation and cross-presentation in the dendritic cell network: Facts, hypothesis, and immunological implications. *Adv Immunol*. 2005;**86**:241–305.

48. Mantegazza AR, Magalhaes JG, Amigorena S, Marks MS. Presentation of phagocytosed antigens by MHC class I and II. *Traffic*. 2013;**14**(2):135–52.

49. Gagliani N, Huber S. Basic aspects of T helper cell differentiation. *Methods Mol Biol*. 2017;**1514**:19–30.

50. Joffre OP, Segura E, Savina A, Amigorena S. Cross-presentation by dendritic cells. *Nat Rev Immunol*. 2012;**12**(8):557–69.

51. Jung S, Unutmaz D, Wong P, Sano GI, De Los Santos K, Sparwasser T, et al. In vivo depletion of CD11c+ dendritic cells abrogates priming of CD8+ T cells by exogenous cell-associated antigens. *Immunity*. 2002;**17**(2):211–20.

52. Smed-Sörensen A, Chalouni C, Chatterjee B, Cohn L, Blattmann P, Nakamura N, et al. Influenza a virus infection of human primary dendritic cells impairs their ability to cross-present antigen to CD8 T cells. *PLoS Pathog*. 2012;**8**(3):e1002572.

53. Bender A, Bui LK, Feldman MAV, Larsson M, Bhardwaj N. Inactivated influenza virus, when presented on dendritic cells, elicits human CD8+ cytolytic T cell responses. *J Exp Med*. 1995;**182**(6):1663–71.

54. Buseyne F, Le Gall S, Boccaccio C, Abastado J-P, Lifson JD, Arthur LO, et al. MHC-I–restricted presentation of HIV-1 virion antigens without viral replication. *Nat Med*. 2001;**7**(3):344–9.

55. Larsson M, Fonteneau JF, Lirvall M, Haslett P, Lifson JD, Bhardwaj N. Activation of HIV-1 specific CD4 and CD8 T cells by human dendritic cells: Roles for cross-presentation and non-infectious HIV-1 virus. *Aids*. 2002;**16**(10):1319–29.

56. Sabado RL, Babcock E, Kavanagh DG, Tjomsland V, Walker BD, Lifson JD, et al. Pathways utilized by dendritic cells for binding, uptake, processing and presentation of antigens derived from HIV-1. *Eur J Immunol*. 2007;**37**(7):1752–63.

57. Sekaly RP, Jacobson S, Richert JR, Tonnelle C, McFarland HF, Long EO. Antigen presentation to HLA class II-restricted measles virus-specific T-cell clones can occur in the absence of the invariant chain. *Proc Natl Acad Sci U S A*. 1988;**85**(4):1209–12.

58. Jacobson S, Sekaly RP, Bellini WJ, Johnson CL, McFarland HF, Long EO. Recognition of intracellular measles virus antigens by HLA class II restricted measles virus-specific cytotoxic T lymphocytes. *Ann N Y Acad Sci*. 1988;**540**:352–3.

59. Tewari MK, Sinnathamby G, Rajagopal D, Eisenlohr LC. A cytosolic pathway for MHC class II-restricted antigen processing that is proteasome and TAP dependent. *Nat Immunol*. 2005;**6**(3):287–94.

60. Miller MA, Ganesan AP V., Luckashenak N, Mendonca M, Eisenlohr LC. Endogenous antigen processing drives the primary CD4+ T cell response to influenza. *Nat Med*. 2015;**21**(10):1216–22.

61. Eisenlohr LC, Luckashenak N, Apcher S, Miller MA, Sinnathamby G. Beyond the classical: Influenza virus and the elucidation of alternative MHC class II-restricted antigen processing pathways. *Immunol Res*. 2011;**51**(2–3):237–48.

62. Coulon P-G, Richetta C, Rouers A, Blanchet FP, Urrutia A, Guerbois M, et al. HIV-infected dendritic cells present endogenous MHC class II-restricted antigens to HIV-specific CD4+ T cells. *J Immunol*. 2016;**197**(2):517–32.

63. Villadangos JA, Schnorrer P. Intrinsic and cooperative antigen-presenting functions of dendritic-cell subsets in vivo. *Nat Rev Immunol*. 2007;**7**(7):543–55.

64. Théry C, Regnault A, Garin J, Wolfers J, Zitvogel L, Ricciardi-Castagnoli P, et al. Molecular characterization of dendritic cell-derived exosomes: Selective accumulation of the heat shock protein hsc73. *J Cell Biol*. 1999;**147**(3):599–610.

65. Théry C, Boussac M, Véron P, Ricciardi-Castagnoli P, Raposo G, Garin J, et al. Proteomic analysis of dendritic cell-derived exosomes: A secreted subcellular compartment distinct from apoptotic vesicles. *J Immunol*. 2001;**166**(12):7309–18.

66. Théry C, Zitvogel L, Amigorena S. Exosomes: Composition, biogenesis and function.

Nat Rev Immunol. 2002;**2**(8):569–79.

67. Théry C, Duban L, Segura E, Véron P, Lantz O, Amigorena S. Indirect activation of naïve CD4+ T cells by dendritic cell-derived exosomes. *Nat Immunol*. 2002;**3**(12):1156–62.

68. Théry C, Ostrowski M, Segura E. Membrane vesicles as conveyors of immune responses. *Nat Rev Immunol*. 2009;**9**(8):581–93.

69. Skotland T, Sandvig K, Llorente A. Lipids in exosomes: Current knowledge and the way forward. *Prog Lipid Res*. 2017;**66**:30–41.

70. Izquierdo-Useros N, Lorizate M, Puertas MC, Rodriguez-Plata MT, Zangger N, Erikson E, et al. Siglec-1 is a novel dendritic cell receptor that mediates HIV-1 trans-infection through recognition of viral membrane gangliosides. *PLoS Biol*. 2012;**10**(12):e1001448.

71. Díaz-Varela M, de Menezes-Neto A, Perez-Zsolt D, Gámez-Valero A, Seguí-Barber J, Izquierdo-Useros N, et al. Proteomics study of human cord blood reticulocyte-derived exosomes. *Sci Rep*. 2018;**8**(1):14046.

72. Saunderson SC, Dunn AC, Crocker PR, McLellan AD. CD169 mediates the capture of exosomes in spleen and lymph node. *Blood*. 2014;**123**(2):208–16.

73. Izquierdo-Useros N, Naranjo-Gómez M, Archer J, Hatch SC, Erkizia I, Blanco J, et al. Capture and transfer of HIV-1 particles by mature dendritic cells converges with the exosome-dissemination pathway. *Blood*. 2009;**113**(12):2732–41.

74. Savina A, Jancic C, Hugues S, Guermonprez P, Vargas P, Moura IC, et al. NOX2 controls phagosomal pH to regulate antigen processing during crosspresentation by dendritic cells. *Cell*. 2006;**126**(1):205–18.

75. Platt CD, Ma JK, Chalouni C, Ebersold M, Bou-Reslan H, Carano RAD, et al. Mature dendritic cells use endocytic receptors to capture and present antigens. *Proc Natl Acad Sci U S A*. 2010;**107**(9):4287–92.

76. Drutman SB, Trombetta ES. Dendritic cells continue to capture and present antigens after maturation in vivo. *J Immunol*. 2010;**185**(4):2140–6.

77. Langerhans P. Uber die nerven der menschlichen haut. *Arch Pathol Anat*. 1868;**44**:325–7.

78. Steinman RM, Cohn Z. Identification of a novel cell type in peripheral lymphoid organs of mice. *J Exp Med*. 1973;**137**:1142–62.

79. Collin M, Mcgovern N, Haniffa M. Human dendritic cell subsets. *Immunology*. 2013;**140**(1):22–30.

80. Haniffa M, Bigley V, Collin M. Human mononuclear phagocyte system reunited. *Semin Cell Dev Biol*. 2015;**41**:59–69.

81. Tussiwand R, Gautier EL. Transcriptional regulation of mononuclear phagocyte development. *Front Immunol*. 2015;**6**:533.

82. Murphy TL, Grajales-Reyes GE, Wu X, Tussiwand R, Briseño CG, Iwata A, et al. Transcriptional control of dendritic cell development. *Annu Rev Immunol*. 2016;**34**:93–119.

83. Swiecki M, Colonna M. The multifaceted biology of plasmacytoid dendritic cells. *Nat Rev Immunol*. 2015;**15**(8):471–85.

84. Sallusto BF, Lanzavecchia A. Efficient presentation of soluble antigen by cultured human dendritic cells is maintained by granulocyte/macrophage colony-stimulating factor plus interleukin 4 and downregulated by tumor necrosis factor α. *J Exp Med*. 1994;**179**(4):1109–18.

85. Pollara G, Kwan A, Newton PJ, Handley ME, Chain BM, Katz DR. Dendritic cells in viral pathogenesis: Protective or defective? *Int J Exp Pathol*. 2005;**86**(4):187–204.

86. Finlay BB, McFadden G. Anti-immunology: Evasion of the host immune system by bacterial and viral pathogens. *Cell*. 2006;**124**(4):767–82.

87. Rescigno M. Dendritic cell functions: Learning from microbial evasion strategies. *Semin Immunol*. 2015;**27**(2):119–24.

88. Cameron PU, Freudenthal PS, Barker JM, Gezelter S, Inaba K, Steinman RM. Dendritic cells exposed to human immunodeficiency virus type-1 transmit a vigorous cytopathic infection to CD4+ T cells. *Science (80-)*. 1992;**257**(5068):383–7.

89. Spira AI, Marx PA, Patterson BK, Mahoney J, Koup RA, Wolinsky SM, et al. Cellular targets of infection and route of viral dissemination after an intravaginal inoculation of simian immunodeficiency virus into rhesus macaques. *J Exp Med*. 1996;**183**(1):215–25.

90. Knight SC, Patterson S. Bone marrow-derived dendritic cells, infection with human immunodeficiency virus, and immunopathology. *Annu Rev Immunol*. 1997;**15**:593–615.

91. Geisbert TW, Hensley LE, Larsen T, Young HA, Reed DS, Geisbert JB, et al. Pathogenesis of Ebola hemorrhagic fever in cynomolgus macaques: Evidence that dendritic cells are early and sustained targets of infection. *Am J Pathol*. 2003;**163**(6):2347–70.

92. Ren X-X, Ma L, Liu Q-W, Li C, Huang Z, Wu L, et al. The molecule of DC-SIGN captures enterovirus 71 and confers dendritic cell-mediated viral trans-infection. *Virol J*. 2014;**11**:47.

93. de Jong MAWP, de Witte L, Bolmstedt A, van Kooyk Y, Geijtenbeek TBH. Dendritic cells mediate herpes simplex virus infection and transmission through the C-type lectin DC-SIGN. *J Gen Virol*. 2008;**89**(10):2398–409.

94. Schönrich G, Raftery MJ. Dendritic cells as Achilles' heel and Trojan horse during varicella zoster virus infection. *Front Microbiol*. 2015;**6**:417.

95. Farrell HE, Bruce K, Lawler C, Oliveira M, Cardin R, Davis-Poynter N, et al. Murine cytomegalovirus spreads by dendritic cell recirculation. *MBio*. 2017;**8**(5):e01264-17.

96. de Witte L, de Vries RD, van der Vlist M, Yüksel S, Litjens M, de Swart RL, et al. DC-SIGN and CD150 have distinct roles in transmission of measles virus from dendritic cells to T-lymphocytes. *PLoS Pathog*. 2008;**4**(4):e1000049.

97. Pham AM, Langlois RA, TenOever BR. Replication in cells of hematopoietic origin is necessary for Dengue virus dissemination. *PLoS Pathog*. 2012;**8**(1):e1002465.

98. Izquierdo-Useros N, Lorizate M, McLaren PJ, Telenti A, Kräusslich HG, Martinez-Picado J. HIV-1 capture and transmission by dendritic cells: The role of viral glycolipids

and the cellular receptor Siglec-1. *PLoS Pathog*. 2014;**10**(7):e1004146.

99. Gummuluru S, Pina Ramirez NG, Akiyama H. CD169-dependent cell-associated HIV-1 transmission: A driver of virus dissemination. *J Infect Dis*. 2014;**210**(Suppl 3):S641–7.

100. Gottlieb MS, Schroff R, Schanker HM, Weisman JD, Fan PT, Wolf RA, et al. Pneumocystis carinii pneumonia and mucosal candidiasis in previously healthy homosexual men: Evidence of a new acquired cellular immunodeficiency. *N Engl J Med*. 1981;**305**(24):1425–31.

101. Barré-Sinoussi F, Chermann JC, Rey F, Nugeyre MT, Chamaret S, Gruest J, et al. Isolation of a T-lymphotropic retrovirus from a patient at risk for acquired immune deficiency syndrome (AIDS). *Science (80-)*. 1983;**220**(4599):868–71.

102. Hahn BH, Shaw GM, Arya SK, Popovic M, Gallo RC, Wong-Staal F. Molecular cloning and characterization of the HTLV-III virus associated with AIDS. *Nature*. 1984;**312**(5990):166–9.

103. Luciw PA, Potter SJ, Steimer K, Dina D, Levy JA. Molecular cloning of AIDS-associated retrovirus. *Nature*. 1984;**312**(5996):760–3.

104. Alizon M, Sonigo P, Barré-Sinoussi F, Chermann JC, Tiollais P, Montagnier L, et al. Molecular cloning of lymphadenopathy-associated virus. *Nature*. 1984;**312**(5996):757–60.

105. Wain-Hobson S, Sonigo P, Danos O, Cole S, Alizon M. Nucleotide sequence of the AIDS virus, LAV. *Cell*. 1985;**40**(1):9–17.

106. Sanchez-Pescador R, Michael D. P, Philip J. B, Kathelyn S. S, Michelle M. S, Sheryl L. B-S, et al. Nucleotide sequence and expression of an AIDS-associated retrovirus (ARV-2). *Science (80-)*. 1985;**227**(4686):484–92.

107. Rabson AB, Martin MA. Molecular organization of the AIDS retrovirus. *Cell*. 1985;**40**(3):477–80.

108. UNAIDS Data Report. 2019;

109. WHO Global Statistics. 2019.

110. ICTV virus taxonomy release. 2018.

111. Whittle H, Morris J, Todd J, Corrah T, Sabally S, Bangali J, et al. HIV-2-infected patients survive longer than HIV-1-infected patients. *AIDS*. 1994;**8**(11):1617–20.

112. Eberle J, Gürtler L. HIV types, groups, subtypes and recombinant forms: Errors in replication, selection pressure and quasispecies. *Intervirology*. 2012;**55**(2):79–83.

113. Korber B, Muldoon M, Theiler J, Gao F, Gupta R, Lapedes A, et al. Timing the ancestor of the HIV-1 pandemic strains. *Science (80-)*. 2000;**288**(5472):1789–96.

114. Yamaguchi J, McArthur C, Vallari A, Sthreshley L, Cloherty G, Berg M, et al. Complete genome sequence of CG-0018a-01 establishes HIV-1 subtype L. *J Acquir Immune Defic Syndr*. 2019;

115. Emerman M, Malim MH. HIV-1 regulatory/accessory genes: Keys to unraveling viral and host cell biology. *Science (80-)*. 1998;**280**(5371):1880–4.

116. Fanales-Belasio E, Raimondo M, Suligoi B, Buttò S. HIV virology and pathogenic mechanisms of infection: A brief overview. *Ann Ist Super Sanita*. 2010;**46**(1):5–14.

117. Freed EO. HIV-1 assembly, release and maturation. *Nat Rev Microbiol*. 2015;**13**(8):484–96.

118. Arthur LO, Bess JW, Sowder RC, Benveniste RE, Mann DL, Chermann JC, et al. Cellular proteins bound to immunodeficiency viruses: Implications for pathogenesis and vaccines. *Science (80-)*. 1992;**258**(5090):1935–8.

119. Abbas AK, Lichtman AH, Pillai S. Cellular and Molecular Immunology. Ninth Edit. Elsevier; 2018.

120. Wilen CB, Tilton JC, Doms RW. HIV: Cell binding and entry. *Cold Spring Harb Perspect Med*. 2012;**2**(8):a006866.

121. Deeks SG, Overbaugh J, Phillips A, Buchbinder S. HIV infection. *Nat Rev Dis Prim*. 2015;**1**:15035.

122. Sarafianos SG, Marchand B, Das K, Himmel D, Parniak MA, Hughes SH, et al. Structure and function of HIV-1 reverse transcriptase: Molecular mechanisms of polymerization and inhibition. *J Mol Biol*. 2009;**385**(3):693–713.

123. Engelman A, Cherepanov P. The structural biology of HIV-1: Mechanistic and therapeutic insights. *Nat Rev Microbiol*. 2012;**10**(4):279–90.

124. Karn J, Stoltzfus M. Transcriptional and posttranscriptional regulation of HIV-1 gene expression. *Cold Spring Harb Perspect Med*. 2012;**2**(2):a006916.

125. Sundquist WI, Kräusslich H-G. HIV-1 assembly, budding, and maturation. *Cold Spring Harb Perspect Med*. 2012;**2**(7):a006924.

126. Nguyen DH, Hildreth JEK. Evidence for budding of human immunodeficiency virus type 1 selectively from glycolipid-enriched membrane lipid rafts. *J Virol*. 2000;**74**(7):3264–72.

127. Hunter E. Macromolecular interactions in the assembly of HIV and other retroviruses. Vol. 5, Seminars in Virology. 1994. p. 71–83.

128. Barré-Sinoussi F, Ross AL, Delfraissy JF. Past, present and future: 30 years of HIV research. *Nat Rev Microbiol*. 2013;**11**(12):877–83.

129. Suligoi B, Raimondo M, Fanales-Belasio E, Buttò S. The epidemic of HIV infection and AIDS, promotion of testing, and innovative strategies. *Ann Ist Super Sanita*. 2010;**46**(1):15–23.

130. Haase AT. Early events in sexual transmission of HIV and SIV and opportunities for interventions. *Annu Rev Med*. 2011;**62**:127–39.

131. Shattock RJ, Moore JP. Inhibiting sexual transmission of HIV-1 infection. *Nat Rev Microbiol*. 2003;**1**(1):25–34.

132. Miller CJ, Li Q, Abel K, Kim E-Y, Ma Z-M, Wietgrefe S, et al. Propagation and dissemination of infection after vaginal transmission of simian immunodeficiency virus. *J Virol*. 2005;**79**(14):9217–27.

133. Masurier C, Salomon B, Guettari N, Pioche C, Guigon M, Klatzmann D, et al. Dendritic

cells route human immunodeficiency virus to lymph nodes after vaginal or intravenous administration to mice. *J Virol*. 1998;**72**(10):7822–9.

134. Hu J, Gardner MB, Miller CJ. Simian immunodeficiency virus rapidly penetrates the cervicovaginal mucosa after intravaginal inoculation and infects intraepithelial dendritic cells. *J Virol*. 2000;**74**(13):6087–95.

135. Coffin J, Swanstrom R. HIV pathogenesis: Dynamics and genetics of viral populations and infected cells. *Cold Spring Harb Perspect Med*. 2013;**3**(1):a012526.

136. Fiebig EW, Wright DJ, Rawal BD, Garrett PE, Schumacher RT, Peddada L, et al. Dynamics of HIV viremia and antibody seroconversion in plasma donors: Implications for diagnosis and staging of primary HIV infection. *AIDS*. 2003;**17**(13):1871–9.

137. Lindbäck S, Thorstensson R, Karlsson AC, von Sydow M, Flamholc L, Blaxhult A, et al. Diagnosis of primary HIV-1 infection and duration of follow-up after HIV exposure. *AIDS*. 2000;**14**(15):2333–9.

138. Little SJ, McLean AR, Spina CA, Rechman DD, Havlir D. Viral dynamics of acute HIV-1 infection. *J Exp Med*. 1999;**190**(6):841–50.

139. Kahn JO, Walker BD. Acute human immunodeficiency virus type 1 infection. *N Engl J Med*. 1998;**339**(1):33–9.

140. Bangham CRM. CTL quality and the control of human retroviral infections. *Eur J Immunol*. 2009;**39**(7):1700–12.

141. Koup RA. Virus escape from CTL recognition. *J Exp Med*. 1994;**180**(3):779–82.

142. Borrow P, Lewicki H, Hahn BH, Shaw GM, Oldstone MB. Virus-specific CD8+ cytotoxic T-lymphocyte activity associated with control of viremia in primary human immunodeficiency virus type 1 infection. *J Virol*. 1994;**68**(9):6103–10.

143. Price DA, Goulder PJR, Klenerman P, Sewell AK, Easterbrook PJ, Troop M, et al. Positive selection of HIV-1 cytotoxic T lymphocyte escape variants during primary infection. *Proc Natl Acad Sci U S A*. 1997;**94**(5):1890–5.

144. Allen TM, O'Connor DH, Jing P, Dzuris JL, Mothé BR, Vogel TU, et al. Tat-specific cytotoxic T lymphocytes select for SIV escape variants during resolution of primary viraemia. *Nature*. 2000;**407**(6802):386–90.

145. Gupta KK. Acute immunosuppression with HIV seroconversion. *N Engl J Med*. 1993;**328**(4):288–9.

146. Maartens G, Celum C, Lewin SR. HIV infection: Epidemiology, pathogenesis, treatment, and prevention. *Lancet*. 2014;**384**(9939):258–71.

147. Brenchley JM, Price DA, Schacker TW, Asher TE, Silvestri G, Rao S, et al. Microbial translocation is a cause of systemic immune activation in chronic HIV infection. *Nat Med*. 2006;**12**(12):1365–71.

148. Estes JD, Harris LD, Klatt NR, Tabb B, Pittaluga S, Paiardini M, et al. Damaged intestinal epithelial integrity linked to microbial translocation in pathogenic simian immunodeficiency virus infections. *PLoS Pathog*. 2010;**6**(8):e1001052.

149. Ford ES, Puronen CE, Sereti I. Immunopathogenesis of asymptomatic chronic HIV Infection: The calm before the storm. *Curr Opin HIV AIDS*. 2009;**4**(3):206–14.

150. Brooks JT, Kaplan JE, Holmes KK, Benson C, Pau A, Masur H. HIV-associated opportunistic infections-going, going, but not gone: The continued need for prevention and treatment guidelines. *Clin Infect Dis*. 2009;**48**(5):609–11.

151. Lackner AA, Lederman MM, Rodriguez B. HIV pathogenesis: The host. *Cold Spring Harb Perspect Med*. 2012;**2**(9):a007005.

152. Hammer SM, Squires KE, Hughes MD, Grimes JM, Demeter LM, Currier JS, et al. A controlled trial of two nucleoside analogues plus indinavir in persons with human immunodeficiency virus infection and CD4 cell counts of 200 per cubic millimeter or less. *N Engl J Med*. 1997;**337**(11):725–33.

153. Palella FJ, Delaney KM, Moorman AC, Loveless MO, Fuhrer J, Satten GA, et al. Declining morbidity and mortality among patients with advanced human immunodeficiency virus infection. *N Engl J Med*. 1998;**338**(13):853–60.

154. Ho DD, Neumann AU, Perelson AS, Chen W, Leonard JM, Markowitz M. Rapid turnover of plasma virions and CD4 lymphocytes in HIV-1 infection. *Nature*. 1995;**373**(6510):123–6.

155. Fischl MA, Richman DD, Grieco MH, Gottlieb MS, Volberding PA, Laskin OL, et al. The efficacy of azidothymidine (AZT) in the treatment of patients with AIDS and AIDS-related complex. *N Engl J Med*. 1987;**317**(4):185–91.

156. Hodges-Mameletzis I, Fonner VA, Dalal S, Mugo N, Msimanga-Radebe B, Baggaley R. Pre-exposure prophylaxis for HIV prevention in women: Current status and future directions. *Drugs*. 2019;**79**(12):1263–76.

157. Dixit NM, Perelson AS. Multiplicity of human immunodeficiency virus infections in lymphoid tissue. *J Virol*. 2004;**78**(16):8942–5.

158. Patterson S, Knight SC. Susceptibility of human peripheral blood dendritic cells to infection by human immunodeficiency virus. *J Gen Virol*. 1987;**68**(4):1177–81.

159. Granelli-Piperno A, Moser B, Pope M, Chen D, Wei Y, Isdell F, et al. Efficient interaction of HIV-1 with purified dendritic cells via multiple chemokine coreceptors. *J Exp Med*. 1996;**184**(6):2433–8.

160. Rubbert A, Combadiere C, Ostrowski M, Arthos J, Dybul M, Machado E, et al. Dendritic cells express multiple chemokine receptors used as coreceptors for HIV entry. *J Immunol*. 1998;**160**(8):3933–41.

161. Turville SG, Cameron PU, Handley A, Lin G, Pöhlmann S, Doms RW, et al. Diversity of receptors binding HIV on dendritic cell subsets. *Nat Immunol*. 2002;**3**(10):975–83.

162. Macatonia SE, Lau R, Patterson S, Pinching AJ, Knight SC. Dendritic cell infection, depletion and dysfunction in HIV-infected individuals. *Immunology*. 1990;**71**(1):38–45.

163. Langhoff E, Terwilliger EF, Bos HJ, Kalland KH, Poznansky MC, Bacon OML, et al. Replication of human immunodeficieacy virus type 1 in primary dendritic cell cultures. *Proc Natl Acad Sci U S A*. 1991;**88**(18):7998–8002.

164. Pope M, Gezelter S, Gallo N, Hoffman L, Steinman RM. Low levels of HIV-1 infection in cutaneous dendritic cells promote extensive viral replication upon binding to memory CD4+ T cells. *J Exp Med*. 1995;**182**(6):2045–56.

165. Kawamura T, Gulden FO, Sugaya M, McNamara DT, Borris DL, Lederman MM, et al. R5 HIV productively infects langerhans cells, and infection levels are regulated by compound CCR5 polymorphisms. *Proc Natl Acad Sci U S A*. 2003;**100**(14):8401–6.

166. Cameron PU, Forsum U, Teppler H, Granelli-Piperno A, Steinman RM. During HIV-1 infection most blood dendritic cells are not productively infected and can induce allogeneic CD4+ T cells clonal expansion. *Clin Exp Immunol*. 1992;**88**(2):226–36.

167. McIlroy D, Autran B, Cheynier R, Wain-Hobson S, Clauvel JP, Oksenhendler E, et al. Infection frequency of dendritic cells and CD4+ T lymphocytes in spleens of human immunodeficiency virus-positive patients. *J Virol*. 1995;**69**(8):4737–45.

168. Granelli-Piperno A, Delgado E, Finkel V, Paxton W, Steinman RM. Immature dendritic cells selectively replicate macrophagetropic (M-tropic) human immunodeficiency virus type 1, while mature cells efficiently transmit both M- and T-tropic virus to T cells. *J Virol*. 1998;**72**(4):2733–7.

169. Granelli-Piperno A, Finkel V, Delgado E, Steinman RM. Virus replication begins in dendritic cells during the transmission of HIV-1 from mature dendritic cells to T cells. *Curr Biol*. 1999;**9**(1):21–9.

170. Lee B, Sharron M, Montaner LJ, Weissman D, Doms RW. Quantification of CD4, CCR5, and CXCR4 levels on lymphocyte subsets, dendritic cells, and differentially conditioned monocyte-derived macrophages. *Proc Natl Acad Sci U S A*. 1999;**96**(9):5215–20.

171. Turville SG, Santos JJ, Frank I, Cameron PU, Wilkinson J, Miranda-Saksena M, et al. Immunodeficiency virus uptake, turnover, and 2-phase transfer in human dendritic cells. *Blood*. 2004;**103**(6):2170–9.

172. Moris A, Nobile C, Buseyne F, Porrot F, Abastado JP, Schwartz O. DC-SIGN promotes exogenous MHC-I-restricted HIV-1 antigen presentation. *Blood*. 2004;**103**(7):2648–54.

173. Laguette N, Sobhian B, Casartelli N, Ringeard M, Chable-Bessia C, Ségéral E, et al. SAMHD1 is the dendritic- and myeloid-cell-specific HIV-1 restriction factor counteracted by Vpx. *Nature*. 2011;**474**(7353):654–7.

174. Hrecka K, Hao C, Gierszewska M, Swanson SK, Kesik-Brodacka M, Srivastava S, et al. Vpx relieves inhibition of HIV-1 infection of macrophages mediated by the SAMHD1 protein. *Nature*. 2011;**474**(7353):658–61.

175. Lahouassa H, Daddacha W, Hofmann H, Ayinde D, Logue EC, Dragin L, et al. SAMHD1 restricts the replication of human immunodeficiency virus type 1 by depleting the intracellular pool of deoxynucleoside triphosphates. *Nat Immunol*. 2012;**13**(3):223–8.

176. Sheehy AM, Gaddis NC, Choi JD, Malim MH. Isolation of a human gene that inhibits HIV-1 infection and is suppressed by the viral Vif protein. *Nature*. 2002;**418**(6898):646–50.

177. Mariani R, Chen D, Schröfelbauer B, Navarro F, König R, Bollman B, et al. Species-specific exclusion of APOBEC3G from HIV-1 virions by Vif. *Cell*. 2003;**114**(1):21–31.

178. Mangeat B, Turelli P, Caron G, Friedli M, Perrin L, Trono D. Broad antiretroviral defence by human APOBEC3G through lethal editing of nascent reverse transcripts. *Nature*. 2003;**424**(6944):99–103.

179. Geijtenbeek TBH, Kwon DS, Torensma R, van Vliet SJ, van Duijnhoven GCF, Middel J, et al. DC-SIGN, a dendritic cell-specific HIV-1-binding protein that enhances trans-infection of T cells. *Cell*. 2000;**100**(5):587–97.

180. Wu L, Bashirova AA, Martin TD, Villamide L, Mehlhop E, Chertov AO, et al. Rhesus macaque dendritic cells efficiently transmit primate lentiviruses independently of DC-SIGN. *Proc Natl Acad Sci U S A*. 2002;**99**(3):1568–73.

181. Gummuluru S, Rogel M, Stamatatos L, Emerman M. Binding of human immunodeficiency virus type 1 to immature dendritic cells can occur independently of DC-SIGN and mannose binding C-type lectin receptors via a cholesterol-dependent pathway. *J Virol*. 2003;**77**(23):12865–74.

182. Trumpfheller C, Park CG, Finke J, Steinman RM, Granelli-Piperno A. Cell type-dependent retention and transmission of HIV-1 by DC-SIGN. *Int Immunol*. 2003;**15**(2):289–98.

183. Granelli-Piperno A, Pritsker A, Pack M, Shimeliovich I, Arrighi J-F, Park CG, et al. Dendritic cell-specific intercellular adhesion molecule 3-grabbing nonintegrin/CD209 is abundant on macrophages in the normal human lymph node and is not required for dendritic cell stimulation of the mixed leukocyte reaction. *J Immunol*. 2005;**175**(7):4265–73.

184. Boggiano C, Manel N, Littman DR. Dendritic cell-mediated trans-enhancement of human immunodeficiency virus type 1 infectivity is independent of DC-SIGN. *J Virol*. 2007;**81**(5):2519–23.

185. Wang J-H, Janas AM, Olson WJ, KewalRamani VN, Wu L. CD4 coexpression regulates DC-SIGN-mediated transmission of human immunodeficiency virus type 1 □. *J Virol*. 2007;**81**(5):2497–507.

186. Izquierdo-Useros N, Blanco J, Erkizia I, Fernández-Figueras MT, Borràs FE, Naranjo-Gómez M, et al. Maturation of blood-derived dendritic cells enhances human immunodeficiency virus type 1 capture and transmission. *J Virol*. 2007;**81**(14):7559–70.

187. Puryear WB, Akiyama H, Geer SD, Ramirez NP, Yu X, Reinhard BM, et al. Interferon-inducible mechanism of dendritic cell-mediated HIV-1 dissemination is dependent on Siglec-1/CD169. *PLoS Pathog*. 2013;**9**(4):e1003291.

188. McDonald D, Wu L, Bohks SM, KewalRamani VN, Unutmaz D, Hope TJ. Recruitment of HIV and its receptors to dendritic cell-T cell junctions. *Science (80-)*. 2003;**300**(5623):1295–7.

189. Yu HJ, Reuter MA, McDonald D. HIV traffics through a specialized, surface-accessible intracellular compartment during trans-infection of T cells by mature dendritic cells. *PLoS Pathog*. 2008;**4**(8):e1000134.

190. Izquierdo-Useros N, Esteban O, Rodriguez-Plata MT, Erkizia I, Prado JG, Blanco J, et al. Dynamic imaging of cell-free and cell-associated viral capture in mature dendritic cells. *Traffic*. 2011;**12**(12):1702–13.

191. Garcia E, Pion M, Pelchen-Matthews A, Collinson L, Arrighi JF, Blot G, et al. HIV-1 trafficking to the dendritic cell-T-cell infectious synapse uses a pathway of tetraspanin sorting to the immunological synapse. *Traffic*. 2005;**6**(6):488–501.

192. Pino M, Erkizia I, Benet S, Erikson E, Fernández-Figueras MT, Guerrero D, et al. HIV-1 immune activation induces Siglec-1 expression and enhances viral trans-infection in blood and tissue myeloid cells. *Retrovirology*. 2015;**12**:37.

193. Akiyama H, Ramirez NGP, Gudheti M V., Gummuluru S. CD169-mediated trafficking of HIV to plasma membrane invaginations in dendritic cells attenuates efficacy of anti-gp120 broadly neutralizing antibodies. *PLoS Pathog*. 2015;**11**(3):e1004751.

194. Bakri Y, Schiffer C, Zennou V, Charneau P, Kahn E, Benjouad A, et al. The maturation of dendritic cells results in postintegration inhibition of HIV-1 replication. *J Immunol*. 2001;**166**(6):3780–8.

195. Cavrois M, Neidleman J, Kreisberg JF, Fenard D, Callebaut C, Greene WC. Human immunodeficiency virus fusion to dendritic cells declines as cells mature. *J Virol*. 2006;**80**(4):1992–9.

196. Williams AF, Barclay AN. The immunoglobulin superfamily - Domains for cell surface recognition. *Annu Rev Immunol*. 1988;**6**:381–405.

197. Crocker PR, Mucklow S, Bouckson V, McWilliam A, Willis AC, Gordon S, et al. Sialoadhesin, a macrophage sialic acid binding receptor for haemopoietic cells with 17 immunoglobulin-like domains. *EMBO J*. 1994;**13**(19):4490–503.

198. Crocker PR, Vinson M, Kelm S, Drickamer K. Molecular analysis of sialoside binding to sialoadhesin by NMR and site-directed mutagenesis. *Biochem J*. 1999;**341**(2):355–61.

199. May AP, Robinson RC, Vinson M, Crocker PR, Jones EY. Crystal structure of the N-terminal domain of sialoadhesin in complex with 3' sialyllactose at 1.85 Å resolution. *Mol Cell*. 1998;**1**(5):719–28.

200. Vinson M, van der Merwe PA, Kelm S, May A, Jones EY, Crocker PR. Characterization of the sialic acid-binding site in sialoadhesin by site-directed mutagenesis. *J Biol Chem*. 1996;**271**(16):9267–72.

201. Hartnell A, Steel J, Turley H, Jones M, Jackson DG, Crocker PR. Characterization of human sialoadhesin, a sialic acid binding receptor expressed by resident and inflammatory macrophage populations. *Blood*. 2001;**97**(1):288–96.

202. Fahy E, Subramaniam S, Brown HA, Glass CK, Merrill AH, Murphy RC, et al. A comprehensive classification system for lipids. *J Lipid Res*. 2005;**46**(5):839–61.

203. Simons K, Ikonen E. How cells handle cholesterol. *Science (80-)*. 2000;**290**(5497):1721–6.

204. Brown DA, London E. Structure and function of sphingolipid- and cholesterol-rich membrane rafts. *J Biol Chem*. 2000;**275**(23):17221–4.

205. Rajendran L, Simons K. Lipid rafts and membrane dynamics. *J Cell Sci*. 2005;**118**(6):1099–102.

206. Lorizate M, Kräusslich H-G. Role of lipids in virus replication. *Cold Spring Harb Perspect Biol*. 2011;**3**(10):a004820.

207. Izquierdo-Useros N, Lorizate M, Contreras F-X, Rodriguez-Plata MT, Glass B, Erkizia I, et al. Sialyllactose in viral membrane gangliosides is a novel molecular recognition

pattern for mature dendritic cell capture of HIV-1. *PLoS Biol*. 2012;**10**(4):e1001315.

208. Puryear WB, Yu X, Ramirez NP, Reinhard BM, Gummuluru S. HIV-1 incorporation of host-cell-derived glycosphingolipid GM3 allows for capture by mature dendritic cells. *Proc Natl Acad Sci*. 2012;**109**(19):7475–80.

209. Macauley MS, Crocker PR, Paulson JC. Siglec regulation of immune cell function in disease. *Nat Rev Immunol*. 2014;**14**(10):653–66.

210. Blixt O, Collins BE, Van den Nieuwenhof IM, Crocker PR, Paulson JC. Sialoside specificity of the siglec family assessed using novel multivalent probes: Identification of potent inhibitors of myelin-associated glycoprotein. *J Biol Chem*. 2003;**278**(33):31007–19.

211. Munday J, Floyd H, Crocker PR. Sialic acid binding receptors (siglecs) expressed by macrophages. *J Leukoc Biol*. 1999;**66**(5):705–11.

212. Crocker PR, Gordon S. Mouse macrophage hemagglutinin (sheep erythrocyte receptor) with specificity for sialylated glycoconjugates characterized by a monoclonal antibody. *J Exp Med*. 1989;**169**(4):1333–46.

213. Rempel H, Calosing C, Sun B, Pulliam L. Sialoadhesin expressed on IFN-induced monocytes binds HIV-1 and enhances infectivity. *PLoS One*. 2008;**3**(4):e1967.

214. York MR, Nagai T, Mangini AJ, Lemaire R, van Seventer JM, Lafyatis R. A macrophage marker, Siglec-1, is increased on circulating monocytes in patients with systemic sclerosis and induced by type I interferons and Toll-like receptor agonists. *Arthritis Rheum*. 2007;**56**(3):1010–20.

215. Pulliam L, Sun B, Rempel H. Invasive chronic inflammatory monocyte phenotype in subjects with high HIV-1 viral load. *J Neuroimmunol*. 2004;**157**(1–2):93–8.

216. Xiong YS, Cheng Y, Lin QS, Wu AL, Yu J, Li C, et al. Increased expression of Siglec-1 on peripheral blood monocytes and its role in mononuclear cell reactivity to autoantigen in rheumatoid arthritis. *Rheumatology*. 2014;**53**(2):250–9.

217. Biesen R, Demir C, Barkhudarova F, Grün JR, Steinbrich-Zöllner M, Backhaus M, et al. Sialic acid-binding Ig-like lectin 1 expression in inflammatory and resident monocytes is a potential biomarker for monitoring disease activity and success of therapy in systemic lupus erythematosus. *Arthritis Rheum*. 2008;**58**(4):1136–45.

218. Chen WC, Kawasaki N, Nycholat CM, Han S, Pilotte J, Crocker PR, et al. Antigen delivery to macrophages using liposomal nanoparticles targeting Sialoadhesin/CD169. *PLoS One*. 2012;**7**(6):e39039.

219. Kirchberger S, Majdic O, Steinberger P, Blüml S, Pfistershammer K, Zlabinger G, et al. Human rhinoviruses inhibit the accessory function of dendritic cells by inducing sialoadhesin and B7-H1 expression. *J Immunol*. 2005;**175**(2):1145–52.

220. von Sydow M, Sönnerborg A, Gaines H, Strannegård Ö. Interferon-alpha and tumor necrosis factor-alpha in serum of patients in various stages of HIV-1 infection. *AIDS Res Hum Retroviruses*. 1991;**7**(4):375–80.

221. Stacey AR, Norris PJ, Qin L, Haygreen EA, Taylor E, Heitman J, et al. Induction of a striking systemic cytokine cascade prior to peak viremia in acute human immunodeficiency virus type 1 infection, in contrast to more modest and delayed

responses in acute hepatitis B and C virus infections. *J Virol*. 2009;**83**(8):3719–33.

222. Estes JD, Gordon SN, Zeng M, Chahroudi AM, Dunham RM, Staprans SI, et al. Early resolution of acute immune activation and induction of PD-1 in SIV-infected sooty mangabeys distinguishes nonpathogenic from pathogenic infection in rhesus macaques. *J Immunol*. 2008;**180**(10):6798–807.

223. Stiksrud B, Aass HCD, Lorvik KB, Ueland T, Trøseid M, Dyrhol-Riise AM. Activated dendritic cells and monocytes in HIV immunological nonresponders: HIV-induced interferon-inducible protein-10 correlates with low future CD4+ recovery. *AIDS*. 2019;**33**(7):1117–29.

224. Ferbas JJ, Toso JF, Logar AJ, Navratil JS, Rinaldo CR. CD4+ blood dendritic cells are potent producers of IFN-alpha in response to in vitro HIV-1 infection. *J Immunol*. 1994;**152**(9):4649–62.

225. Yonezawa A, Morita R, Takaori-Kondo A, Kadowaki N, Kitawaki T, Hori T, et al. Natural alpha interferon-producing cells respond to human immunodeficiency virus type 1 with alpha interferon production and maturation into dendritic cells. *J Virol*. 2003;**77**(6):3777–84.

226. Lepelley A, Louis S, Sourisseau M, Law HKW, Pothlichet J, Schilte C, et al. Innate sensing of HIV-infected cells. *PLoS Pathog*. 2011;**7**(2):e1001284.

227. Lehmann C, Harper JM, Taubert D, Hartmann P, Fätkenheuer G, Jung N, et al. Increased interferon alpha expression in circulating plasmacytoid dendritic cells of HIV-1-infected patients. *J Acquir Immune Defic Syndr*. 2008;**48**(5):522–30.

228. Lehmann C, Lafferty M, Garzino-Demo A, Jung N, Hartmann P, Fätkenheuer G, et al. Plasmacytoid dendritic cells accumulate and secrete interferon alpha in lymph nodes of HIV-1 patients. *PLoS One*. 2010;**5**(6):e11110.

229. Li G, Cheng M, Nunoya J, Cheng L, Guo H, Yu H, et al. Plasmacytoid dendritic cells suppress HIV-1 replication but contribute to HIV-1 induced immunopathogenesis in humanized mice. *PLoS Pathog*. 2014;**10**(7):e1004291.

230. Fonteneau J-F, Larsson M, Beignon A, Mckenna K, Dasilva I, Amara A, et al. Human immunodeficiency virus type 1 activates plasmacytoid dendritic cells and concomitantly induces the bystander maturation of myeloid dendritic cells. *J Virol*. 2004;**78**(10):5223–32.

231. Cella M, Salio M, Sakakibara Y, Langen H, Julkunen I, Lanzavecchia A. Maturation, activation, and protection of dendritic cells induced by double-stranded RNA. *J Exp Med*. 1999;**189**(5):821–9.

232. Hashimoto SI, Suzuki T, Nagai S, Yamashita T, Toyoda N, Matsushima K. Identification of genes specifically expressed in human activated and mature dendritic cells through serial analysis of gene expression. *Blood*. 2000;**96**(6):2206–14.

233. Montoya M, Schiavoni G, Mattel F, Gresser I, Belardelli F, Borrow P, et al. Type I interferons produced by dendritic cells promote their phenotypic and functional activation. *Blood*. 2002;**99**(9):3263–71.

234. Gautier G, Humbert M, Deauvieau F, Scuiller M, Hiscott J, Bates EEM, et al. A type I interferon autocrine-paracrine loop is involved in Toll-like receptor-induced interleukin-12p70 secretion by dendritic cells. *J Exp Med*. 2005;**201**(9):1435–46.

235. Pollara G, Handley ME, Kwan A, Chain BM, Katz DR. Autocrine type I interferon amplifies dendritic cell responses to lipopolysaccharide via the nuclear factor-κB/p38 pathways. *Scand J Immunol*. 2006;**63**(3):151–4.

236. Hensley-McBain T, Berard AR, Manuzak JA, Miller CJ, Zevin AS, Polacino P, et al. Intestinal damage precedes mucosal immune dysfunction in SIV infection. *Nat Mucosal Immunol*. 2018;**11**(5):1429–40.

237. Sewald X, Ladinsky MS, Uchil PD, Beloor J, Pi R, Herrmann C, et al. Retroviruses use CD169-mediated trans-infection of permissive lymphocytes to establish infection. *Science (80-)*. 2015;**350**(6260):563–7.

238. Kader M, Smith AP, Guiducci C, Wonderlich ER, Normolle D, Watkins SC, et al. Blocking TLR7- and TLR9-mediated IFN-α production by plasmacytoid dendritic cells does not diminish immune activation in early SIV infection. *PLoS Pathog*. 2013;**9**(7):e1003530.

239. Li Q, Estes JD, Schlievert PM, Duan L, Brosnahan AJ, Southern PJ, et al. Glycerol monolaurate prevents mucosal SIV transmission. *Nature*. 2009;**458**(7241):1034–8.

240. Shang L, Duan L, Perkey KE, Wietgrefe S, Zupancic M, Smith AJ, et al. Epithelium-innate immune cell axis in mucosal responses to SIV. *Mucosal Immunol*. 2017;**10**(2):508–19.

241. Hladik F, Sakchalathorn P, Ballweber L, Lentz G, Fialkow M, Eschenbach D, et al. Initial events in establishing vaginal entry and infection by human immunodeficiency virus type-1. *Immunity*. 2007;**26**(2):257–70.

242. Ballweber L, Robinson B, Kreger A, Fialkow M, Lentz G, McElrath MJ, et al. Vaginal Langerhans cells nonproductively transporting HIV-1 mediate infection of T cells. *J Virol*. 2011;**85**(24):13443–7.

243. Shen R, Kappes JC, Smythies LE, Richter HE, Novak L, Smith PD. Vaginal myeloid dendritic cells transmit founder HIV-1. *J Virol*. 2014;**88**(13):7683–8.

244. Trifonova RT, Bollman B, Barteneva NS, Lieberman J. Myeloid cells in intact human cervical explants capture HIV and can transmit it to CD4 T cells. *Front Immunol*. 2018;**9**:2719.

245. Fackler OT, Murooka TT, Imle A, Mempel TR. Adding new dimensions: Towards an integrative understanding of HIV-1 spread. *Nat Rev Microbiol*. 2014;**12**(8):563–71.

246. Wu L, KewalRamani VN. Dendritic-cell interactions with HIV: Infection and viral dissemination. *Nat Rev Immunol*. 2006;**6**(11):859–68.

247. Slenczka W, Klenk HD. Forty years of Marburg virus. *J Infect Dis*. 2007;**196**(Suppl 2):S131–5.

248. Messaoudi I, Amarasinghe GK, Basler CF. Filovirus pathogenesis and immune evasion: Insights from Ebola virus and Marburg virus. *Nat Rev Microbiol*. 2015;**13**(11):663–76.

249. Kuhn JH, Amarasinghe GK, Basler CF, Bavari S, Bukreyev A, Chandran K, et al. ICTV virus taxonomy profile: Filoviridae. *J Gen Virol*. 2019;**100**(6):911–2.

250. Johnson KM, Lange J V., Webb PA, Murphy FA. Isolation and partial characterisation of a new virus causing acute hæmorrhagic fever in Zaire. *Lancet*. 1977;**309**(8011):569–

71.

251. WHO International Study Team. Ebola haemorrhagic fever in Sudan, 1976. *Bull World Health Organ*. 1978;**56**(2):247–70.

252. Baseler L, Chertow DS, Johnson KM, Feldmann H, Morens DM. The pathogenesis of Ebola virus disease. *Annu Rev Pathol Mech Dis*. 2017;**12**:387–418.

253. WHO Ebola situation report. 10 June 2016.

254. Ebola health update [Internet]. 2019.

255. A. FHS, W. GT. Filoviridae: Marburg and Ebola viruses. In: Knipe DM, Howley PM, editors. Fields Virology. Sixth edit. Philadelphia: Wolters Kluwer Health/Lippincott Williams & Wilkins; 2013. p. 923–56.

256. Feldmann H, Geisbert TW. Ebola haemorrhagic fever. *Lancet*. 2011;**377**(9768):849–62.

257. Noda T, Sagara H, Suzuki E, Takada A, Kida H, Kawaoka Y. Ebola virus VP40 drives the formation of virus-like filamentous particles along with GP. *J Virol*. 2002;**76**(10):4855–65.

258. Mühlberger E, Weik M, Volchkov VE, Klenk HD, Becker S. Comparison of the transcription and replication strategies of marburg virus and Ebola virus by using artificial replication systems. *J Virol*. 1999;**73**(3):2333–42.

259. Mehedi M, Falzarano D, Seebach J, Hu X, Carpenter MS, Schnittler H-J, et al. A new Ebola virus nonstructural glycoprotein expressed through RNA editing. *J Virol*. 2011;**85**(11):5406–14.

260. Sanchez A, Trappier SG, Mahy BWJ, Peters CJ, Nichol ST. The virion glycoproteins of Ebola viruses are encoded in two reading frames and are expressed through transcriptional editing. *Proc Natl Acad Sci U S A*. 1996;**93**(8):3602–7.

261. Manicassamy B, Wang J, Jiang H, Rong L. Comprehensive analysis of Ebola virus GP1 in viral entry. *J Virol*. 2005;**79**(8):4793–805.

262. Basler CF, Wang X, Mühlberger E, Volchkov V, Paragas J, Klenk HD, et al. The Ebola virus VP35 protein functions as a type I IFN antagonist. *Proc Natl Acad Sci U S A*. 2000;**97**(22):12289–94.

263. Reid SP, Leung LW, Hartman AL, Martinez O, Shaw ML, Carbonnelle C, et al. Ebola virus VP24 binds karyopherin 1 and blocks STAT1 nuclear accumulation. *J Virol*. 2006;**80**(11):5156–67.

264. ViralZone; SIB Swiss Institute of Bioinformatics [Internet]. 2014.

265. Baskerville A, Fisher-Hoch SP, Neild GH, Dowsett AB. Ultrastructural pathology of experimental Ebola haemorrhagic fever virus infection. *J Pathol*. 1985;**147**(3):199–209.

266. Geisbert TW, Jahrling PB, Hanes MA, Zack PM. Association of Ebola-related Reston virus particles and antigen with tissue lesions of monkeys imported to the United States. *J Comp Pathol*. 1992;**106**(2):137–52.

267. Moller-Tank S, Maury W. Ebola virus entry: A curious and complex series of events. *PLoS Pathog*. 2015;**11**(4):e1004731.

268. Davey RA, Shtanko O, Anantpadma M, Sakurai Y, Chandran K, Mauri W. Mechanisms

of filovirus entry. *Curr Top Microbiol Immunol*. 2017;**411**:323–52.

269. Curtis BM, Scharnowske S, Watsont AJ. Sequence and expression of a membrane-associated C-type lectin that exhibits CD4-independent binding of human immunodeficiency virus envelope glycoprotein gp120. *Proc Natl Acad Sci U S A*. 1992;**89**(17):8356–60.

270. Pöhlmann S, Soilleux EJ, Baribaud F, Leslie GJ, Morris LS, Trowsdale J, et al. DC-SIGNR, a DC-SIGN homologue expressed in endothelial cells, binds to human and simian immunodeficiency viruses and activates infection in trans. *Proc Natl Acad Sci U S A*. 2001;**98**(5):2670–5.

271. Baribaud F, Doms RW, Pöhlmann S. The role of DC-SIGN and DC-SIGNR in HIV and Ebola virus infection: Can potential therapeutics block virus transmission and dissemination? *Expert Opin Ther Targets*. 2002;**6**(4):423–31.

272. Dominguez-Soto A, Aragoneses-Fenoll L, Martin-Gayo E, Martinez-Prats L, Colmenares M, Naranjo-Gomez M, et al. The DC-SIGN-related lectin LSECtin mediates antigen capture and pathogen binding by human myeloid cells. *Blood*. 2007;**109**(12):5337–45.

273. Salvador B, Sexton NR, Carrion R, Nunneley J, Patterson JL, Steffen I, et al. Filoviruses utilize glycosaminoglycans for their attachment to target cells. *J Virol*. 2013;**87**(6):3295–304.

274. O'Hearn A, Wang M, Cheng H, Lear-Rooney CM, Koning K, Rumschlag-Booms E, et al. Role of EXT1 and glycosaminoglycans in the early stage of filovirus entry. *J Virol*. 2015;**89**(10):5441–9.

275. Tamhankar M, Gerhardt DM, Bennett RS, Murphy N, Jahrling PB, Patterson JL. Heparan sulfate is an important mediator of Ebola virus infection in polarized epithelial cells. *Virol J*. 2018;**15**(1):135.

276. Uhlin-Hansen L, Wik T, Kjellén L, Berg E, Forsdahl F, Kolset SO. Proteoglycan metabolism in normal and inflammatory human macrophages. *Blood*. 1993;**82**(9):2880–9.

277. Jones M, Tussey L, Athanasou N, Jackson DG. Heparan sulfate proteoglycan isoforms of the CD44 hyaluronan receptor induced in human inflammatory macrophages can function as paracrine regulators of fibroblast growth factor action. *J Biol Chem*. 2000;**275**(11):7964–74.

278. Manakil JF, Sugerman PB, Li H, Seymour GJ, Bartold PM. Cell-surface proteoglycan expression by lymphocytes from peripheral blood and gingiva in health and periodontal disease. *J Dent Res*. 2001;**80**(8):1704–10.

279. Wegrowski Y, Milard A-L, Kotlarz G, Toulmonde E, Maquart F-X, Bernard J. Cell surface proteoglycan expression during maturation of human monocytes-derived dendritic cells and macrophages. *Clin Exp Immunol*. 2006;**144**(3):485–93.

280. Moller-Tank S, Maury W. Phosphatidylserine receptors: Enhancers of enveloped virus entry and infection. *Virology*. 2014;**468**–**470**:565–80.

281. Ravichandran KS. Beginnings of a good apoptotic meal: The find-me and eat-me signaling pathways. *Immunity*. 2011;**35**(4):445–55.

282. Jemielity S, Wang JJ, Chan YK, Ahmed AA, Li W, Monahan S, et al. TIM-family proteins promote infection of multiple enveloped viruses through virion-associated phosphatidylserine. *PLoS Pathog*. 2013;**9**(3):e1003232.

283. Kondratowicz AS, Lennemann NJ, Sinn PL, Davey RA, Hunt CL, Moller-Tank S, et al. T-cell immunoglobulin and mucin domain 1 (TIM-1) is a receptor for Zaire Ebolavirus and Lake Victoria Marburgvirus. *Proc Natl Acad Sci U S A*. 2011;**108**(20):8426–31.

284. Moller-Tank S, Kondratowicz AS, Davey RA, Rennert PD, Maury W. Role of the phosphatidylserine receptor TIM-1 in enveloped-virus entry. *J Virol*. 2013;**87**(15):8327–41.

285. Dahlmann F, Biedenkopf N, Babler A, Jahnen-Dechent W, Karsten CB, Gnirß K, et al. Analysis of Ebola virus entry into macrophages. *J Infect Dis*. 2015;**212**(Suppl 2):S247–57.

286. Shimojima M, Takada A, Ebihara H, Neumann G, Fujioka K, Irimura T, et al. Tyro3 family-mediated cell entry of Ebola and Marburg viruses. *J Virol*. 2006;**80**(20):10109–16.

287. Brindley MA, Hunt CL, Kondratowicz AS, Bowman J, Sinn PL, McCray PB, et al. Tyrosine kinase receptor Axl enhances entry of Zaire ebolavirus without direct interactions with the viral glycoprotein. *Virology*. 2011;**415**(2):83–94.

288. Bavari S, Bosio CM, Wiegand E, Ruthel G, Will AB, Geisbert TW, et al. Lipid raft microdomains: A gateway for compartmentalized trafficking of Ebola and Marburg viruses. *J Exp Med*. 2002;**195**(5):593–602.

289. Perez-Zsolt D, Martinez-Picado J, Izquierdo-Useros N. Receptors on primary phagocytes as therapeutic targets against highly pathogenic emerging viruses. In: Antiviral discovery for highly pathogenic emerging viruses.

290. Takada A, Watanabe S, Ito H, Okazaki K, Kida H, Kawaoka Y. Downregulation of β1 integrins by Ebola virus glycoprotein: Implication for virus entry. *Virology*. 2000;**278**(1):20–6.

291. Mulherkar N, Raaben M, de la Torre JC, Whelan SP, Chandran K. The Ebola virus glycoprotein mediates entry via a non-classical dynamin-dependent macropinocytic pathway. *Virology*. 2011;**419**(2):72–83.

292. Nelson EA, Dyall J, Hoenen T, Barnes AB, Zhou H, Liang JY, et al. The phosphatidylinositol-3-phosphate 5-kinase inhibitor apilimod blocks filoviral entry and infection. *PLoS Negl Trop Dis*. 2017;**11**(4):e0005540.

293. Kondratowicz AS, Hunt CL, Davey RA, Cherry S, Maury WJ. AMP-activated protein kinase is required for the macropinocytic internalization of ebolavirus. *J Virol*. 2013;**87**(2):746–55.

294. Saeed MF, Kolokoltsov AA, Albrecht T, Davey RA. Cellular entry of Ebola virus involves uptake by a macropinocytosis-like mechanism and subsequent trafficking through early and late endosomes. *PLoS Pathog*. 2010;**6**(9):e1001110.

295. Simmons JA, D'Souza RS, Ruas M, Galione A, Casanova JE, White JM. Ebolavirus glycoprotein directs fusion through NPC1+ endolysosomes. *J Virol*. 2016;**90**(1):605–10.

296. Spence JS, Krause TB, Mittler E, Jangra RK, Chandran K. Direct visualization of Ebola virus fusion triggering in the endocytic pathway. *MBio*. 2016;**7**(1):e01857-15.

297. Carette JE, Raaben M, Wong AC, Herbert AS, Obernosterer G, Mulherkar N, et al. Ebola virus entry requires the cholesterol transporter Niemann-Pick C1. *Nature*. 2011;**477**(7364):340–3.

298. Sakurai Y, Kolokoltsov AA, Chen C-C, Tidwell MW, Bauta WE, Klugbauer N, et al. Two-pore channels control Ebola virus host cell entry and are drug targets for disease treatment. *Science (80-).* 2015;**347**(6225):995–8.

299. Takada A, Robison C, Goto H, Sanchez A, Murti KG, Whitt MA, et al. A system for functional analysis of Ebola virus glycoprotein. *Proc Natl Acad Sci U S A*. 1997;**94**(26):14764–9.

300. Wool-Lewis RJ, Bates P. Characterization of Ebola virus entry by using pseudotyped viruses: Identification of receptor-deficient cell lines. *J Virol*. 1998;**72**(4):3155–60.

301. Martinez O, Johnson J, Manicassamy B, Rong L, Olinger GG, Hensley LE, et al. Zaire Ebola virus entry into human dendritic cells is insensitive to cathepsin L inhibition. *Cell Microbiol*. 2010;**12**(2):148–57.

302. Côté M, Misasi J, Ren T, Bruchez A, Lee K, Filone CM, et al. Small molecule inhibitors reveal Niemann-Pick C1 is essential for Ebola virus infection. *Nature*. 2011;**477**(7364):344–8.

303. Jasenosky LD, Neumann G, Lukashevich I, Kawaoka Y. Ebola virus VP40-induced particle formation and association with the lipid bilayer. *J Virol*. 2001;**75**(11):5205–14.

304. Harty RN, Brown ME, Wang G, Huibregtse J, Hayes FP. A PPxY motif within the VP40 protein of Ebola virus interacts physically and functionally with a ubiquitin ligase: Implications for filovirus budding. *Proc Natl Acad Sci U S A*. 2000;**97**(25):13871–6.

305. Peterson AT, Carroll DS, Mills JN, Johnson KM. Potential mammalian filovirus reservoirs. *Emerg Infect Dis*. 2004;**10**(12):2073–81.

306. Groseth A, Feldmann H, Strong JE. The ecology of Ebola virus. *Trends Microbiol*. 2007;**15**(9):408–16.

307. WHO International Study Team. Ebola haemorrhagic fever in Zaire, 1976. *Bull World Health Organ*. 1978;**56**(2):271–93.

308. Dowell SF, Mukunu R, Ksiazek TG, Khan AS, Rollin PE, Peters CJ. Transmission of Ebola hemorrhagic fever: A study of risk factors in family members, Kikwit, Democratic Republic of the Congo, 1995. *J Infect Dis*. 1999;**179**(Suppl 1):S87–91.

309. Ajelli M, Parlamento S, Bome D, Kebbi A, Atzori A, Frasson C, et al. The 2014 Ebola virus disease outbreak in Pujehun, Sierra Leone: Epidemiology and impact of interventions. *BMC Med*. 2015;**13**:281.

310. Nielsen CF, Kidd S, Sillah ARM, Davis E, Mermin J, Kilmarx PH. Improving burial practices and cemetery management during an Ebola virus disease epidemic - Sierra Leone, 2014. *Morb Mortal Wkly Rep*. 2015;**64**(1):20–7.

311. Geisbert TW, Jaax NK. Marburg hemorrhagic fever: Report of a case studied by immunohistochemistry and electron microscopy. *Ultrastruct Pathol*. 1998;**22**(1):3–17.

312. Ryabchikova EI, Kolesnikova L V., Luchko S V. An analysis of features of pathogenesis in two animal models of Ebola virus infection. *J Infect Dis*. 1999;**179**(Suppl 1):S199–202.

313. Chertow DS, Kleine C, Edwards JK, Scaini R, Giuliani R, Sprecher A. Ebola virus disease in West Africa - Clinical manifestations and management. *N Engl J Med*. 2014;**371**(22):2054–7.

314. Hunt L, Gupta-Wright A, Simms V, Tamba F, Knott V, Tamba K, et al. Clinical presentation, biochemical, and haematological parameters and their association with outcome in patients with Ebola virus disease: An observational cohort study. *Lancet Infect Dis*. 2015;**15**(11):1292–9.

315. Uyeki TM, Mehta AK, Davey RT, Liddell AM, Wolf T, Vetter P, et al. Clinical management of ebola virus disease in the United States and Europe. *N Engl J Med*. 2016;**374**(7):636–46.

316. Chertow DS, Childs RW, Arai AE, Davey RT. Cardiac MRI findings suggest myocarditis in severe Ebola virus disease. *JACC Cardiovasc Imaging*. 2017;**10**(6):711–3.

317. Mattia JG, Vandy MJ, Chang JC, Platt DE, Dierberg K, Bausch DG, et al. Early clinical sequelae of Ebola virus disease in Sierra Leone: A cross-sectional study. *Lancet Infect Dis*. 2016;**16**(3):331–8.

318. Emond RTD, Evans B, Bowen ETW, Lloyd G. A case of Ebola virus infection. *Br Med J*. 1977;**2**(6086):541–4.

319. Rodriguez LL, De Roo A, Guimard Y, Trappier SG, Sanchez A, Bressler D, et al. Persistence and genetic stability of Ebola virus during the outbreak in Kikwit, Democratic Republic of the Congo, 1995. *J Infect Dis*. 1999;**179**(Suppl 1):S170–6.

320. Rowe AK, Bertolli J, Khan AS, Mukunu R, Muyembe-Tamfum JJ, Bressler D, et al. Clinical, virologic, and immunologic follow-up of convalescent Ebola hemorrhagic fever patients and their household contacts, Kikwit, Democratic Republic of the Congo. *J Infect Dis*. 1999;**179**(Suppl 1):S28–35.

321. Bausch DG, Towner JS, Dowell SF, Kaducu F, Lukwiya M, Sanchez A, et al. Assessment of the risk of Ebola virus Transmission from bodily fluids and fomites. *J Infect Dis*. 2007;**196**(Suppl 2):S142–7.

322. Mate SE, Kugelman JR, Nyenswah TG, Ladner JT, Wiley MR, Cordier-Lassalle T, et al. Molecular evidence of sexual transmission of Ebola virus. *N Engl J Med*. 2015;**373**(25):2448–54.

323. Maxmen A. Experimental Ebola drugs face tough test in war zone. *Nature*. 2018;**561**(7721):14.

324. Bradfute SB, Swanson PE, Smith MA, Watanabe E, McDunn JE, Hotchkiss RS, et al. Mechanisms and consequences of ebolavirus-induced lymphocyte apoptosis. *J Immunol*. 2010;**184**(1):327–35.

325. Menicucci AR, Versteeg K, Woolsey C, Mire CE, Geisbert JB, Cross RW, et al. Transcriptome analysis of circulating immune cell subsets highlight the role of monocytes in Zaire Ebola virus Makona pathogenesis. *Front Immunol*. 2017;**8**:1372.

326. Martines RB, Ng DL, Greer PW, Rollin PE, Zaki SR. Tissue and cellular tropism, pathology and pathogenesis of Ebola and Marburg viruses. *J Pathol*. 2015;**235**(2):153–74.

327. Zaki SR, Goldsmith CS. Pathologic features of filovirus infections in humans. *Curr Top Microbiol Immunol*. 1999;**235**:97–116.

328. Bosio CM, Aman MJ, Grogan C, Hogan R, Ruthel G, Negley D, et al. Ebola and Marburg viruses replicate in monocyte-derived dendritic cells without inducing the production of cytokines and full maturation. *J Infect Dis*. 2003;**188**(11):1630–8.

329. Mahanty S, Hutchinson K, Agarwal S, Mcrae M, Rollin PE, Pulendran B. Impairment of dendritic cells and adaptive immunity by Ebola and Lassa viruses. *J Immunol*. 2003;**170**(6):2797–801.

330. Lubaki NM, Ilinykh P, Pietzsch C, Tigabu B, Freiberg AN, Koup RA, et al. The lack of maturation of Ebola virus-infected dendritic cells results from the cooperative effect of at least two viral domains. *J Virol*. 2013;**87**(13):7471–85.

331. Yen B, Mulder LCF, Martinez O, Basler CF. Molecular basis for ebolavirus VP35 suppression of human dendritic cell maturation. *J Virol*. 2014;**88**(21):12500–10.

332. Lubaki NM, Younan P, Santos RI, Meyer M, Iampietro M, Koup RA, et al. The Ebola interferon inhibiting domains attenuate and dysregulate cell-mediated immune responses. *PLoS Pathog*. 2016;**12**(12):e1006031.

333. Gupta M, Mahanty S, Ahmed R, Rollin PE. Monocyte-derived human macrophages and peripheral blood mononuclear cells infected with Ebola virus secrete MIP-1α and TNF-α and inhibit poly-IC-induced IFN-α in vitro. *Virology*. 2001;**284**(1):20–5.

334. Mohamadzadeh M, Coberley SS, Olinger GG, Kalina W V., Ruthel G, Fuller CL, et al. Activation of triggering receptor expressed on myeloid cells-1 on human neutrophils by Marburg and Ebola viruses. *J Virol*. 2006;**80**(14):7235–44.

335. Ströher U, West E, Bugany H, Klenk H-D, Schnittler H-J, Feldmann H. Infection and activation of monocytes by Marburg and Ebola viruses. *J Virol*. 2001;**75**(22):11025–33.

336. Escudero-Pérez B, Volchkova VA, Dolnik O, Lawrence P, Volchkov VE. Shed GP of Ebola virus triggers immune activation and increased vascular permeability. *PLoS Pathog*. 2014;**10**(11):e1004509.

337. Colavita F, Biava M, Castilletti C, Lanini S, Miccio R, Portella G, et al. Inflammatory and humoral immune response during Ebola virus infection in survivor and fatal cases occurred in Sierra Leone during the 2014–2016 outbreak in West Africa. *Viruses*. 2019;**11**(4):E373.

338. Reynard S, Journeaux A, Gloaguen E, Schaeffer J, Varet H, Pietrosemoli N, et al. Immune parameters and outcomes during Ebola virus disease. *JCI Insight*. 2019;**4**(1):e125106.

339. Feldmann H, Bugany H, Mahner F, Klenk H-D, Drenckhahn D, Schnittler H-J. Filovirus-induced endothelial leakage triggered by infected monocytes/macrophages. *J Virol*. 1996;**70**(4):2208–14.

340. Geisbert TW, Young HA, Jahrling PB, Davis KJ, Larsen T, Kagan E, et al. Pathogenesis of Ebola hemorrhagic fever in primate models: Evidence that hemorrhage is not a direct

effect of virus-induced cytolysis of endothelial cells. *Am J Pathol*. 2003;**163**(6):2371–82.

341. Geisbert TW, Young HA, Jahrling PB, Davis KJ, Kagan E, Hensley LE. Mechanisms underlying coagulation abnormalities in Ebola hemorrhagic fever: Overexpression of tissue factor in primate monocytes/macrophages is a key event. *J Infect Dis*. 2003;**188**(11):1618–29.

342. Sanchez A, Lukwiya M, Bausch D, Mahanty S, Sanchez AJ, Wagoner KD, et al. Analysis of human peripheral blood samples from fatal and nonfatal cases of Ebola (Sudan) hemorrhagic fever: Cellular responses, virus load, and nitric oxide levels. *J Virol*. 2004;**78**(19):10370–7.

343. Wauquier N, Becquart P, Padilla C, Baize S, Leroy EM. Human fatal zaire Ebola virus infection is associated with an aberrant innate immunity and with massive lymphocyte apoptosis. *PLoS Negl Trop Dis*. 2010;**4**(10):e837.

344. Rasmussen AL. Host factors in Ebola infection. *Annu Rev Genomics Hum Genet*. 2016;**17**:333–51.

345. Escudero-Pérez B, Muñoz-Fontela C. Role of type I interferons on filovirus pathogenesis. *Vaccines*. 2019;**7**(1):E22.

346. Jin H, Yan Z, Prabhakar BS, Feng Z, Ma Y, Verpooten D, et al. The VP35 protein of Ebola virus impairs dendritic cell maturation induced by virus and lipopolysaccharide. *J Gen Virol*. 2010;**91**(2):352–61.

347. Ilinykh PA, Lubaki NM, Widen SG, Renn LA, Theisen TC, Rabin RL, et al. Different temporal effects of Ebola virus VP35 and VP24 proteins on global gene expression in human dendritic cells. *J Virol*. 2015;**89**(15):7567–83.

348. Yen BC, Basler CF. Effects of filovirus interferon antagonists on responses of human monocyte-derived dendritic cells to RNA virus infection. *J Virol*. 2016;**90**(10):5108–18.

349. Edwards MR, Liu G, Mire CE, Sureshchandra S, Luthra P, Yen B, et al. Differential regulation of interferon responses by Ebola and Marburg virus VP35 proteins. *Cell Rep*. 2016;**14**(7):1632–40.

350. Villinger F, Rollin PE, Brar SS, Chikkala NF, Winter J, Sundstrom JB, et al. Markedly elevated levels of interferon (IFN)-γ, IFN-α, interleukin (IL)-2, IL-10, and tumor necrosis factor-α associated with fatal Ebola virus infection. *J Infect Dis*. 1999;**179**(Suppl 1):S188–91.

351. Connor JH, Yen J, Caballero IS, Garamszegi S, Malhotra S, Lin K, et al. Transcriptional profiling of the immune response to Marburg virus infection. *J Virol*. 2015;**89**(19):9865–74.

352. Caballero IS, Honko AN, Gire SK, Winnicki SM, Melé M, Gerhardinger C, et al. In vivo Ebola virus infection leads to a strong innate response in circulating immune cells. *BMC Genomics*. 2016;**17**:707.

353. Liu X, Speranza E, Muñoz-Fontela C, Haldenby S, Rickett NY, Garcia-Dorival I, et al. Transcriptomic signatures differentiate survival from fatal outcomes in humans infected with Ebola virus. *Genome Biol*. 2017;**18**(1):4.

354. Eisfeld AJ, Halfmann PJ, Wendler JP, Kyle JE, Burnum-Johnson KE, Peralta Z, et al.

Multi-platform ’omics analysis of human Ebola virus disease pathogenesis. *Cell Host Microbe*. 2017;**22**(6):817–29.

355. Kerber R, Krumkamp R, Korva M, Rieger T, Wurr S, Duraffour S, et al. Kinetics of soluble mediators of the host response in Ebola virus disease. *J Infect Dis*. 2018;**218**(Suppl 5):S496–503.

356. Kreuels B, Wichmann D, Emmerich P, Schmidt-Chanasit J, de Heer G, Kluge S, et al. A case of severe Ebola virus infection complicated by gram-negative septicemia. *N Engl J Med*. 2014;**371**(25):2394–401.

357. Medzhitov R. Recognition of microorganisms and activation of the immune response. *Nature*. 2007;**449**(7164):819–26.

358. Blanco J, Barretina J, Clotet B, Esté JA. R5 HIV gp120-mediated cellular contacts induce the death of single CCR5-expressing CD4 T cells by a gp41-dependent mechanism. *J Leukoc Biol*. 2004;**76**(4):804–11.

359. Herbeuval J-P, Hardy AW, Boasso A, Anderson SA, Dolan MJ, Dy M, et al. Regulation of TNF-related apoptosis-inducing ligand on primary CD4+ T cells by HIV-1: Role of type I IFN-producing plasmacytoid dendritic cells. *Proc Natl Acad Sci*. 2005;**102**(39):13974–9.

360. Meier A, Chang JJ, Chan ES, Pollard RB, Sidhu HK, Kulkarni S, et al. Sex differences in the Toll-like receptor-mediated response of plasmacytoid dendritic cells to HIV-1. *Nat Med*. 2009;**15**(8):955–9.

361. Harman AN, Lai J, Turville S, Samarajiwa S, Gray L, Marsden V, et al. HIV infection of dendritic cells subverts the IFN induction pathway via IRF-1 and inhibits type 1 IFN production. *Blood*. 2011;**118**(2):298–308.

362. Harman AN, Nasr N, Feetham A, Galoyan A, Alshehri AA, Rambukwelle D, et al. HIV blocks interferon induction in human dendritic cells and macrophages by dysregulation of TBK1. *J Virol*. 2015;**89**(13):6575–84.

363. Luft T, Pang KC, Thomas E, Hertzog P, Hart DN, Trapani J, et al. Type I IFNs enhance the terminal differentiation of dendritic cells. *J Immunol*. 1998;**161**(4):1947–53.

364. Paquette RL, Hsu NC, Kiertscher SM, Park AN, Tran L, Roth MD, et al. Interferon-α and granulocyte-macrophage colony-stimulating factor differentiate peripheral blood monocytes into potent antigen-presenting cells. *J Leukoc Biol*. 1998;**64**(3):358–67.

365. Sallusto F, Cella M, Danieli C, Lanzavecchia A. Dendritic cells use macropinocytosis and the mannose receptor to concentrate macromolecules in the major histocompatibility complex class II compartment: Downregulation by cytokines and bacterial products. *J Exp Med*. 1995;**182**(2):389–400.

366. Sriram U, Biswas C, Behrens EM, Dinnall J-A, Shivers DK, Monestier M, et al. IL-4 suppresses dendritic cell response to type I interferons. *J Immunol*. 2007;**179**(10):6446–55.

367. Cella M, Scheidegger D, Palmer-Lehmann K, Lane P, Lanzavecchia A, Alber G. Ligation of CD40 on dendritic cells triggers production of high levels of interleukin-12 and enhances T cell stimulatory capacity: T-T help via APC activation. *J Exp Med*. 1996;**184**(2):747–52.

368. Wang J-H, Janas AM, Olson WJ, Wu L. Functionally distinct transmission of human immunodeficiency virus type 1 mediated by immature and mature dendritic cells. *J Virol*. 2007;**81**(17):8933–43.

369. Schwartz S, Campbell M, Nasioulas G, Harrison J, Felber BK, Pavlakis GN. Mutational inactivation of an inhibitory sequence in human immunodeficiency virus type 1 results in Rev-independent gag expression. *J Virol*. 1992;**66**(12):7176–82.

370. Hermida-Matsumoto L, Resh MD. Localization of human immunodeficiency virus type 1 Gag and Env at the plasma membrane by confocal imaging. *J Virol*. 2000;**74**(18):8670–9.

371. Lindwasser OW, Resh MD. Myristoylation as a target for inhibiting HIV assembly: Unsaturated fatty acids block viral budding. *Proc Natl Acad Sci*. 2002;**99**(20):13037–42.

372. Perlman M, Resh MD. Identification of an intracellular trafficking and assembly pathway for HIV-1 Gag. *Traffic*. 2006;**7**(6):731–45.

373. Abel K, Rocke DM, Chohan B, Fritts L, Miller CJ. Temporal and anatomic relationship between virus replication and cytokine gene expression after vaginal simian immunodeficiency virus infection. *J Virol*. 2005;**79**(19):12164–72.

374. UNAIDS estimates. 2018.

375. Eid SG, Mangan NE, Hertzog PJ, Mak J. Blocking HIV-1 transmission in the female reproductive tract: from microbicide development to exploring local antiviral responses. *Clin Transl Immunol*. 2015;**4**(10):e43.

376. Hu Q, Frank I, Williams V, Santos JJ, Watts P, Griffin GE, et al. Blockade of attachment and fusion receptors inhibits HIV-1 infection of human cervical tissue. *J Exp Med*. 2004;**199**(8):1065–75.

377. Haase AT. Targeting early infection to prevent HIV-1 mucosal transmission. *Nature*. 2010;**464**(7286):217–23.

378. Sanders RW, de Jong EC, Baldwin CE, Schuitemaker JHN, Kapsenberg ML, Berkhout B. Differential transmission of human immunodeficiency virus type 1 by distinct subsets of effector dendritic cells. *J Virol*. 2002;**76**(15):7812–21.

379. Rodriguez-Garcia M, Shen Z, Barr FD, Boesch AW, Ackerman ME, Kappes JC, et al. Dendritic cells from the human female reproductive tract rapidly capture and respond to HIV. *Mucosal Immunol*. 2017;**10**(2):531–44.

380. Stieh DJ, Maric D, Kelley ZL, Anderson MR, Hattaway HZ, Beilfuss BA, et al. Vaginal challenge with an SIV-based dual reporter system reveals that infection can occur throughout the upper and lower female reproductive tract. *PLoS Pathog*. 2014;**10**(10):e1004440.

381. Cantero J, Genescà M. Maximizing the immunological output of the cervicovaginal explant model. *J Immunol Methods*. 2018;**460**:26–35.

382. Li M, Gao F, Mascola JR, Stamatatos L, Polonis VR, Koutsoukos M, et al. Human immunodeficiency virus type 1 env clones from acute and early subtype B infections for standardized assessments of vaccine-elicited neutralizing antibodies. *J Virol*. 2005;**79**(16):10108–25.

383. Trifonova RT, Lieberman J, van Baarle D. Distribution of immune cells in the human cervix and implications for HIV transmission. *Am J Reprod Immunol*. 2014;**71**(3):252–64.

384. Duluc D, Gannevat J, Anguiano E, Zurawski S, Carley M, Boreham M, et al. Functional diversity of human vaginal APC subsets in directing T-cell responses. *Mucosal Immunol*. 2013;**6**(3):626–38.

385. Soper A, Kimura I, Nagaoka S, Konno Y, Yamamoto K, Koyanagi Y, et al. Type I interferon responses by HIV-1 infection: Association with disease progression and control. *Front Immunol*. 2018;**8**:1823.

386. WHO. Consolidated guidelines on HIV prevention, diagnosis, treatment and care for key populations. 2016 update.

387. Derking R, Ozorowski G, Sliepen K, Yasmeen A, Cupo A, Torres JL, et al. Comprehensive antigenic map of a cleaved soluble HIV-1 envelope trimer. *PLoS Pathog*. 2015;**11**(3):e1004767.

388. Myszka DG. Kinetic, equilibrium, and thermodynamic analysis of macromolecular interactions with BIACORE. *Methods Enzymol*. 2000;**323**:325–32.

389. Corti D, Misasi J, Mulangu S, Stanley DA, Kanekiyo M, Wollen S, et al. Protective monotherapy against lethal Ebola virus infection by a potently neutralizing antibody. *Science (80-)*. 2016;**351**(6279):1339–42.

390. Pino Claveira M. HIV-1 immune activation induces Siglec-1 expression and enhances viral transmission in myeloid cells. Universitat Autònoma de Barcelona; 2016.

391. Kuhn JH, Adachi T, Adhikari NKJ, Arribas JR, Bah IE, Bausch DG, et al. New filovirus disease classification and nomenclature. *Nat Rev Microbiol*. 2019;**17**(5):261–3.

392. Alvarez CP, Lasala F, Carrillo J, Muñiz O, Corbí AL, Delgado R. C-type lectins DC-SIGN and L-SIGN mediate cellular entry by Ebola virus in cis and in trans. *J Virol*. 2002;**76**(13):6841–4.

393. Baribaud F, Pöhlmann S, Leslie G, Mortari F, Doms RW. Quantitative expression and virus transmission analysis of DC-SIGN on monocyte-derived dendritic cells. *J Virol*. 2002;**76**(18):9135–42.

394. Simmons G, Reeves JD, Grogan CC, Vandenberghe LH, Baribaud F, Whitbeck JC, et al. DC-SIGN and DC-SIGNR bind Ebola glycoproteins and enhance infection of macrophages and endothelial cells. *Virology*. 2003;**305**(1):115–23.

395. Versteeg K, Menicucci AR, Woolsey C, Mire CE, Geisbert JB, Cross RW, et al. Infection with the Makona variant results in a delayed and distinct host immune response compared to previous Ebola virus variants. *Sci Rep*. 2017;**7**(1):9370.

396. Peskova M, Heger Z, Janda P, Adam V, Pekarik V. An enzymatic assay based on luciferase Ebola virus-like particles for evaluation of virolytic activity of antimicrobial peptides. *Peptides*. 2017;**88**:87–96.

397. Kaletsky RL, Francica JR, Agrawal-Gamse C, Bates P. Tetherin-mediated restriction of filovirus budding is antagonized by the Ebola glycoprotein. *Proc Natl Acad Sci U S A*. 2009;**106**(8):2886–91.

398. Goujon C, Jarrosson-Wuillème L, Bernaud J, Rigal D, Darlix JL, Cimarelli A. With a little help from a friend: Increasing HIV transduction of monocyte-derived dendritic cells with virion-like particles of SIVMAC. *Gene Ther*. 2006;**13**(12):991–4.

399. Martin-serrano J, Perez-caballero D, Bieniasz PD. Context-dependent effects of L domains and ubiquitination on viral budding. *J Virol*. 2004;**78**(11):5554–63.

400. Lin G, Simmons G, Pöhlmann S, Baribaud F, Ni H, Leslie GJ, et al. Differential N-linked glycosylation of human immunodeficiency virus and Ebola virus envelope glycoproteins modulates interactions with DC-SIGN and DC-SIGNR. *J Virol*. 2003;**77**(2):1337–46.

401. Panchal RG, Ruthel G, Kenny TA, Kallstrom GH, Lane D, Badie SS, et al. In vivo oligomerization and raft localization of Ebola virus protein VP40 during vesicular budding. *Proc Natl Acad Sci U S A*. 2003;**100**(26):15936–41.

402. Feizpour A, Yu X, Akiyama H, Miller CM, Edmans E, Gummuluru S, et al. Quantifying lipid contents in enveloped virus particles with plasmonic nanoparticles. *Small*. 2015;**11**(13):1592–602.

403. Yuan S, Cao L, Ling H, Dang M, Sun Y, Zhang X, et al. TIM-1 acts a dual-attachment receptor for Ebolavirus by interacting directly with viral GP and the PS on the viral envelope. *Protein Cell*. 2015;**6**(11):814–24.

404. Tscherne DM, Manicassamy B, García-Sastre A. An enzymatic virus-like particle assay for sensitive detection of virus entry. *J Virol Methods*. 2010;**163**(2):336–43.

405. Martinez-Picado J, McLaren PJ, Erkizia I, Martin MP, Benet S, Rotger M, et al. Identification of Siglec-1 null individuals infected with HIV-1. *Nat Commun*. 2016;**7**:12412.

406. PREVAIL II Writing Group, Multi-National PREVAIL II Study Team, Davey RT, Dodd L, Proschan MA, Neaton J, et al. A randomized, controlled trial of ZMapp for Ebola virus infection. *N Engl J Med*. 2016;**375**(15):1448–56.

407. Martinez O, Johnson JC, Honko A, Yen B, Shabman RS, Hensley LE, et al. Ebola virus exploits a monocyte differentiation program to promote its entry. *J Virol*. 2013;**87**(7):3801–14.

408. Leroy EM, Baize S, Volchkov VE, Fisher-Hoch SP, Georges-Courbot MC, Lansoud-Soukate J, et al. Human asymptomatic Ebola infection and strong inflammatory response. *Lancet*. 2000;**355**(9222):2210–5.

409. Leung LW, Martinez O, Reynard O, Volchkov VE, Basler CF. Ebola virus failure to stimulate plasmacytoid dendritic cell interferon responses correlates with impaired cellular entry. *J Infect Dis*. 2011;**204**(Suppl 3):S973–7.

410. Ayithan N, Bradfute SB, Anthony SM, Stuthman KS, Dye JM, Bavari S, et al. Ebola virus-like particles stimulate type I interferons and proinflammatory cytokine expression through the Toll-like receptor and interferon signaling pathways. *J Interf Cytokine Res*. 2014;**34**(2):79–89.

411. Olejnik J, Forero A, Deflubé LR, Hume AJ, Manhart WA, Nishida A, et al. Ebolaviruses associated with differential pathogenicity induce distinct host responses in human macrophages. *J Virol*. 2017;**91**(11):e00179-17.

412. Perez-Zsolt D, Martinez-Picado J, Izquierdo-Useros N. When dendritic cells go viral: The role of Siglec-1 in host defense and dissemination of enveloped viruses. In press. *Viruses*.

413. Rustagi A, Gale M. Innate antiviral immune signaling, viral evasion and modulation by HIV-1. *J Mol Biol*. 2014;**426**(6):1161–77.

414. Sandstrom TS, Ranganath N, Angel JB. Impairment of the type I interferon response by HIV-1: Potential targets for HIV eradication. *Cytokine Growth Factor Rev*. 2017;**37**:1–16.

415. Akiyama H, Pina Ramirez N-G, Gibson G, Kline C, Watkins S, Ambrose Z, et al. Interferon-inducible CD169/Siglec1 attenuates anti-HIV-1 effects of alpha interferon. *J Virol*. 2017;**91**(21):e00972-17.

416. Doyle T, Goujon C, Malim MH. HIV-1 and interferons: Who's interfering with whom? *Nat Rev Microbiol*. 2015;**13**(7):403–13.

417. Hickey DK, Patel M V., Fahey J V., Wira CR. Innate and adaptive immunity at mucosal surfaces of the female reproductive tract: Stratification and integration of immune protection against the transmission of sexually transmitted infections. *J Reprod Immunol*. 2011;**88**(2):185–94.

418. Iwasaki A. Antiviral immune responses in the genital tract: Clues for vaccines. *Nat Rev Immunol*. 2010;**10**(10):699–711.

419. Iyer SS, Bibollet-Ruche F, Sherrill-Mix S, Learn GH, Plenderleith L, Smith AG, et al. Resistance to type 1 interferons is a major determinant of HIV-1 transmission fitness. *Proc Natl Acad Sci U S A*. 2017;**114**(4):E590–9.

420. Chang JJ, Woods M, Lindsay RJ, Doyle EH, Griesbeck M, Chan ES, et al. Higher expression of several interferon-stimulated genes in HIV-1-infected females after adjusting for the level of viral replication. *J Infect Dis*. 2013;**208**(5):830–8.

421. Pope M, Betjes MGH, Romani N, Hirmand H, Cameron PU, Hoffman L, et al. Conjugates of dendritic cells and memory T lymphocytes from skin facilitate productive infection with HIV-1. *Cell*. 1994;**78**(3):389–98.

422. Iwasaki A. Mucosal dendritic cells. *Annu Rev Immunol*. 2007;**25**:381–418.

423. Ganor Y, Real F, Sennepin A, Dutertre CA, Prevedel L, Xu L, et al. HIV-1 reservoirs in urethral macrophages of patients under suppressive antiretroviral therapy. *Nat Microbiol*. 2019;**4**(4):633–44.

424. Hirbod T, Nilsson J, Andersson S, Uberti-Foppa C, Ferrari D, Manghi M, et al. Upregulation of interferon-α and RANTES in the cervix of HIV-1-seronegative women with high-risk behavior. *J Acquir Immune Defic Syndr*. 2006;**43**(2):137–43.

425. Wang Y, Abel K, Lantz K, Krieg AM, McChesney MB, Miller CJ. The Toll-like receptor 7 (TLR7) agonist, imiquimod, and the TLR9 agonist, CpG ODN, induce antiviral cytokines and chemokines but do not prevent vaginal transmission of simian immunodeficiency virus when applied intravaginally to rhesus macaques. *J Virol*. 2005;**79**(22):14355–70.

426. Agrawal T, Vats V, Wallace PK, Singh A, Salhan S, Mittal A. Recruitment of myeloid and plasmacytoid dendritic cells in cervical mucosa during Chlamydia trachomatis

infection. *Clin Microbiol Infect*. 2009;**15**(1):50–9.

427. Lund JM, Linehan MM, Iijima N, Iwasaki A. Plasmacytoid dendritic cells provide innate immune protection against mucosal viral infection in situ. *J Immunol*. 2006;**177**(11):7510–4.

428. Segura E, Touzot M, Bohineust A, Cappuccio A, Chiocchia G, Hosmalin A, et al. Human inflammatory dendritic cells induce Th17 cell differentiation. *Immunity*. 2013;**38**(2):336–48.

429. Stieh DJ, Matias E, Xu H, Fought AJ, Blanchard JL, Marx PA, et al. Th17 cells are preferentially infected very early after vaginal transmission of SIV in macaques. *Cell Host Microbe*. 2016;**19**(4):529–40.

430. Booth AM, Fang Y, Fallon JK, Yang JM, Hildreth JEK, Gould SJ. Exosomes and HIV Gag bud from endosome-like domains of the T cell plasma membrane. *J Cell Biol*. 2006;**172**(6):923–35.

431. Fang Y, Wu N, Gan X, Yan W, Morrell JC, Gould SJ. Higher-order oligomerization targets plasma membrane proteins and HIV Gag to exosomes. *PLoS Biol*. 2007;**5**(6):e158.

432. Rodriguez-Plata MT, Puigdomènech I, Izquierdo-Useros N, Puertas MC, Carrillo J, Erkizia I, et al. The infectious synapse formed between mature dendritic cells and CD4+ T cells is independent of the presence of the HIV-1 envelope glycoprotein. *Retrovirology*. 2013;**10**:42.

433. Ruffin N, Gea-Mallorquí E, Brouiller F, Jouve M, Silvin A, See P, et al. Constitutive Siglec-1 expression confers susceptibility to HIV-1 infection of human dendritic cell precursors. *Proc Natl Acad Sci U S A*. 2019;**116**(43):21685–93.

434. Geisbert TW, Hensley LE, Gibb TR, Steele KE, Jaax NK, Jahrling PB. Apoptosis induced in vitro and in vivo during infection by Ebola and Marburg viruses. *Lab Investig*. 2000;**80**(2):171–86.

435. Davis KJ, Anderson AO, Geisbert TW, Steele KE, Geisbert JB, Vogel P, et al. Pathology of experimental Ebola virus infection in African green monkeys: Involvement of fibroblastic reticular cells. *Arch Pathol Lab Med*. 1997;**121**(8):805–19.

436. Lasala F, Arce E, Otero JR, Rojo J, Delgado R. Mannosyl glycodendritic structure inhibits DC-SIGN-mediated Ebola virus infection in cis and in trans. *Antimicrob Agents Chemother*. 2003;**47**(12):3970–2.

437. Chandran K, Sullivan NJ, Felbor U, Whelan SP, Cunningham JM. Endosomal proteolysis of the Ebola virus glycoprotein is necessary for infection. *Science (80-)*. 2005;**308**(5728):1643–5.

438. Schornberg K, Matsuyama S, Kabsch K, Delos S, Bouton A, White J. Role of endosomal cathepsins in entry mediated by the Ebola virus glycoprotein. *J Virol*. 2006;**80**(8):4174–8.

439. Marzi A, Möller P, Hanna SL, Harrer T, Eisemann J, Steinkasserer A, et al. Analysis of the interaction of Ebola virus glycoprotein with DC-SIGN (dendritic cell-specific intercellular adhesion molecule 3-grabbing nonintegrin) and its homologue DC-SIGNR. *J Infect Dis*. 2007;**196**(Suppl 2):S237–46.

440. Gramberg T, Hofmann H, Möller P, Lalor PF, Marzi A, Geier M, et al. LSECtin interacts with filovirus glycoproteins and the spike protein of SARS coronavirus. *Virology*. 2005;**340**(2):224–36.

441. Bray M, Geisbert TW. Ebola virus: The role of macrophages and dendritic cells in the pathogenesis of Ebola hemorrhagic fever. *Int J Biochem Cell Biol*. 2005;**37**(8):1560–6.

442. Martinez O, Leung LW, Basler CF. The role of antigen-presenting cells in filoviral hemorrhagic fever: Gaps in current knowledge. *Antiviral Res*. 2012;**93**(3):416–28.

443. McElroy AK, Akondy RS, Davis CW, Ellebedy AH, Mehta AK, Kraft CS, et al. Human Ebola virus infection results in substantial immune activation. *Proc Natl Acad Sci*. 2015;**112**(15):4719–24.

444. Luo D, Zheng R, Wang D, Zhang X, Yin Y, Wang K, et al. Effect of sexual transmission on the West Africa Ebola outbreak in 2014: A mathematical modelling study. *Sci Rep*. 2019;**9**(1):1653.

445. Bart SM, Cohen C, Dye JM, Shorter J, Bates P. Enhancement of Ebola virus infection by seminal amyloid fibrils. *Proc Natl Acad Sci*. 2018;**115**(28):7410–5.

446. De Saint Jean A, Lucht F, Bourlet T, Delézay O. Transforming growth factor beta 1 up-regulates CD169 (sialoadhesin) expression on monocytederived dendritic cells: Role in HIV sexual transmission. *Aids*. 2014;**28**(16):2375–80.

447. Steiniger B, Barth P, Herbst B, Hartnell A, Crocker PR. The species-specific structure of microanatomical compartments in the human spleen: Strongly sialoadhesin-positive macrophages occur in the perifollicular zone, but not in the marginal zone. *Immunology*. 1997;**92**(2):307–16.

448. Basler CF. Molecular pathogenesis of viral hemorrhagic fever. *Semin Immunopathol*. 2017;**39**(5):551–61.

449. Qiu X, Wong G, Audet J, Bello A, Fernando L, Alimonti JB, et al. Reversion of advanced Ebola virus disease in nonhuman primates with ZMapp. *Nature*. 2014;**514**(7520):47–53.

450. Nature news: Two Ebola drugs show promise amid ongoing outbreak [Internet]. 2019.

451. Pascal KE, Dudgeon D, Trefry JC, Anantpadma M, Sakurai Y, Murin CD, et al. Development of clinical-stage human monoclonal antibodies that treat advanced Ebola virus disease in nonhuman primates. *J Infect Dis*. 2018;**218**(Suppl 5):S612–26.

452. Flyak AI, Shen X, Murin CD, Turner HL, David JA, Fusco ML, et al. Cross-reactive and potent neutralizing antibody responses in human survivors of natural ebolavirus infection. *Cell*. 2016;**164**(3):392–405.

453. Duehr J, Wohlbold TJ, Oestereich L, Chromikova V, Amanat F, Rajendran M, et al. Novel cross-reactive monoclonal antibodies against ebolavirus glycoproteins show protection in a murine challenge model. *J Virol*. 2017;**91**(16):e00652-17.

454. Luczkowiak J, Lasala F, Mora-Rillo M, Arribas JR, Delgado R. Broad neutralizing activity against ebolaviruses lacking the mucin-like domain in convalescent plasma specimens from patients with Ebola virus disease. *J Infect Dis*. 2018;**218**(Suppl 5):S574–81.

455. Mohan GS, Li W, Ye L, Compans RW, Yang C. Antigenic subversion: A novel mechanism of host immune evasion by Ebola virus. *PLoS Pathog*. 2012;**8**(12):e1003065.

456. Kugelman JR, Kugelman-Tonos J, Ladner JT, Pettit J, Keeton CM, Nagle ER, et al. Emergence of Ebola virus escape variants in infected nonhuman primates treated with the MB-003 antibody cocktail. *Cell Rep*. 2015;**12**(12):2111–20.

457. Muñoz A, Sigwalt D, Illescas BM, Luczkowiak J, Rodríguez-Pérez L, Nierengarten I, et al. Synthesis of giant globular multivalent glycofullerenes as potent inhibitors in a model of Ebola virus infection. *Nat Chem*. 2016;**8**(1):50–7.

458. Henß L, Beck S, Weidner T, Biedenkopf N, Sliva K, Weber C, et al. Suramin is a potent inhibitor of Chikungunya and Ebola virus cell entry. *Virol J*. 2016;**13**:149.

459. Lump E, Castellano LM, Meier C, Seeliger J, Erwin N, Sperlich B, et al. A molecular tweezer antagonizes seminal amyloids and HIV infection. *Elife*. 2015;**4**:e05397.

460. Röcker AE, Müller JA, Dietzel E, Harms M, Krüger F, Heid C, et al. The molecular tweezer CLR01 inhibits Ebola and Zika virus infection. *Antiviral Res*. 2018;**152**:26–35.

461. Akiyama H, Miller C, Patel H V., Hatch SC, Archer J, Ramirez N-GP, et al. Virus particle release from glycosphingolipid-enriched microdomains is essential for dendritic cell-mediated capture and transfer of HIV-1 and henipavirus. *J Virol*. 2014;**88**(16):8813–25.

462. Madrid PB, Chopra S, Manger ID, Gilfillan L, Keepers TR, Shurtleff AC, et al. A systematic screen of FDA-approved drugs for inhibitors of biological threat agents. *PLoS One*. 2013;**8**(4):e60579.

463. Madrid PB, Panchal RG, Warren TK, Shurtleff AC, Endsley AN, Green CE, et al. Evaluation of Ebola virus inhibitors for drug repurposing. *ACS Infect Dis*. 2015;**1**(7):317–26.

464. Dowall SD, Bosworth A, Watson R, Bewley K, Taylor I, Rayner E, et al. Chloroquine inhibited Ebola virus replication in vitro but failed to protect against infection and disease in the in vivo guinea pig model. *J Gen Virol*. 2015;**96**(12):3484–92.

465. Falzarano D, Safronetz D, Prescott J, Marzi A, Feldmann F, Feldmann H. Lack of protection against Ebola virus from chloroquine in mice and hamsters. *Emerg Infect Dis*. 2015;**21**(6):1065–7.

466. Gignoux E, Azman AS, de Smet M, Azuma P, Massaquoi M, Job D, et al. Effect of artesunate-amodiaquine on mortality related to Ebola virus disease. *N Engl J Med*. 2016;**374**(1):23–32.

467. Lindstrom A, Anantpadma M, Baker L, Raghavendra NM, Davey R, Davisson VJ. Phenotypic prioritization of diphyllin derivatives that block filoviral cell entry by vacuolar (H+)-ATPase inhibition. *ChemMedChem*. 2018;**13**(24):2664–76.

468. Johansen LM, Branna JM, Delos SE, Shoemaker CJ, Stossel A, Lear C, et al. FDA-approved selective estrogen receptor modulators inhibit Ebola virus infection. *Sci Transl Med*. 2013;**5**(190):190ra79.

469. Shoemaker CJ, Schornberg KL, Delos SE, Scully C, Pajouhesh H, Olinger GG, et al. Multiple cationic amphiphiles induce a Niemann-Pick C phenotype and inhibit Ebola

virus entry and infection. *PLoS One*. 2013;**8**(2):e56265.

470. Carstea ED, Morris JA, Coleman KG, Loftus SK, Zhang D, Cummings C, et al. Niemann-Pick C1 disease gene: Homology to mediators of cholesterol homeostasis. *Science (80-)*. 1997;**277**(5323):228–31.

471. Naureckiene S, Sleat DE, Lacklan H, Fensom A, Vanier MT, Wattiaux R, et al. Identification of HE1 as the second gene of Niemann-Pick C disease. *Science (80-)*. 2000;**290**(5500):2298–301.

472. Guedj J, Piorkowski G, Jacquot F, Madelain V, Nguyen THT, Rodallec A, et al. Antiviral efficacy of favipiravir against Ebola virus: A translational study in cynomolgus macaques. *PLoS Med*. 2018;**15**(3):e1002535.

473. Warren TK, Jordan R, Lo MK, Ray AS, Mackman RL, Soloveva V, et al. Therapeutic efficacy of the small molecule GS-5734 against Ebola virus in rhesus monkeys. *Nature*. 2016;**531**(7594):381–5.

474. Lüdtke A, Ruibal P, Wozniak DM, Pallasch E, Wurr S, Bockholt S, et al. Ebola virus infection kinetics in chimeric mice reveal a key role of T cells as barriers for virus dissemination. *Sci Rep*. 2017;**7**:43776.

475. Oestereich L, Lüdtke A, Ruibal P, Pallasch E, Kerber R, Rieger T, et al. Chimeric mice with competent hematopoietic immunity reproduce key features of severe Lassa fever. Fernandez-Sesma A, editor. *PLOS Pathog*. 2016;**12**(5):e1005656.

476. Sun W, He S, Martínez-Romero C, Kouznetsova J, Tawa G, Xu M, et al. Synergistic drug combination effectively blocks Ebola virus infection. *Antiviral Res*. 2017;**137**:165–72.

477. Dyall J, Nelson EA, DeWald LE, Guha R, Hart BJ, Zhou H, et al. Identification of combinations of approved drugs with synergistic activity against Ebola virus in cell cultures. *J Infect Dis*. 2018;**218**(Suppl 5):S672–8.

Chapter 11

PUBLICATIONS

1. Míriam Díaz-Varela, Armando de Menezes-Neto, **Daniel Perez-Zsolt**, Ana Gámez-Valero, Joan Seguí-Barber, Nuria Izquierdo-Useros, Javier Martinez-Picado, Carmen Fernández-Becerra and Hernando A. del Portillo. Proteomics study of human cord blood reticulocyte-derived exosomes. *Scientific Reports*. 2018. 8(1):14046. doi: 10.1038/s41598-018-32386-2.

2. **Daniel Perez-Zsolt**, Jon Cantero-Pérez, Itziar Erkizia, Susana Benet, Maria Pino, Carla Serra-Peinado, Alba Hernández-Gallego, Josep Castellví, Gustavo Tapia, Vicent Arnau-Saz, Julio Garrido, Antoni Tarrats, Maria J. Buzón, Javier Martinez-Picado, Nuria Izquierdo-Useros and Meritxell Genescà. Dendritic cells from the cerivcal mucosa capture and transfer HIV-1 via Siglec-1. 2019. *Frontiers in Immunology*. 10:825. doi: 10.3389/fimmu.2019.00825.

3. **Daniel Perez-Zsolt**, Itziar Erkizia, Maria Pino, Mónica García-Gallo, Maria Teresa Martin, Susana Benet, Jakub Chojnacki, María Teresa Fernández-Figueras, Dolores Guerrero, Victor Urrea, Xabier Muñiz-Trabudua, Leonor Kremer, Javier Martinez-Picado and Nuria Izquierdo-Useros. Anti-Siglec-1 antibodies block Ebola viral uptake and decrease cytoplasmic viral entry. 2019. *Nature Microbiology*. 4(9):1558-1570. doi: 10.1038/s41564-019-0453-2.

4. **Daniel Perez-Zsolt**, Javier Martinez-Picado, Nuria Izquierdo-Useros. When dendritic cells go viral: The role of Siglec-1 in host defense and dissemination of enveloped viruses. *Viruses. 2019* (in press).

5. **Daniel Perez-Zsolt**, Javier Martinez-Picado, Nuria Izquierdo-Useros. Receptors on primary phagocytes as therapeutic targets against highly pathogenic emerging viruses in *Antiviral discovery for highly pathogenic emerging viruses* (under review).

Chapter 12

ACKNOWLEDGEMENTS

La ciencia es ante todo trabajo en equipo, y eso es algo que he aprendido durante estos cinco años en IrsiCaixa. Por eso no podía faltar un apartado como este, en el que quiero agradecer su ayuda a todos aquéllos que se han implicado, directa o indirectamente, en este trabajo.

En primer lugar, a **Javier** por darme la oportunidad de formar parte de este gran equipo que es GREC. Porque aunque la prueba de acceso fue dura, y no sé si a día de hoy sería capaz de formular la D-glucosa (o cualquier otra de sus formas), una vez superada la cosa cambia, y siempre he encontrado la puerta de tu despacho abierta para atender cualquier duda o problema que pudiera tener. Además, siempre he salido de allí con algún buen consejo bajo el brazo. A **Nuria**, por todo lo que he podido aprender de ti. Eres una gran maestra en el arte de conseguir que parezca fácil lo que no lo es. Porque siempre se entiende mejor cómo funciona el mundo de los virus cuando éstos son palomitas a repartir entre los espectadores en una sala de cine, o cuando sus vías de entrada en las células son una tubería que gotea, y que sólo podrá repararse cuando se tapen todas y cada una de sus fugas. Ah! Y además me salvaste de la indigencia aquella vez en Hong Kong. En fin, muchas gracias a los dos por todo lo que me habéis enseñado sobre ciencia y sobre el mundo. Si al principio de la tesis me hubieran dicho todas las cosas geniales que iba a hacer durante estos años no me lo hubiera creído. No sé qué me deparará el futuro; pero en lo que a materia de jefes se refiere, dejáis el listón muy alto!

También quiero agradecer al Dendris Team por todo el apoyo durante todo este tiempo. A **Itziar**, la reina malísssim… digo bueníssimaaa de P3. Por todas las veces que me has salvado el experimento después de que algún citómetro hiciera de las suyas, y por tantas horas compartidas mano a mano en la cabina, escuchando las obras maestras de Tchaikovsky o Camela, indistintamente. A **Susana**, per tots els moments compartits, els nervis abans de les presentacions, els congressos, les estones a P3. Tantes coses! Ara que et toca començar amb la tesi, molts ànims perquè segur que va tot súper bé, i d'aquí res seràs una doctora… doctora! **Maria Pino**, encara que hagis passat dels monos d'Irsi als monos d'Atlanta no ens oblidem de tu. Recordo els primers anys de tesi, quan tot el que feia intentava fer-ho com tu, perquè sabia que aleshores estaria bé. Potser no li posava tant de swing, però! En qualsevol cas, t'estic molt agraït per la part en què has col·laborat en aquesta tesi amb les cèl·lules plasmacitoides. **Xabi**, el nuevo fichaje dendriticólogo, eres un crack y cortas los mAbs de maravilla, además de sorprendernos de vez en cuando con cookies brutales o con los productos de tu huerto. Seguro que haces una tesis genial! **Pat**, companya de fatigues en l'apassionant món de la proteòmica/transcriptòmica, gràcies per

tots els consells de post-doc experta en múltiples i diversos virus, és molt guai tenir-te a l'equip! And **Jakub**, thank you for always looking at the bright side, and also for super-helping us with the super-resolution microscopy. I am afraid I will never see donuts the same way again.

Y cómo no, gracias también al Erradication Team, la otra mitad del grupo. **Mari Carmen**, porque siempre que he tenido alguna duda relacionada con molecular (y han sido bastantes) he podido acudir en tu ayuda. **María Salgado**, durante mucho tiempo vecina de mesa, a ti también he acudido en muchas ocasiones, ya que los episodios de Juego de Tronos siempre requerían de nuestro profundo análisis. **Cristina**, gracias por pasarme las células! Y también por acompañarme a todos esos seminarios de la UAB para conseguir autógrafos. A **Sara**, por hablarme de la película de It Follows, aunque algunos días que me quedé hasta tarde en el hospital la recordaba y tenía miedito. Y a **Maria Francesca**, gracias a ti y a Nico por invitarme a vuestra terraza aquella tarde, lo pasamos genial! A **Ángel**, que siempre deja lo que esté haciendo (aunque sea un interesante curso de bioestadística) cuando bajo de visita a la mazmorra. Espero que podamos volver a esquiar, pero major si es un día que haya nieve. Aunque contigo a las duras... y a las maduras! I **Sílvia Bernal**, merci per amenitzar tant els dinars, i per introduir-me al món del cross-fit en aquell dia d'IrsiGym.

Y gestionando tanto a Dendris como Erradicadores: **Judith**, la money manager! Eres genial, muchas gracias por todo durante estos años. Por los trayectos en bus y Renfe, que se hacían muchísimo más llevaderos contigo, por presentarme a los que serían mis compis de piso durante tanto tiempo, por todas las fiestas habidas y por haber, por los encuentros fortuitos por Sabadell que le alegran a uno el día, por esa súper boda (gracias a ti y a Miquel, claro), etc. etc. Senkiu very very much! También a **Mari** y a **Diana**, por estar siempre dispuestas a ayudar. Y cómo no, gracias a **Víctor**, por hacernos accessible ese mundo a veces extraño que es la bioestadística, pero que entra mucho mejor en forma de cápsula. Muchas gracias por ayudar a que ningún bioestadístico que lea nuestros papers se lleve las manos a la cabeza!

Siguiendo con el tema de publicaciones, me gustaría agradecer por su trabajo a todos los colaboradores que han hecho posible que tantos resultados, incluidos muchos de los que contiene esta tesis, vieran la luz. A nuestros vecinos del IGTP y ahora investigadores en el grupo de Investigación Traslacional en VIH del VHIR **Txell Genescà** y **Jon Cantero**. Gracias por vuestra dedicación y trabajo para que el proyecto de mucosa cervical saliera adelante tan bien como lo ha hecho. Aunque solíamos quedarnos hasta tarde el día que

llegaba tejido, al final el esfuerzo a merecido la pena! Y por supuesto, gracias a **Arnau Saz** y **Maria José Buzón** por su colaboración en este proyecto, así como al resto de co-autores de la publicación. Vull agrair motl especialment a la **Isabel Crespo** de la plataforma de citometría del IDIBAPS per la seva inestimable ajuda amb l'Amnis. Por lo que respecta al trabajo de anticuerpos contra Siglec-1, quisiera reconocer la gran labor del grupo de **Leonor Kremer** en el CNB/CSIC, con la participación de **Mónica García-Gallo**, **Maria Teresa Martin, M. García-Cabrero** y **M. Lozano**. Por su excelente asistencia, consejo y procesamiento de imágenes, a **Elena Rebollo** de la Unidad de Microscopia de Fluorescencia Avanzada del IBMB-PCB, así como a **Jaume Boix** y **Matías**. Siguiendo con los microscopios, no puedo dejar de agradecerle a **Maite Fernández-Figueras** su ayuda en el microscopio electrónico, y por su incansable entusiasmo en busca siempre de la mejor imagen. También a **Ester Sayós**, **Laia Pérez-Roca** e **Irian Lorencés** por el procesamiento de muestras. Asimismo, quiero agradecer a **Dolores Guerrero** y al equipo de otorrinolaringología del HUGTiP por proporcionarnos valiosas muestras de tejido. También a **César Muñoz-Fontela**, **Beatriz Escudero-Pérez** y **Sergio Gómez-Medina**, del HPI en Hamburgo por sus constructivos comentarios. A **Míriam Díaz-Varela** y **Hernando del Portillo** por su interesante colaboración en el proyecto de vesículas extracelulares. Y como en esta tesis no ha faltado la citometría, también a **Marco A. Fernández** y **Gerard Requena** de la plataforma de citometría del IGTP por su ayuda con el Fortessa y el Sorter.

Del grupo VIC, quisiera agradecer a **Jorge** toda su ayuda durante estos años, en especial con los ELISAs y siempre que me ha surgido alguna duda en inmunología, una materia en la que es un verdadero maestro. A **Montse**, que se apunta a los mejores planes. Desde un viaje a Edimburgo o la visita al festival de terror de Sitges hasta un brunch en Barcelona. Eso sin olvidar una sesión de Mysterium! Al **Ferran**, perquè li agrada Edimburg i per tant m'agrada ell (Yahahai!). A **Carlos**, el sevillano que monta las mejores fiestas en su piso y que pronto será el más cachas de todo Irsi. Y **Raquel**, la pre-doc Otaku que es más rica que un sushi. A **Edwards**, que ha conseguido no volverse volando a Chile después de conocernos. I al **Francesc**, per totes aquestes curses en les que m'ha guanya… que hem partipat. També a la **Marisa**, **Silvia Marfil**, l'**Ester Aparicio** i en **Víctor**, sempre disposats a treure't un somriure dintre i fora de P3. A **Carmen**, per aquell passeig pels Champs Élysées. I al **Julià**, perquè m'ha ajudat sempre que ho he necessitat.

Y llegan los VIRIs! Gràcies Òscar per la portada d'aquesta tesi, ets un gran artista i a més súper bona persona, així que intenta no canviar gaire eh! Ah, i em va encantar visitar el teu

poble, m'ho vaig passar genial! A **Ester**, por tantos momentos de risa que hemos pasado, en especial el de la fusión de caras que fue brutal. También por grandes momentos como los Mysteriums y la esquiada. Y porque eres guay y punto. **Miguel**! Influencer de la siensia y mi queridísimo Piscis. Sabemos que no eres una ONG pero te queremos igual. Gracias por las meriendas a horas en que solamente quedamos los verdaderos trabajadores de IrsiCaixa. Y cómo no a la jefa, **Julia**. Gracias por llevarme en coche hasta Montcada tantas veces, aunque para eso tuviéramos que ir hasta el merendero. No pasa nada, se compensaba cuando me ponías una cinta del Pau durante el trayecto! Además, muchas gracias por los consejos y por tener siempre un rato para mi cuando te encuentro por Irsi.

It's Brander's time. Gracias **Samandhy** por tus consejos sobre cómo escribir la tesis, y por compartir conmigo los vídeos de baile! A **Marta Ruiz** (Sexy Lady), porque siempre que paso por tu rincón sé que las risas están aseguradas. A **Luis**, que siempre me deja probar de su cachimba aunque no sea una NK. A **Anuska**, porque aunque haya muchas enfermedades que curar también hay momentos para pasarlo bien. I a l'**Àlex**, per tantes estones compartides a P3 (i a la cafeteria). l'També a la **Míriam**, **Bruna** i **Sandra**, perquè sou estupendes què carai. En el Roger Paredes' group, querría agradecer a **Alexandra** por los buenos momentos hablando en el bus o en Irsi, y por compartir mi gusto por los libros horrorosos/divertidos como el de Mme Raquin y el Passage du Pont-Neuf (Arghhh!). També a l'**Aleix**, que sempre em deixa veure els seus salvapantalles tan xulos. I a la **Maria Casadellà**, perquè la seva manera de ser et contagia de bon humor. Al **Marc**, que està fent un codi que fa una mica de por però segur que té bones intencions (oi?). A la **Mariona**, la meva companya de P3 els dies que hi havia teixit i sortia a les tantes de P3. Y a **Carmen**, la vecina de mesa que nunca me veía porque siempre estaba escribiendo la tesis. Finalment, al **Roger Paredes**, perquè sempre és molt amable i a més li agrada el piano. Toma ya.

En VITI, quiero agradecer a **Eli García** por los desayunos, que contigo son más divertidos. També a la **Sònia**, amb la que sempre trobem algún tema graciós per comentar, com les amígdales ravioli. También a **Ceci**, no vaya a ser que si no la pongo en agradecimientos no quiera ir conmigo a la próxima Gala de los Óscars. També al **Jordi**, un reincorporat a IrsiCaixa que sempre t'alegra amb el seu bon humor. I arriba el torn del grup de l'Ester Ballana. Vull agraïr a l'**Edurne** per compartir aquests moments finals de la tesi, que han estat durillos però entre tots han passat millor. Ah, i també per seguir-me parlant tot i que m'agradi el Bloody Mary que lleva anchoa. También a **Lucía**, porque eres encantadora y eso es de agradecer. Al **Roger Badia**, perquè creu que sóc un hombre del renacimiento i un piano-man i això em fa molta ilu. També a la **Maria Pujantell**, l'**Eva** i l'**Ester Ballana**,

perquè sempre heu estat súper amables amb mi i porque vosotras lo valéis. En el grupo de Miguel Ángel, quiero agradecer a **Ana Jordán** que haya sido mi compañera de beca todos estos años, apoyándonos en los buenos y en los malos momentos. Y por todas esas tardes de patinaj… ah no, pero sí que te agradezco que hagas ese brownie tan espectacular ;). També a la **Sandra Franco**, amb qui puc anar a veure pelis de terror i també Dirty Dancing! I a la Maria Nevot, per compartir els nervis d'abans de les presentacions del GeSIDA i moments sempre agradables a Irsi.

A la **Júlia** i la **Rita** de comunicació, perquè un dels millors moments a IrsiCaixa va ser quan vaig poder donar una xerrada divulgativa a alumnes d'instituts. I també a la **Rosina** i a la **Marina**, per ensenyar-nos tantes coses sobre la investigació responsable i l'alimentació (ese súper póster!). A **Julián**, por ayudarme a recuperar mis carpetas perdidas. I al **Pep Coll**, per ensenyar-nos estudis tan interessants sobre la PrEP. A los tres en raya de recepción. **Penélope**, muchas gracias por solucionar de forma súper rápida cualquiera de los problemas con los que venimos. **Arnau**, gracias por ese Danieleeee cuando paso por delante de la recepción, así no se me olvida cómo me llamo. Y a **Cristina Mesa**, por ser siempre tan amable conmigo y ayudarme en cualquier trámite con una sonrisa. Y a Lidia Ruiz, gracias por gestionar tan bien el AutoMACS y también por las charlas en tu despacho acompañadas de Ferrero Rocher, la expresión del buen gusto. A las chicas de muestras! **Rafi**, gracias por ayudarme en P3 siempre que lo he necesitado. Además, me lo pasé genial en el concierto de OT, y no sólo dentro sino también en la cola porque estabais vosotras. A **Lucía**, por dejarme usar tu centrífuga algunas veces. Sé que fue un gran esfuerzo, pero demuestra gran generosidad por tu parte jajajaj. Y gracias **Cristina Ramírez** y **Susana Esteban** por la ayuda que siempre nos dais en P3 y por los buenos momentos en la cafetería. También a **Eulàlia** y **Teresa**, porque siempre es agradable hablar con vosotras en los desayunos.

A los que estuvieron conmigo en Irsi y volaron del nido. A **Luis**, por tantos momentos 'pachachos' y esos fresquitos en París. A l'**Alba**, per la teva calidesa i per aquel gran momento de críticos de arte al museo Chillida. A **Javi**, que compilabas tus códigos mientras yo hacía mis 'puntitos'. A **Yolanda**, por compartir una nueva etapa además de la carrera. A **Eli Gómez**, una verdadera aventurera. A la **Muntsa**, una altra aventurera fent les Amèriques. I al **Josep**, el més aventurer de tots! A **Marta Marszalek**, por esos momentos al sol después de comer. Y a **Ferrán**, por lo divertido que fue pasar ratos contigo y por compartir tus fotos en Insta, que así puedo seguir lo que haces! Y a tantos que han pasado por el laboratorio durante estos 5 años…

També voldria agrair molt especialment al **Bonaventura Clotet** i a la **Lourdes Grau** per donar-me l'oportunitat de formar part d'aquesta gran família (y cada vez más) que és IrsiCaixa. Per mi ha estat un veritable privilegi poder fer la tesi en un ambient tan agradable i professional com és el d'IrsiCaixa.

A banda d'Irsi, m'agradaria donar les gràcies a tota la gent de Lluita, sempre al nostre costat fent posible que la investigació estigui lligada a la clínica. A l'**Anna Bassols**, en **Francesc Borràs** i la **Sílvia Vidal** els vull agrair els seus comentaris sempre constructius i tota la seva ajuda. Així mateix, vull donar les gràcies a la **Victòria Nogués** per la seva gran ajuda des de la UAB durant tota la tesi. And I would like to acknowledge all the people from the Imagine Institute in Paris for their warm welcome. In particular, I want to express my gratitude to **Antonio Rausell**, **Anne-Françoise Batto**, **Francisco Requena** and **Akira** for their help during my stage in Paris. Merci beaucoup!

A la gente del máster y de la carrera. En especial a **Jéssica**, **Marta**, **Sarai**, **Alba**, **Ana Villar**, **Agrin**, **Laura**, **Meri**. Gracias a todas por hacer de los años de carrera una pasada! A més de pels anys de carrera, a l'**Estela** i l'**Olívia** també vull agraïr-vos especialment que em féssiu arribar l'oferta per fer el doctorat a IrsiCaixa. I també voldria agair a les meves professores de biologia i química de l'IES Sant Quirze, **Empar Solanes** i **Maria Antònia Sanz**, per introduir-me en el món de la ciència.

Finalmente, quisiera agradecer muy especialmente a mis amigos y a toda mi familia por haberme apoyado siempre en todo lo que me he propuesto. Estoy muy feliz de estar rodeado por todos vosotros. Gracias **papa**, **mama** i **Ari** por todo vuestro cariño y por estar siempre a mi lado.